Volume 47 *September 1961* *Number 9*

Proceedings of the
National Academy of Sciences
of the United States of America

The Proceedings of the National Academy of Sciences

OFFICERS OF THE ACADEMY

DETLEV W. BRONK
President

J. A. STRATTON
Vice President

H. P. ROBERTSON
Foreign Secretary

HUGH L. DRYDEN
Home Secretary

L. V. BERKNER
Treasurer

EDITORIAL BOARD OF THE PROCEEDINGS

SAUNDERS MAC LANE
Chairman

HUGH L. DRYDEN, *Home Secretary*
L. V. BERKNER, *Treasurer*
H. P. ROBERTSON, *Foreign Secretary*
EDWIN B. WILSON, *Managing Editor*

HARRISON BROWN
S. CHANDRASEKHAR
ERNST CLOOS
THOMAS FRANCIS, JR.
C. H. GRAHAM
G. EVELYN HUTCHINSON
WILLARD F. LIBBY
H. W. MAGOUN
J. R. PIERCE

Subscription price is $17.50 for one year, $33.50 for two years, and $48.00 for three years. The price of a single issue beginning with volume 47 (1961), is $2.25; through volume 46 (1960), $1.50. Make all remittances payable to the National Academy of Sciences in U.S. currency or its equivalent.

Editorial correspondence should be addressed to the PROCEEDINGS OF THE NATIONAL ACADEMY OF SCIENCES, 2101 Constitution Avenue, Washington 25, D. C.

Business correspondence should be addressed to the Printing and Publishing Office, National Academy of Sciences, 2101 Constitution Ave., Washington 25, D. C.

Subscribers are requested to notify the Printing and Publishing Office of the Academy and their local postmaster immediately of change of address. Notices to the Academy should provide both the old and the new address.

Microfilms of complete volumes of this journal are available to regular subscribers only and may be obtained at the end of the volume year from University Microfilms, 313 N. First Street, Ann Arbor, Michigan.

Second-class postage paid at Easton, Pennsylvania. This publication is authorized to be mailed at the special rates of postage prescribed by Section 132.122.

PRINTED IN THE U. S. A.

THE PROCEEDINGS OF THE NATIONAL ACADEMY OF SCIENCES
is published monthly by
THE NATIONAL ACADEMY OF SCIENCES

Proceedings of the

NATIONAL ACADEMY OF SCIENCES

Volume 47 · Number 9 · September 15, 1961

THE KINETICS OF FORMATION OF NATIVE RIBONUCLEASE DURING OXIDATION OF THE REDUCED POLYPEPTIDE CHAIN

By C. B. Anfinsen, E. Haber,* M. Sela,† and F. H. White, Jr.

LABORATORY OF CELLULAR PHYSIOLOGY AND METABOLISM, NATIONAL HEART INSTITUTE, NATIONAL INSTITUTES OF HEALTH

Communicated by John T. Edsall, July 31, 1961

Bovine pancreatic ribonuclease is completely reduced by treatment with mercaptoethanol in 8 *M* urea to yield a randomly coiled polypeptide chain containing eight cysteine residues.[1–3] Under optimal conditions of polypeptide concentration and pH, essentially complete reformation of the disulfide bonds of the native enzyme occurs in the presence of molecular oxygen.[2, 3] From chemical and physical studies of the reformed enzyme, it may be concluded that the information for the correct pairing of half-cystine residues in disulfide linkage, and for the assumption of the native secondary and tertiary structures, is contained in the amino acid sequence itself.

Preliminary to studies on the interactions involved in the refolding process, and to establish the order of chemical events during the formation of active protein, we have followed the rates of disappearance of sulfhydryl groups, and of the appearance of the spectral properties characteristic of the native enzyme and its active derivatives. The appearance of increased positive optical rotation associated with secondary structure was also studied. The results rule out the sequential formation of one active molecule after another. They suggest as a major possibility that some disulfide bonds formed during the early stages of oxidation are not identical with those of the native protein but undergo rearrangement to yield the native configuration.

Materials and Methods.—Bovine pancreatic ribonuclease (RNase) was purchased from the Sigma Chemical Company, St. Louis, Missouri. Test samples of the lot employed in these studies (#R60B-204, "chromatographic grade") were subjected, before use, to chromatography[4] on the cation exchanger, carboxymethylcellulose[5] (Brown Paper Company, Lot 1069; 0.6 meq/gm) and on IRC-50,[6] and were found to consist almost entirely of the major "A" peak with a smaller peak (approximately 5% of the major peak) running in the position of the usual "B" component Amino acid analysis according to the procedure of Spackman, Stein and Moore[7] yielded values in good agreement with those reported for the commercial preparations that have been used for most of the structural studies on this enzyme.

Reduced RNase was prepared by treatment of the native enzyme with mercaptoethanol in 8 *M* urea followed by separation of the reduced chain from reagents on Sephadex-G25 (Pharmacia, Uppsala, Lot 6493) as described earlier.[3]

The procedure employed for oxidation of fully reduced RNase consisted of adjustment of the concentration of the solution of reduced protein in 0.1 *M* acetic acid that emerged from the

Sephadex-G25 columns with water to the desired protein concentration, followed by adjustment to pH 8.2 with tris (hydroxymethyl) aminomethane (tris)-acetate buffer. Three large-scale oxidations were carried out, two at 2.0 mg/ml and one at 0.1 mg/ml. Oxidation in two experiments was allowed to proceed at room temperature (23–24°C) in open beakers without stirring. In a third experiment (at 2.0 mg/ml), slow stirring was employed, without detectable differences in results except for a slight increase in the amount of turbidity produced. The soluble protein concentration, after as long as 24 hr, was still 95% or more of the original concentration. During oxidation, and particularly frequently during the early stages, samples were withdrawn, diluted to the desired concentrations with 0.1*M* acetate buffer, pH 5.0, and assayed[8] for enzyme activity against ribonucleic acid prepared according to Crestfield, Smith, and Allen,[9] and against uridylic-2′,3′-cyclic phosphate (barium salt, Schwarz BioResearch). The latter assays were carried out with the Cary Recording ultraviolet spectrophotometer as previously described.[2, 10] Each analysis was compared with simultaneous controls run on native RNase solutions.

The Cary spectrophotometer was also employed for the serial determination of the absorption spectra of the solutions, with the speed of reading adjusted to yield curves that permitted accurate estimation of the differences in absorbancy at various wavelengths. Protein concentrations were estimated from the same spectra at 275 mμ where RNase and reduced RNase have the same molar extinction ($E = 9{,}200$).

Optical rotatory measurements were made with a Rudolph precision ultraviolet polarimeter, model 80, equipped with the Rudolph photometric polarimeter attachment and an oscillating polarizer prism. The measurements were carried out at a wavelength of 366 mμ, using a mercury lamp as the light source. At this wavelength, the changes in specific optical rotation were sufficiently large to permit reasonable accuracy with 20 cm polarimetric tubes even with relatively dilute solutions of protein (2 mg/ml). The specific optical rotation for native RNase at this wave length was −288°, and for fully reduced RNase, −372°. In one experiment, where oxidation was carried out on a solution of reduced RNase at a concentration of 0.1 mg/ml, samples of the reoxidation mixture were taken at various times, acidified with acetic acid to approximately pH 4, and lyophilized. The resulting material, when dissolved in water at a concentration of 2 mg/ml, gave optical rotations in excellent agreement with corresponding samples taken at similar times of oxidation in other experiments at higher protein concentrations. Most samples taken during the latter stages of oxidation were somewhat turbid and required brief centrifugation at approximately 15,000 *g* before measurement.

The extent of reduction and the kinetics of SH disappearance during oxidation were determined both by titration with *p*-chloromercuribenzoate[11] and by reaction with 1-C_{14}-iodoacetic acid of known specific radioactivity followed by determination of radioactivity on the alkylated protein.[3] Aliquots of the protein solution (approximately 2 mg protein in 1.0 ml were added to 1.0 ml 1.0 *M* tris-acetate buffer, pH 8.5 containing 10 μmoles C_{14} iodoacetic acid (0.2 μcurie) and the alkylation was allowed to proceed for 10 min. After this time, excess iodoacetic acid was immobilized by the addition of an excess (5 μl) of mercaptoethanol. After reaction for 15 min, the alkylated protein was separated from the various reagents by passage of the sample through a (1 × 40) cm column of Sephadex G25 in 0.1 *M* acetic acid, and the radioactivity was subsequently counted in the Packard Scintillation counter in the presence of a water-miscible phosphor.[12] Protein concentration in the samples counted was calculated from absorbancy measurements at 275 mμ.

Results.—The data in Figure 1 summarize the changes in the sulfhydryl group content, specific optical rotation and enzyme activity during oxidation of the SH groups of fully reduced RNase under the conditions presented in the experimental section. Final values obtained, expressed as percentages of the differences between fully reduced RNase and native RNase, are shown at the right of the figure. These values indicate essentially complete restoration of the native properties. A final value for the activity of the oxidation mixture toward the synthetic substrate is not given since this value was quite variable (generally 60–70% of the native level) due, possibly, to inhibition by components of the solution. This possibility has not been investigated as part of the present study. It has been found, however,

that on chromatography of samples of reformed RNase, the major component is identical to that present in commercial samples of the enzyme and possesses completely normal activity toward both RNA and synthetic substrates.[2]

The most striking phenomenon observed in these studies is the marked lag phase before enzymatic activity appears, during which period the sulfhydryl titer and the specific optical rotation change along a curve similar to that of a first-order reaction. The presence of this lag phase (various explanations for which are offered in the discussion) immediately rules out the possibility that disulfide bonds are formed in such a way that detectable amounts of complete, native molecules are produced in a one-by-one fashion.

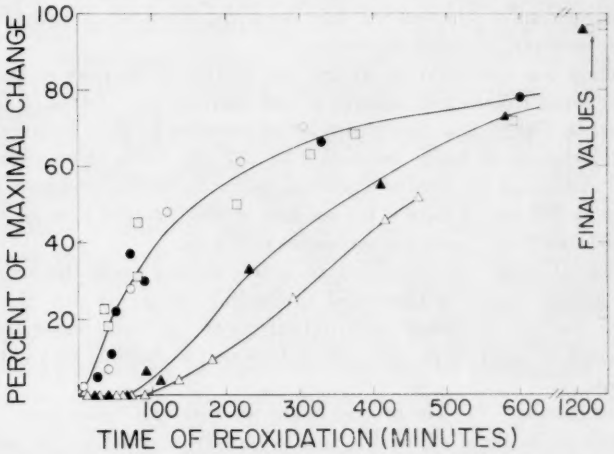

FIG. 1.—Changes, during the oxidation of reduced ribonuclease, in SH groups as followed by titration with *p*-chloromercuribenzoate (●) and by reaction with radioactive iodoacetate (○), in optical rotation (□), and in enzymatic activity as measured against ribonucleic acid (▲) and against uridylic-2′,3′-cyclic phosphate (△).

Changes in spectral properties during oxidation (from one typical experiment) are summarized in Table 1 and conform, in general, to earlier observations on the relationship between activity and spectral properties. Native RNase shows an absorption maximum at 277.5 mμ, which is also shown by such active derivatives[13, 14] as RNase-S, carboxypeptidase-treated RNase and RNase which has been modified by addition of polyalanine side chains of considerable length on available amino groups.[15] On the other hand, inactive derivatives still possessing intact SS bonds (pepsin-inactivated RNase, methylated RNase, etc.) have shown a maximum at 276 mμ.[13, 14] Both oxidized and reduced RNase show still another absorption maximum, at 275 mμ, which appears to be characteristic of the chain devoid of disulfide cross-links.

In the present studies (see Table 1) the position of the maximum changes from 275 mμ to 276 mμ during the lag period prior to the appearance of enzyme activity, and then increases roughly in parallel with the appearance of enzyme activity to a

TABLE 1

SPECTRAL CHANGES

Time, min	Wavelength of maximum absorption, mμ	Molar extinction, E_{287} mμ
0	275.0	3600
72	275.4	4600
177	276.2	5080
296	276.2	5470
453	276.4	5900
800	276.8	5700
Native RNase	277.5	6360

final value of 277.5 mμ. The presence of a maximum at 276 mμ is, incidentally, also characteristic of the randomly cross-linked derivative obtained during oxidation in urea, guanidine, and other disorienting reagents[15] and may be characteristic of tyrosine interactions of a nonspecific sort, occurring when the *specific* interaction of the phenolic hydroxyl groups is prevented.

The reaction was also followed at 287 mμ, as this is the peak of the difference spectrum between RNase and inactive RNase derivatives. Although the data are not included in Figure 1, a direct correlation becomes evident between change in activity and change in molar extinction at 287 mμ when these parameters are plotted as functions of the time of oxidation, assuming as final and initial values the absorptions at 287 mμ of native RNase and of the inactive form of the enzyme with "shifted spectrum," having a maximum at 276 mμ.

Discussion.—During the formation of native RNase from the reduced chain, sulfhydryl groups might be converted to disulfide bonds by one of two general mechanisms, the first involving the initial pairing of the *correct* half-cystine residues and the second, of random pairing with subsequent reshuffling to yield the native arrangement.

A. *Correct pairing:* (1) The process might proceed by a *"one-by-one" mechanism* in which each molecule of reduced RNase is rapidly oxidized to the native, active form without the accumulation of significant quantities of partial oxidation products. The formation of the first bond would, in this system, greatly increase the likelihood that a *second* bond would form in the same molecule over the probability that a *first* bond would form in another molecule. (2) The rates of formation of successive disulfide bonds might be sufficiently different that, at any time, the population of molecules would be *predominantly of one kind;* e.g., one SS bond with six SH groups, two SS bonds with four SH groups, etc. Although the correct pairing of SH groups is assumed in this mechanism, enzyme activity would first appear only after the formation of the final, fourth, bond (if all four are indeed essential). (3) A variation of mechanism No. 2 would involve rates of oxidation of the four pairs of SH groups that are *essentially the same.* This variation would lead to the formation of a mixture of partially oxidized molecules; *activity* would appear upon oxidation of the *fourth* pair or possibly earlier, should some molecules having only two or three disulfide bonds possess activity. (4) A situation might be visualized in which the *correct* arrangement of disulfide bonds has been formed but where the resulting molecules are inactive because of *incorrect secondary and tertiary structure.* The appearance of enzyme activity and "native" spectral properties would result from the rearrangement of noncovalent interactions to yield the native form.

B. *Random pairing:* Pairing might be random in the initial stages of reaction and activity might first appear after reshuffling, through disulfide interchange, to yield the native configuration.

The results presented in this paper make it possible to rule out mechanism *A*1 since only traces of enzyme activity and of the native spectral characteristics have appeared even after the disappearance of approximately half of the total SH group content of the reduced protein. Alternatives *A*2 and *A*3 are somewhat more difficult to rule out, particularly without a careful examination of the chemical nature of the disulfide bridges that have formed at various times by techniques similar to those used in establishing the disulfide bridges of the native enzyme.[16] However, on a purely kinetic basis, these mechanisms seem unlikely since, when three-fourths of the SH groups have disappeared, enzyme activity has risen to more than half of the theoretical value. Mechanisms *A*2 and *A*3 would require that no activity appear before three of the four final SS bonds were complete in all the molecules present (unless partially oxidized molecules with only three SS bonds reformed possess some activity).

Mechanism *A*4 permits a lag in the appearance of activity even if the conditions of mechanism *A*1 obtain. Nevertheless, this mechanism is somewhat improbable on the basis of the known characteristics of rearrangement of the secondary and tertiary structures of native RNase after distortion in solutions of 8 *M* urea. It has been shown, for example, that the modifications in spectral and optical rotatory properties of RNase occurring in urea solutions are entirely reversible upon dilution to lower urea concentrations or upon dialysis.[14, 17] Further, the time required for reversal is relatively short, and certainly only a small fraction of the time involved in the 1–2-hour lag period found in the present experiments. The rapid refolding of the urea-distorted configuration of native RNase by polyanions[13] (presumably including ribonucleic acid itself) yields an active enzyme, also militates against aberrant three dimensional structure as a major reason for the existence of a lag phase in activity in the present experiments on the reformation of SS bonds.

Mechanism *B* is consistent with the kinetic data presented here and becomes even more probable when other available information is taken into account. As mentioned above, oxidation of the SH groups of reduced RNase may be carried out in the presence of various agents that cause the formation of enzymatically inactive molecules, for which the typical spectrum of RNase, with a maximum at 277.5 mμ, is not obtained. When such randomly cross-linked molecules are incubated under the conditions employed for oxidations as described in the present paper, no detectable changes occur. However, the addition of SH compounds (including reduced RNase) under conditions known to favor disulfide interchange,[18] induces the rearrangement of the molecule to yield an active product in high yield, possessing the physical properties of native RNase.[19] The requirement for SH catalysis supports the idea that the inactive materials are inactive because of random pairing of half-cystine residues and that, in the case of the lag in appearance of enzyme activity in the present experiments, a similar situation obtains.

It is tentatively concluded, therefore, that oxidation of SH groups in this system occurs initially through relatively random formation of SS bonds with subsequent rearrangement taking place under the influence of disulfide interchange driven by

thermodynamic forces toward the most probable form, native ribonuclease. Some of the less likely possibilities mentioned above can only be rigorously excluded upon completion of current experiments on the nature of the pairing of half-cystine residues during the lag phase.

The authors wish to thank Mrs. Juanita Cooke for her expert assistance in many of these experiments.

* Present address: Massachusetts General Hospital, Boston 14, Massachusetts.

† On leave of absence from The Weizmann Institute of Science, Rehovoth, Israel.

[1] Sela, M., F. H. White, Jr., and C. B. Anfinsen, *Biochim. et Biophys. Acta*, **31**, 417 (1959).

[2] White, F. H., Jr., *J. Biol. Chem.*, **236**, 1353 (1961).

[3] Anfinsen, C. B., and E. Haber, *ibid.*, **236**, 1361 (1961).

[4] Aqvist, S. E. G., and C. B. Anfinsen, *ibid.*, **234**, 1112 (1959).

[5] Peterson, E. A., and H. A. Sober, *J. Am. Chem. Soc.*, **78**, 751 (1956).

[6] Hirs, C. H. W., S. Moore, and W. H. Stein, *J. Biol. Chem.*, **200**, 493 (1953).

[7] Spackman, D. H., W. H. Stein, and S. Moore, *Anal. Chem.*, **30**, 1190 (1958).

[8] Anfinsen, C. B., R. R. Redfield, W. L. Choate, J. Page, and W. R. Carroll, *J. Biol. Chem.*, **207**, 201 (1954).

[9] Crestfield, A. M., Smith, K. C., and F. W. Allen, *ibid.*, **216**, 185 (1956).

[10] Richards, F. M., *Compt. rend. trav. lab. Carlsberg, Ser. Chim.*, **29**, 315 (1955).

[11] Boyer, P. D., *J. Am. Chem. Soc.*, **76**, 4331 (1954).

[12] Bray, G. A., *Anal. Biochem.*, **1**, 279 (1960).

[13] Sela, M., and C. B. Anfinsen, *Biochim. et Biophys. Acta*, **24**, 229 (1957).

[14] Sela, M., C. B. Anfinsen, and W. F. Harrington, *ibid.*, **26**, 502 (1957).

[15] Haber, E., M. Sela, and C. B. Anfinsen, *Federation Proc.*, **20**, Part I, 217 (1961).

[16] Experimental work is now in progress to determine the nature of the pairing of half-cystine residues at various times during the early stages of reoxidation. Preliminary results indicate that pairing is quite random and that "incorrectly" formed bonds are present.

[17] Harrington, W. F., and J. A. Schellman, *Compt. rend. trav. lab. Carlsberg, Ser. Chim.*, **30**, 21 (1956).

[18] Sluyterman, L. A. A., *Biochim. et Biophys. Acta*, **48**, 429 (1961).

[19] Haber, E., and C. B. Anfinsen, unpublished data.

---

*PHOTOSYNTHETIC PHOSPHORYLATION AND MOLECULAR OXYGEN**

BY DANIEL I. ARNON,† M. LOSADA, F. R. WHATLEY, H. Y. TSUJIMOTO, D. O. HALL, AND A. A. HORTON

DEPARTMENT OF CELL PHYSIOLOGY, UNIVERSITY OF CALIFORNIA, BERKELEY

Communicated July 3, 1961

Oxygen and photosynthesis were first linked about 200 years ago when both were discovered almost simultaneously. The earliest concept of photosynthesis was that of planetary ventilation in which illuminated plants exchanged CO_2 or "bad air" for O_2 or "vital air" (see historical review[1]). A mechanism for this gas exchange was proposed in 1796 by Ingenhousz.[2] Green plants, he suggested, absorb from "carbonic acid in the sunshine, the carbon, throwing out at that time the oxygen alone, and keeping the carbon to itself as nourishment." [2]

For over a hundred years afterward, the view that CO_2 assimilation always involved a liberation of oxygen gas was so firmly entrenched that it was even extended to the dark CO_2 assimilation by chemosynthetic bacteria.[3–5] The idea

of photosynthesis without oxygen evolution seemed a contradiction of terms until the conclusive work of van Niel[6, 7] with photosynthetic bacteria firmly established that, basically, the assimilation of CO_2 at the expense of light energy does not depend on the liberation of oxygen or on the presence of oxygen. Bacterial photosynthesis occurs under strictly anaerobic conditions and includes organisms that are obligate anaerobes (for example, *Chlorobium* and *Chromatium*[6, 7]).

Although molecular oxygen was shown to be unnecessary and often even detrimental to bacterial photosynthesis, its role in the energy transformations that occur during photosynthesis in green plants has gained more attention with time. In 1939, Hill postulated[8] that the consumption of molecular oxygen is necessary for photosynthesis of green plants in order to supply additional energy for CO_2 assimilation. He envisaged "first a reduction of a substance by chloroplasts giving oxygen and then a reoxidation of the reduced substances by part of the oxygen together with a simultaneous reduction of the necessary equivalent of carbon dioxide." [9] In 1951 Burk and Warburg[10] reported the separation of photosynthesis into a light reaction and a dark reaction on the basis of manometric measurements with intact *Chlorella* cells. In the words of Warburg, "in the light reaction, one molecule of O_2 will develop per molecule of chlorophyll . . . whereas during the dark period following the end of illumination it can be observed manometrically . . . that two-thirds of the oxygen gas developed during the light period undergoes a back reaction." [11] This dark consumption of oxygen is, in Warburg and Burk's view, a photosynthetically induced respiration that supplies two-thirds of the needed energy and is, therefore, indispensable for CO_2 assimilation in photosynthesis. As summed up recently by Warburg, "Keine (CO_2) Fixierung ohne Atmung." [12]

A biochemical model for oxygen consumption in photosynthesis in accordance with the views of Hill and Warburg was proposed by Vishniac and Ochoa.[13] They suggested that the ATP used for CO_2 assimilation in photosynthesis is formed by a collaboration between chloroplasts and mitochondria. In their model, chloroplasts reduced pyridine nucleotide in light and ATP was formed when mitochondria reoxidized the reduced pyridine nucleotide with molecular oxygen, by the dark process of oxidative phosphorylation. A similar model for ATP formation has been used in several general schemes of photosynthesis, as, for example, in the one proposed in 1951 by Holzer[14] and in 1954 by Calvin's group (ref. 15, Fig. 7). In all these schemes, oxidative phosphorylation by mitochondria, and hence oxygen consumption, was an essential feature of the mechanism of photosynthesis.

A mechanism of photosynthesis that includes a consumption of molecular oxygen cannot apply to the strictly anaerobic bacterial photosynthesis and leads, therefore, to the inference that the mechanism of energy conversion in bacterial photosynthesis is basically different from that in plant photosynthesis. However, the discovery of photosynthetic phosphorylation in isolated spinach chloroplasts[16] and, shortly thereafter, in cell-free preparations of *Rhodospirillum rubrum*,[17] has pointed to mechanisms for ATP formation at the expense of light energy that are common to green plants and photosynthetic bacteria. A unified concept of photosynthesis in plants and bacteria, based on photosynthetic phosphorylation as the common denominator is now possible and has been presented elsewhere.[18–20]

A key premise in this concept is that, in green plants as in bacteria, photosynthetic phosphorylation is fundamentally independent of molecular oxygen. Since this

has recently been questioned[12, 21] we have re-examined the relation of oxygen to photosynthetic phosphorylation. The purpose of this article is to bring together and add to the evidence which confirms and extends our earlier conclusions that photosynthetic phosphorylation, both in green plants and photosynthetic bacteria, is basically independent of molecular oxygen and hence of respiration.

Cyclic and Noncyclic Photophosphorylation.—Photosynthetic phosphorylation (photophosphorylation) is a term coined in 1954 to describe a light-induced ATP formation by isolated chloroplasts, without the aid of mitochondria and without the consumption of oxygen.[16] The over-all reaction of photosynthetic phosphorylation is represented by equation (1):

$$\mathrm{ADP} + \mathrm{P} \xrightarrow{\text{light}} \mathrm{ATP} \qquad (1)$$

Reaction 1, in which the sole product is ATP, was subsequently designated cyclic photophosphorylation, to distinguish it from a second photophosphorylation reaction by isolated chloroplasts (equation (2)) which was found a few years later[22] and named noncyclic photophosphorylation.[18]

$$\mathrm{TPN} + 2\mathrm{H}^+ + \mathrm{ADP} + \mathrm{P} + 2\mathrm{OH}^- \xrightarrow{\text{light}} \mathrm{TPNH_2} + \mathrm{ATP} + \mathrm{H_2O} + {}^1/_2\mathrm{O_2} \qquad (2)$$

The terms "cyclic" and "noncyclic" refer to the electron flow mechanisms which have been proposed[18, 19] for these two reactions that now jointly constitute the process of photosynthetic phosphorylation. In cyclic photophosphorylation all of the biochemically effective light energy is used for ATP formation. In noncyclic photophosphorylation only a portion of the biochemically effective light energy is used for the formation of ATP; the remainder is used for the formation of a reductant, $\mathrm{TPNH_2}$, and the excretion (evolution) of oxygen. A nonphysiological variant of noncyclic photophosphorylation (reaction 2) is reaction 3, in which TPN is replaced by ferricyanide[22, 23] (represented here by Fe^{3+}).

$$2\mathrm{Fe}^{3+} + \mathrm{ADP} + \mathrm{P} + 2\mathrm{OH}^- \xrightarrow{\text{light}} 2\mathrm{Fe}^{2+} + \mathrm{ATP} + \mathrm{H_2O} + {}^1/_2\mathrm{O_2} \qquad (3)$$

The significance of cyclic and noncyclic photophosphorylation to the over-all mechanism of photosynthesis in green plants is that they supply—aside from oxygen as the excreted by-product—the two products, ATP and $\mathrm{TPNH_2}$, which alone suffice for converting $\mathrm{CO_2}$ into carbohydrates in the dark.[24, 25] Both ATP and $\mathrm{TPNH_2}$ (also oxygen) are formed by noncyclic photophosphorylation (equation (2)) but cyclic photophosphorylation (equation (1)), which supplies only ATP, is also needed for $\mathrm{CO_2}$ assimilation because the ATP formed in noncyclic photophosphorylation is insufficient to convert $\mathrm{CO_2}$ to carbohydrate.[26]

Chloroplast fragments ("grana") do not respire[27, 28] and hence, according to Warburg, would not be expected to fix $\mathrm{CO_2}$ ("Grana atmen *nicht* und fixierien *nicht*" [12]). However, by fractionating isolated chloroplasts we have shown that grana fail to assimilate $\mathrm{CO_2}$ not because they are unable to respire but because they lack the requisite chloroplast enzymes. These are water-soluble and are readily leached out in the preparation of "grana."[29] The soluble chloroplast enzymes, either *in situ* or when extracted from chloroplasts, assimilate $\mathrm{CO_2}$ to the level of carbohydrates and do so solely[24] at the expense of ATP and $\mathrm{TPNH_2}$—

the two compounds formed in chloroplasts by cyclic and noncyclic photophosphorylation (equations (1) and (2)) and not by respiration.

CO_2 assimilation proper in photosynthesis, whether in whole cells[30] or in isolated chloroplasts,[24, 25] consists of the same exclusively dark, enzymatic reactions[31] that are now known to operate in nonphotosynthetic cells.[32-34] There is, so far as we know, no valid experimental basis, for postulating in photosynthesis a peculiar photochemically produced "reducing power" that is capable of direct reduction of CO_2 to the level of carbohydrate by some special mechanism unknown elsewhere in biochemistry (see, for example, ref. 35 and 36). If we abandon the notion of an unspecified, hypothetical "reducing power" and interpret photosynthesis in terms of known biochemical mechanisms, then the unique feature of photosynthesis as a biological process is not CO_2 assimilation—a dark process driven, in both photosynthetic and nonphotosynthetic cells, by ATP and reduced pyridine nucleotide—but the formation of these two compounds by cyclic and noncyclic photophosphorylation.

The discovery of photosynthetic phosphorylation was part of a coincident, broader finding[16, 27] that isolated chloroplasts are capable of carrying out a complete extracellular photosynthesis, i.e., a conversion of CO_2 to starch and sugar, at physiological temperatures and with no energy supply except visible light. The view that chloroplasts are the sites of complete photosynthesis was once widely held without the support of critical experimental evidence and was later abandoned because of evidence to the contrary, only to be formulated anew on the basis of improved methods for isolating functional chloroplasts from leaves (see review[1]).

The discovery of cyclic and noncyclic photophosphorylation by isolated chloroplasts (also of CO_2 assimilation, see review[1]) was confirmed and extended in other laboratories, notably those of Jagendorf,[37-40] Wessels,[41, 42] Vennesland,[43, 44] and Hill.[45] Most of the work has been done with spinach chloroplasts but recently Whatley *et al.*[46] have also demonstrated cyclic and noncyclic photophosphorylation (and CO_2 assimilation) in chloroplasts isolated from several other species of plants.[47]

Of the two photophosphorylation reactions (equations (1) and (2)), the cyclic type (equation (1)) appeared the more basic from the standpoint of a general mechanism of energy transformation in photosynthesis since this reaction was found in representatives of all the different groups of photosynthetic organisms. Williams[50] found photosynthetic phosphorylation in the obligately anaerobic photosynthetic bacteria, *Chromatium* and *Chlorobium*. Cyclic photophosphorylation in algal preparations was found by Thomas and Haans[51] and Petrack and Lipmann.[52] (For a more complete review of literature see ref. 53.)

Special Features of Cyclic and Noncyclic Photophosphorylation.—The unique features of cyclic photophosphorylation are that ATP is formed with no added electron donor and no added electron acceptor. Cyclic photophosphorylation consumes neither respiratory substrate nor molecular oxygen. Both are replaced by light[53] which provides the free energy required for the synthesis of pyrophosphate bonds of ATP. This seemed at first not to be the case in photosynthetic bacteria. Frenkel's cell-free preparations of *R. rubrum* became substrate-dependent after washing; the rate of phosphorylation was doubled on adding α-ketoglutarate.[17] But in subsequent experiments Frenkel[54] ruled out the dependence on an added chemical substrate and once this fundamental point was clarified, the equivalence

of cyclic photophosphorylation in chloroplasts and bacterial particles seemed probable.[55]

The independence of photosynthetic phosphorylation from a respiratory substrate is confirmed by the independence of this process from CO_2 assimilation. Photosynthetic phosphorylation occurs when the enzymes of the reductive carbon cycle are removed by washing the chloroplasts, CO_2 is not supplied to the reaction mixture, and the reaction vessels contain KOH in the center well. This would not exclude a possible *catalytic* participation of CO_2 in photophosphorylation (cf. Warburg *et al.*[12] and Vennesland *et al.*[56]). What can be definitely excluded is that substrate amounts of carbon compound(s) are first synthesized in light from CO_2 and are then used as electron donors for the formation of ATP.

While cyclic photophosphorylation was recognized as a common denominator of all photosyntheses, noncyclic photophosphorylation as represented by equation (2)—a reaction that liberates oxygen—seemed at first destined to remain a special feature of plant photosynthesis, since oxygen is not evolved in bacterial photosynthesis. However, Losada *et al.*[57] (cf. also Duysens *et al.*[58]) have recently separated reaction 2 into two distinct photochemical reactions (*a*) a photooxidation of hydroxyl ions that yields oxygen (equation (4)) and (*b*) a photophosphorylation reaction proper in which the photoreduction of triphosphopyridine nucleotide is coupled with the formation of adenosine triphosphate (equation 5).

$$2A + 2OH^- \xrightarrow{\text{light}} 2A^- + H_2O + {}^1/_2O_2 \qquad (4)$$

$$TPN + 2H^+ + ADP + P + 2A^- \xrightarrow{\text{light}} TPNH_2 + ATP + 2A \qquad (5)$$

$$\text{Sum: } TPN + 2H^+ + ADP + P + 2OH^- \xrightarrow{\text{light}} TPNH_2 + ATP + H_2O + {}^1/_2O_2 \qquad (2)$$

Only the photooxidation of hydroxyl ions (equation (4)) is peculiar to green plants since only green plants seem capable of using OH^- as an electron donor with the resultant excretion of molecular oxygen. Reaction 5, the noncyclic photophosphorylation reaction proper, occurs also in photosynthetic bacteria.[59] Since they use inorganic or organic electron donors, such as thiosulfate or succinate instead of OH^-, oxygen evolution does not occur in the reaction.

Figure 1 depicts the over-all scheme for noncyclic photophosphorylation in green plants that we now envisage. The intermediate *A* in Figure 1 is both the electron acceptor for the first light reaction and the electron donor for the second light reaction (cf. equations (4) and (5)). We have used indophenol dyes as an experimental device to separate the two photochemical reactions. The natural intermediates with which the dyes have interacted have not been identified. They may include cytochrome components[60] or a quinone.[61, 62] The terminal physiological electron acceptor in noncyclic photophosphorylation (B in Fig. 1) is pyridine nucleotide.

Our original scheme for noncyclic photophosphorylation (ref. 22, Fig. 3) envisaged the phosphorylation step as occurring between the unknown reductant (H), formed by the photolysis of water and TPN, whereas our present scheme, based on the electron flow theory,[18, 53] links the phosphorylation step with the oxidation of cytochrome by photoactivated chlorophyll.

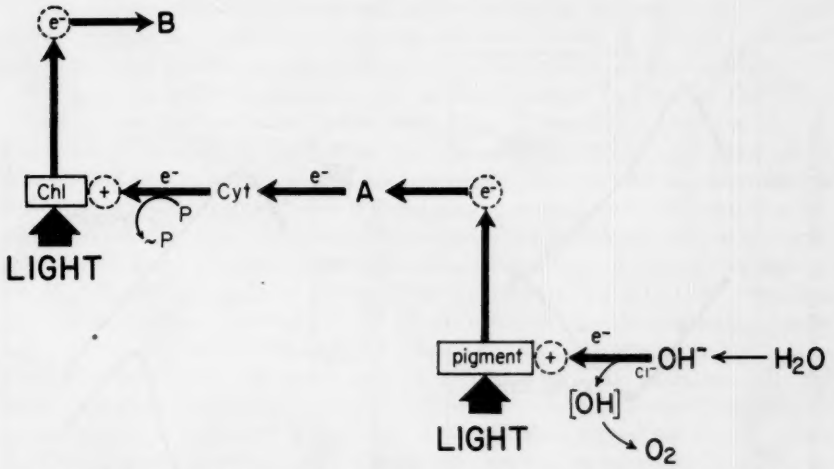

FIG. 1.—*Scheme for noncyclic photophosphorylation of the green plant type.* In the first light reaction, the pigment molecule (see text) becomes excited by the absorption of a quantum of light. The excited pigment donates its high-energy electron (e^-) to an intermediate electron acceptor (A) and accepts an electron from an hydroxyl ion. The oxidation product (OH) of the hydroxyl ion is the precursor of molecular oxygen. In the second light reaction, the chlorophyll molecule (Chl), excited by the absorption of a quantum of light, donates its high-energy electron (e^-) to the terminal electron acceptor (B) and accepts, via the cytochrome system (Cyt), an electron from the reduced intermediate (A^-) formed in the first light reaction. The phosphorylation step is linked with the transfer of the electron from cytochrome to chlorophyll.

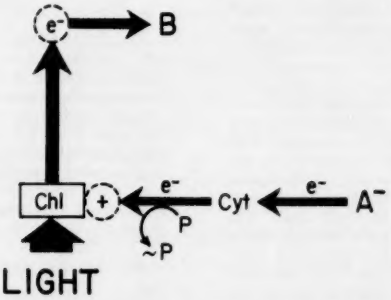

FIG. 2.—*Scheme for noncyclic photophosphorylation of the bacterial type.* The chlorophyll molecule (Chl) becomes excited by the absorption of a quantum of light. The excited chlorophyll donates its high energy electron (e^-) to the electron acceptor (B) and accepts, via the cytochrome system (Cyt), an electron from an external electron donor (A^-). The phosphorylation step is linked with the transfer of the electron from cytochrome to chlorophyll.

TPN reduction in noncyclic photophosphorylation (reaction 2), although normally coupled with, may also be uncoupled from, ATP formation. Trebst *et al.* (ref. 63, Table 1) have shown that ammonia[64] suppresses almost completely the formation of ATP in reaction 2 in light without inhibiting the formation of $TPNH_2$. These results speak against the suggestion of Chance and Olson[65] that the photoreduction of TPN may be driven by ATP, formed perhaps by cyclic photophosphorylation (cf. also Marrè and Forti[66]). The contrary is, in fact, the case. Elec-

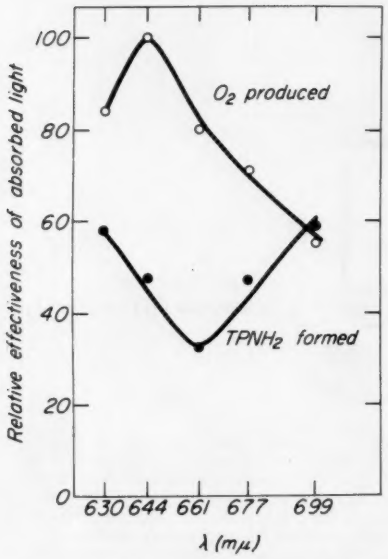

FIG. 3.—*Effectiveness of monochromatic light, in the red region of the spectrum, on oxygen evolution and TPN reduction, occurring as separate chloroplast reactions.*[57] Oxygen was measured manometrically when the photochemical reaction was limited to the photooxidation of OH^- (equation (4)) in a reaction mixture which included, in a final volume of 3 ml, chloroplast fragments (C_{1a}) containing 1 mg. of chlorophyll and the following in μmoles: tris/acetate buffer, pH 8, 40; potassium ferricyanide, 15; and 2, 6 - dichlorophenol indophenol (DCPIP), 0.2. TPN reduction (measured spectrophotometrically at 340 mμ) was carried out in a parallel experiment in which the photooxidation of water was blocked by the omission of chloride and the addition of 2×10^{-5} *M* CMU. The electron donor system for TPN reduction consisted of 20 μmoles ascorbate and 0.05 μmoles of 2,3′,6-trichlorophenol indophenol (equation (5)). The reactions were run for 15 min at 15°C. Gas phase, nitrogen.

100 on the ordinate scale is equivalent to 0.15 μatoms oxygen evolved per μmole quanta of light absorbed. 58 on the ordinate scale is equivalent to 0.09 μmoles $TPNH_2$ formed per μmole quanta of light absorbed.

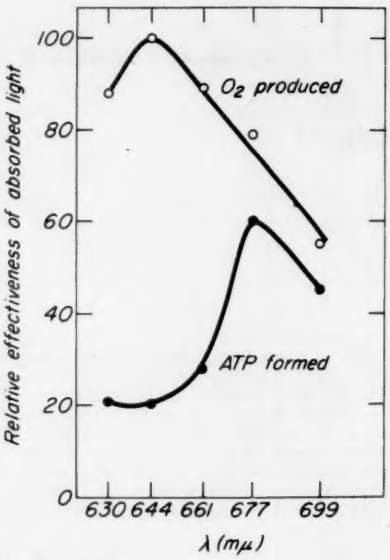

FIG. 4.—*Effectiveness of monochromatic light, in the red region of the spectrum, on oxygen evolution and cyclic photophosphorylation, occurring as separate chloroplast reactions.*[57] Oxygen evolution was measured as described in Figure 3. ATP formation by cyclic photophosphorylation (equation (1)) was measured in a parallel experiment in a reaction mixture which included, in a final volume of 3 ml, chloroplast fragments (C_{1a}) containing 1 mg chlorophyll and the following in μmoles: tris/HCl buffer, pH 8.3, 80; $MgSO_4$, 5; ADP, 10; $K_2HP^{32}O_4$, 10; and vitamin K_3 (menadione), 0.3.

100 on the ordinate scale is equivalent to 0.16 μatoms oxygen evolved per μmole quanta of light absorbed. 60 on the ordinate scale is equivalent to 0.10 μmole ATP formed per μmole quanta of light absorbed.

tron transport, resulting in TPN reduction, may proceed without ATP formation, but no photophosphorylation can occur unless it is coupled with electron transport.

Experimentally, it is possible to convert noncyclic photophosphorylation in chloroplasts (equation (2) and Fig. 1) to a "bacterial" type (equation (5) and Fig.

2) by replacing OH^- with an exogenous electron donor at the level of A^-. Reduction of pyridine nucleotide is then coupled with the oxidation of the exogenous electron donor and a simultaneous ATP formation but *without* oxygen evolution.[57]

We have not definitely identified the "pigment" shown in Figure 1 that is involved in the photooxidation of hydroxyl ions. Recent experiments on the effectiveness of monochromatic light on the photochemical reactions of chloroplasts suggest that this may be a special photosynthetic pigment such as chlorophyll *b* or another accessory pigment that is found only in oxygen-evolving organisms, i.e. higher plants and algae, rather than chlorophyll *a* (or the closely related bacteriochlorophyll) found in all photosynthetic cells. (See review of related literature in ref. 57.) In the red region of the spectrum the photooxidation of OH^- (equation (4)) was most effective around 644 mμ, which corresponds to the maximum absorption peak[67] in the red for chlorophyll *b* (Figs. 3 and 4). The effectiveness of monochromatic light in the red region on photoreduction of TPN (equation (5)) and cyclic photophosphorylation (equation (1)) was distinctly different from that on oxygen evolution (equation (4) and Figs. 3 and 4), thus supporting the view that these are different light reactions. The experiments with monochromatic light favor the conclusion that the photochemical reaction which produces oxygen is different from the other photochemical reactions which produce ATP and reduced pyridine nucleotide. The relation of oxygen produced to ATP formation in noncyclic photophosphorylation will now be examined in more detail.

Oxygen as an Excreted By-Product of Noncyclic Photophosphorylation.—The essence of noncyclic photophosphorylation, both in plants and in photosynthetic bacteria, appears to be the formation of ATP which is coupled with an electron transport from an external electron donor to pyridine nucleotide acting as the electron acceptor. As already mentioned, in plants, as in photosynthetic bacteria, oxygen is *not consumed* in these essential aspects of noncyclic photophosphorylation. Oxygen may be *liberated* in this process but only in the specific instance, that is characteristic of plant but not of bacterial photosynthesis, when OH^- is the external electron donor.

This concept is supported by the experimental findings that ATP formation greatly *increases* the rate of oxygen evolution and the concomitant reduction of the electron acceptor, whether it is ferricyanide or TPN[22, 23, 39, 68, 69] (equations (2) and (3)). These results run counter to Hill's original hypothesis that in chloroplasts "the reduced product formed in the light might be reoxidized by molecular oxygen to give a phosphorylating system similar to that in chemosynthetic bacteria."[45] As Hill and Bonner have recently pointed out, "In such a hypothesis one would expect that addition of inorganic phosphate and ADP to the system would result in *decreased* rates of (H) acceptor reduction and of oxygen production"[60] (italics ours).

Hill has accepted the new experimental findings and concluded that "the above... hypothesis has to be abandoned."[60] Warburg,[12] however, has retained the hypothesis of oxygen consumption in energy transformations in photosynthesis and questioned the new experimental facts. Specifically, Warburg *et al.*[12] found that with naphthoquinone sulfonate as the hydrogen acceptor, the stoichiometry of oxygen evolution by chloroplasts is not affected by phosphorylation. Warburg *et al.*[12] suggested that the increase in photoproduction of oxygen as a consequence of

photophosphorylation—first observed by other investigators[22, 68] with ferricyanide (equation (3))—was the result of an uncontrolled change in acidity.

Since the increased production of oxygen that accompanied photophosphorylation in the ferricyanide system was found in solutions that were strongly buffered with tris (hydroxymethyl) aminomethane buffer,[23] it seemed unlikely that the observed effect was the result of uncontrolled pH changes as suggested by Warburg *et al.*[12] Moreover, Davenport[69] has recently found that the rate of photoreduction of TPN, the physiological hydrogen acceptor in noncyclic photophosphorylation (equation (2)), was also greatly increased at two different pH's when a phosphate-accepting system was present.

We have now reinvestigated the effect of photophosphorylation on oxygen evolution by isolated chloroplasts at different hydrogen ion concentrations, using either TPN or ferricyanide as electron acceptors. The pH value of each reaction mixture was checked at the end of the experiment. The results are shown in Figures 5 and 6. With either TPN or ferricyanide as the electron acceptor, we observed a signifi-

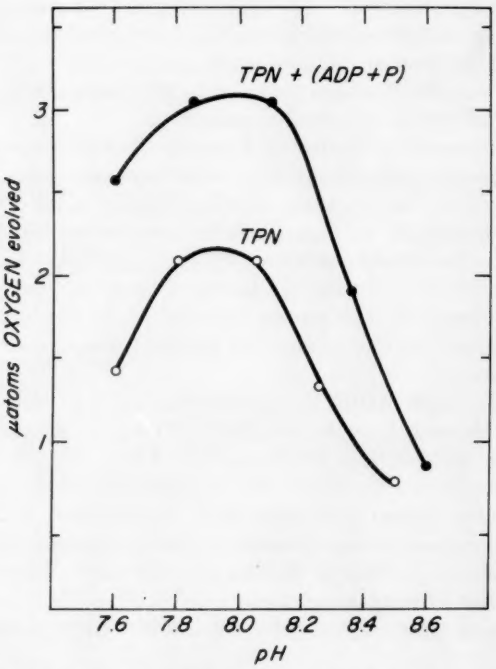

FIG. 5.—*Effect of photophosphorylation at various pH values on oxygen evolution accompanying TPN reduction.* The reaction was carried out in Warburg manometer vessels at 15°C. Illumination, 25,000 Lux for 6 min.; gas phase, nitrogen. In all vessels the reaction mixture contained, in a final volume of 3 ml, 200 μmoles tris-HCl buffer, 4 μmoles TPN, purified TPN-reductase from spinach, and broken chloroplasts (P_{1s}) containing 0.2 mg chlorophyll. To the phosphorylating series [TPN plus (ADP plus P)] were added 10 μmoles $MgSO_4$, 10 μmoles potassium phosphate and 10 μmoles ADP. Tris buffer, potassium phosphate, and ADP were each adjusted to the selected pH; the TPN was adjusted to pH 7.5. The pH shift, as determined at the end of the reaction, was found not to exceed 0.1 unit.

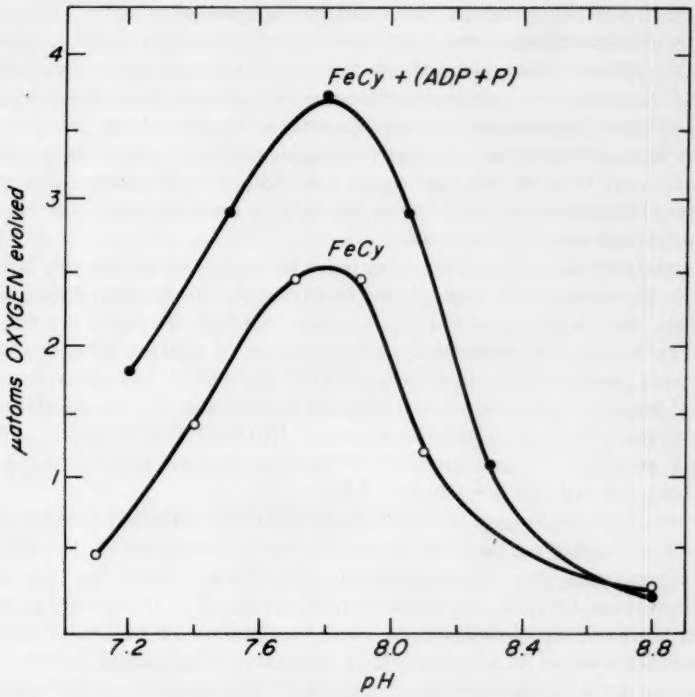

FIG. 6.—*Effect of photophosphorylation at various pH values on oxygen evolution accompanying ferricyanide (FeCy) reduction.* Experimental conditions as described for Figure 5 except that TPN and TPN reductase were omitted and 15 μmoles $K_3Fe(CN)_6$ were added to each vessel.

cantly higher photoproduction of oxygen by isolated chloroplasts when the reaction was coupled with ATP formation. The increase in oxygen evolution occurred over a wide range of pH (cf. Avron *et al.*[68]).

These results confirm and extend those reported earlier[22, 23] and are in harmony with the view that oxygen is an excreted by-product of electron transfer in noncyclic photophosphorylation incidental to the use of OH^- as the electron donor. The electron transfer is more rapid when it is coupled with ATP formation and since OH^- is the electron donor, (compare the anode reaction in the electrolysis of water), more oxygen will be produced per unit of time when ATP is formed simultaneously.

To recapitulate, oxygen is not essential to the two main events of noncyclic photophosphorylation in plants and bacteria: the photoreduction of pyridine nucleotide and the coupled formation of ATP. In fact, oxygen gas is an excreted by-product of photosynthesis in green plants, although not in photosynthetic bacteria, because only green plants can use hydroxyl ions as the electron donor in noncyclic photophosphorylation. When other electron donors are substituted, noncyclic photophosphorylation in green plants resembles that in photosynthetic bacteria: it proceeds without oxygen evolution.[57]

Oxygen as an Electron Acceptor in Noncyclic Photophosphorylation.—When photosynthetic phosphorylation was first discovered it proceeded at a sustained rate only in the presence of oxygen (ref. 16, Fig. 2b). However, since there was no net evolution (as measured by manometric pressure change) of molecular oxygen, we concluded then[16] that oxygen acted as a catalyst in photosynthetic phosphorylation and not as a substrate as in oxidative phosphorylation. A decisive difference, then and now, between photosynthetic and oxidative phosphorylation was the inability of chloroplasts to form ATP in the dark by oxidizing substrates of oxidative phosphorylation with molecular oxygen.[70, 71]

The catalytic action of oxygen may now be explained by the mechanism for noncyclic photophosphorylation shown in Figure 1. As already stated, pyridine nucleotide, the physiological electron acceptor in noncyclic photophosphorylation (B in Fig. 1), may be replaced by non-physiological electron acceptors, such as ferricyanide [compare equations (2) and (3)]. Mehler[72–74] has shown earlier that in a Hill reaction molecular oxygen may act in the same manner as ferricyanide. When oxygen acts as an electron acceptor in a Hill reaction it is usually reduced to hydrogen peroxide. It now appears[44, 75] that the photoreduction of oxygen may also be coupled with the formation of ATP.

The reduction of oxygen to hydrogen peroxide by illuminated chloroplasts is ordinarily a sluggish reaction but it can be greatly accelerated by the addition of one of several catalysts. Among these are FMN[76] and vitamin K_3. On the basis of the mechanism for noncyclic photophosphorylation (Fig. 1), it would be expected that, in the presence of oxygen and catalytic amounts of FMN or vitamin K_3, ATP formation would be accompanied by the reduction of oxygen. Oxygen would then act as the terminal electron acceptor, like TPN or ferricyanide in equations (2) or (3) (see also B in Fig. 1). With oxygen acting as the terminal electron acceptor and OH^- as the electron donor there would be no net evolution of oxygen because the oxygen released is now offset by the oxygen consumed. The $H_2\overset{*}{O}_2$ formed by the reduction of $\overset{*}{O}_2$ (equation (6)) is then decomposed by the endogenous catalase of chloroplasts[12, 75] (equation (7)). ATP is therefore formed without any net consumption of oxygen (equation (8)).

$$\overset{*}{O}_2 + 2H^+ + ADP + P + 2OH^- \xrightarrow[\text{catalyst}]{\text{light}} H_2\overset{*}{O}_2 + ATP + H_2O + {}^1/_2O_2 \qquad (6)$$

$$H_2\overset{*}{O}_2 \xrightarrow[\text{endogenous catalase}]{\text{dark}} H_2\overset{*}{O} + {}^1/_2\overset{*}{O}_2 \qquad (7)$$

$$\text{Sum: } \overset{*}{O}_2 + 2H^+ + ADP + P + 2OH^- \xrightarrow[\text{catalyst}]{\text{light}} H_2\overset{*}{O} + {}^1/_2\overset{*}{O}_2 + ATP + H_2O + {}^1/_2O_2 \qquad (8)$$

The over-all reaction 8 becomes an oxygen-dependent photophosphorylation without a manometrically measurable oxygen consumption. The oxygen consumed ($\overset{*}{O}_2$) is exchanged with the oxygen produced (O_2). We have previously called this an "oxygen-catalyzed cyclic photophosphorylation."[53] We prefer now to abandon this term and to identify the mechanism of this pseudocyclic process

more precisely as a special case of an oxygen-dependent noncyclic photophosphorylation, one in which molecular oxygen acts like ferricyanide in replacing TPN as the terminal electron acceptor. As a result, oxygen becomes reduced to hydrogen peroxide. Superficially, reaction 8 is of the cyclic type since its over-all balance is the same as reaction 1. What characterizes the pseudocyclic reaction 8 and indicates that it has a mechanism different from the truly cyclic reaction 1 is a dependence on oxygen.

The hydrogen peroxide formed in reaction 6 can be trapped with the use of an ethanol-catalase trapping system.[72] In this case reaction 9 would replace reaction 7 and ATP formation would be accompanied by oxygen consumption, as shown by equation (10), which is a sum of reactions 6 and 9.

$$\overset{*}{O}_2 + 2H^+ + ADP + P + 2OH^- \xrightarrow[\text{catalyst}]{\text{light}} H_2\overset{*}{O}_2 + ATP + H_2O + {}^1/_2O_2 \qquad (6)$$

$$H_2\overset{*}{O}_2 + C_2H_5OH \xrightarrow[\text{added catalase}]{\text{dark}} 2H_2\overset{*}{O} + CH_3{\cdot}CHO \qquad (9)$$

$$\text{Sum: } \overset{*}{O}_2 + 2H^+ + C_2H_5OH + ADP + P + 2OH^- \xrightarrow[\text{catalyst, added catalase}]{\text{light}}$$

$$2H_2\overset{*}{O} + CH_3{\cdot}CHO + ATP + H_2O + {}^1/_2O_2 \qquad (10)$$

Figure 7 shows that the stoichiometry of these reactions has been experimentally verified. In an atmosphere of oxygen, ATP formation in noncyclic photophosphorylation (*a*) was accompanied by oxygen evolution when TPN or ferricyanide were added in substrate amounts as electron acceptors, (*b*) gave no significant oxygen evolution or uptake when FMN was added in catalytic amounts (equation (8)), and (*c*) was accompanied by oxygen consumption (equation (10)) when catalytic amounts of FMN were added jointly with substrate amounts of ethanol and excess catalase.

These results demonstrate the fundamental independence of noncyclic photophosphorylation of chloroplasts from molecular oxygen. Depending on the composition of the reaction mixture, the same ATP formation has occurred whether oxygen is produced (equations (2) or (3)), consumed (equation (10)) or merely exchanged (equation (8)).

Krogmann[77] has recently investigated oxygen-dependent photophosphorylations using indophenol dyes as cofactors. He concluded that his results could not be satisfactorily explained by the reduction of molecular oxygen to hydrogen peroxide. However, the recent work of Trebst and Eck[75] and our own evidence using ethanol-catalase as a hydrogen peroxide trapping system[72] (Fig. 7) shows that oxygen is indeed reduced to hydrogen peroxide.

Molecular oxygen can also serve as the terminal electron acceptor B (Fig. 1) in an experimentally contrived system in which the use of water as the electron donor for chloroplasts is blocked by inhibitors and an external electron donor is supplied instead. Krogmann and Vennesland[21] have described a system of this kind in which ATP formation was accompanied by the simultaneous consumption of O_2 and of an external electron donor. An apparent "oxidative photosynthetic

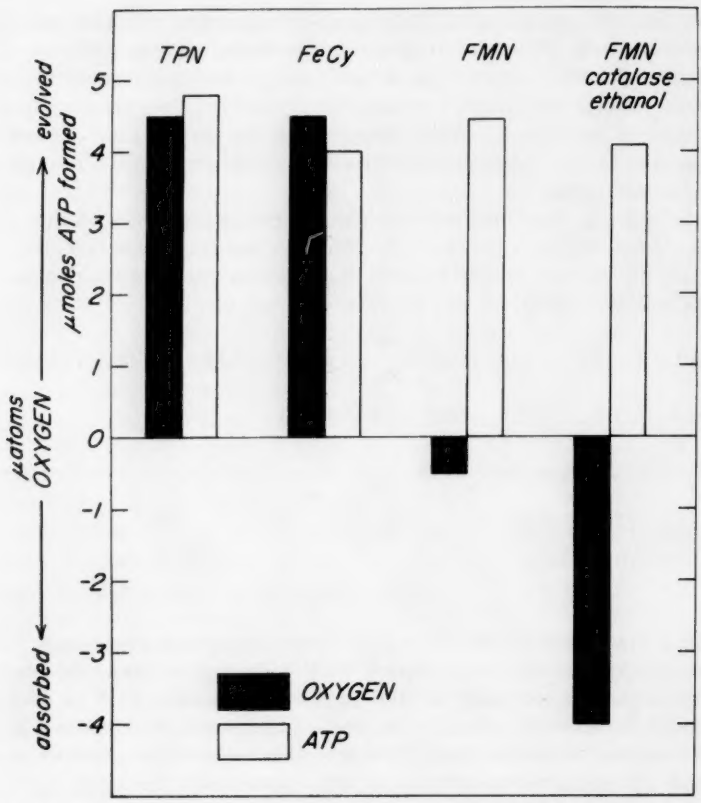

FIG. 7.—*ATP formation accompanied by oxygen evolution, oxygen exchange, or oxygen consumption, in noncyclic photophosphorylation by chloroplasts.* Oxygen was evolved when TPN or ferricyanide was the electron acceptor. In the presence of FMN, oxygen evolution was balanced by oxygen absorption (equation (8)). (We consider the slight oxygen absorption found in this treatment to be within the limits of experimental error.) In the presence of FMN, ethanol and catalase, ATP formation was accompanied by oxygen uptake (equation (10)).

The reaction mixtures contained, in a total volume of 3 ml, the following in μmoles: tris buffer, pH 7.8, 80; $MgCl_2$, 10; ADP, 10; $K_2H^{32}PO_4$, 10; and broken chloroplasts (P_{1s}) containing 0.4 mg chlorophyll. The following were added (in μmoles) where indicated: TPN, 6; $K_3Fe(CN)_6$, 15; FMN, 0.1; ethanol, 600; and crystalline catalase, 1 mg. TPN was added together with purified TPN-reductase from spinach. The experiment was carried out in Warburg manometer vessels, at 15°C. Gas phase, air; illumination, 25,000 Lux for 6 min.

phosphorylation" resulted that resembled oxidative phosphorylation by mitochondria, especially when $DPNH_2$ was used as the electron donor. However, the analogy between such "oxidative photosynthetic phosphorylation" and oxidative phosphorylation by mitochondria appears to be fortuitous. The role of $DPNH_2$ in this chloroplast system was not that of a physiological electron donor but that of a nonspecific reducing agent for the dye, one of several possible reducing agents.

That the consumption of oxygen was artificially induced and was not a physiological component of photophosphorylation is made clear by the observations of Krogmann and Vennesland[21] that "there was ample energy released by the dark oxidation of the DPNH to form the high energy phosphate bonds. Nevertheless, the reaction gave no phosphorylation unless the system was illuminated, even though the light caused no increase in the rate of oxygen consumption." We interpret this example of "oxidative photosynthetic phosphorylation" in chloroplasts as an instance of noncyclic photophosphorylation of the "bacterial type" in which oxygen acts as a nonspecific terminal electron acceptor (B in Fig. 2).

Nonparticipation of Oxygen in Cyclic Photophosphorylation.—In the preceding discussion, noncyclic photophosphorylation in chloroplasts was shown to be fundamentally independent of oxygen in that oxygen was either merely an excreted by-product of photooxidation of hydroxyl ions or a nonspecific electron acceptor. An even more direct demonstration of the independence of photosynthetic phosphorylation from oxygen is afforded by cyclic photophosphorylation. Here oxygen does not take part in the process at all, since, as already mentioned, neither an external electron acceptor nor an external electron donor is involved; oxygen thus cannot participate in the process as a substitute for one or as the by-product of the other. In cyclic photophosphorylation both the electron donor and the electron acceptor are endogenously generated by the light reaction.

Investigations of the mechanism of cyclic photophosphorylation in chloroplasts and bacterial particles have led to the conclusion that the formation of ATP is coupled with a cyclic, "closed circuit" transport of electrons from an endogenous electron donor to an endogenous electron acceptor, through a chain of carriers associated with the photosynthetic apparatus (cf. review[53]). Experimentally, a vigorous cyclic photophosphorylation by chloroplasts *in vitro* requires the addition, in *catalytic* amounts, of an electron carrier which can be either a known component of chloroplasts (vitamin K or FMN) or a nonphysiological agent such as phenazine methosulfate. (Fresh bacterial particles require no addition of external cofactors for vigorous cyclic photophosphorylation, but on aging respond to the addition of vitamin K and PMS[53].) The role assigned to the added electron carriers in cyclic photophosphorylation is illustrated diagrammatically for phenazine methosulfate in Figure 8.

The full identity of the photosynthetic electron carrier system is not yet established but the main components appear to include cytochromes,[18, 53] quinones (a naphthoquinone[78] or a benzoquinone[61, 62]) and flavin compounds.[78, 79] There is thus a parallelism between cyclic photophosphorylation of chloroplasts and oxidative phosphorylation of mitochondria with respect to several components of the electron transport chain although, it will be recalled, not with respect to the electron donor and electron acceptor. Nevertheless, suggestions have come recently, mainly from the laboratory of Vennesland,[21] that photophosphorylation by chloroplasts usually resembles oxidative phosphorylation in mitochondria in being dependent on molecular oxygen. Vennesland *et al.* have recently expressed their position in these words: "It is our opinion that chloroplasts which have not suffered damage to their oxygen-evolving mechanism prefer a cyclic process in which oxygen is evolved when FMN or menadione are cofactors. A truly anaerobic cycling involving neither production nor reconsumption of molecular oxygen *can apparently*

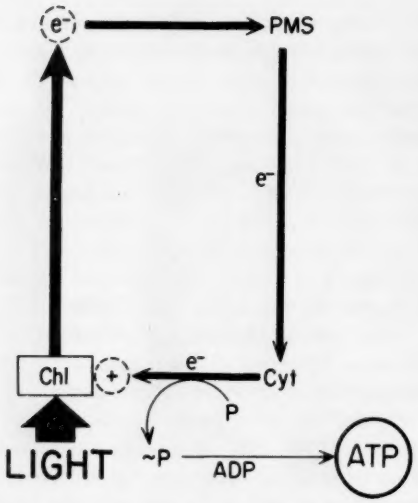

FIG. 8.—*Scheme for cyclic photophosphorylation.* The chlorophyll molecule (Chl) becomes excited by the absorption of a quantum of light. The excited chlorophyll donates its high-energy electron to oxidized phenazine methosulfate (PMS) and accepts an electron from reduced cytochrome (Cyt). The cycle is completed when the reduced PMS donates an electron to the oxidized cytochrome. The phosphorylation step is envisaged as being linked with the transfer of the electron from cytochrome to chlorophyll.

occur also, and is most pronounced with pyocyanine and phenazine methosulfate, less so with vitamin K_3, and hardly at all with FMN" [56] (our italics).

Thus there seems to be general agreement that a "truly anaerobic" cyclic photophosphorylation by isolated chloroplasts occurs in the presence of phenazine methosulfate. The question seems to turn on the role of oxygen in cyclic photophosphorylations catalyzed by vitamin K and FMN. Vennesland *et al.*[56] suggest that these are mainly of the oxygen-dependent type. We consider the participation of oxygen to be a special case of noncyclic photophosphorylation, where oxygen acts as a nonspecific substitute for TPN (Fig. 7). From our point of view, the main interest in vitamin K and FMN as catalysts of photophosphorylation lies not in their ability to catalyze an electron flow in which oxygen participates as a nonspecific electron acceptor (equations (6) and (8)) but rather in their ability to catalyze a truly anaerobic cyclic electron flow in which oxygen does not participate (equation (1)). We consider the anaerobic cyclic photophosphorylation as a common denominator of plant and bacterial photosynthesis and we regard the oxygen-dependent pseudocyclic type as merely a special case of noncyclic photophosphorylation in chloroplasts.

The experimental conditions required for demonstrating an anaerobic, cyclic photophosphorylation catalyzed by vitamin K and FMN differ from those required for demonstrating the oxygen-dependent, pseudocyclic photophosphorylation. Aside from the absence of oxygen, the effective operation of the anaerobic system requires higher concentrations (catalytic versus "microcatalytic") of vitamin K and FMN, and, particularly for the anaerobic FMN system, high concentrations of the chloroplast material in relation to illumination. The need

for a relatively high concentration of chloroplast material suggests that the anaerobic FMN and vitamin K systems require more chloroplast factor(s) than the pseudocyclic oxygen-dependent system. No similar requirements were observed for the anaerobic phenazine methosulfate system.

Despite the similarity of the over-all reactions (equations (1) and (8)), the anaerobic, cyclic photophosphorylations catalyzed by vitamin K and FMN can be distinguished experimentally from their oxygen-dependent, pseudocyclic analogues. The latter depend on the photoproduction of oxygen (equations (6), (7), and 8)) which requires chloride[53, 80] and are sensitive to two well-known inhibitors of oxygen evolution in photosynthesis, CMU[81] (*p*-chlorophenyldimethyl urea) and *o*-phenanthroline.[80]

Table 1 shows that, under experimental conditions favorable for each system,

TABLE 1

EFFECT OF CHLORIDE ON PHOTOPHOSPHORYLATION IN NITROGEN OR AIR

Treatment	μmoles ATP Formed	
	Minus chloride	Plus chloride
Nitrogen, FMN	5.1	5.7
Nitrogen, vitamin K_3	9.7	9.9
Air, FMN	0.5	6.1
Air, vitamin K_3	0.4	5.5

In the nitrogen series the illumination was 2,000 Lux for 30 min, and the reaction mixture included, in a final volume of 3 ml, chloroplast fragments (C_{18}) containing 2.5 mg chlorophyll and 0.3 μmoles of FMN or vitamin K_3. In the air series, the illumination was 50,000 Lux for 30 min and the reaction mixture included, in a final volume of 3 ml, chloroplast fragments (C_{18}) containing 0.2 mg chlorophyll and 0.003 μmoles of FMN or vitamin K_3. Other components of the reaction mixture were, in μmoles: tris buffer, pH 8.3, 80; $K_2H^{32}PO_4$, 15; ADP, 15; and $MgSO_4$, 5. Chloroplasts were prepared in 0.5 *M* sucrose and chloride-free reagents were used. In the plus chloride series 10 μmoles NaCl were added. Nitrogen gas was purified by passing through a zinc-methylene blue solution (A. T. Jagendorf, personal communication).

the omission of chloride had scarcely an effect on the anaerobic cyclic photophosphorylation with FMN or vitamin K, but severely inhibited their oxygen-dependent, pseudocyclic counterparts. Likewise, CMU (also *o*-phenanthroline[53]) inhibited the oxygen-dependent, pseudocyclic photophosphorylation but had relatively little effect on their anaerobic, cyclic counterparts (Table 2).

TABLE 2

EFFECT OF CMU ON PHOTOPHOSPHORYLATION IN NITROGEN AND AIR WITH HIGH CHLOROPHYLL AT LOW LIGHT INTENSITY

Treatment	μmoles ATP Formed			
	Nitrogen		Air	
	Control	CMU	Control	CMU
FMN	7.0	6.6	4.2	1.7
Vitamin K_3	8.1	7.6	3.3	1.3
PMS	2.7	2.4	2.9	2.8

The reaction mixture included, in a final volume of 3.0 ml, chloroplast fragments (C_{18}) containing 2.5 mg chlorophyll and, in μmoles: tris buffer, pH 8.3, 80; $MgSO_4$, 10; $K_2H^{32}PO_4$, 15; ADP, 15; and, where indicated, FMN, 0.3; vitamin K_3, 0.3, or, phenazine methosulfate (PMS), 0.1. The final concentration of CMU was 2×10^{-6} *M*. The reaction was run for 30 min at an illumination of 2,000 Lux. The nitrogen gas was purified as described in Table 1.

When some experimental conditions are unfavorable for anaerobic, cyclic photophosphorylation, the high affinity of reduced FMN or vitamin K_3 for molecular oxygen may still give rise to a pseudocyclic, oxygen-dependent photophosphorylation. Thus, we have observed in the presence of 10^{-4} *M* FMN or vitamin K_3 at a high light intensity, and with a relatively low concentration of chloroplast material (0.25 mg chlorophyll/3 ml) that photophosphorylation became oxygen-dependent, even when the reaction was started in purified nitrogen gas that was

TABLE 3

EFFECT OF CMU ON PHOTOPHOSPHORYLATION IN NITROGEN AND AIR WITH LOW CHLOROPHYLL AT HIGH LIGHT INTENSITY

Treatment	μmoles ATP Formed			
	Nitrogen		Air	
	Control	CMU	Control	CMU
FMN	5.6	1.5	5.4	1.1
Vitamin K_3	8.6	4.7	5.3	1.0
PMS	9.3	9.9	8.9	8.6

Experimental conditions as in Table 2 except that less chloroplast material (C_{15}) was used (0.25 mg chlorophyll) and the illumination was increased to 20,000 Lux. Reaction time, 15 min.

treated to remove oxygen impurities (Table 3). Phosphorylation became oxygen-dependent when the catalytic amounts of FMN or vitamin K_3 were photochemically reduced by chloroplasts. An equivalent amount of oxygen was then liberated which was sufficient to sustain an oxygen-dependent photophosphorylation (cf. Trebst and Eck[75]). The oxygen dependence of the system was determined by blocking the oxygen evolution reaction with CMU. ATP formation then became strongly inhibited. (It seems likely that a similar dependence on photochemically generated oxygen accounts for the results reported by Vennesland *et al.* in ref. 56, Table 2.) Photophosphorylations catalyzed by phenazine methosulfate were resistant to inhibition by CMU and *o*-phenanthroline,[53] regardless whether the reaction was carried out under conditions favoring the anaerobic cyclic, or the oxygen-dependent pseudocyclic pathway (Tables 2 and 3).

Concluding Remarks.—From the standpoint of cellular physiology, the role of oxygen in ATP formation in photosynthesis provides an interesting contrast to the role of oxygen in ATP formation in respiration. The high thermodynamic efficiency of respiration, and its superiority over fermentation in using the free energy of the degradation of foodstuffs for synthesis of the pyrophosphate bonds of ATP, is made possible by the key role that molecular oxygen plays as the terminal electron acceptor in oxidative phosphorylation by mitochondria. Only with oxygen can the oxidation of foodstuffs be complete (to CO_2 and water) and their free energy released in full for metabolic purposes. In the last seven years biochemical investigations of photosynthesis in cell-free systems revealed no such role for oxygen in ATP formation by chloroplasts and bacterial particles. Here, ATP formation occurs in cyclic photophosphorylation under strictly anaerobic conditions where the participation of oxygen is excluded. In noncyclic photophosphorylation, oxygen may replace TPN as a terminal electron acceptor, but, as discussed later, this results in a loss instead of a gain in the yield of physiologically useful energy.

The strictly anaerobic character of cyclic photophosphorylation in bacterial preparations needs no elaboration since photosynthesis in bacteria is firmly established as an anaerobic process.[7] In isolated chloroplasts, anaerobic cyclic photophosphorylation has been demonstrated with phenazine methosulfate as a catalyst, and also with vitamin K_3 and FMN. With the latter, a far more rigid control of experimental conditions was required than with phenazine methosulfate.

Special experimental safeguards are needed for demonstrating in chloroplasts an anaerobic cyclic photophosphorylation catalyzed by vitamin K_3 and FMN, because these substances, when reduced photochemically, readily react with small concentrations of molecular oxygen. Phenazine methosulfate also reacts readily

with oxygen, but its affinity for oxidized cytochromes[82] seems to be greater than for oxygen; it is thus able to catalyze a cyclic electron flow (Fig. 8) even in the presence of molecular oxygen.

Noncyclic photophosphorylation consists of ATP formation that is coupled with the reduction of pyridine nucleotide and the oxidation of an exogenous electron donor. The process, which was originally found in isolated chloroplasts,[22] has now also been demonstrated in bacterial particles.[59] The difference between noncyclic photophosphorylation in the two cases centers on the electron donor. For isolated chloroplasts the electron donors are hydroxyl ions which on oxidation form oxygen; this accounts for oxygen evolution in plant photosynthesis. Photosynthetic bacteria cannot use hydroxyl ions but only such electron donors as organic acids or reduced sulfur compounds[6, 7]; this accounts for the absence of oxygen evolution in bacterial photosynthesis. Instead of oxygen, oxidized bacterial electron donors are formed, which may be further metabolized or may accumulate and yield, for example, elemental sulfur.[6]

The role of oxygen in photosynthesis is, therefore, only incidental and not vital to the energy transformation reactions, as it is in respiration. Oxygen is evolved because it is an excreted product of the oxidation of hydroxyl ions—the electron donor in noncyclic photophosphorylation by chloroplasts. Experimentally, when another electron donor is substituted for hydroxyl ions, noncyclic photophosphorylation in chloroplasts becomes converted to the bacterial type: ATP formation is coupled with pyridine nucleotide reduction but no oxygen is evolved.[57]

In a cell-free system, oxygen evolution by chloroplasts will be observed manometrically only under certain conditions. First, the acceptor for the electrons "expelled" from chlorophyll in the primary photochemical reaction must not react preferentially with the components of the photosynthetic electron transport chain (cf. Trebst and Eck[83]). If it does react, as in the case of phenazine methosulfate, then cyclic photophosphorylation, in which oxygen is not evolved, will result. Second, the electron acceptor must not be easily oxidized by molecular oxygen. This is often, but not always, related to redox potential. Thus, TPN with a redox potential, at pH 7, of $E'_0 = -324$ mV shares this property with ferricyanide ($E'_0 = 360$ mV) and p-benzoquinone ($E'_0 = 293$ mV). In the intact plant, oxygen is normally evolved during photosynthesis because the $TPNH_2$ formed in noncyclic photophosphorylation is not reoxidized by the oxygen formed, but is used up in carbon assimilation.

A special case of noncyclic photophosphorylation by isolated chloroplasts occurs when oxygen acts as the terminal electron acceptor and becomes reduced to hydrogen peroxide. The photoreduction of oxygen by isolated chloroplasts, discovered by Mehler,[72] has been investigated by Brown and Good[84] and Good and Hill,[76] who suggested that it is "an artifact" [84] and that "the direct reduction of oxygen does not ordinarily occur to a significant extent *in vivo*." [76]

In a cell-free system containing microcatalytic amounts of FMN or vitamin K_3, oxygen may replace TPN as the electron acceptor in noncyclic photophosphorylation by chloroplasts and give rise to an oxygen-dependent, pseudocyclic photophosphorylation. The substitution of oxygen for TPN is analogous to the substitution of ferricyanide for TPN. ATP is still formed in each case, but the reductant produced is no longer $TPNH_2$ but either ferrocyanide, or, when oxygen

is the electron acceptor, H_2O_2 or water. Thus, the intervention of oxygen in noncyclic photophosphorylation results in a loss of biochemically useful energy which would have normally been used for forming a strong reductant, i.e. $TPNH_2$. When oxygen is the electron acceptor and water is the final product of oxygen reduction (equations (6) and (7)) the energy loss is equivalent to a redox potential of 1139 mV (difference between $E_0' = 815$ mV for the water/oxygen system and $E_0' = -324$ mV for the $TPN/TPNH_2$ system). If hydrogen peroxide is allowed to accumulate as the final product of the oxygen reduction, the computed energy loss would be equivalent to a redox potential of 1006 mV.

* The following abbreviations are used: ATP, adenosine triphosphate; ADP, adenosine diphosphate; P, orthophosphate; TPN, $TPNH_2$, oxidized and reduced forms of triphosphopyridine nucleotide; FMN, riboflavin phosphate (flavin mononucleotide); PMS, phenazine methosulfate.

† Aided by grants from the National Institutes of Health and the Office of Naval Research.

[1] Arnon, D. I., *Bull. Torrey Botan. Club*, **88** (1961).

[2] Ingenhousz, J., *Essay on the food of plants and the renovation of soils*, London (1796).

[3] Lebedev, A., *Biochem. Z.*, **7**, 1 (1907).

[4] Lebedev, A., *Ber. deut. botan. Ges.*, **27**, 598 (1909).

[5] Lebedev, A. F., *Izvest. Donskovo Gosudarst. Univ.*, **3**, 25 (1921), translated in *Am. Rev. Soviet Med.*, **5**, 15 (1948).

[6] Van Niel, C. B., *Arch. Mikrobiol.*, **3**, 1 (1931).

[7] Van Niel, C. B., in *Photosynthesis in Plants*, ed. J. Franck and W. E. Loomis (Ames, Iowa: Iowa State College Press, 1949), p. 437.

[8] Hill, R., *Proc. Roy. Soc. (London)*, **B 127**, 209 (1939).

[9] Hill, R., *Symposia Soc. Exptl. Biol.*, **5**, 221 (1951).

[10] Burk, D., and O. Warburg, *Z. Naturforsch.*, **6b**, 12 (1951).

[11] Warburg, O., *Science*, **128**, 68 (1958).

[12] Warburg, O., G. Krippahl, H. S. Gewitz, and W. Z. Volker, *Z. Naturforsch.*, **14b**, 712 (1959).

[13] Vishniac, W., and S. Ochoa, *J. Biol. Chem.*, **198**, 501 (1952).

[14] Holzer, H., *Z. Naturforsch.*, **6b**, 424 (1951).

[15] Bassham, J. A., A. A. Benson, L. D. Kay, A. Z. Harris, A. T. Wilson, and M. Calvin, *J. Am. Chem. Soc.*, **76**, 1760 (1954).

[16] Arnon, D. I., M. B. Allen, and F. R. Whatley, *Nature*, **174**, 394 (1954).

[17] Frenkel, A. W., *J. Am. Chem. Soc.*, **76**, 5568 (1954).

[18] Arnon, D. I., *Nature*, **184**, 10 (1959).

[19] Arnon, D. I., M. Losada, M. Nozaki, and K. Tagawa, *ibid.*, **190**, 601 (1961).

[20] Stanier, R. Y., *Bacteriol. Rev.*, **25**, 1 (1961).

[21] Krogmann, D. W., and B. Vennesland, *J. Biol. Chem.*, **234**, 2205 (1959).

[22] Arnon, D. I., F. R. Whatley, and M. B. Allen, *Science*, **127**, 1026 (1958).

[23] Arnon, D. I., F. R. Whatley, and M. B. Allen, *Biochim. et Biophys. Acta*, **32**, 47 (1959).

[24] Trebst, A. V., H. Y. Tsujimoto, and D. I. Arnon, *Nature*, **182**, 351 (1958).

[25] Losada, M., A. V. Trebst, and D. I. Arnon, *J. Biol. Chem.*, **235**, 832 (1960).

[26] Trebst, A. V., M. Losada, and D. I. Arnon, *ibid.*, **234**, 3055 (1959).

[27] Arnon, D. I., in *Enzymes: Units of Biological Structure and Function*, ed. O. H. Gaebler (New York: Academic Press, Inc., 1956), p. 279.

[28] Arnon, D. I., M. B. Allen, and F. R. Whatley, *Biochim. et Biophys. Acta*, **20**, 449 (1956).

[29] Whatley, F. R., M. B. Allen, L. L. Rosenberg, J. B. Capindale, and D. I. Arnon, *ibid.*, **20**, 462 (1956).

[30] Calvin, M., *Proc. Intern. Congr. Biochem., 3rd Congr., Brussels*, 1955 (New York: Academic Press, Inc., 1956), p. 211.

[31] Vishniac, W., B. L. Horecker, and S. Ochoa, *Advances in Enzymol.*, **19**, 1 (1957).

[32] Trudinger, P. A., *Biochem. J.*, **64**, 274 (1956).

[33] Aubert, J. P., G. Milhaud, and J. Millet, *Ann. inst. Pasteur*, **92**, 515 (1957).

[34] McFadden, B. A., and D. E. Atkinson, *Arch. Biochem. Biophys.*, **66**, 16 (1957); McFadden, B. A., *J. Bacteriol.*, **77**, 339 (1959).

[35] Strehler, B. L., *Arch. Biochem. Biophys.*, **43,** 67 (1953).

[36] Gaffron, H., in *Autotrophic Microorganisms*, ed. B. A. Fry and J. L. Peel (Cambridge, England: Cambridge University Press, 1954), p. 163.

[37] Avron, M., and A. T. Jagendorf, *Nature*, **179,** 428 (1957).

[38] Avron, M., A. T. Jagendorf, and M. Evans, *Biochim. et Biophys. Acta*, **26,** 262 (1957).

[39] Jagendorf, A. T., in *The Photochemical Apparatus*, Brookhaven Symposia in Biology, No. 11 (1958).

[40] Jagendorf, A. T., and M. Avron, *J. Biol. Chem.*, **231,** 277 (1958).

[41] Wessels, J. S. C., *Biochim. et Biophys. Acta*, **25,** 97 (1957).

[42] *Ibid.*, **29,** 113 (1958).

[43] Chow, C. T., and B. Vennesland, *Plant Physiol.*, **32** (Supp.), iv (1957).

[44] Nakamoto, T., D. W. Krogmann, and B. Vennesland, *J. Biol. Chem.*, **234,** 2783 (1959).

[45] Hill, R., and D. A. Walker, *Plant Physiol.*, **34,** 240 (1959).

[46] Whatley, F. R., M. B. Allen, A. V. Trebst, and D. I. Arnon, *ibid.*, **35,** 188 (1960).

[47] Other accounts of the discovery of photosynthetic phosphorylation and CO_2 assimilation by isolated chloroplasts are sometimes found in the literature. Thus in 1956, J. A. Bassham and M. Calvin, in *Currents in Biochemical Research*, ed. D. E. Green (New York: Interscience, 1956), ascribed the discovery of CO_2 assimilation by isolated chloroplasts to Boychenko and Baranov.[48] In 1959, Calvin (ref. 49, p. 152) ascribed the discovery of both CO_2 assimilation and ATP synthesis by isolated chloroplasts to his own laboratory.

[48] Boychenko, E. A., and V. I. Baranov, *Doklady Akad. Nauk S.S.S.R.*, **95,** 1025 (1954); *Chem. Abstr.*, **48,** 8881 (1954).

[49] Calvin, M., *Rev. Modern Phys.*, **31,** 147 (1959); also in *Biophysical Science—A Study Program*, ed. J. C. Oncley (New York: John Wiley and Sons, 1959), p. 152.

[50] Williams, A. M., *Biochim. et Biophys. Acta*, **19,** 570 (1956).

[51] Thomas, J. B., and A. M. Haans, *ibid.*, **18,** 286 (1955).

[52] Petrack, B., and F. Lipmann, in *Light and Life*, ed. W. D. McElroy and B. Glass (Baltimore: Johns Hopkins Press, 1961), p. 621.

[53] Arnon, D. I., *ibid.*, p. 489.

[54] Frenkel, A. W., *J. Biol. Chem.*, **222,** 823 (1956).

[55] Geller, D. M., "Photophosphorylation by *Rhodospirillum rubrum* preparations," Doctoral Dissertation, Div. Med. Sci., Harvard University (1957).

[56] Vennesland, B., T. Nakamoto, and B. Stern, in *Light and Life*, ed. W. D. McElroy and B. Glass (Baltimore: Johns Hopkins University Press, 1961), p. 609.

[57] Losada, M., F. R. Whatley, and D. I. Arnon, *Nature*, **190,** 606 (1961.)

[58] Duysens, L. N. M., J. Amesz, and B. M. Kamp, *ibid.*, **190,** 510 (1961).

[59] Nozaki, M., K. Tagawa, and D. I. Arnon, these PROCEEDINGS, **47,** 1334 (1961).

[60] Hill, R., and W. D. Bonner, in *Light and Life*, ed. W. D. McElroy and B. Glass (Baltimore: Johns Hopkins University Press, 1961), p. 424.

[61] Crane, F. L., *Plant Physiol.*, **34,** 128 (1959); Bishop, N. I., these PROCEEDINGS, **45,** 1696 (1959).

[62] Krogmann, D. W., *Biochem. Biophys., Research Commun.*, **4,** 275 (1961).

[63] Trebst, A. V., M. Losada, and D. I. Arnon, *J. Biol. Chem.*, **235,** 840 (1960).

[64] Krogmann, D. W., A. T. Jagendorf, and M. Avron, *Plant Physiol.*, **34,** 272 (1959).

[65] Chance, B., and J. M. Olson, *Arch. Biochem. Biophys.*, **88,** 54 (1960).

[66] Marrè, E., and E. Forti, *Science*, **126,** 976 (1957).

[67] French, C. S., in *Handbuch der Pflanzenphysiologie*, ed. W. Ruhland (Heidelberg: Springer, 1960), vol. 5, part 1, p. 252.

[68] Avron, M., D. W. Krogmann, and A. T. Jagendorf, *Biochim. et Biophys. Acta*, 30, 144 (1958).

[69] Davenport, H. E., *Biochem. J.*, **77,** 471 (1960).

[70] Arnon, D. I., paper presented at the *Cell Symposium, Amer. Assn. for the Advancement of Sci.*, Berkeley Meeting (1954); *Science*, **122,** 9 (1955).

[71] Arnon, D. I., M. B. Allen, and F. R. Whatley, *Biochim. et Biophys. Acta*, **20,** 449 (1956).

[72] Mehler, A. H., *Arch. Biochem. Biophys.*, **33,** 65 (1951).

[73] *Ibid.*, **34,** 339 (1951).

[74] Mehler, A. H., and A. H. Brown, *ibid.*, **38,** 365 (1952).

[75] Trebst, A., and H. Eck, *Z. Naturforsch.* (in press).

[76] Good, N., and R. Hill, *Arch. Biochem. Biophys.*, **57**, 355 (1955).
[77] Krogmann, D. W., *J. Biol. Chem.*, **235**, 3630 (1960).
[78] Arnon, D. I., in *Handbuch der Pflanzenphysiologie*, ed. W. Ruhland (Heidelberg: Springer, 1960), vol. 5, part 1, p. 773.
[79] Baltscheffsky, H., *Svensk Kemisk Tidskrift*, **72**, 4 (1960).
[80] Warburg, O., in *Heavy Metal Prosthetic Groups and Enzyme Action* (Oxford, England: Clarendon Press, 1949), p. 213.
[81] Wessels, J. S. C., *Biochim. et Biophys. Acta*, **19**, 548 (1956).
[82] Massey, V., *ibid.*, **34**, 255 (1959).
[83] Trebst, A., and H. Eck, *Z. Naturforsch.*, **16b**, 44 (1961).
[84] Brown, A. H., and N. Good, *Arch. Biochem. Biophys.*, **57**, 340 (1955).

NONCYCLIC PHOTOPHOSPHORYLATION IN PHOTOSYNTHETIC BACTERIA

BY M. NOZAKI, K. TAGAWA, AND DANIEL I. ARNON*

LABORATORY OF CELL PHYSIOLOGY, UNIVERSITY OF CALIFORNIA, BERKELEY

Communicated August 2, 1961

Noncyclic photophosphorylation is the formation of adenosine triphosphate in a light-induced electron flow from an external electron donor to an electron acceptor such as pyridine nucleotide. In photosynthesis of green plants the electron donors are the hydroxyl ions of water and hence the over-all reaction also produces, aside from ATP and PNH_2,[1] molecular oxygen, which is liberated when OH^- is photooxidized (see Fig. 1 in preceding article[2]).

Photosynthetic bacteria cannot use OH^- as an electron donor for photosynthesis but use a variety of reductants stronger than OH^-, among them hydrogen gas, succinate, or thiosulfate. With hydrogen gas no input of light energy is required for the reduction of pyridine nucleotide, since hydrogen gas, with the aid of bacterial hydrogenase, can reduce pyridine nucleotide in the dark.[3] The contribution of light to bacterial photosynthesis is then limited to the formation of ATP by cyclic photophosphorylation.[4, 5] With other electron donors such as, for example, succinate, the additional input of energy that is necessary to reduce pyridine nucleotide is provided by light. Thus, in bacterial photosynthesis with succinate as the electron donor, light energy serves a dual purpose: it supplies ATP by cyclic photophosphorylation and, by photooxidizing the electron donor, it also provides electrons for reducing pyridine nucleotides by a noncyclic electron flow mechanism.

Photoreduction of pyridine nucleotide (DPN) by cell-free preparations of *Rhodospirillum rubrum*[6, 7] and *Chromatium*[3] has been observed but attempts to find a simultaneous ATP formation, analogous to the noncyclic photophosphorylation in chloroplasts, led to negative results.[7, 8] As pointed out by Vernon and Ash,[8] a demonstration of ATP formation by a noncyclic electron flow mechanism is more difficult in chromatophores than in chloroplasts because in chromatophores it cannot be experimentally distinguished from a simultaneous ATP formation by cyclic photophosphorylation. In chromatophores, a vigorous cyclic photophosphorylation occurs under anaerobic conditions and without added cofactors,[3] whereas in chloroplasts cyclic photophosphorylation is always under experimental

control since it will not proceed anaerobically to a significant extent without the addition of co-factors.

Evidence for noncyclic photophosphorylation in photosynthetic bacteria, which we now wish to report, has been obtained under conditions when cyclic photophosphorylation was suppressed, thereby making it possible to distinguish the ATP formed by a noncyclic electron flow mechanism from that formed by a cyclic mechanism. In chromatophores of *R. rubrum*, in which cyclic photophosphorylation was made inoperative, ATP formation was obligatorily coupled with a light-dependent electron flow from an external electron donor to DPN as the terminal electron acceptor.

Methods.—Rhodospirillum rubrum (kindly supplied by R. Y. Stanier) was grown anaerobically, at room temperature, under continuous illumination by a bank of fluorescent lights in a medium of Gest *et al.*[9] supplemented with 0.017 *M* NH_4Cl. *Chromatium* cells were grown under similar conditions in a culture medium to be described elsewhere. Two-day-old cultures were centrifuged, the sedimented cells washed with 0.1 *M* tris-HCl buffer, pH 7.8 (used also in subsequent operations) and recentrifuged. A paste of the washed cells was ground by hand, under argon gas, with an equal volume of levigated alumina, the slurry suspended in tris buffer (gassed with argon), and centrifuged at 3,000 × *g* for 15 min. The supernatant fluid was further centrifuged at 12,000 × *g* for 15 min., the residue was discarded, and the supernatant fluid (PS) was used for the isolation of chromatophores. Centrifugations were carried out in the cold and the centrifuge chamber was filled beforehand with argon gas.

The PS preparation was centrifuged in a Spinco, Model L centrifuge, at 144,000 × *g* for 1 hr. The supernatant fluid (S) was frozen for later use. The residue (P), which constituted the chromatophore fraction, was resuspended in tris buffer (gassed with argon) and recentrifuged at 144,000 × *g* for 1 hr. The residue, after suspension in tris buffer, constituted the washed chromatophores (P_1), and the corresponding supernatant fluid (S_1) was saved for later use. In certain experiments the washing procedure was repeated, yielding twice-washed chromatophores (P_2) and a corresponding supernatant fluid (S_2), etc.

The photochemical reactions were carried out in Thunberg-type cuvettes, which were made anaerobic, by five consecutive cycles of evacuation (to 5 mm Hg) followed by flushing with argon gas. The cuvettes were placed in an illuminated glass-walled water bath. DPN reduction was measured periodically (with a Cary recording spectrophotometer) as the difference in optical density at 340 mμ between an illuminated cuvette and a dark control. The reaction was stopped by adding 0.3 ml of 40% trichloracetic acid to each cuvette. The reaction mixture was centrifuged and 1 ml of the supernatant fluid was used for determining the ATP formed,[10] and, where applicable, 0.3 ml of the supernatant fluid was used for determining the lactate formed.[8]

Bacteriochlorophyll was measured at 810 mμ by diluting a suspension of chromatophores with distilled water, as described by Anderson and Fuller.[11]

Results.—Suppression of cyclic photophosphorylation: Cyclic photophosphorylation in cell-free preparations of *R. rubrum* and *Chromatium* was suppressed by the use of antimycin A or 2-heptyl-4-hydroxy-quinoline-N-oxide[12–15] (HOQNO) (a gift of D. P. Hackett). The effect of these inhibitors was most pronounced

with washed chromatophores. As shown in Table 1, unwashed chromatophores had an appreciable photophosphorylation that was resistant to the action of these two inhibitors. This resistant photophosphorylation seemed to depend on factor(s) present in the supernatant fluid as evidenced by the addition of the supernatant fluid to washed chromatophores (Table 1).

TABLE 1

EFFECTS OF INHIBITORS ON PHOTOPHOSPHORYLATION IN CELL-FREE PREPARATIONS OF *Chromatium* AND *R. rubrum*

	Inhibitor added	μmoles of ATP formed/mg chl/hr Chromatium	R. rubrum
Crude extract (PS)	none	103	90
PS	Antimycin A	71	33
PS	HOQNO	33	29
Unwashed chromatophores (P)	none	96	139
P	Antimycin A	42	22
P	HOQNO	13	26
Washed chromatophores (P_1)	none	82	142
P_1	Antimycin A	7	8
P_1	HOQNO	1	15
P_1 + washings (S_1)	none	..	139
$P_1 + S_1$	Antimycin A	..	24
$P_1 + S_1$	HOQNO	..	22

The reaction mixture contained in a final volume of 3 ml: chromatophores, containing 0.1 mg bacteriochlorophyll; hexokinase, 1 mg; and the following in μmoles: tris buffer, pH 7.8, 100; $MgCl_2$, 5; ADP, 0.5; $K_2HP^{32}O_4$, 10; D-glucose 30. Antimycin A (10 μg) or HOQNO (0.03 μmole) was added as indicated. The reaction was run at 20° for 30 min in the light (10,000 Lux).

Aside from inhibiting cyclic photophosphorylation (Table 1), antimycin A and HOQNO were also found to inhibit photoreduction of DPN when succinate was the electron donor (Fig. 1). Succinate could not, therefore, be used as the electron donor for noncyclic photophosphorylation in the presence of either one of these inhibitors. However, antimycin A or HOQNO gave practically no inhibition when ascorbate, together with catalytic amounts of 2,6-dichlorophenol indophenol (DPIP), served as the electron donor for DPN reduction (Fig. 2). It thus became possible to measure ATP formation that is coupled with the electron flow from ascorbate to DPN, under conditions when cyclic photophosphorylation was blocked. Neither the photoreduction of DPN with succinate or ascorbate, nor photophosphorylation, was diminished by repeated washing of chromatophores ($P \rightarrow P_3$). In fact, the once-washed chromatophores (P_1) were more active than the unwashed particles (P).

We have previously reported[20] that photosynthetic bacteria contain a soluble pyridine nucleotide reductase which, when assayed in a chloroplast system, reduced (in the light) triphosphopyridine nucleotide (TPN) in preference to DPN. In the present experiments, however, chromatophores were found to have a tightly bound, DPN-specific pyridine nucleotide reductase. In addition, the chromatophores had a bound transhydrogenase which made possible a light-dependent reduction of TPN in the presence of traces of DPN.

Noncyclic photophosphorylation: As shown in Table 2, a noncyclic photophosphorylation system was functioning with chromatophores from *R. rubrum*. The formation of ATP required the simultaneous presence of an electron donor system (substrate amounts of ascorbate plus catalytic amounts of DPIP) and of an electron acceptor (DPN). The stoichiometry of this reaction appears to be the same

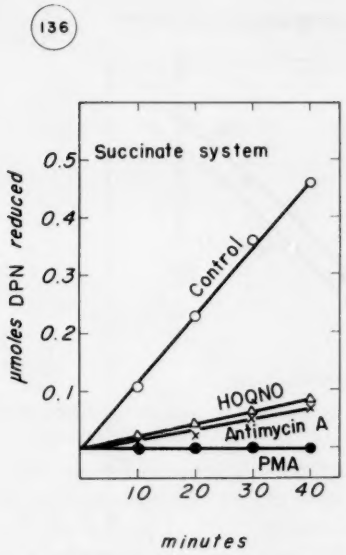

FIG. 1.—Photoreduction of DPN by washed chromatophores of *R. rubrum* (P_1) with succinate. The reaction mixture contained in a total volume of 3 ml, 0.03 mg bacteriochlorophyll, as washed *R. rubrum* chromatophores (P_1), and in μmoles: tris buffer (pH 7.8), 100; $MgCl_2$, 5; DPN, 2; and succinate, 20. The following inhibitors were added as indicated: antimycin A, 10 μg; 2-heptyl 4-hydroxyquinoline N-oxide (HOQNO), 0.03 μmole; or phenyl mercuric acetate (PMA), 0.3 μmole. The reaction was carried out in Thunberg-type cuvettes at 20°C. Gas phase, argon; illumination, 10,000 Lux.

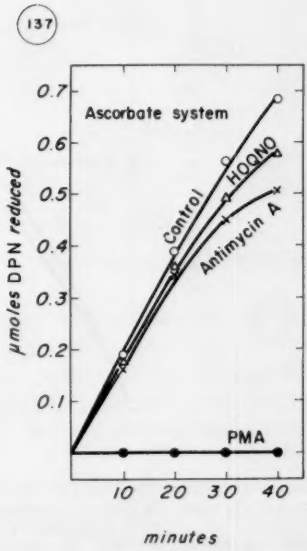

FIG. 2.—Photoreduction of DPN by washed *R. rubrum* chromatophores with ascorbate. The reaction mixture and experimental conditions were the same as described for Figure 1 except that succinate was replaced by 20 μmoles of ascorbate and 0.2 μmole of 2,6-dichlorophenol indophenol.

TABLE 2

NONCYCLIC PHOTOPHOSPHORYLATION IN *R. rubrum*

Components added	Substances added	μmoles ATP formed/mg chl/hr
Electron donor and acceptor	Ascorbate, DPIP, DPN	44.8
Electron donor system	Ascorbate, DPIP	5.4
Electron acceptor	DPN	7.6
None	.....	5.0
Electron donor, acceptor, and inhibitor	Ascorbate, DPIP, DPN, PMA	6.2

All vessels contained antimycin A, 10 μg. The following additions were made where indicated: ascorbate, 20 μmoles; 2,6-dichlorophenol indophenol (DPIP), 0.2 μmole; DPN, 2 μmoles; phenyl mercuric acetate (PMA), 0.3 μmole. Other components of the reaction mixture and conditions were the same as in the control treatment of Table 1.

as in noncyclic photophosphorylation by isolated chloroplasts: one mole of ATP is formed for each mole of pyridine nucleotide reduced (Fig. 3). Experimentally, this stoichiometry was obtained only when the reduced DPN was trapped by an added lactic dehydrogenase system. Without this addition, the reduced DPN was

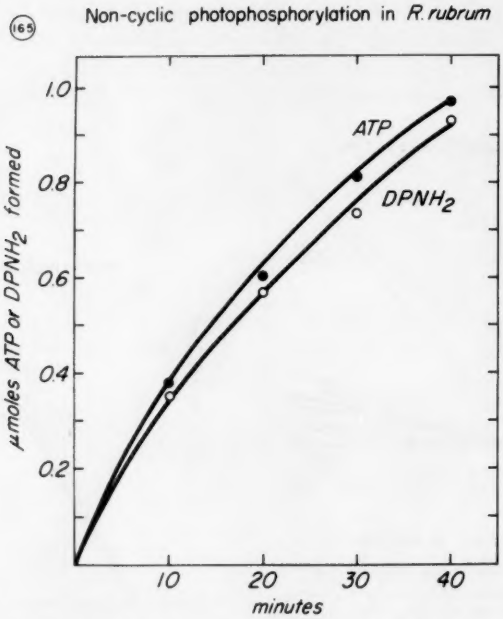

FIG. 3.—Stoichiometry of ATP formation and DPN reduction (as measured by lactate formation) in noncyclic photophosphorylation with *R. rubrum* chromatophores. The reaction mixture contained 0.04 mg bacteriochlorophyll, as washed chromatophores (P_1), and in μmoles: tris buffer (pH 7.8), 100; $MgCl_2$, 5; ADP, 5; $K_2HP^{32}O_4$, 5; ascorbate, 20; 2,6-dichlorophenol indophenol, 0.2; DPN, 0.3; and pyruvate, 10. 25 μg of crystalline lactic dehydrogenase (muscle) and 10 μg of antimycin A were also added. Other experimental conditions were the same as described for Figure 1.

reoxidized in the reaction mixture, resulting in low recoveries of $DPNH_2$ and high $P/DPNH_2$ ratios.

The effectiveness of substrate amount of ascorbate as the electron donor for noncyclic photophosphorylation by *R. rubrum* chromatophores depended on the addition of catalytic amounts of DPIP, which evidently acted as an electron carrier between ascorbate and the electron transport system within the chromatophore. We have also observed a cyclic photophosphorylation, which is resistant to antimycin A (resembling in this respect the cyclic photophosphorylation catalyzed by phenazine methosulfate[13, 15]), when we replaced substrate amounts of ascorbate (20 μmoles) with catalytic amounts (0.5 μmole) and added it jointly with a catalytic amount of DPIP (0.2 μmole).

Phenyl mercuric acetate (PMA) completely inhibited non-cyclic electron flow whether the electron flow was measured as DPN reduction (Figs. 1 and 2) or as ATP formation accompanying the DPN reduction (Table 2). However, in other experiments, we have observed that PMA at this same concentration only partially inhibited the cyclic photophosphorylation. The PMA, therefore, seems to inhibit the step(s) involved between the e^- and the DPN (see Fig. 4).

A diagrammatic representation of noncyclic photophosphorylation in bacteria is given in Figure 4 (compare Fig. 2 in preceding article). It seems likely that

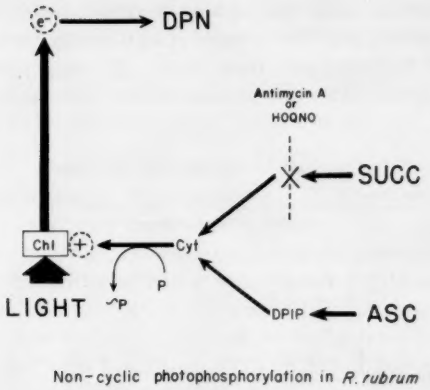

FIG. 4.—Scheme for noncyclic photophosphorylation in *R. rubrum* with either succinate or ascorbate as an electron donor. Details in the text.

electron transport from succinate to DPN shares with the electron transport system of cyclic photophosphorylation, the same step, sensitive to inhibition by antimycin A and HOQNO, that involves electron transfer between a cytochrome of the b type and a cytochrome of the c type.[14, 15] A possible participation of coenzyme Q in this sector of the electron transport chain in bacterial photophosphorylations is discussed elsewhere.[16]

Additional support for noncyclic electron flow in photosynthetic bacteria has come from recent experiments of Losada *et al.*[17–19] on photoproduction of H_2 and photofixation of N_2 by *Chromatium* at the expense of thiosulfate as the electron donor. The results are consistent with the view that electrons expelled from chlorophyll, following the primary photochemical act, are responsible for the reduction of H^+ to H_2 and for the reduction of N_2. The electrons lost by chlorophyll would be replaced by those donated by thiosulfate, via the bacterial cytochrome system. The expected occurrence of photophosphorylation coupled with the electron flow to H_2 or N_2 is now under investigation.

Concluding Remarks.—Since noncyclic photophosphorylation in bacteria (Fig. 4) is analogous to noncyclic photophosphorylation (without oxygen evolution) in chloroplasts (see Fig. 2 in preceding article), photosynthesis in plants and bacteria is now seen as having in common two photochemical processes: cyclic and noncyclic photophosphorylation. In both plants and bacteria light energy, when it supplies ATP by cyclic and by noncyclic photophosphorylation, also brings about a reduction of pyridine nucleotide and oxidation of an exogenous electron donor that is coupled with the formation of ATP.

The differences between bacterial and plant photosynthesis seem to center on the electron donors that are consumed in the reduction of pyridine nucleotide. With some bacterial electron donors, as for example, hydrogen gas, the reduction of pyridine nucleotide requires no input of light energy. With other electron donors, such as thiosulfate or succinate, an input of light energy, in a noncyclic electron flow mechanism, becomes necessary for the reduction of pyridine nucleotide. Thus in bacterial photosynthesis, the reduction of pyridine nucleotide may occur with or without an input of light energy depending on the particular electron

donor used. By contrast, in photosynthesis of green plants, the reduction of pyridine nucleotide invariably requires an input of light energy because the physiological electron donors are hydroxyl ions from water. A comparison of photosynthetic phosphorylation in green plants and photosynthetic bacteria is given in Table 3.

TABLE 3

PHOTOSYNTHETIC PHOSPHORYLATION

GREEN PLANTS	PHOTOSYNTHETIC BACTERIA
noncyclic photophosphorylation:	
a) $2A + 2OH^- \xrightarrow{Cl^-} 2A^- + H_2O + {}^1/_2O_2$	
b) $TPN + 2H^+ + ADP + P + 2A^- \rightarrow TPNH_2 + ADP + 2A$	$DPN + 2H^+ + ADP + P + 2A^- \rightarrow DPNH_2 + ATP + 2A$
Sum:	
$TPN + 2H^+ + ADP + P + 2OH^- \xrightarrow{Cl^-} TPNH_2 + ATP + H_2O + {}^1/_2O_2$	$DPN + 2H^+ + ADP + P + 2A^- \rightarrow DPNH_2 + ATP + 2A$
cyclic photophosphorylation:	
$ADP + P \rightarrow ATP$	$ADP + P \rightarrow ATP$

It now appears that plants, but not photosynthetic bacteria, are able to use hydroxyl ions as electron donors in photosynthesis because plants have evolved an additional pigment system[2] and an auxiliary light-dependent reaction[20] in which the electrons from OH^- are first raised to a potential similar to that of the electron donors in bacterial photosynthesis and are then used in a second photochemical reaction—i.e. the photophosphorylation reaction proper common to plants and bacteria—in which pyridine nucleotide reduction is coupled with the formation of ATP.

* Aided by grants from the National Institutes of Health and the Office of Naval Research.

[1] The following abbreviations are used: ATP, adenosine triphosphate; ADP, adenosine diphosphate; P, orthophosphate; PN, PNH_2, DPN, $DPNH_2$, oxidized and reduced forms of pyridine nucleotide and diphosphopyridine nucleotide; DPIP, 2,6-dichlorophenol indophenol.

[2] Arnon, D. I., M. Losada, F. R. Whatley, H. Y. Tsujimoto, D. O. Hall, and A. A. Horton, these PROCEEDINGS, **47,** 1314 (1961).

[3] Arnon, D. I., in *Light and Life*, ed. W. D. McElroy and B. Glass (Baltimore: Johns Hopkins Press, 1961), p. 489.

[4] Losada, M., A. V. Trebst, S. Ogata, and D. I. Arnon, *Nature*, **186,** 753 (1960).

[5] Stanier, R. Y., *Bacteriol. Rev.*, **25,** 1 (1961).

[6] Frenkel, A. W., in *The Photochemical Apparatus*, Brookhaven Symposia in Biology, No. 11 (1958).

[7] Vernon, L. P., and O. K. Ash, *J. Biol. Chem.*, **234,** 1878 (1959).

[8] *Ibid.*, **235,** 2721 (1960).

[9] Gest, H., M. D. Kamen, and H. M. Bregoff, *J. Biol. Chem.*, **182,** 153 (1950).

[10] Arnon, D. I., M. B. Allen, and F. R. Whatley, *Biochim. et Biophys. Acta*, **20,** 449 (1956).

[11] Anderson, I. C., and R. C. Fuller, *Archiv. Biochem. Biophys.*, **76,** 168 (1958).

[12] Geller, D. M., "Photophosphorylation by *Rhodospirillum rubrum* preparations," Doctoral Dissertation, Harvard University (1957).

[13] Geller, D. M., and F. Lipmann, *J. Biol. Chem.*, **235,** 2478 (1960).

[14] Smith, L., and M. Baltscheffsky, *ibid.*, **234,** 1575 (1959).

[15] Baltscheffsky, H., and M. Baltscheffsky, *Acta Chemica Scand.*, **14,** 257 (1960).

[16] Arnon, D. I., *Federation Proc.* (in press).

[17] Losada, M., M. Nozaki, and D. I. Arnon, in *Light and Life*, ed. W. D. McElroy and B. Glass (Baltimore: Johns Hopkins Press, 1961), p. 570.

[18] Arnon, D. I., M. Losada, M. Nozaki, and K. Tagawa, *Biochem. J.*, **77,** 23 P (1960).

[19] Arnon, D. I., M. Losada, M. Nozaki, and K. Tagawa, *Nature*, **190,** 601 (1961).

[20] Losada, M., F. R. Whatley, and D. I. Arnon, *Nature*, **190,** 606 (1961).

AN INTERPRETATION OF THE KINETIC BEHAVIOR OF MODEL SUBSTRATES OF α-CHYMOTRYPSIN†*

By George Hein and Carl Niemann

California Institute of Technology

Communicated July 24, 1961

Reactions catalyzed by α-chymotrypsin involve substrates whose structures and molecular dimensions may vary over wide limits.[1] It has become increasingly evident with polypeptide and protein substrates that the pattern of action observed for this enzyme is not entirely predictable from present knowledge of the behavior of the acylated α-amino acid derivatives used as models for these higher-molecular-weight substrates. While the results from these two sources must eventually be reconciled and correlated with a postulated active site of limited dimensions, this problem is of less immediate concern than the interpretation of interactions of substrates and inhibitors of widely varying structure but with molecular dimensions which approximate those of a postulated active site.

For α-chymotrypsin the experimental evidence for an active site of limited dimensions is based upon: (*a*) loss of catalytic activity of the enzyme, with respect to protein and ester type substrates, upon reaction with diisopropylphosphorfluoridate under conditions where diisopropylphosphorylation of the enzyme proceeds with approximately 1:1 molecular stoichiometry; (*b*) mediation of the preceding reaction by compounds known to be totally competitive inhibitors of the α-chymotrypsin catalyzed hydrolysis of acylated α-amino acid derivatives; (*c*) studies analogous to those described in (*a*) and (*b*) above but involving *p*-nitrophenyl acetate rather than diisopropylphosphorfluoridate; and (*d*) the observation that many substrate-inhibitor and a few substrate-substrate pairs of varying molecular structure, including inhibitors used in (*b*) and (*c*) above, interact with the enzyme at loci sufficiently close to each other so that totally competitive inhibition is observed.[2–4] While the preceding chain of evidence is still incomplete, it is sufficiently well founded to justify interpretation of α-chymotrypsin catalyzed reactions involving substrates and inhibitors of modest molecular dimensions in terms of interactions occurring at a single active site.

Possible Kinetic Interpretations.—For model synthetic substrates the primary data, the dependence of the rate of the over-all reaction upon enzyme [E] and initial substrate [S] concentrations is described by equation (1).

$$-d\,[\mathrm{S}]/dt = d\,[\mathrm{P}]/dt = k_0\,[\mathrm{E}][\mathrm{S}]/(K_\mathrm{O} + [\mathrm{S}]) \qquad (1)$$

Without regard to the interpretation of the two constants, K_O and k_0, of equation (1), it is possible to decide whether any relationship exists between them. Table 1 lists variations in values of K_O for ranges of values of k_0 observed for 45 representative substrates of α-chymotrypsin. It is apparent that low K_O values are compatible with any k_0 value, while high K_O values are possible for all k_0 values except the highest and lowest. However, the latter observation may only illustrate experimental limitations. It follows from equation (1) that values of K_O will tend to be inversely proportional to the rate of reaction while those of k_0 will be directly proportional to it. Thus, a low k_0 and a high K_O value would indicate a very slow

TABLE 1

RELATION OF VALUES OF K_O TO THOSE OF k_0*

k_0† × 10^3	No. of substrates	K_O‡ × 10^3
10^4–10^3	2	1.1–0.7
10^3–10^2	6	5.7–0.09
10^2–10	3	611–2.9
10 –1	18	177–1.37
1 –0.1	14	460–2.42
0.1 –0.01	2	9.8–0.25

* Of 45 representative substrates of α-chymotrypsin whose constants are given in Tables 2 through 6.
† In units of M/min/mg protein-nitrogen per ml.
‡ In units of M.

reaction, probably one too slow to evaluate. Alternatively, few high k_0 values have been observed and experimental difficulties, such as the limited solubilities of many substrates in water, make it reasonable to assume that high values for both K_O and k_0 will not be observed frequently, if at all. Thus, except for a possible, but unlikely, requirement of a low K_O value for a high k_0 value there is no parallel between observed K_O and k_0 values for an extensive series of substrates of α-chymotrypsin.

Equation (1) can be represented by a number of kinetic paths leading to an interpretation of the constants K_O and k_0. We shall consider three that appear to be the most pertinent.

The simplest is given by equation (2)

$$E + S \underset{k_{-1}}{\overset{k_1}{\rightleftharpoons}} ES \xrightarrow{k_2} E + P \tag{2}$$

where $K_O = K_S = (k_{-1} + k_2)/k_1$ and $k_0 = k_2$. This representation suffers from the oversimplification of considering only a single, irreversible step leading to products from a single enzyme-substrate complex. Another hazard lies in the unsupported assumption that K_S is necessarily at or close to one of its two limits, i.e., $K_S \doteq k_{-1}/k_1$ or k_2/k_1.

The second representation is given by equations (3) and (4)

$$E + S \underset{k_{-1}}{\overset{k_1}{\rightleftharpoons}} ES \xrightarrow{k_2} E + P \tag{3}$$

$$E + S \underset{k_{-4}}{\overset{k_4}{\rightleftharpoons}} ES' \tag{4}$$

where $K_S = (k_{-1} + k_2)/k_1$ and $K_{S_1} = k_{-4}/k_4$. In this instance it is assumed that the substrate may combine with the enzyme in two ways, one producing products and the other totally competitive with the first and unproductive. This leads to a rate equation identical in form to equation (1) but with $k_0 = k_2K_{S_1}/(K_S + K_{S_1})$ and $K_O = K_SK_{S_1}/(K_S + K_{S_1})$. With the requirement that K_O, K_S, and K_{S_1} all be positive, then both K_S and $K_{S_1} > K_O$. If either K_S or K_{S_1} are significantly smaller than each other, then K_O, the observed value, will tend to approximate the lower value. Similarly, k_0, the observed value, will be smaller than k_2 whenever K_{S_1} becomes appreciably smaller than K_S, otherwise k_0 will approximate k_2.

The third and final representation, given in equation (5),

$$E + S \underset{k_{-1}}{\overset{k_1}{\rightleftharpoons}} ES \xrightarrow{k_2} ES' + P_1 \xrightarrow{k_3} E + P_2 \tag{5}$$

has been proposed for the case of an acyl-enzyme intermediate,[5] but need not be restricted to this particular interpretation. The over-all reaction is again described by equation (1) but in this instance $k_0 = [k_2k_3/(k_2 + k_3)]$ and $K_O = [(k_{-1} + k_2)/k_1][k_3/(k_2 + k_3)]$. The inclusion of two irreversible steps leading to products adds a further source of ambiguity to the interpretation of K_O and k_0. In this case when $k_3 \doteq k_2$, $k_{-1} > k_2$ and $k_1 \geqslant k_3$ an increase in the value of k_0 will cause a decrease in the value of K_S. This is in contrast to the more common Michaelis-Menton representation of equation (2) and its extension in equations (3) and (4), where an increase in k_0 can only cause an increase in K_O if it effects K_O at all.

Structures of Substrates.—Although no simple relation between K_O and k_0 is observed, it is desirable to attempt a correlation between the magnitudes of these constants and variations in structure of groups of substrates. Such an interpretation must bear in mind the complexities inherent in the kinetic expressions employed to describe the experimental results, as outlined above.

The substrates we wish to consider are largely acylated α-amino acid derivatives or analogues of these compounds. Their structures may be represented by the formula $R_1CHR_2COR_3$ where, R_1 is the α-acylamino group, which occasionally will be represented as $R_1'CONH$, R_2 the α-amino acid side chain, and R_3 the functional derivative of the carboxyl group that, for substrates, is transformed into reaction products. The formulas $R_1CHR_2COR_3$ and $R_1'CONHCHR_2COR_3$ provide a convenient basis for the identification of a relatively large number of substrates of α-chymotrypsin but they are not to be interpreted as defining the scope of action of this enzyme. It is not our present intention to catalogue all known substrates of α-chymotrypsin, but to arrive at a set of generalizations that can be used for correlating the structures and kinetic behavior of substrates of the above formulae where $R_2 \neq H$.

Acylated α-Amino Acid Esters.—As a first approximation we assume with some justification that values of K_O may be taken as indices of the degree to which substrates are bound to the active site.[5] The question then arises as to the extent to which each of the structural components $R_1 = R_1'CONH$, R_2 and COR_3 contribute to an observed value of K_O. Since COR_3 clearly participates in the over-all reaction of a substrate, it is appropriate that we first direct attention to the relation between values of K_O and the nature of R_3.

It is seen from the data given in Table 2[3, 6–10] that when $R_1 = CH_3CONH$ and $R_2 = p\text{-}HOC_6H_4CH_2$ the variation of K_O is *ca.* 160 fold but, excluding $R_3 = OC_2H_5$, is less than 5 fold. Considering only those compounds where $COR_3 = CONHR$ leads to a mean value of 38 ± 23 for K_O,[11] a relatively small variation consistent

TABLE 2

EFFECT OF COR_3 IN L-$R_1'CONHCHR_2COR_3$ ON VALUES OF K_O AND k_0

$R_1' = CH_3$; $R_2 = p\text{-}HOC_6H_4CH_2$

R_3	K_O*	k_0†	Ref.
OH	110	v. small	3
$NHCH_3$	61	small	6
$NHNH_2$	30	1.1	7
NH_2	32	2.4	3
$NHCH_2CONH_2$	23	7.5	8
NHOH	43	33	3
OC_2H_5	0.7	2,900, 4,400	9, 10

* In units of 10^{-3} M

† In units of 10^{-3} M/min/mg protein-nitrogen per ml.

with the structural similarity of these members of the larger series. Thus, in addition to its more obvious role in determining the magnitude of k_0, COR_3 may contribute to the binding of substrate, substantially when $R_3 = OC_2H_5$ and less when $COR_3 = CONHR$.

It can be argued that the decrease in the value of K_O observed for $R_3 = OC_2H_5$, relative to that for $R_3 = NH_2$ is simply a consequence of a change in the relative magnitudes of k_2 and k_3 of equation (5) and that the value of K_O for $R_3 = OC_2H_5$ no longer approximates k_{-1}/k_1. With $K_O = K_S(k_3/(k_2 + k_3))$, $K_O \doteq K_S$ when $k_3 > k_2$ but $K_O < K_S$ when $k_2 \geqslant k_3$. However, in order that the steady-state assumption inherent in the preceding relation is not violated, i.e., for equation (5) to remain valid, $k_3 \geqslant k_2$ and thus the minimum $K_O \doteq K_S/2$. Thus, while we cannot exclude the possibility that when $k_2 \doteq k_3$ the value of K_O may be less than that of K_S we can assert that this effect cannot by itself account for the drastically lower K_O values observed when $R_3 = OC_2H_5$ than when $R_3 = NHR$ and that simple ester groups contribute substantially to decreasing values of K_O compared to the corresponding amides and related compounds. Further evidence for this assertion is found in the K_O and k_0 values of substrates with $R_1 = CH_3CONH$, $R_2 = (CH_3)_2CHCH_2$, $(CH_3)_2CH$, and CH_3, and $R_3 = OCH_3$, OC_2H_5, $OCH(CH_3)_2$, and OCH_2CH_2Cl (cf. Table 3).[9, 10, 12–17] The corresponding compounds with $R_3 = NHR$

TABLE 3

VALUES OF K_O AND k_0 FOR ESTERS OF L-R_1'CONHCHR_2COR$_3$ WHERE $R_2 \neq H$

R_2	R_1'	R_3	K_O*	k_0†	Ref.
β-(C_8H_6N)CH_2	CH_3	OC_2H_5	0.09	760	9
p-$HOC_6H_4CH_2$	CH_3	OC_2H_5	0.7	2,900, 4,400	9, 10
	C_6H_5	OC_2H_5	(3.9)	(820) 30% methanol	12
$C_6H_5CH_2$	H	OCH_3	0.25	0.05 D-antipode	...
	CH_3	OCH_3	1.8	918	13
	CH_3	OC_2H_5	1.1	2600	14
	C_6H_5	OCH_3	(4.3)	(530) 30% methanol	12
	C_6H_5	OC_2H_5	(5.7)	(390) 20% methanol	12
$(CH_3)_2CHCH_2$	CH_3	OCH_3	2.9	67	...
$(CH_3)_2CH$	CH_3	OCH_3	117	2.26	15, 16
	CH_3	OC_2H_5	110	1.93	15
	CH_3	$OCH(CH_3)_2$	177	1.22	15
	CH_3	OCH_2CH_2Cl	19	3.32	15
	CH_2Cl	OCH_3	39	1.6	15, 16
	C_6H_5	OCH_3	4.3	0.65	15, 16
CH_3	CH_3	OCH_3	611	19	17
	C_6H_5	OCH_3	9.8	3.8	...
	C_6H_5	OCH_3	3.2	0.155 D-antipode	...

* In units of 10^{-3} M.
† In units of 10^{-3} M/min./mg protein-nitrogen per ml.

not only are not substrates, or very poor ones, but also have K_I values so high as to be indeterminable when evaluated as inhibitors.[18]

A second conclusion to be drawn from the data summarized in Table 3 is that while COR_3 may make a substantial contribution to the binding of substrate to the active site, the magnitude of this effect is dependent upon the nature of R_2. In general, the magnitude of K_O increases with decreasing size of the R_2 component. The data for the valine derivatives are also instructive in that their uniformly low k_0 values, relative to those of the corresponding leucine and alanine derivatives,

coupled with the individual K_O and k_0 values for the four acetyl valine esters implicate the carbonyl group of COR_3 as a binding locus.

For the acylated aromatic α-amino acid esters it is evident that both R_2 and COR_3 contribute in a major way to the binding of substrate. A question remains as to the relative contribution of $R_1 = R_1'CONH$ for this class of compounds. A direct answer cannot be provided because the only information available is for reactions in 20–30 per cent methanol, a solvent known to cause a substantial increase in K_O and a decrease in k_0 values of esters.[19] However, from the values given in Table 3 for $R_1' = CH_3$ and C_6H_5, $R_2 = p\text{-}HOC_6H_4CH_2$ or $C_6H_5CH_2$, and $R_3 = OCH_3$ or OC_2H_5 we conclude that the K_O values for the benzoyl derivatives, even when corrected for the above solvent effect, will approximate those of the corresponding acetyl derivatives and for this class of substrates R_1 does not contribute significantly to the binding of substrate except in a stereochemical sense.

Types of Binding and Limit Cases.—In examining the role of R_1, R_2, and COR_3 in binding substrate to the active site, it is necessary to distinguish between forces which assure orientation of the substrate and those of sufficient magnitude to decrease the dissociation constant of a complex. It is in this latter sense that R_2 and COR_3 are of major importance for the acylated aromatic α-amino acid esters and R_1 is relatively unimportant whereas in the former all three assume significance. The fact that the degree of stereospecificity ordinarily observed is radically decreased when $R_1 = H$, $R_2 = C_6H_5CH_2$, and $R_3 = OCH_3$, indicates that the size of R_1' must be at least that of a methyl group if $R_1'CONH$ is to be reasonably effective in a stereochemical sense for this class of substrates.

Turning to the acylated aliphatic α-amino acid esters listed in Table 3 it is seen that R_1 assumes a role different from that noted above in that the magnitudes of the K_O values when $R_2 = (CH_3)_2CH$ or CH_3 and $R_3 = OCH_3$ are in the order $R_1' = CH_3 > CH_2Cl > C_6H_5$, the difference between $R_1' = CH_3$ and C_6H_5 being *ca.* 30 fold for $R_2 = (CH_3)_2CH$ and *ca.* 60 fold for $R_2 = CH_3$.

From the preceding observations we can recognize two limiting situations for the acylated α-amino acid ester type of substrate. In one the dissociation constant is primarily determined by R_2 and COR_3 while R_1 is effective primarily in its stereochemical orienting role. In the other, where R_2 is no longer an aromatic side chain or its steric equivalent, the roles of R_1 and R_2 are reversed, the former contributing to binding while the latter, smaller substituent is reduced to an orienting role. For convenience we shall represent substrates of the first limiting type by $S^{3E}_{R_2R_3}$ and those of the second by $S^{3E}_{R_1R_3}$.[20]

From the values of K_O and k_0 given in Table 3 it is evident that substrates of the $S^{3E}_{R_2R_3}$ limit type are characterized by low K_O and high k_0 values. This implies that substrates of this type, involving minimal contribution of the R_1 group to the overall binding energy other than that required for its stereochemical function, are effectively bound to the active site and that the orientation of the substrate in the complex is such as to permit formation of products at a rapid rate. On the other hand, for substrates of the $S^{3E}_{R_1R_3}$ limit type K_O values are markedly dependent upon R_1, and when effective combination with the active site is achieved, as indicated by a low K_O value, it is at the expense of a diminished k_0 value. In the transition $S^{3E}_{R_1R_3} \rightarrow S^{3E}_{R_1R_2R_3} \rightarrow S^{3E}_{R_2R_3}$ increasing participation of R_2 in the binding process, generally increasing with the size of R_2, will be reflected in decreasing values of K_O

and increasing values of k_0. Statements about the "specificity" of α-chymotrypsin, and its preference for aromatic amino acid substrates[1] refer to the effectiveness of $S^{3E}_{R_2R_3}$ type substrates, compared to the $S^{3E}_{R_1R_3}$ type.

With substrates of the $S^{3E}_{R_1R_3}$ limit type a decrease in K_O determined by R_3 is accompanied by an increase in k_0. The opposite behavior is observed when a decrease in K_O is determined by R_1.

Substrates of type $S^{3E}_{R_2R_3}$ are approximated when R_2 = p-$HOC_6H_4CH_2$, $C_6H_5CH_2$, or β-$(C_8H_6N)CH_2$ and R_3 = OCH_3, or OC_2H_5. However, within this series there are several discordant values of K_O and k_0. It is unfortunate that lack of agreement as to the k_0 value of acetyl-L-tyrosine ethyl ester does not permit a decision as to whether the k_0 value is approximately equal to or significantly greater than that of the corresponding phenylalanine derivative. While the latter possibility is indicated by the behavior of the analogous benzoyl derivatives the values are for different solvent systems. The only clear anomaly is the low value of k_0 for ethyl acetyl-L-tryptophanate associated with the lowest K_O value of the series. This suggests that the observed K_O and k_0 values may not be those of equation (2) but instead those derived from equations (3) and (4). If it is assumed that $k_2 \doteq k_0$ for the analogous phenylalanine derivative, the relation $K_O = k_0K_S/k_2$ leads to a value of 3.8 for K_S and the implication that a low K_{S_1} value due to effective, nonproductive combination overides the K_S value in determining K_O and is responsible for the low k_0 value. This interpretation is consistent with the anomalous behavior observed for the system acetyl-L-tryptophanmethylamide and methyl hippurate[18] and the hydrolysis of methyl acetyl-D-tryptophanate at high enzyme concentrations.[21]

In order that a substrate approximate the $S^{3E}_{R_1R_3}$ limit type R_2 must be only of sufficient size to fulfil its stereochemical function but it must be sufficiently small not to give a substrate within the zone between the $S^{3E}_{R_1R_3}$ and $S^{3E}_{R_2R_3}$ limit types. It is evident from the data given in Table 3 for methyl benzoyl-D- and L-alaninate that R_2 must be larger than CH_3 to insure the degree of stereospecificity which can be observed for the $S^{3E}_{R_1R_3}$ type when R_1 = C_6H_5CONH, R_3 = OCH_3, and R_2 = $(CH_3)_2CH$. The decrease of stereochemical specificity when R_2 = CH_3 in the $S^{3E}_{R_1R_3}$ limit case is analogous to the same occurrence in the $S^{3E}_{R_2R_3}$ limit case when R_1' = H.

Peptides and Acylated Amino-Acid Amides.—The wide range of data available for the acylated α-amino acid esters suggests that these compounds are more suitable models than the corresponding amides for predicting the course of an α-chymotrypsin catalyzed proteolysis, granting the independent knowledge that in all cases hydrolysis will be limited to peptide bonds involving only α-amino acids. The interpretation given above predicts that cleavage of all peptide bonds involving the carboxyl group of aromatic α-amino acid residues will occur irrespective of their position in the peptide chain and that cleavage of peptide bonds involving the carboxyl group of all other amino acid residues will be dependent upon the size of the side chain and the nature of the adjacent amino acid residues. In the latter case, an observable rate of hydrolysis requires increased size of the side chain, enhanced binding capacity of the extended R_1 moiety or a diminished steric contribution of the R_3 moiety.

The data given in Tables 2 and 4[3, 7, 22–25] and the knowledge that acylated ali-

TABLE 4

VALUES OF K_O AND k_0 FOR AMIDES OF L-R_1'CONHCHR_2COR_3 WHERE $R_2 \neq H$

R_2	R_1'	R_3	K_O*	k_0†	Ref.
β-(C_8H_6N)CH_2	CH_3	NH_2	5.0	0.55	3
	β-C_6H_4N	NH_2	2.5	1.5	3
p-$HOC_6H_4CH_2$	H	NH_2	12	0.45	3
	CH_3	NH_2	32	2.6	3
	CF_3	NH_2	26	2.4	3
	C_2H_3O	NH_2	7	0.85	22
	CH_2Cl	NH_2	27	4.0	3
	β-C_6H_4N	NH_2	12	5.0	3
	α-C_6H_4N	NH_2	9.2	6.4	3
	C_6H_5	NH_2	2.5	4.0	3
$C_6H_5CH_2$	CH_3	NH_2	31	0.8	3
	β-C_6H_4N	NH_2	19	2.0	3
$C_6H_{11}CH_2$	CH_3	NH_2	27	0.65	23
p-$HOC_6H_4CH_2$	H	$NHNH_2$	9.8	0.058	24
	CH_3	$NHNH_2$	29.5	1.1	7
	$CHCl_2$	$NHNH_2$	5.2	0.7	24
	$C(CH_3)_3$	$NHNH_2$	40	0.4	24
	β-C_6H_4N	$NHNH_2$	8	0.84	25
	C_6H_5	$NHNH_2$	2.2	0.5	24

* In units of 10^{-2} M.
† In units of 10^{-3} M/min/mg protein-nitrogen per ml.

phatic α-amino-acid amides are hydrolyzed slowly, if at all,[1] suggests that with the acylated aromatic α-amino acid amides R_2 has an important role in diminishing the dissociation constant of the complex in which orientation of the substrate is determined by R_1, R_2, and R_3. A choice between R_1 or R_3 as the other major binding component is difficult because of the narrow limits observed for variation of K_O with R_1'; of the order of 13 fold for the amides and hydrazides compared with less than 3 fold for the substituted amides of Table 2. As a first approximation the acylated α-amino acid amides of Table 4 will be regarded as approximating the $S^{3A}_{R_1R_2}$[26] limit type to a greater degree than the type $S^{3A}_{R_2R_3}$ and in this respect differ from the corresponding esters of Table 3.

For the eight substrates of Table 4 where $R_2 = p$-$HOC_6H_4CH_2$ and $R_3 = NH_2$, variation of the ratio k_0/K_O is approximately 40 fold and increases nonlinearly with decreasing values of K_O. Two exceptions are $R_1' = H$ and C_2H_3O where the k_0/K_O ratios are lower than expected from the relationship just noted. Furthermore, the k_0 values for those two substrates are exceptionally low when compared with those of other members of the series. These two features suggest that in a formal sense both substrates combine with the active site of the enzyme in two ways, only one of which leads to products, the other being totally competitive with the first and nonproductive. If it is assumed that K_O and k_0 observed for these derivatives are derived from equations (3) and (4) instead of K_S and k_2 values of equation (2) and that the K_S value of each is approximated by the K_O values of the derivatives immediately preceding or following it in Table 4, values of k_2 can be obtained from the relation $k_0 = K_O k_2/K_S$. This treatment gives k_2 values of 1.8 and 3.1 or 3.2 for the formyl and carbethoxy derivatives, respectively. These results are now consistent with those of other members of the series.

The view that the values of K_O and k_0 for the formyl derivative are low because they represent two modes of combination with the value of K_{S_i} lower than that of K_S is supported by other considerations. It can be argued that the size of the R_1', or R_1, group of the formyl derivative is sufficiently small to allow access to non-

productive modes of combination that are not accessible to analogous L-antipodes containing R_1 groups of larger size. Thus, the low K_O and k_0 values observed for the formyl derivative should be associated with a diminished stereospecificity. This is supported by the observation that not only formyl L-phenylalanine methyl ester but also the D-antipode are substrates under conditions where acetyl-D-phenylalanine methyl ester is not a substrate.

Alternative, nonproductive binding of the carbethoxy derivative can arise if the ester function in R_1 can interact with ρ_3, the locus at the site otherwise involved in interaction with COR_3.[27, 28]

The variation in values of K_O and k_0, excluding those of the formyl and carbethoxy derivatives is remarkably small, less than 13 and 3 fold, respectively. While there is a tendency for k_0 to increase as K_O decreases, the trend is not uniform. If the values of the acetyl and nicotinyl derivatives are taken as representative indicators of variation in K_O and k_0 when $R_2 = p\text{-}HOC_6H_4CH_2$ and $R_3 = NH_2$ the trend noted above is maintained when $R_2 = C_6H_5CH_2$ or $\beta\text{-}(C_5H_6N)CH_2$ and $R_3 = NH_2$. However, for $R_2 = p\text{-}HOC_6H_4CH_2$ and $R_3 = NHNH_2$ a decrease in the value of K_O has little or no effect upon the value of k_0. The only element of consistency in the behavior of the acylated-L-tyrosinamides and hydrazides is that both formyl derivatives have relatively low K_O values and exceptionally low k_0 values.

The fact that the K_O values of the acylated-L-tyrosinamides and hydrazides are dependent upon the nature of R_1' but the dependence of k_0 upon R_1' is different for the amides and hydrazides may be explained on the basis of a greater participation of the R_3 group in the binding process in the case of the amides, a not unreasonable assumption in view of the generally higher k_0 values of amides relative to hydrazides and the behavior noted previously in the transition from $S^{3E}_{R_1R_3} \rightarrow S^{3E}_{R_1R_2R_3} \rightarrow S^{3E}_{R_2R_3}$ for the acylated aliphatic amino acid esters.

Structural Factors Other than Size.—In the preceding discussion binding energies have been related to the size of the R_1' and R_2 groups although for the COR_3 group attention has been directed to evidence indicating participation of the carbonyl group *per se*. While size in the case of the R_1' and R_2 groups remains a good approximation, if steric implications are considered, there is evidence for factors of a more subtle nature. For $R_1' = CH_2Cl$, $\beta\text{-}C_5H_4N$, or $\alpha\text{-}C_5H_4N$ differences in values of K_O and k_0 are observed beyond those anticipated on the basis of size alone. Similarly with R_2, although acetyl-L-phenylalaninamide and the corresponding cyclohexyl derivative are kinetically indistinguishable, acylated-L-tyrosine derivatives have k_0 values greater than those of the analogous phenylalanine derivatives and it has been noted that aromatic inhibitors have lower K_I values than the corresponding hydroaromatic compounds. However, discussion of these more detailed features will not be attempted here and instead attention will be restricted to structural features associated with variations in K_O and k_0 of an order of magnitude difference or more.

From Table 2 it is seen that the dependence of k_0 upon R_3 is in the order expected for a reaction whose rate increases with increasing polarizability of the carbonyl group of COR_3. While the detailed mechanism of the bond breaking process is obscure, we concur with the view that reaction involves concerted attack on the carbonyl group of COR_3 by nucleophilic and electrophilic groups of the active site.[29] The question of the reality of an acyl enzyme intermediate for the substrates herein

TABLE 5

VALUES OF K_O AND k_0 FOR SUBSTRATES OF TYPE $R_2ACO_2CH_2$ | CH_3COB

Configuration	R_2	A	B	K_I*	K_O*	k_0†	Ref.
L	$C_6H_5CH_2$	CH	NH	...	1.8	918	13
D	$C_6H_5CH_2$	CH	NH	2.5	...	...	3
(+)	$C_6H_5CH_2$	CCH_3	NH	8.7	...	0.01	30
(−)	$C_6H_5CH_2$	CCH_3	NH	8.2	...	0.01	30
L	p-$HOC_6H_4CH_2$	CH	NCH_3	...	...	very unreactive substrate	31
...	$C_6H_5CH_2$	N	NH	20	...	...	32
(±)	$C_6H_5CH_2$	CH	CH_2	...	0.49	0.91	33
L	CH_3	CH	NH	...	611	19	17
(±)	CH_3	CH	CH_2	...	460	0.30	33
(−)	CH_3	CH	CH_2	...	141	0.17	33

* In units of 10^{-3} *M*.
† In units of 10^{-3} *M*/min/mg protein-nitrogen per ml.

considered is, in our opinion, still an open one.

In Table 5[3, 13, 17, 30–33] are listed compounds that provide examples of order of magnitude effects not previously considered. The first four relate to replacement of the α-hydrogen atom of $R_1'CONHCHR_2COR_3$ by a methyl group. While this structural change reduces the value of k_0 by a factor greater than 10^4, the increase in K_O, actually evaluated as K_I, is only about 5 fold. The implication is that this structural change does not markedly effect combination of the substrate with the active site but does depress the value of k_0, possibly by distortion of the position of the substrate in the complex and probably by interfering with either nucleophilic or electrophilic attack on the carbonyl group of COR_3.

The consequences of replacement of the α-amido hydrogen atom by a methyl group are not known beyond the point that this structural change converts a very reactive substrate into a slightly reactive one. Preliminary experiments with α-N-methyl acetyl-L-tyrosinamide suggest that this behavior is due primarily to a large decrease in the value of k_0.

Replacement of the α-CH group by a nitrogen atom abolishes substrate activity and the K_I value for the inhibitory nitrogen analogue is an order of magnitude greater than the K_O value of the analogous substrate. Models of the former compound, containing two planar amide bonds, show that its stereochemical features are very different from those of the analogous substrate and it may be inferred that orientation of the inhibitor in the complex differs markedly from that of the related substrate. Further evidence relating substrate activity of compounds of the type $R_1CHR_2COR_3$ with a tetrahedral disposition of R_1, R_2, and COR_3 was obtained when it was found that methyl α-acetamido acrylate was incapable of functioning as a substrate.[17]

For substrates approximating the $S^{3E}_{R_2R_3}$ limit type it has been assumed that the role of $R_1 = R_1'CONH$ is largely restricted to orientation of the substrate and contributes only in a minor way to the dissociation constant of the complex leading to products. Replacement of the α-amido NH by a CH_2 group, in a substrate approximating the $S^{3E}_{R_2R_3}$ limit type, cf. Table 5, results in less than a 4-fold increase in the value of K_O for the DL-analogue but a decrease in the corresponding value of k_0 of the order of 10^3. While these data are more ambiguous than those for a pair of antipodes, they establish the point that the NH group in $R_1'CONH$ is a critica

structural element of R_1 with respect to the effectiveness of the latter in orienting the substrate at the active site. Similar results have been obtained for the corresponding alanine derivatives where for methyl acetyl-L-alaninate the substrate may approximate the $S^{3E}_{R_1R_2}$ limit type. The two antipodes of the analogue where $R_1 = CH_3CONH$ is replaced by $R_1 = CH_3COCH_2$ and $R_2 = CH_3$ show a substantial loss in stereospecificity, a relatively large difference in the K_O values and a relatively small difference in k_0 values. This behavior is characteristic of the situation represented by equations (3) and (4). Thus, the decrease in values of k_0 by several orders of magnitude when $R_1 = R_1'CONH$ is replaced by $R_1 = R_1'COCH_2$ is a consequence of an increased incidence of unproductive modes of combination that are competitive with those leading to products.

Other structural modifications of substrates of the type $R_1'CONHCHR_2COR_3$ than those considered above are known to lead to order of magnitude consequences. When $R_1' = CH_3$ and $R_3 = OCH_3$ DL-compounds with $R_2 = (CH_3)_3C$ or $C_6H_5C(CH_3)_2$ are no longer substrates and the L-compound with $R_2 = 1\text{-HO-}3,5(CH_3)_2\text{-}C_6H_2CH_2$ is hydrolyzed much less rapidly than when $R_2 = 1\text{-}HOC_6H_4CH_2$.[34] These qualitative observations are consistent with the behavior noted previously for the analogous valine derivatives.

Replacement of $R_1 = R_1'CONH$ by $R_1 = NH_2$; NH_3^+, when $R_2 = p\text{-}HOC_6H_4CH_2$ or $C_6H_5CH_2$ and $R_3 = OCH_3$ or OC_2H_5, results in a marked decrease in the rate of hydrolysis as well as a partial loss of stereospecificity which normally favors the L-antipode. The absence of unambiguous kinetic data does not permit comment beyond the fact that such behavior is not unexpected and is in accord with other results involving diminished size of R_1 groups, starting with HCONH and decreasing to OH and Cl.[12]

There are examples of alteration of the COR_3 group in which the carbonyl oxygen atom is replaced by another atom or group. In both cases involving $R_1' = CH_3$, $R_2 = C_6H_5CH_2$, and COR_3 replaced by CNH(NHOH); $CNH_2(NOH)$, or $CSNH_2$ neither of the L-antipodes are substrates and their K_I values are approximately equal to or less than the K_O values of the corresponding carbonyl derivatives.[15, 35] The implication is that neither of the above replacements have a profound influence on the ability of those compounds to combine with the active site, which is in accord with the interpretation given previously for the corresponding amides, hydrazides, and hydroxamides, but that transformation into products is excluded for other reasons.

Generalizations.—In the preceding discussion attention has been directed to substrates of the type $R_1CHR_2COR_3$ possessing the L-configuration. The kinetic properties of these substrates have been interpreted on the basis of the following generalizations.

Interaction of substrate with the asymmetric active site of the enzyme proceeds with R_1, R_2, and COR_3 and the configuration about the asymmetric carbon atom of the substrate determining its orientation at the active site. However, not all of these interactions need contribute significantly to the dissociation constant of the complex. Supplementary to the preceding interaction in which incipient orientation of the substrate is achieved, one or more of the three groups R_1, R_2, and COR_3 interact with their complementary loci on the active site to decrease the dissociation constant of the complex maintaining the previously determined orientation of the

substrate. In three limit cases, two of which have been discussed above, only two of the three groups are so bound. Pictorially:

$$\left.\begin{array}{l} \\ S^3R_1R_2R_3 \rightarrow S^3R_1R_3 \\ \\ \end{array}\right\} \text{Arbitrary "Limit" Types}$$

Orientation Binding

In the interpretation of values of K_O and k_0 it was assumed that values of K_O were apparent dissociation constants and that whenever K_O and k_0 values significantly lower than those of other members of a structurally related series of substrates were encountered the anomalous values were K_O and k_0 values derived from equations (3) and (4) rather than K_S and k_2 values of equation (2).

Substrates approximating several of the limit types have been identified, and as a first approximation binding effectiveness has been related to the size of R_1 and R_2 and polarizability of the carbonyl group of COR_3. Further, within each group, attention has been directed to additional structural features that appear to play a significant role; e.g., the CONH group in R_1, aromatic structures in R_2, and the carbonyl group in COR_3.

It was concluded that a substrate of the $S^3_{R_2R_3}$ limit type is characterized by a nonlinear increase in values of k_0 with decreasing values of K_O whereas with one of the $S^3_{R_1R_3}$ limit type a decrease in K_O is accompanied by a decrease in k_0 that may be minimized by increasing participation of R_2 in the binding process. This suggests that in a binding mode involving R_1 and COR_3 increased binding leads to disorientation of the substrate which can be prevented or minimized by increased participation of R_2 in the binding process.

In the preceding interpretation, developed for trifunctional substrates $R_1CHR_2COR_3$ with $R_2 \neq H$, it was tacitly assumed that the α-hydrogen atom had no role in orientation and binding of substrate to the active site, other than that inherent in its presence at an asymmetric center. The interpretation recognizes the well-known specificity of α-chymotrypsin for substrates possessing the L-configuration. However, it provides for the reaction of certain D-antipodes by invoking a loss in steric control in the orienting process normally favoring the L-antipode accompanied by alternative interactions in an orienting or binding sense for the D-antipode.

When a particular R group present in an L-antipode fails to function effectively in the orienting process, e.g., it is too small, then the L-antipode can assume other orientations all of which place an R group in the position otherwise occupied by the α-hydrogen atom as long as COR_3 continues to interact with ρ_3. This situation should approximate that observed for L-substrates of the type $R_1'CONHCHR_2COR_3$ in which the α-hydrogen atom is replaced by a methyl group, a replacement leading to a dramatic decrease in the magnitude of k_0. The same R group responsible for loss of stereospecificity of the L-antipode, when present in the D-antipode, will allow the latter access to orienting and binding loci at the active site but, except for one case, will again result in placing an R group in the position normally occupied by the α-hydrogen atom of an L-substrate. The one exception occurs when, for the D-antipode, R_1 interacts with the locus ρ_2 and R_2 with ρ_1. Thus, except for the case

where the structures of R_1 and R_2 are such as to optimize an "interaction exchange" of the above kind, the interpretation predicts that k_0 values for the D-antipodes will be orders of magnitude smaller than those of the L-substrates. For the one exception the difference in k_0 values of D- and L-antipodes would be substantially smaller. Experimental results compatible with this view have been discussed above. Neither the interpretation nor the data considered previously predict reaction of a D-antipode at a rate order of magnitude greater than the L-antipode.

Inversion of Antipodal Specificity.—D-3-Carbomethoxy-3,4-dihydroisocarbostyril(D-3CDIC) is a substrate of α-chymotrypsin and under limiting first-order reaction conditions would be hydrolyzed at a rate 2.8×10^3 times that of its L-antipode and 1.2 times that of methyl acetyl-L-phenylalaninate, cf. Table 6. The K_O and k_0 values for methyl acetyl-L-phenylalaninate and D-3CDIC suggest that these two compounds are similarly oriented at the active site and that their kinetic constants are determined by essentially the same structural factors. The former approximates a substrate of the $S^{3E}_{R_2R_3}$ limit type in which $R_1 = R_1'CONH$ is important for orientation of the substrate at the active site.

The compound D-3CDIC is a special kind of bifunctional substrate in that R_1 and R_2 are fused retaining the CONH elements of $R_1'CONH$ but replacing R_1' by R_2. If D-3CDIC is to be regarded as approximating a $S^{3E}_{R_2R_3}$ limit type it must contain structural elements to replace the role of R_1 in methyl acetyl-L-phenylalaninate in contributing to orientation of the substrate in the complex. This property is found in the conformationally restricted structure of 3CDIC, in which COR_3 can assume two limiting positions, axial or equatorial, with respect to the essentially planar bicyclic ring system. We have noted previously that the one case where a D-antipode can assume a favorable orientation at a site normally accommodating an L-substrate is where R_1 can interact with the R_2 locus ρ_2 and R_2 with the R_1 locus ρ_1. Stereospecificity is achieved for methyl acetyl-L-phenylalaninate, in a formal sense, by interaction at three points while D-3CDIC is stereospecifically bound by interactions with a plane and a point. The plane of interaction provides for the fusion of the otherwise separate R_2-ρ_1 and R_1-ρ_2 interactions while that of the point involving the COR_3 locus at ρ_3 is limited only by the conformations accessible to COR_3. While it is not certain that the interactions envisaged as occurring in the plane actually involve subtending of the ρ_1 and ρ_2 loci by the dihydroisocarbostyril nucleus we favor this view even though it may require minor displacement of the ρ loci of the site. The alternative would require special features of the ρ_2 locus for which there is no independent evidence. Finally, for the same reasons that would place the COR_3 group of methyl acetyl-L-phenylalaninate above the planes of the ρ_1 and ρ_2 loci, a fusion of the R_1-ρ_2, R_2-ρ_1 loci in the plane of the dihydroisocarbostyril nucleus, would place the COR_3 group of D-3CDIC in a predominantly axial position above the plane of the nucleus.

The COR_3 group of L-3CDIC cannot be placed in the same position as that occupied in the complex with methyl acetyl-L-phenylalaninate or D-3CDIC without at the same time requiring an inversion in the disposition of the ρ_1 and ρ_2 loci at the site for interaction with the dihydroisocarbostyril nucleus. However, L-3CDIC can assume an orientation at the site in which an equatorially disposed COR_3 group can interact with the ρ_3 locus and the dihydroisocarbostyril nucleus with the ρ_1 site. This view was favored when it was found that the conformationally de-

terminate 3-carbomethoxyisocarbostyril(3-CIC) with an equatorial COR_3 group was a substrate with a k_0 value the same order of magnitude as that of L-3CDIC.

The assignment of different binding modes to D-3CDIC and L-3CDIC received support when it was found that the inhibition of hydrolysis of D-3CDIC by indole was totally competitive whereas that of L-3CDIC was of the mixed type and similar to that observed previously for methyl benzoylglycinate.[28]

The assignment of L-3CDIC to a particular limit type substrate is uncertain. There are two possibilities, either the trifunctional $S^{3E}_{R_1R_2}$ limit type in which the orienting function of R_2 is approaching minimum effectiveness, or the bifunctional $S^{2E}_{R_1R_2}$ limit type in which R_2 could have no orienting function and because of its absence may permit R_1 to interact with ρ_2 as well as ρ_1. However, one would expect the kinetic constants of L-3CDIC to approximate those of examples of either of the previous limit types. The similarity of the values of K_O and k_0 for L-3CDIC and those of methyl benzoylglycinate and methyl benzoyl-L-alaninate is evident from the data given in Table 6.

TABLE 6

VALUES OF K_O AND k_0 FOR A SELECTED SET OF SUBSTRATES

	K_O*	k_0†	k_0/K_O‡
D-3CDIC**	0.55	331	602
Methyl Acetyl-L-phenylalaninate	1.8	918	510
3CIC††	1.37	1.70	1.24
Methyl Benzoylglycinate	7.55	2.98	0.394
Methyl Benzoyl-L-alaninate	9.75	3.80	0.390
L-3CDIC‡‡	11.3	2.42	0.214
Methyl Formyl-D-phenylalaninate	0.25	0.05	0.200
Methyl Benzoyl-D-alaninate	3.21	0.155	0.048

* In units of 10^{-3} M.
† In units of 10^{-3} M/min/mg protein-nitrogen per ml.
‡ In units of min/mg protein-nitrogen per ml.
** D-3-Carbomethoxydihydroisocarbostyril.
†† 3-Carbomethoxyisocarbostyril.
‡‡ L-antipode of **.

The compound D-3CDIC is the first example of inversion of the usual antipodal specificity of α-chymotrypsin. The structural feature of the substrate responsible for this behavior is the rigid planar bicyclic nucleus which permits the R_1-ρ_2, R_2-ρ_1 interactions required for an inversion of antipodal specificity to proceed in an essentially concerted manner. The effectiveness of this kind of interaction is illustrated by comparison of the kinetic constants of D-3CDIC and methyl formyl-D-phenyl-alaninate, where it may be presumed that the same kind of exchange proceeds but in a nonconcerted sense. While the K_O values of the two substrates are of the same order of magnitude, their values of k_0 differ by a factor of 6.6×10^3 with that of D-3CDIC being the faster.

Conclusions.—The argument developed in this communication has as its goal: first, the establishment of generalizations to be used for the interpretation of the kinetic behavior of relatively low molecular weight substrates of α-chymotrypsin and, secondly, elaboration of limit cases for a more detailed description of the geometrical disposition and molecular nature of the orienting and binding loci at the active site of the enzyme. We believe that the first objective has been achieved for trifunctional substrates $R_1'CONHCHR_2COR_3$, where $R_2 \neq H$, and that the same principles can be applied for substrates of other types and for competitive inhibitors.

As for the second objective, it is now possible to suggest a probable conformation for a representative trifunctional substrate at the active site, which in turn provides a partial description of the site itself. Figure 1 illustrates methyl acetyl-L-phenylalaninate in a conformation suggested by the data and arguments discussed previously.

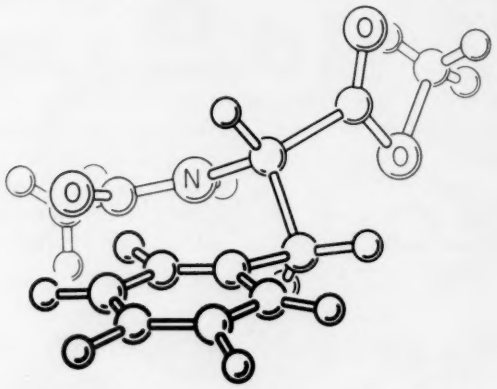

FIG. 1.—Representation of methyl acetyl-L-phenyalaninate at the active site of α-chymotrypsin in a conformation leading to products.

It recognizes the need for accommodating R_1 and COR_3 groups of the dimensions encountered in polypeptide substrates and provides for the decrease in k_0 values arising from substituents which interfere with attack on the carbonyl group of the potentially reactive bond by electro- and nucleophilic groups of the site.

The disposition of the loci ρ_1, ρ_2, and ρ_3 is described in terms of a complementary substrate. Although in a formal sense these loci have been regarded as points it is probable that they are planes capable of deformation. If ρ_2 is taken as a plane of reference that of ρ_1 is adjacent in a clockwise direction, but tilted out of the plane of ρ_2 the plane of ρ_3 is postulated as being above and possibly perpendicular to that of ρ_2.

* This investigation was supported in part by a grant from the National Institutes of Health, U. S. Public Health Service.

† Contribution No. 2733, Gates and Crellin Laboratories of Chemistry.

[1] Dixon, M., and E. C. Webb, *Enzymes* (New York: Academic Press, 1958) pp. 252–265, 268–271.

[2] Cohen, J. A., R. A. Oosterbaan, H. S. Jansz, and F. Berends, *J. Cell. Comp. Physiol.*, **54** (Suppl. 1), 231 (1959).

[3] Foster, R. J., and C. Niemann, *J. Am. Chem. Soc.*, **77**, 1886, 3370 (1955).

[4] Foster, R. J., H. J. Shine, and C. Niemann, *ibid.*, **77**, 2378 (1955).

[5] Neurath, H., and B. S. Hartley, *J. Cell. Comp. Physiol.*, **54** (Suppl. 1), 179 (1959).

[6] Lands, W. E. M., and C. Niemann, *J. Am. Chem. Soc.*, **81**, 2204 (1959).

[7] Braunholtz, J. T., R. J. Kerr, and C. Niemann, *ibid.*, **81**, 2852 (1959).

[8] MacAllister, R. V., K. M. Harmon, and C. Niemann, *J. Biol. Chem.*, **177**, 767 (1949).

[9] Cunningham, L. V., and C. S. Brown, *ibid.*, **221**, 287 (1956).

[10] Hearon, J. Z., *et al.* in *The Enzymes*, ed., P. D. Boyer, H. Lardy, and K. Myrbäck (New York: Academic Press, 1959), vol. 1, p. 127.

[11] Here and throughout the text values of K_0 are in units of 10^{-3} M and those of k_0 in units of $10^{-3}M$/min/mg protein-nitrogen per ml.

[12] Neurath, H., and G. W. Schwert, *Chem. Rev.*, **46**, 69 (1950).

[13] Bender, M. A., and W. L. Glasson, *J. Am. Chem. Soc.*, **82**, 3336 (1960).
[14] Hammond, B. R., and H. Gutfreund, *Biochem. J.*, **61**, 187 (1955).
[15] Waite, H., and C. Niemann, unpublished results.
[16] Applewhite, T. H., H. Waite, and C. Niemann, *J. Am. Chem. Soc.*, **80**, 1465 (1958).
[17] Wolf, J. P., III, and C. Niemann, unpublished results.
[18] Applewhite, T. H., and C. Niemann, *J. Am. Chem. Soc.*, **81**, 2208 (1959).
[19] Applewhite, T. H., R. B. Martin, and C. Niemann, *ibid.*, **80**, 1457 (1958).
[20] $S^{3E}_{R_3R_2}$ symbolizes a trifunctional ester type substrate with R_2 and COR_3 contributing to binding, and $S^{3E}_{R_1R_3}$ symbolizes a similar type but with R_1 and COR_3 in binding roles.
[21] Bock, R. M., and C. Niemann, unpublished results.
[22] Manning, D. T., and C. Niemann, *J. Am. Chem. Soc.*, **81**, 747 (1959).
[23] Jennings, R. R., and C. Niemann, *ibid.*, **75**, 4687 (1953).
[24] Lutwack, R., H. F. Mower, and C. Niemann, *ibid.*, **79**, 5690 (1957).
[25] Kerr, R. J., and C. Niemann, *ibid.*, **80**, 1469 (1958).
[26] $S^{3A}_{R_1R_2}$ and $S^{3A}_{R_2R_3}$ symbolize trifunctional amide-type substrates analogous to the ester types discussed previously.
[27] The symbols ρ_1, ρ_2, and ρ_3 are used to identify loci at the active site complementary to R_1, R_2, and COR_3, respectively.
[28] Huang, H. T., and C. Niemann, *J. Am. Chem. Soc.*, **75**, 1395 (1953).
[29] Bender, J. L., *Chem. Rev.*, **60**, 53 (1960).
[30] Almond, H. R., Jr., and C. Niemann, unpublished results.
[31] Hubele, K., and C. Niemann, unpublished results.
[32] Kurtz, A. N., and C. Niemann, *J. Am. Chem. Soc.*, **83**, 1879 (1961).
[33] Isaacs, N. S., and C. Niemann, unpublished results.
[34] Abrash, H. I., and C. Niemann, unpublished results.
[35] Peterson, P. E., and C. Niemann, *Biochim. Biophys. Acta*, **48**, 331 (1961).

---

*AN ELECTRON SPIN RESONANCE ANALYSIS OF THE MECHANISM OF SUCCINIC DEHYDROGENASE ACTIVITY**

BY THOMAS C. HOLLOCHER, JR., AND BARRY COMMONER

THE HENRY SHAW SCHOOL OF BOTANY AND THE ADOLPHUS BUSCH III LABORATORY OF MOLECULAR BIOLOGY, WASHINGTON UNIVERSITY, ST. LOUIS

Communicated by Albert Szent-Györgyi, July 10, 1961

This present paper reports experimental evidence, based on the electron spin resonance (ESR) technique, which describes quantitatively the relationship among various reaction parameters and the resultant concentrations of free radicals observed in systems consisting solely of succinic dehydrogenase (SDH), succinate, and fumarate. These data lead to the derivation of a reaction mechanism and to calculations of associated thermodynamic constants. The resultant values are in good agreement with the values of those constants which can be derived from conventional biochemical observations of the SDH system. In addition, certain other reaction constants which cannot be deduced from the older observations have been calculated from the ESR data. Electron spin resonance observations thereby lead to the establishment of a reaction mechanism for the process catalyzed by SDH in which a main feature is the occurrence of a free radical form of the enzyme-substrate complex. The data also show that the chemical change in the substrate molecule which occurs during SDH activity is closely associated with the process

which results in electron-unpairing in the enzyme-substrate complex. These results confirm and extend earlier studies which showed that ESR signals observed in mitochondrial particles from heart muscle are due to a free radical form of the enzyme-substrate complex formed by SDH.[1, 2]

In spite of the extensive literature on the properties and biochemical activity of SDH, the mechanism of the enzymatic reaction is not clearly understood. Succinic dehydrogenase catalyzes reversibly the redox interaction between succinate and fumarate. Potentiometric studies prove the reversibility of the succinate-fumarate interaction and indicate that SDH is a perfect catalyst in the sense that the equilibrium redox potential is that predicted by the succinate-fumarate couple and is not influenced by the enzyme.[3]

While SDH has been shown to be an iron-containing flavoprotein,[4–7] it is not known with certainty whether the iron atoms or the flavin prosthetic group undergo redox transitions in the enzyme-catalyzed reaction. Most redox enzymes in the presence of their natural substrates exhibit profound spectral effects which can be interpreted as a change in the redox state of the enzyme's prosthetic group. However, the changes in absorbancy observed in SDH are not subject to such unequivocal interpretations. Upon the addition of succinate to purified, soluble SDH, the characteristic spectrum of the enzyme is altered slightly[4, 6, 8–10] Since the principle change occurs in the absorbancy at 460 mμ and thereby resembles the more pronounced effects due to the strong reducing agent, hydrosulfite, this result suggests that the flavin moiety of the enzyme is reduced by succinate. This conclusion is supported by the observation that malonate inhibits the effect of succinate on the enzyme's absorption spectrum.

However, certain other considerations suggest that the above effects may not necessarily reflect changes in the redox state of the enzyme's prosthetic group: (*a*) Compounds other than succinate (malonate and "activators," for example) also produce spectral alterations in SDH of approximately the same magnitude, although differing in some detail from those induced by succinate.[9] (*b*) It has not been shown that fumarate can reverse the succinate-induced spectral changes in a regular manner predictable from thermodynamic considerations. (*c*) If it is assumed that the spectral changes produced by succinate at 460 mμ do reflect flavin reduction, one can calculate that the potential, E_0' (at pH 7.6), characteristic of this redox transition in SDH is about -0.2 volts. However, this value does not agree with the redox potential of the enzyme as a whole, which can be estimated from the published Michaelis-Menten constants for SDH,[9, 11–16] for these estimates give potentials near 0 volts at pH 7 to 7.6. The possibility exists, therefore, that the effect of succinate on the spectrum of SDH may relate to events other than redox transitions, such as configurational or electronic rearrangements associated with complex formation.

The succinate-fumarate-SDH system interacts with a wide variety of secondary redox reactants, which mediate the net oxidation of succinate or net reduction of fumarate. Such redox coupling is the basis for the biological oxidation of succinate by oxygen through the electron transport system and is employed in all *in vitro* studies of SDH kinetics and of SDH activity. In such systems, the principal redox reaction catalyzed by SDH is between substrate and secondary redox mediator rather than between succinate and fumarate, and there is evidence that the nature

of the redox mediator can profoundly influence the kinetics and, perhaps, the mechanism of the redox reactions observed. Thus, the Michaelis-Menten constants for SDH calculated from experiments of this type frequently depend on the nature of the secondary coupling system employed to promote the net redox reaction.[6, 9, 11–16] Also, it has been shown that although the kinetics of succinate oxidation by phenazine methosulfate are strongly influenced by the iron content of SDH, the reduction of fumarate by reduced FMN is not.[9] There is, therefore, some uncertainty regarding the correspondence of Michaelis-Menten and inhibitor constants with their related equilibrium constants for the succinate-fumarate interaction.

In the absence of unequivocal data regarding the redox properties of the enzyme itself, little can be said about the number and details of the redox reactions which take place in the SDH system or about the nature of possible redox intermediates. In the absence of a confirmed reaction mechanism and of data on the equilibrium properties of the system, critical thermodynamic constants, such as ΔF°, ΔH° and ΔS°, for the reactions among SDH and its substrates are also lacking.

In general, these difficulties result from an inability to derive from conventional biochemical data on the SDH system evidence which can describe the electronic processes which occur in the system. If these processes involve unpaired electrons, this difficulty can be remedied by using ESR techniques which are capable of characterizing and determining the concentration of unpaired electrons in the system. As shown below, ESR observations on the SDH system indicate that electron unpairing and free radical formation are associated with SDH activity in equilibrium systems containing only succinate, fumarate, and SDH. The ESR observations define in certain detail the redox mechanism of the SDH system and lead to calculations of thermodynamic constants of the reactions involved.

Experimental Methods.—Succinic dehydrogenase: Succinic dehydrogenase was prepared by the method of Singer and co-workers from beef heart.[11, 12] Succinic dehydrogenase activity was assayed at 38°C by the manometric phenazine methosulfate method of Singer, and protein content was determined by use of Biuret color coefficients published for this preparation.[11, 12] The succinoxidase activity of the preparations was determined manometrically, while succinate-cytochrome *c* reductase activity was measured spectrophotometrically at 550 mμ, using ferric cytochrome *c* (Sigma Company).

All reagents used in the preparation and assays of SDH and in the subsequent experiments were commercial reagents of high purity. Distilled water further purified by ion exchange resins was used exclusively. All experiments were carried out in 0.005 *M* phosphate buffer at pH 7.6.

Prior to use, SDH in the form of acetone powder was stored at −20°C under vacuum. Aqueous samples of the enzyme were stored at −20°C. The maximum time of storage was about two weeks.

ESR techniques: The ESR spectrometer employed in these studies was designed and constructed by Dr. Jonathan Townsend of the Washington University Department of Physics. A brief description of this X-band spectrometer has been published elsewhere.[17, 18, 35] For ESR observations, aqueous samples, contained in Pyrex cells, were inserted through a slot into the resonance cavity of the spectrometer. These cells accommodate 0.1 to 0.2 ml of sample with a sensitive volume of about 0.05 ml. All observations were made at 32°C to 35°C unless otherwise stipulated.

The sensitivity of this ESR spectrometer (at a signal:noise ratio of 1/2) with aqueous samples at about 30°C is 1 to $2 \cdot 10^{12} \cdot \Delta H$ spins under the following conditions: A 1-mc field modulation amplitude of 12 to 16 gauss, an integration time of 0.1 second, and a microwave power level at the sample of a few milliwatts. In the case of free radicals with line widths of about 15 gauss, such as those observed in these studies, this sensitivity corresponds to a detectable concentration

of about $5 \cdot 10^{-7}$ *M* free radicals at a signal:noise ratio of 1 to 2.

The control of sample temperature during ESR studies was accomplished by the flow of gas at a desired temperature past the sample cell. Buffered solutions of potassium peroxylamine disulfonate[19, 20] were used as a magnetic field marker. Spin counts were made by comparing the areas under ESR absorption (integral) curves with those obtained with manganous ion standards and by making appropriate corrections for the difference in electron quantum spin number.[21, 22] The ESR absorption curves were obtained by integration from the derivative curves which represent the curves displayed by the spectrometer.

Experimental Results.—Succinic dehydrogenase (general properties): Most SDH preparations used in these studies were purified to a level of 40–60 per cent and exhibit an activity (determined by the phenazine manometric assay) of about 100 to 200 μg atoms $O \cdot min^{-1} \cdot ml^{-1}$. In all preparations the succinate-cytochrome *c* reductase activity is about three decimal orders of magnitude or more lower than the SDH activity while succinoxidase activity is undetectable.

Upon storage of SDH in the form of acetone powder or at a purity of 40–60% in aqueous solutions in the manner described above, it is found that SDH activity declines only very slightly over a period of one to two weeks.

Spectra of preparations rendered optically clear by centrifugation are typical of the 4-iron-atom form of SDH and exhibit no evidence of the presence of additional flavoproteins or cytochromes.[6, 9, 11, 12] The optical density ratio $E_{440m\mu}/E_{580m\mu}$ for the preparations is 2.5 ± 0.1. The 4-iron-atom enzyme is characterized by a value of 2.5, while the 2-iron enzyme preparations exhibit a ratio of 3.2.[6] Biochemical SDH activity is proportional to optical density as measured at 580 mμ. In the calculations which follow, SDH concentration is determined on the basis of a molecular weight of $2 \cdot 10^5$ $gm \cdot mole^{-1}$ and a specific activity of the 4-iron enzyme of 30 μg atom $O \cdot min^{-1} \cdot mg^{-1}$.[11, 12]

ESR observations (general considerations): Succinic dehydrogenase, succinate, and fumarate do not exhibit an ESR signal when examined separately. When the three components are present together, an ESR signal is observed which corresponds with respect to line shape, line width, and *g* value to the signals previously observed under similar circumstances in particles of heart muscle mitochondria.[1, 2]

Because appreciable concentrations of SDH are obtainable with Singer preparations (of the order 5 to $8 \cdot 10^{-5}$ *M*), it has been possible to obtain relatively intense ESR signals from them.

Accordingly, one can study the characteristics of the signal under instrument conditions which maximize resolution although at the expense of sensitivity.[23] Figure 1 shows typical ESR signals observed in a mixture of SDH, fumarate, and succinate under conditions of maximum sensitivity (and low resolution) and of maximum resolution (and low sensitivity). The signal observed at maximum sensitivity (Figure 1*E*) is essentially simple except for a minor deflection on the lower field side of the main peak, and a certain degree of asymmetry. The data of Figure 1 show that the symmetry of the signal improves and the minor peak becomes less pronounced under conditions of maximum resolution.

As a result, neither aspect of the original ESR signal can be regarded as evidence of partially-resolved hyperfine structure. This effect, and the total absence of hyperfine structure under conditions of maximum resolution (Signal D in Figure 1) indicate either that the SDH signal lacks hyperfine lines or that any hyperfine lines present are 1 gauss or less in width (the limit of resolution under the instrument

conditions employed).

From Figure 1 the following estimates of the characteristic features of the SDH free radical can be made: g value, 2.003 ± 0.001; line width between regions of maximum slope, 15.8 ± 1.0 gauss; hyperfine lines separated by 1 gauss or more, none. These characteristics are consistent with the association of the signal with a complex organic free radical.[21] It has been shown previously that the free radical forms of free FMN and FAD yield ESR signals which are similar to the above, except that hyperfine lines with line widths of about 2 to 4 gauss are observed.[24–27] Signals similar to those of Figure 1 have been detected with "old yellow enzyme" in the presence of TPNH.[26, 27]

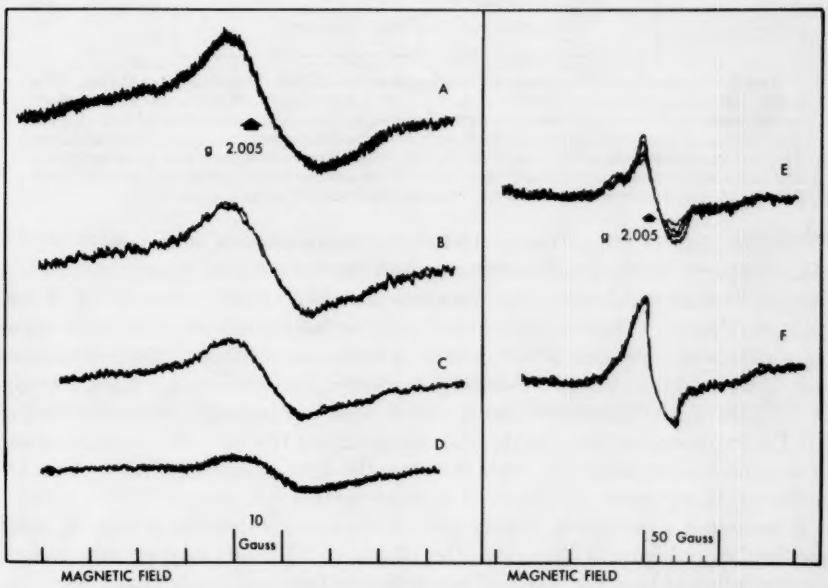

FIG. 1.—ESR signals obtained from soluble SDH under different instrumental conditions. The curves all represent the derivative of resonance absorption with respect to magnetic field (dX''/dH) as a function of magnetic field (H), which increases from left to right in each frame. The sum of the concentrations of succinate and fumarate is 0.05 M and the fumarate:succinate mole ratio is 1. The concentrations of SDH and free radicals are about $6 \cdot 10^{-5}$ M and $1.5 \cdot 10^{-5} M$, respectively. Each curve results from the superimposition of two or more individual curves. The magnetic field modulation amplitude in gauss, the spectrometer's minimum response time in seconds, and the time in minutes required to scan a 100-gauss segment of magnetic field are, respectively, the following: (*a*) 12, 0.1, 13; (*b*) 9, 0.1, 3.3; (*c*) 6, 0.1, 13; (*d*) 2, 1, 13; (*e*) 12, 0.1, 0.95; (*f*) 12, 0.1, 0.95. Curves (*a*), (*b*), (*c*), (*d*), and (*f*) are obtained under conditions of maximum resolution (minimum crystal detector current), while the curves of (*e*) were obtained under conditions of maximum sensitivity.

The integral forms of several signals observed in the SDH system containing different concentrations of enzyme are shown in Figure 2. Although the free radical concentrations (and therefore the areas under the integrals) vary, the signal characteristics (line width and shape) remain constant within the limits of instrumental error.

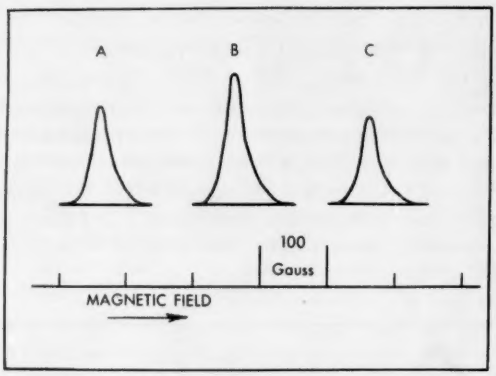

FIG. 2.—Integrated ESR signals obtained with soluble SDH, illustrating line shape. The curves all represent resonance absorption (X'') as a function of magnetic field (H), which increases from left to right, and are derived through numerical integration of first derivative curves of the kind illustrated in Figure 1. The free radical concentrations of curves (*a*), (*b*), and (*c*) are $8.9\cdot$, $11.8\cdot$, and $7.9\cdot10^{-6}M$, respectively, and they are proportional to the areas under their respective curves. Sum of the succinate and fumarate concentrations is 0.05 M, and the fumarate:succinate mole ratio is 1 for all curves.

The free radical concentration, ESR signal characteristics, and, indeed, all the results reported in this paper are unaffected by the presence or absence of dissolved oxygen, at least up to the partial pressure of oxygen in air. Once the SDH systems reach chemical and thermal equilibrium, the free radical concentration remains constant for an indefinite period of time at room temperature. The free radicals can, however, be destroyed irreversibly by heating the systems for a few minutes at 70°C or a few seconds at 100°C. This observation, and the parallel loss of SDH activity suggest that the thermal destruction of free radicals is a consequence of enzyme denaturation. In these respects, the ESR signals in SDH systems are similar to those previously observed in heart particle systems.[1, 2]

Relationship between free radical concentration and enzymatic activity of SDH preparations: Figure 3 illustrates the effects of SDH activity on free radical concentration at constant levels of succinate and fumarate (mole ratio 1:1). The points represent enzyme samples taken at different stages during the purification of two SDH preparations derived from the same sample of acetone powder. The curve is linear with a (0, 0) intercept. Thus, free radical concentration is proportional to SDH activity, as assayed manometrically, and bears no relationship to enzyme purity. While this linear relationship applies to all preparations studied, it is found that the slope of the line depends somewhat on the particular sample of acetone powder employed as starting material. This result shows that free radical formation is associated with SDH activity and is not a spurious effect produced by a contaminant.

Effect of equilibrium parameters on free radical concentration: A series of ESR determinations have been carried out to establish, quantitatively, the relation of free radical concentration to various parameters that affect the SDH reaction In each case, the enzyme used was a sample taken from several successive preparations of SDH, each purified to the 40–60% level. In each case, the system contained only measured concentrations of SDH, fumarate, and succinate in pH 7.6 phos-

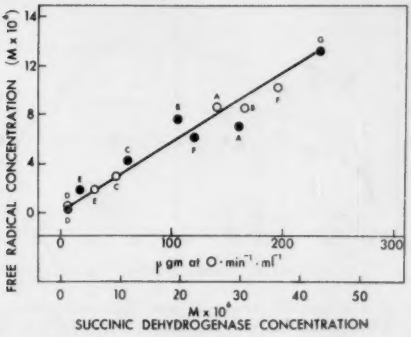

FIG. 3.—The effect of SDH concentration on free radical concentration during the purification of two SDH preparations from a common sample of acetone powder. Open and closed circles represent the two preparations. The letters A, B, C, D, E, and F represent samples of SDH increasing in purity in this order during purification. The point corresponding to G represents preparation F after having been concentrated by dialysis against *Carbowax 20* (Carbide and Carbon Chemicals Company). During preparation, the purity of SDH samples shown range between about 1 and 50%. The sum of the succinate and fumarate concentrations is 0.05 *M* and the fumarate:succinate mole ratio is 1.

phate buffer. ESR determinations were made under conditions of maximum instrument sensitivity at regulated temperatures. Equilibrium conditions prevailed in all cases; repeated ESR signals were determined at approximately 1-min intervals until a number of signals of constant amplitude were obtained. Free radical concentration was then calculated from the integral of an average of 6–8 successive differential signals in the manner described above.

Figure 4 shows the relationship between free radical and SDH concentration

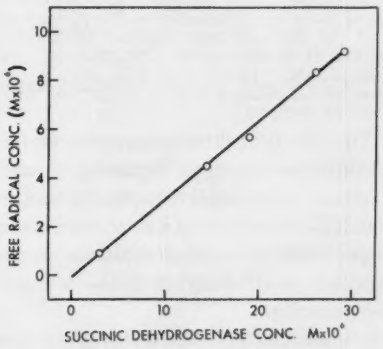

FIG. 4.—The influence of SDH concentration, as varied through dilution, on the free radical concentration. The sum of the succinate and fumarate concentrations is 0.05 *M* and the fumarate:succinate mole ratio is 0.5.

In this experiment, the SDH activity and concentration of a single preparation of enzyme were altered by dilution while maintaining constant concentrations of succinate and fumarate. The curve again is linear with a (0, 0) intercept.

For any given enzyme sample, the slope of the dilution line is a function of the fumarate/succinate mole ratio, the total concentration of succinate and fumarate,

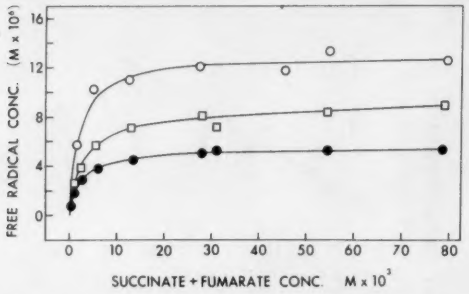

FIG. 5.—The effect of the sum of succinate and fumarate concentrations on the free radical concentration. The upper, middle, and lower curves are obtained with $5.0\cdot$, $3.3\cdot$, and $2.0\cdot10^{-5}$ M SDH, respectively. The fumarate:succinate mole ratio is 1 throughout.

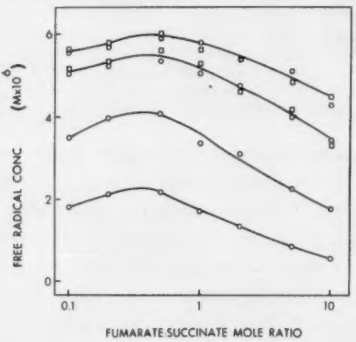

FIG. 6.—Semilog plots of the effect of fumarate:succinate mole ratio on free radical concentration. The sum of the succinate and fumarate concentrations are the following. Upper curve: squares, $3.92\cdot10^{-2}$ M; circles $3.52\cdot10^{-2}$ M. Second curve: squares, $1.69\cdot10^{-2}$ M; circles $1.35\cdot10^{-2}$ M. Third curve: $0.50\cdot10^{-2}$ M. Bottom curve: $0.12\cdot10^{-2}$ M. The concentration of soluble purified SDH is $2.6\cdot10^{-5}$ M throughout.

and the temperature. The effects of these parameters on free radical concentration under equilibrium conditions are shown in Figures 5, 6, and 7.

In Figure 5, the free radical concentration is plotted as a function of the fumarate plus succinate concentration. The curves are characterized by a (0, 0) intercept and approach asymptotes with increasing substrate concentration. The slopes of the curves are everywhere positive and decrease with increasing substrate concentration, approaching zero slope.

Figure 6 illustrates in a semilog plot the effect of the fumarate/succinate mole ratio on the free radical concentration. Here, the individual curves are defined by the sum of the succinate and fumarate concentrations. The curves pass through a maximum which is invariant within any single SDH preparation at constant temperature.

The effect of temperature on free radical concentration is shown in Figure 7. Within the temperature range covered, from about 5°C to 46°C, the free radical concentration is freely reversible.

The influence of malonate concentration on a system composed of SDH, suc-

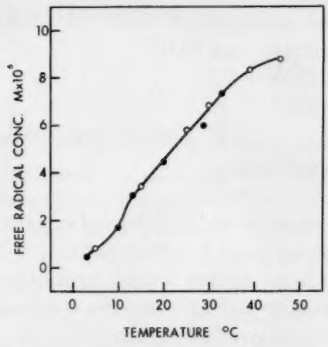

FIG. 7.—The reversible influence of temperature on free radical concentration. The concentration of SDH is $2.74 \cdot 10^{-5}$ *M*; the sum of the succinate and fumarate concentrations is $5 \cdot 10^{-3}$ *M*; the fumarate:succinate mole ratio is 0.5. Solid circles represent decreasing temperature and open circles represent increasing temperature.

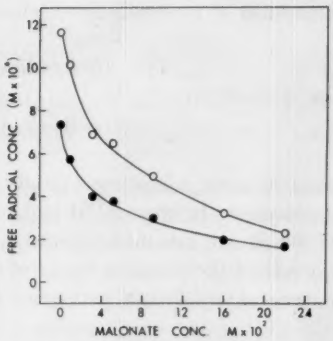

FIG. 8.—The influence of malonate concentration on free radical concentration. The sum of the succinate and fumarate concentrations is 0.05 *M* and the fumarate:succinate mole ratio is 1. Open circles: $5.0 \cdot 10^{-5}$ *M* SDH. Solid circles: $3.3 \cdot 10^{-5}$ *M* SDH.

cinate, and fumarate (1:1) is shown in Figure 8. The free radical concentration decreases with increasing malonate concentration, approaching zero asymptotically. The slopes of the curves are everywhere negative and increase with malonate concentration, approaching zero slope as the limit.

Interpretation of results and thermodynamic considerations: We shall undertake to interpret the following results of the ESR experiments just described: (*a*) Line width and *g* value considerations indicate that the ESR signals observed in the SDH system arise from free radicals. (*b*) The observed free radicals have a functional relationship to SDH activity: They cannot be formed when the enzyme is inactive, and free radical concentration is proportional to SDH activity while being independent of enzyme purity. (*c*) The free radicals are formed through equilibrium reactions in systems containing only succinate, fumarate, and SDH as reactants. (*d*) An examination of the relationship of the various equilibrium parameters to the free radical concentration indicates the following: To a close approximation, free radical concentration is linear in SDH concentration, quadratic in the sum of the succinate and fumarate concentrations, cubic with an invariant maximum in the fumarate-to-succinate mole ratio, and quadratic with respect to malonate concentration.

The above results and the reversible and irreversible effects of temperature are exactly analogous to those reported previously from ESR studies of the heart particle systems.[1, 2] As in the case of the earlier studies, the foregoing data impose certain severe restrictions on possible reaction mechanisms, and these restrictions together with considerations based on the biochemistry of the SDH system enable us to reject as unlikely or inconsistent with observed data a variety of possible free-radical–forming mechanisms. Since the reasoning employed in developing these limitations has been described in detail in the earlier papers,[1, 2, 28] we shall here state as a conclusion that only a mechanism of the following general type

appears to be capable of accounting for the relationships observed among the concentrations of free radical, succinate, fumarate, and SDH.

$$\text{Succ.} + \text{ox. SDH} \rightleftharpoons \left[\begin{array}{c}\text{(free radical complexes)} \\ \Uparrow\Downarrow \\ \text{(Non-free radical complexes)}\end{array}\right] \rightleftharpoons \text{Fum.} + \text{red. SDH.} \quad (1)$$

This mechanism comprises a family of mechanisms which differ only in the number of complexes between SDH and substrate (or some 4-carbon derivatives of the latter) which are assumed to exist. All such complexes are in equilibrium and differ one from the other by virtue of internal structure and electron configuration.

The general equilibrium expression for this family of mechanisms is:

$$R = \frac{mCEQ}{n(Q + K_1)\ (Q + 1) + mCQ\ (n + 1)}, \quad (2)$$

where n and m are constants representing the sum of functions of equilibrium constants, R is the free radical concentration, C is the sum of the succinate and fumarate concentration, E is the total SDH concentration, and Q is the fumarate-to-succinate mole ratio. K_1, the over-all equilibrium constant, is defined by

$$K_1 = \frac{\text{(Fum) (red. SDH)}}{\text{(Succ) (ox. SDH)}} \quad (3)$$

The reciprocal of (2) is

$$\frac{1}{R} = \frac{n(Q + K_1)\ (Q + 1)}{mCEQ} + \frac{n + 1}{E}. \quad (4)$$

The simplest case of the family of mechanisms given by equation (1) and the one chiefly considered in our previous papers[1, 2, 28] is one in which a single species of non-free radical complex and of free radical complex occur. In this case, we consider, besides the overall equilibrium defined by (3), the following equilibria: Succ + ox. SDH $\rightleftharpoons$ binary complex:

$$\frac{\text{(complex)}}{\text{(Succ) (ox. SDH)}} = K_2. \quad (5)$$

Fum + red. SDH $\rightleftharpoons$ binary complex:

$$\frac{\text{(complex)}}{\text{(Fum) (red. SDH)}} = K_3. \quad (6)$$

Free radical form of binary complex $\rightleftharpoons$ binary complex:

$$\frac{\text{(complex)}}{\text{(Free radical complex)}} = K_4 \quad (7)$$

Since

$$K_1 = \frac{K_2}{K_3}, \quad (8)$$

equation (4) reduces to:

$$\frac{1}{R} = \frac{K_4\,(Q + K_1)\,(Q + 1)}{K_2 \qquad CEQ} + \frac{K_4 + 1.}{E} \tag{9}$$

Since there are no compelling reasons which require the consideration of more complex cases, we shall consider only the above relationships in our treatment of the data and in subsequent discussions.

It is clear from a cursory examination of the above relationships that the proposed equilibrium expression possesses the same power relationships, intercepts, and limit characteristics exhibited by the observed free radical data. Equation (2) requires, for example, proportionality between R and E and that $Q_{R_{max}} = \sqrt{K_1}$ (that is, the value of Q at which R is a maximum is invariant in the other parameters). Both of these conditions are observed in the free radical data (see Figs. 4 and 6). That $Q_{R_{max}} = \sqrt{K_1}$ is shown by taking the partial of R with respect to Q, $\partial R/\partial Q$, for equation (2) or (9), setting $\partial R/\partial Q, = 0$ for the condition of zero slope at the maximum, and solving the resultant expression for $Q_{R_{max}}$.

However, the most critical tests of the correspondence between the ESR data and the proposed reaction mechanism are the following: (*a*) The value of $1/R$ should be linear in the function $\frac{[(Q + K_1)(Q + 1)]}{Q}$, and the family of lines given by variations in C all should have a common intercept which equals $(K_4 + 1)/E$. (*b*) Also, $1/R$ should be linear in $1/C$ with the same common intercept for the family of lines defined by variations in Q.

To test the degree to which the ESR data conform to the foregoing relationships, the data shown directly in Figure 6 have been replotted in accordance with the required functions. In these curves, K_1 is taken to be equal to $(Q_{R_{max}})^2$, in keeping with the relationship expressed above.

Figure 9 represents a plot of $1/R$ against $1/C$, for various values of Q, with E being constant throughout. In keeping with the above requirements, the data conform to a family of lines with a common extrapolated intercept within experimental error.

In Figure 10, $1/R$ is plotted against the function $[(Q + 1)(Q + K_1)]/Q$, with C as the second variable and E constant. Again, the data conform to the required relationships and fall on a series of lines for the various values of C, which extrapolate to a common intercept that is identical with that found in Figure 9.

Figures 9 and 10 show that the quantitative relationships between free radical concentration (R) and total substrate concentration (C) and between R and the succinate/fumarate ratio (Q) conform quite closely to the requirements of the equilibrium expression (equation 9) which describes the proposed SDH reaction mechanism. In view of the agreement, the foregoing relationships may be used to calculate the equilibrium constants characteristic of the proposed reaction mechanism.

The common intercept established by both of these linear relationships, which is equal to $(K_4 + 1)/E$, leads to a direct calculation of K_4 (the constant for the equilibrium between the nonfree radical complex and its free radical form), since the value of E is known from the conditions of the experiments. As already indicated

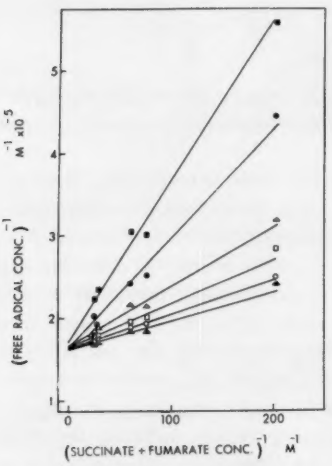

FIG. 9.—Curves of reciprocal free radical concentration as a function of reciprocal sum of the succinate and fumarate concentrations. The fumarate:succinate mole ratios are the following. Solid squares: 10; solid circles: 5; open triangles: 2; open squares: 0.1; open circles: 0.2; and solid triangles: 0.5. The data are those plotted in Figure 6.

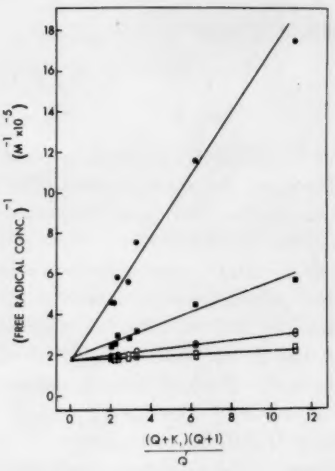

FIG. 10.—Curves of reciprocal free radical concentration plotted against the function $\frac{(Q + K_1)(Q + 1)}{Q}$. See text for definition of this function. The sum of the succinate and fumarate concentrations are the following: Solid circles: $0.12 \cdot 10^{-2}$ M; solid squares: $0.50 \cdot 10^{-2}$ M; open circles: $1.32 \cdot 10^{-2}$ M and $1.69 \cdot 10^{-2}$ M; and open squares: $3.52 \cdot 10^{-2}$ M and $3.92 \cdot 10^{-2}$ M. The data are those plotted in Figure 6.

above, the overall equilibrium constant (K_1) can be calculated from the value of Q where the free radical concentration (R) is at a maximum. The equilibrium constant (K_2) for the reaction between succinate and the oxidized form of SDH can be calculated from equation (9), since $1/K_2$ will appear as the slope of the straight line which should result from a plot of $1/R$ against the expression

$$\frac{K_4}{E} \cdot \frac{(Q + 1)\,(Q + K_1)}{CQ}.$$

Figure 11 is a plot of this relationship, the data employed being those shown directly in Figure 6. All of the available data conform quite well to the expected linear relationship, over a rather considerable range of values, so that the slope, and therefore the value of K_2, is readily obtained. The values of K_1 and K_2 being known, K_3 can be calculated from equation (8). Thus, Figures 9, 10, and 11 show that the experimental values of free radical concentration determined at various values of C and Q conform to the relationships expected from the proposed reaction mechanism and lead graphically to a calculation of the relevant equilibrium constants.

The foregoing considerations are readily expanded to include the effects of malonate on the observed free radical concentrations in the SDH system. Since malonate is a competitive inhibitor of SDH,[9, 12, 14, 29–31] we may expect the following relationships to hold:

Malonate + ox. SDH $\rightleftharpoons$ Mal-SDH complex$_1$:

$$\frac{(\text{Mal-SDH complex}_1)}{(\text{Malonate})(\text{ox. SDH})} = K_5. \tag{10}$$

Malonate + red. SDH $\rightleftharpoons$ Mal-SDH complex$_2$:

$$\frac{(\text{Mal-SDH complex}_2)}{(\text{Malonate})(\text{red SDH})} = K_6. \tag{11}$$

The above expression may now be combined with equation (9) in the form:

$$\frac{1}{R_M} = \frac{K_4 M\ (K_5 Q + K_1 K_6)\ (Q + 1)}{K_2\ \ CQE} + \frac{1}{R'}, \tag{12}$$

where M is malonate concentration, R_M is the free radical concentration of the SDH system in the presence of malonate, and the remaining symbols are those defined above. Should this or a similar relationship apply, $1/R_M$ should be linear

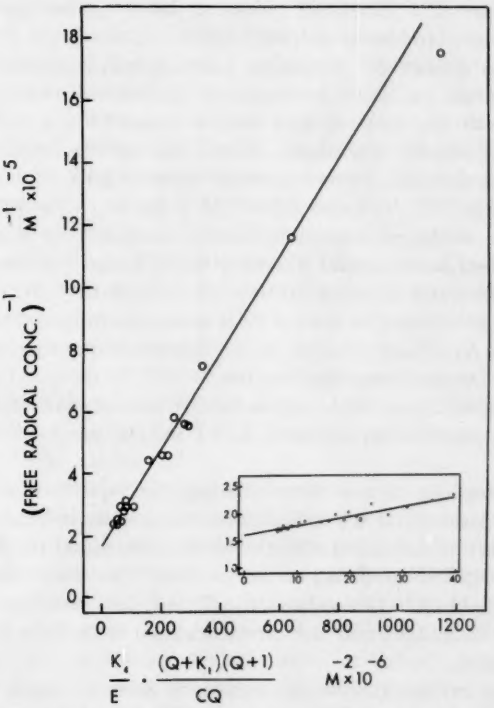

FIG. 11.—Curve of reciprocal free radical concentration plotted against the function $\frac{K_4}{E} \cdot \frac{(Q + 1)(Q + K_1)}{CQ}$. See text for definition of this function. The data are those plotted in Figure 6.

in M and the slope at constant values of Q and C should be proportional to $1/E$. To test the conformity of the ESR data obtained from the malonate-inhibited SDH system to this relationship, the data of Figure 8 have been appropriately

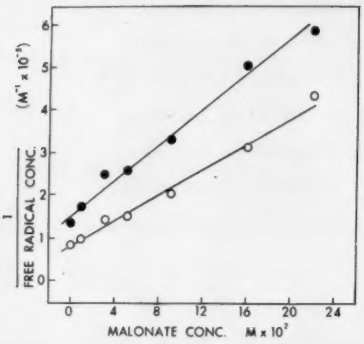

FIG. 12.—Curves of reciprocal free radical concentration plotted against malonate concentration. The concentrations of SDH for open circles and solid circles are $5.0 \cdot 10^{-5}$ M and $3.3 \cdot 10^{-5}$ M, respectively. The data are those plotted in Figure 8.

replotted in Figure 12. The fit of points on linear curves appears to be quite good, and the slopes are closely proportional to $1/E$.

While the data do not yet permit an unambiguous evaluation of K_5 and K_6, we can assume from published estimates of the kinetic constants for malonate inhibition for both the forward and reverse reactions[9, 12, 14, 29–31] that $K_6 \cong K_5/4$. If this relationship is assumed, K_5 and K_6 can be calculated from equation (12). The values obtained in this way range between $2 \cdot 10^4$ M^{-1} and $2 \cdot 10^3$ M^{-1} for K_5 and between $0.5 \cdot 10^4$ M^{-1} and $0.5 \cdot 10^3$ M^{-1} for K_6. The reciprocals of these constants, which would correspond to kinetic constants for malonate inhibition (K_I) obtained from conventional kinetic studies, range between $5 \cdot 10^{-5}$ M and $5 \cdot 10^{-4}$ M for $1/K_5$ and between $20 \cdot 10^{-5}$ M and $20 \cdot 10^{-4}$ M for $1/K_6$. These values, obtained solely on the basis of ESR observations, are of the same order of magnitude as the K_I values reported in the literature for succinate → fumarate and fumarate → succinate reaction kinetics.[9, 14, 29–31] It would appear therefore, that the effects of malonate inhibition on the free radical concentration of the SDH system conform to the expectations based on the proposed enzyme reaction mechanism.

Given the foregoing means of calculating the equilibrium constants which describe the proposed SDH mechanism, the values of the relevant thermodynamic constants can also be estimated. Such calculations, based on the ESR data obtained from two SDH preparations made from the same acetone-powder are summarized in Table 1. The values of $\Delta F°$ and $\Delta E_0'$ are calculated from ESR observations at 32°; $\Delta H°$ and $\Delta S°$ are calculated from data obtained at 10°C, 32°C, and 46°C.

The values of the thermodynamic constants given in Table 1 are such that, qualitatively, the free radical concentration always decreases with decreasing temperature over the range studied. This effect is observed both in ESR studies of the purified SDH system (see Figure 7) and in the earlier studies of the SDH free radicals found in heart muscle particles.[1, 2]

The values of $\Delta F°$, $\Delta H°$, and $\Delta S°$ are of a reasonable order of magnitude for the reactions with which they are associated in the proposed reaction mechanism. Determination of the value of $\Delta E_0'$, the redox potential difference for the enzyme-

TABLE 1

THERMODYNAMIC DATA FOR THE REACTIONS OF SUCCINIC DEHYDROGENASE

Reaction		Preparation	Equilibrium constant (32°C)	$\Delta F°$ (32°) cal mole^{-1}	$\Delta E_0'$ (32°, pH 7.6) volts	$\Delta H°$ (10°C to 46°C) cal mole^{-1}	$\Delta S°$ (10°C to 46°C) cal. mole^{-1}/°K
(1) $\frac{(\text{Fum})(\text{red SDH})}{(\text{Succ})(\text{ox SDH})}$	$= K_1$	1*a*	0.11	1300	−0.029	−9510	−36
		1*b*	0.25	840	−0.018	−9520	−34
(2) $\frac{(\text{Complex})}{(\text{Succ})(\text{ox SDH})}$	$= K_2$	1*a*	311	−3460	...	−4210	−2.5
		1*b*	724	−4000	...	−6500	−8
(3) $\frac{(\text{Complex})}{(\text{Fum})(\text{red SDH})}$	$= K_3$	1*a*	2830	−4790	...	3930	29
		1*b*	2890	−4730	...	3020	25
(4) $\frac{(\text{Complex})}{(\text{Free Radical complex})}$	$= K_4$	1*a*	1.33	−180	...	−8050	−26
		1*b*	1.88	−380	...	−8060	−25

substrate system, permits the calculation of the redox potential of the enzyme alone, a value not previously available from biochemical studies of SDH. The over-all redox potential difference, $\Delta E_0'$, equals E_0' (enzyme) − E_0' (substrate). Since the E_0' (substrate), which is readily determined by conventional methods, is about 0 volts at pH 7.6,[3] the redox potential of the enzyme itself is about equal to $\Delta E_0'$. The conclusion (see Tables 1 and 2) that the SDH redox potential is about 0 volts is in keeping with expectations based on the redox properties of the biochemical reactions with which it is normally coupled in the electron transport system.[2, 32–35]

The conventional Michaelis-Menten constants ($K_{M(S)}$ and $K_{M(F)}$) which describe the affinity of SDH for succinate and fumarate respectively can also be estimated from the equilibrium constants descriptive of the proposed reaction mechanism. $K_{M(S)}$ is approximately equal to $1/[K_2\ (1 + 1/K_4)]$ and $K_{M(F)}$ is approximately equal to $1/[K_3\ (1 + 1/K_4)]$. The values of these constants calculated from the data summarized in Tables 1 and 2 are of the order of 10^{-3} *M* and 10^{-4} *M* respectively, and fall within the fairly wide range of values reported from kinetic determinations of these constants.[9, 11–15]

While equilibrium and thermodynamic constants derived from ESR measurements on separate SDH preparations made from the same acetone-powder are similar (see Table 1), noticeably greater variations are observed when wholly independent preparations are compared. This can be seen from Table 2, which summarizes the results obtained from preparations derived from eight different acetone powders, including the one which provided the data summarized in Table 1. It is evident from the consistency of data based on a single enzyme preparation (see, for example, Figure 6) that the variations in the values of the constants are not due to experimental errors. While we cannot at present define the cause of these differences among enzyme preparations, it would appear either that they are due to original variations in the character of the enzymes present in different tissue samples or that they are introduced by some step in the treatment of the preparation prior to the preparation of the acetone powder.

Discussion.—The foregoing analysis of the data regarding free radical concentrations in the SDH system shows that a particular mechanism accounts for the

TABLE 2

EQUILIBRIUM CONSTANTS AND FREE ENERGY CHANGES FOR THE REACTIONS OF SDH

Preparation	Temp (°C)	Reaction (1) K_1	Reaction (1) $\Delta F°$ (cal mole^{-1})	Reaction (1) ΔE_0 (pH 7.6) (v)	Reaction (2) K_2 (M^{-1})	Reaction (2) $\Delta F°$ (cal mole^{-1})	Reaction (3) K_3 (M^{-1})	Reaction (3) $\Delta F°$ (cal mole^{-1})	Reaction (4) K_4	Reaction (4) $\Delta F°$ (cal mole^{-1})	Michaelis constant (succinate) $\frac{1}{K_2(1+1/K_4)}$ ($M \cdot 10^4$)	Michaelis constant (fumarate) $\frac{1}{K_3(1+1/K_4)}$ ($M \cdot 10^4$)
1(a)	46	0.12	1340	−0.029	412	−3800	3430	−5150	0.92	52	11.6	1.4
1(a)	32	0.25	840	−0.018	724	−3980	2890	−4730	1.88	−380	9.0	2.3
1(a)	10	0.74	170	−0.004	1520	−4120	1780	−4210	5.25	−930	5.5	4.7
1(b)	46	0.06	1790	−0.039	238	−3460	3970	−5250	0.84	110	19.2	1.2
1(b)	32	0.11	1330	−0.029	311	−3460	2830	−4790	1.33	−180	18.4	2.0
1(b)	13	0.25	790	−0.017	493	−3540	1970	−4330	3.33	−680	15.6	3.9
2	32	0.12	1290	−0.028	174	−3120	1410	−4390	1.77	−350	36.6	4.5
3	35	0.16	1120	−0.024	635	−3940	3970	−5080	3.25	−720	12.0	1.9
4	35	3.00	−660	0.015	2770	−4850	900	−4160	3.15	−700	2.8	8.4
5	32	2.56	−570	0.012	3020	−4850	1140	−4270	3.26	−720	2.5	6.6
6	32	3.24	−710	0.015	3090	−4860	950	−4150	3.33	−730	2.5	8.1
7	35	1.56	−270	0.006	1980	−4650	1270	−4370	2.73	−610	3.7	5.8
8	35	0.90	70	−0.002	2600	−4810	2900	−4880	1.95	−410	2.6	2.3

reactions which occur in a system containing SDH, succinate, and fumarate at equilibrium. However, further considerations indicate that this mechanism is also characteristic of the nonequilibrium systems which mediate net oxidation or reduction of substrate by this enzyme.

The reaction constants calculated from the ESR data refer, of course, to an equilibrium system. On the other hand, the corresponding constants determined from biochemical studies of the effects of reaction parameters on the rate of SDH activity, as measured by interaction with an added redox system, refer to non-equilibrium conditions. As shown in Tables 2 and 3, the range of values of the SDH Michaelis-Menten constants and the malonic acid inhibition constants, calculated from the ESR data, agree with the range of values previously reported on the basis of biochemical determinations of non-equilibrium systems. Furthermore, in both of these cases there is correspondence between the physical significance of the reaction constants deduced from ESR data on the equilibrium system and those based on biochemical rate measurements.

It is also relevant that the reaction mechanism proposed on the basis of the free radical concentrations observed in the purified SDH system is identical with that previously deduced from ESR studies of SDH in heart muscle particles.[1, 2] In the latter case, it was found that the ESR signals observed under equilibrium conditions were also found during net oxidation of succinate in the presence of oxygen (the system being, therefore, not in complete equilibrium) as long as succinate remained.

These considerations indicate that the free radical mechanism characteristic of the simple SDH system in equilibrium (and lacking a secondary redox couple) occurs also in nonequilibrium systems in which net redox consumption of substrate is promoted through added redox agents or through interactions with the electron-transport system present, for example, in the heart muscle particle. We may conclude, therefore, that the SDH reaction mechanism deduced from the ESR data is descriptive of the enzymatic activity of SDH generally.

TABLE 3

RANGE OF VALUES FOR SDH REACTION CONSTANTS*

Source of data	Michaelis constant (succinate) ($M \cdot 10^4$)	Michaelis constant (fumarate) ($M \cdot 10^4$)	Malonate inhibition constant (forward reaction) ($M \cdot 10^4$)	Malonate inhibition constant (reverse reaction) ($M \cdot 10^4$)
Free radical concentrations (ESR data)	2 to 37†	1 to 8†	5 to 48‡	20 to 192‡
Oxidation-reduction rates (published values)§	1 to 20	2 to 20	1 to 15	4 to 60

* All values are for temperatures of 25° to 35°C.
† See Table 2 for method of calculation and individual values.
‡ See text for method of calculation.
§ From references (9, 12–16, 29–31).

The ESR observations describe several properties of the SDH system that have been hitherto uncertain or inaccessible to experiment. The data show that the enzyme itself undergoes oxidation-reduction and lead to a calculation of the redox potential for the enzyme (about 0.0 v.) which conforms to expectations based on its position in the biological electron-transport chain. The observations also elucidate the apparent inhibitory effects of fumarate on the oxidation of succinate by SDH and of succinate on the reduction of fumarate. The common interpretation of these effects is that succinate and fumarate act, each against the other, as classical competitive inhibitors by reversibly combining with the active sites of reduced and oxidized SDH, respectively. Calculations based upon the ESR data show, however, that complexes of the type succinate-reduced SDH and fumarate-oxidized SDH can exist in only trivial concentrations, if at all. This indicates that fumarate does not compete with succinate for the oxidized enzyme and that succinate does not compete with fumarate for the reduced enzyme. The effect is probably due to a competition between substrate and the appropriate redox form of the secondary redox couple usually present in the system, and reflects an effective partial reversal of a reaction rather than competitive inhibition. Finally, the ESR results show that a free radical form of the enzyme-substrate complex occurs in the system, and the data lead to a reaction mechanism that accounts for this new observation and to the calculation of thermodynamic constants for the SDH reaction and for several partial reactions.

The ESR data also provide new evidence regarding the electronic processes which occur within the SDH enzyme-substrate complex, and their relationship to the overall chemical reaction catalyzed by the enzyme. The ESR signal observed in the SDH system arises within the complex formed when the substrate becomes bound to the enzyme. Neither the free enzyme nor the substrate exhibit ESR signals, so that neither component contains unpaired electrons associated with the organic portions of the molecule. It follows, then, that the observed ESR signal

results from the *unpairing* of some pair of electrons present in the enzyme-substrate complex. There are three types of electronic configurations, involving organic moieties of the complex, that might result from this process: (*a*) a triplet with a pair of electrons closely coupled in antiparallel alignment, (*b*) a multiplet (biradical) with two uncoupled and independent unpaired electrons, or (*c*) a doublet (free radical) with a single unpaired electron.

The triplet state is an unlikely source of the signal, for we observe no resonance at $g = 4$, which frequently occurs with these states. Triplet states giving rise to signals at $g = 2$ are usually too broad to be detected in the conditions of our experiments (dilute aqueous and randomly oriented systems). While we cannot completely rule out a biradical state, the structure of the ESR signal places certain restrictions on the location of the two unpaired electrons within the complex. Since neither g value nor line shape considerations suggest the existence of two different types of spin environments, it must be concluded that if a biradical state exists, both electrons occupy similar but physically separated environments so that their individual ESR signals superimpose closely. Because all electrons associated with the organic moieties of the SDH system appear to be originally paired and not paramagnetic, the existence of a doublet state in the complex would require that one member of a pair of electrons must become associated with a spin state which is unobservable by ESR techniques. The iron atoms present in SDH provide a reasonable basis for such an event. If one of the unpaired electrons served to reduce a ferric atom in SDH to the ferrous state, the latter would be expected to produce an ESR signal that would be too broad to be detected at room temperatures in an aqueous medium.

Thus, the ESR data show that an electron transfer process occurs within the SDH enzyme-substrate complex and that this process gives rise to one or two uncoupled, unpaired electrons. This type of event has been described in charge transfer complexes,[36, 37] and on the whole, the SDH free radical complex bears a general resemblance to a charge transfer complex of the "strong" or π-onium type described by Mulliken.[38] The available data provide no specific evidence regarding the location of the unpaired electron(s). A signal of the type observed is consistent with localization of a single unpaired electron in the flavin prosthetic group, provided that anisotropic effects, electron exchange processes or spin-spin interactions between electrons are sufficient to account for the absence of the hyperfine lines that are otherwise observed in flavin free radicals.[24–27] It is also possible that the unpaired electron(s) are associated with some part of the protein moiety of the enzyme.

An important consequence of the ESR studies is the conclusion that the enzyme-substrate complexes, whether of the free radical or non-free radical types, do not dissociate into products which are themselves free radicals, such as a succinate radical or a free radical form of the enzyme itself. In particular, the observed dependence of free radical concentration on the fumarate/succinate mole ratio requires that neither SDH nor substrate can exist in the system as separate free radicals. Nevertheless, it is clear that free radical forms of the complex must arise as a consequence of univalent electron transfer between the substrate and the enzyme, so that free radical states of both of these components are to be expected. The central conclusion to be drawn from our observations is that these states

exist only when the enzyme and substrate are bound together in the form of a complex.

There are two possible causes for the failure of the free radical complex to dissociate, measurably, into separate free radical forms of either of its components: (*a*) the lifetime of the particular electronic states may be so short as to preclude the relatively slow process involved in the physical separation of the enzyme and substrate, or (*b*) the electronic configuration of the complex may be such as to induce a binding between substrate and enzyme which is so strong as to be essentially covalent.

In the latter case, one would expect to find a major entropy change associated with the transition between free radical and non-free radical forms of the complex. The entropy change associated with this process, which can be calculated from the ESR data (see Table 1) is consistent with the second of these effects. The value (about 30 cal $mole^{-1}/°K$) is much greater than any effect expected directly simply from the unpairing of electrons in a common resonance system and must reflect a profound change in the molecular structure of the complex. This change is probably localized in the substrate part of the complex or in a neighboring region of the protein, for there is no evidence (for example from optical studies) of major changes in flavin structure during SDH activity.

In sum, these considerations show that (*a*) One of the events that follows the binding of substrate to SDH is the uncoupling of a pair of electrons as a consequence of electron transfer between enzyme and substrate. (*b*) As a result of this process, the complex possesses one, or possibly two, unpaired electrons capable of inducing the observed ESR signals and is therefore a free radical. (*c*) While the ESR data do not distinguish among possible members of the class of free radical enzyme-substrate complexes, the data do show that there must exist at least one member of this class from which substrate does not measurably dissociate. This last effect appears to result from major structural changes, which are probably covalent in character and which appear to be localized in or near the substrate part of the complex.

These considerations indicate that free radical complexes play an essential role in the chemical change in the substrate that is catalyzed by SDH. This conclusion, in keeping with the ESR observations generally, is evidence that free radicals are decisive intermediates in the reactions catalyzed by SDH. It is expected that further ESR and biochemical studies will provide a more precise description of the relationships which exist among the electronic states of the complexes, their thermodynamic constants, and the configurations of possible complexes in which strong binding of substrate to enzyme may occur.

* This work was supported in part by the Office of Naval Research and by research grant C-3983 from the National Cancer Institute, U. S. Public Health Service.

[1] Commoner, B., and T. C. Hollocher, Jr., these PROCEEDINGS, **46**, 405 (1960).

[2] Hollocher, T. C., Jr., and B. Commoner, these PROCEEDINGS, **46**, 416 (1960).

[3] Borsook, H., and H. F. Schott, *J. Biol. Chem.*, **92**, 535, 559 (1931).

[4] Kearney, E. B., and T. P. Singer, *Biochim. Biophys. Acta*, **17**, 596 (1955).

[5] Singer, T. P., E. B. Kearney, and V. Massey, *Arch. Biochem. Biophys.*, **60**, 255 (156).

[6] Singer, T. P., E. B. Kearney, and V. Massey, in *International Symposium. Enzymes: Units of Biological Structure and Function*, ed. O. H. Gaebler (New York: Academic Press, 1956), pp. 417–432.

[7] Kearney, E. B., T. P. Singer, and N. Zastrow, *Arch. Biochem. Biophys.*, **55,** 579 (1955).
[8] Singer, T. P., and E. B. Kearney, *Biochim. Biophys. Acta*, **15,** 151 (1954).
[9] Singer, T. P., E. B. Kearney, and V. Massey, *Adv. Enzymol.*, **18,** 65 (1957).
[10] Singer, T. P., E. B. Kearney, and N. Zastrow, *Biochim. Biophys. Acta*, **17,** 154 (1955).
[11] Singer, T. P., and E. B. Kearney, in *Methods of Biochemical Analysis*, ed. D. Glick (New York: Interscience Publishers, 1957), vol. 4, pp. 307–333.
[12] Singer, T. P., E. B. Kearney, and P. Bernath, *J. Biol. Chem.*, **223,** 599 (1956).
[13] Slater, E. C., and W. D. Bonner, *Biochem. J.*, **52,** 185 (1952).
[14] Thorn, M. B., *Biochem. J.*, **54,** 540 (1953).
[15] Ackermann, W. W., and V. R. Potter, *Proc. Soc. Exptl. Biol. Med.*, **72,** 1 (1949).
[16] Slater, E. C., *Disc. Faraday Soc.*, **20,** 311 (1955).
[17] Commoner, B., J. J. Heise, and J. Townsend, these PROCEEDINGS, **42,** 710 (1956).
[18] Hahs, T. S., Master's thesis, Washington University, 1960.
[19] Pake, G. E., J. Townsend, and S. I. Weissman, *Phys. Rev.*, **85,** 682 (1952).
[20] Townsend, J., S. I. Weissman, and G. E. Pake, *Phys. Rev.*, **89,** 606 (1953).
[21] Wertz, J. E., *Chem. Revs.*, **55,** 729 (1955).
[22] Van Vleck, J. H., *The Theory of Electric and Magnetic Susceptibilities* (Oxford University Press, 1932).
[23] Commoner, B., in *Light and Life*, ed. W. D. McElroy and B. Glass, (Baltimore: Johns Hopkins Press), pp. 356–377.
[24] Commoner, B., and B. B. Lippincott, these PROCEEDINGS, **44,** 1110 (1958).
[25] Lippincott, B. B., Ph. D. thesis, Washington University, 1959.
[26] Ehrenberg, A., *Acta Chem. Scand.*, **14,** 766 (1960).
[27] Ehrenberg, A., in *Free Radicals in Biological Systems*, ed. M. S. Blois (New York: Academic Press, 1961), pp. 337–350.
[28] Hollocher, T. C., and B. Commoner, *Federation Proc.*, **19,** 28 (1960).
[29] Quastel, J. H., and W. R. Wooldridge, *Biochem. J.*, **22,** 689 (1928).
[30] Quastel, J. H., and A. H. M. Wheatley, *Biochem. J.*, **25,** 117 (1931).
[31] Mann, P. J. G., and J. H. Quastel, *Biochem. J.*, **35,** 502 (1941).
[32] Yakushiji, E., and K. Okunuki, *Proc. Imp. Acad. (Tokyo)*, **16,** 299 (1940).
[33] Keilin, D., and E. F. Hartree, *Nature*, **176,** 200 (1955).
[34] Ball, E. G., *Biochem. Z.*, **295,** 262 (1938).
[35] Stotz, E., A. E. Sidwell, and T. R. Hogness, *J. Biol. Chem.*, **124,** 11 (1938).
[36] Miller, R. E., and W. F. K. Wynne-Jones, *J. Chem. Soc.*, 2378 (1959).
[37] Bijl, D., H. Kainer, and A. C. Rose-Innes, *J. Chem. Phys.*, **30,** 765 (1959).
[38] Mulliken, R. S., *J. Am. Chem. Soc.*, **74,** 811(1952); *J. Phys. Chem.*, **56,** 801 (1952).

---

*FREE RADICALS IN SURVIVING TISSUES**

BY BARRY COMMONER AND JESSIE L. TERNBERG

THE HENRY SHAW SCHOOL OF BOTANY, THE ADOLPHUS BUSCH III LABORATORY OF MOLECULAR BIOLOGY AND THE DEPARTMENT OF SURGERY, WASHINGTON UNIVERSITY, ST. LOUIS

Communicated by Albert Szent-Györgyi, July 10, 1961

The first experimental evidence that free radicals occur in animal tissues (and in other biological materials), reported from this laboratory in 1954, was based on electron spin resonance (ESR) studies of frozen-dried samples.[1] ESR signals indicative of low concentrations of free radicals were observed in frozen-dried samples prepared from a variety of animal tissues. The ubiquitous occurrence of the ESR signals and their relative intensities in different tissues suggested that they were due to free radicals associated with metabolic processes.

However, the dry condition of the samples, which was dictated by the relatively low sensitivity of the ESR apparatus then available (the presence of water, being an effective absorber of microwave energy, causes an appreciable loss in the sensitivity of ESR detection), precluded more direct evidence regarding the physiological significance of the observed free radicals.

The development by Jonathan Townsend of more sensitive ESR apparatus has now permitted direct investigation of this question. In the present communication, we report results obtained from a series of ESR investigations of surviving tissues from several laboratory animals and from man. The results show that free radicals occur in living animal tissues and that their concentrations are related to the biological origin of the tissue and vary with certain physiological and pathological conditions. The properties of the free radicals detected in surviving animal tissues are consistent with those previously observed in functional oxidation-reduction enzyme systems, and there is evidence that they are associated with the mitochondria present in the tissue.

Materials and Methods.—Tissue samples from laboratory animals are prepared from organs removed whole, as quickly as possible after anesthetization (by ether) of the animal. The entire organ is stored on cracked ice, and tissue slices, about 0.5 mm. thick, are prepared when required. About 50 mg (wet weight) of tissue is suspended in 0.2 ml of 5% glucose solution contained in a flat pyrex ESR cell ($1 \times 5 \times 20$ mm). The tissue is oriented in the cell so that the entire sample occupies the sensitive zone of the ESR spectrometer cavity. The ESR spectrometer employed in these studies, which has been described briefly elsewhere,[2] employs microwave radiation of 9,000 mc/sec, so that resonance absorption due to the spin of the unpaired electron occurs at an external magnetic field of about 3,000 gauss. ESR signals are obtained by scanning the microwave energy absorption as a function of magnetic field strength. About 2 min are required for each run. In the experiments reported below, the instrument was operated with an inherent time-constant of 0.1 sec. The instrument will detect about 10^{-11} moles of free radical (of the line width typical of free radicals encountered in biological materials) in a sample containing about 0.1 ml of liquid water.

The ESR signal produced by the spectrometer represents the rate of change in the microwave energy absorbed by the sample with respect to the strength of the external magnetic field. The signal intensity, which is proportional to the number of unpaired electrons sensed by the instrument, is given by the integral of the original signal. To determine the actual free radical content of a tissue sample (on the assumption that each free radical molecule contains one unpaired electron), the integral of the sample signal is compared with the integral of the signal given by a standard solution ($10^{-4}M$) of $MnCl_2$, taking into account that the electron quantum spin number for Mn is $^5/_2$. The free radical concentration of the tissue is then calculated from the wet weight or the nitrogen content (by microKjeldahl) of the sample.

Results.—The ESR signals obtained from approximately 50-mg samples of surviving tissue from various guinea pig organs are shown in Figure 1. These observations are typical of results obtained with comparable tissues from rat, mouse, and man. The signals are centered in the region $g = 2.003$ to $g = 2.005$, and line widths (at the point of maximum slope) are 10–20 gauss. In general, the line

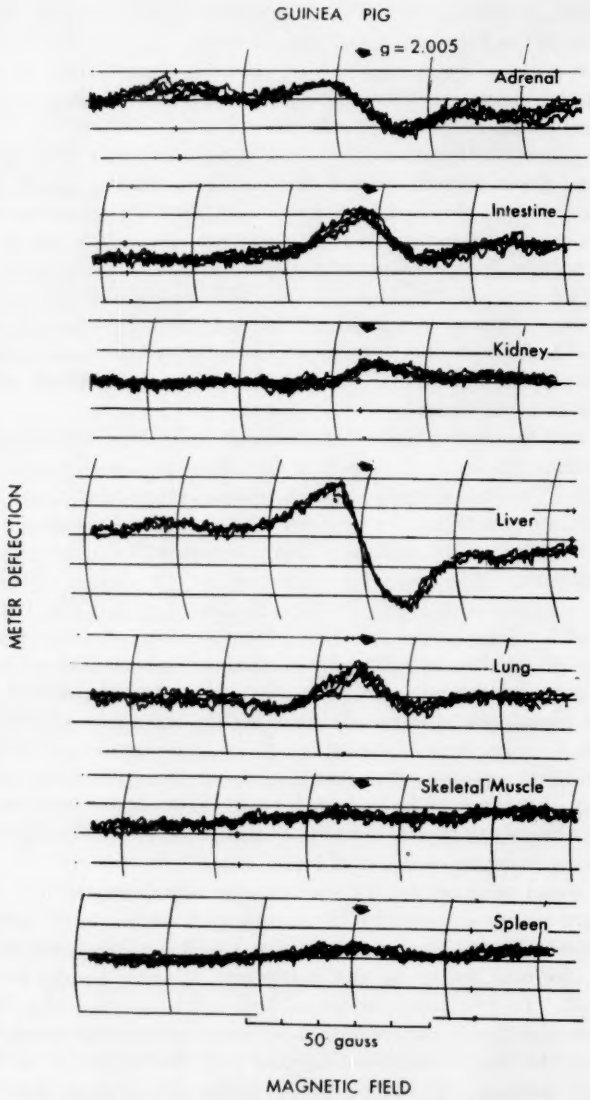

FIG. 1.—ESR signals obtained from surviving samples of guinea pig tissues. Each signal represents superimposed tracings of 3–6 successive runs. The magnetic field increases to the right along the abscissa. The meter deflection (ordinate) represents the rate of change of absorption of microwave energy (9,000 mc/sec) with respect to the field strength. Samples were about 50 mg (wet weight) and the suspending medium was 5 per cent glucose in water. Instrument conditions are described in the text.

shapes are simple and rather similar. The signals are indistinguishable from those exhibited by free radicals formed in redox enzyme systems or in mitochondrial particles which contain such systems.[3–5]

The ESR signal from guinea pig adrenal tissue is unusual and exhibits two subsidiary symmetrical peaks at an interval of about 40 gauss on either side of the main signal at $g = 2.005$. However, adrenal tissue from rat and man exhibit only a simple signal.

By the methods described above, we have determined the total free radical content of a number of single samples of liver, kidney, and heart, removed from a series of adult guinea pigs, rats, and mice (standard laboratory strains). The results illustrated in Figure 2 show that the free radical contents, expressed on either a

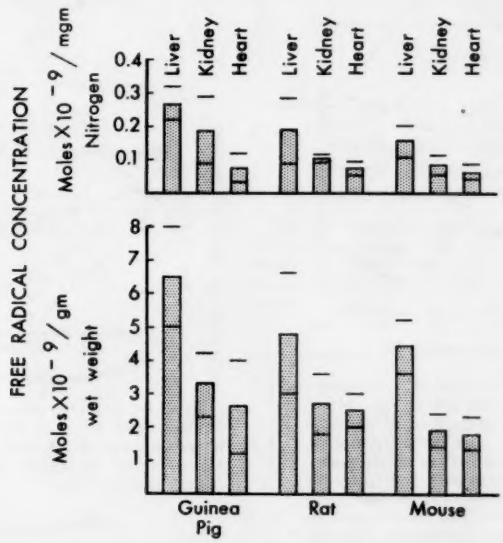

FIG. 2.—Comparison of the free radical concentrations (calculated as described in the text) of surviving liver, kidney, and heart tissue from the guinea pig, rat, and mouse. Bar heights represent average values of 6–8 samples from separate animals. Horizontal lines indicate the standard deviation relevant to each average.

wet-weight or nitrogen basis, while somewhat variable, exhibit mean values which appear to be characteristic both of a given tissue and of a given animal. The free radical content of liver, kidney, and heart declines in the order guinea pig > rat > mouse. In all three animals, the free radical content declines in the order liver > kidney > heart. ESR signals are usually undetectable in samples of skeletal muscle from all three animals; occasionally, it is possible to detect a very weak signal. Comparable relationships among the free radical contents of these tissues have been observed in less complete studies of tissues from man and dog.

The ESR signals observed in surviving animal tissues are characteristically sensitive to ambient temperature. Figure 3(*a*) shows how the free radical content of guinea pig kidney changes as the ambient temperature is varied. The free radical level increases noticeably as the temperature is reduced from 28° to 0°C and persists in the frozen tissue. When the temperature is again elevated, the free radical content falls, but the curves for rising and falling temperature do not coincide. The effects of ambient temperature on free radical content are generally

reversible if the temperature does not exceed about 30°C. However, as shown in Figure 3(*b*) when the temperature of guinea pig kidney tissue is increased from 0° to 38°, an irreversible loss of most of the original signal occurs.

The foregoing results suggest that the free radical contents of surviving tissue samples vary not only with the ambient temperature but also with time. To elucidate this effect, the signal intensity of a series of equivalent samples of rat liver was followed with time at different ambient temperatures. The results, illustrated in Figure 4, show that free radical concentration falls with time, at a constant

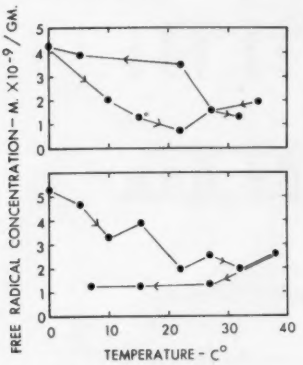

FIG. 3.—Free radical concentration of surviving guinea pig kidney slices during variations in ambient temperature. In the experiment shown in the upper curve (*a*), measurements began with the tissue at 36°C. The temperature was then lowered to 0°C and then raised to 32°C. In the experiment shown in the lower curve (*b*), measurements began at 0°C, and the temperature was increased to 38°C and then reduced again.

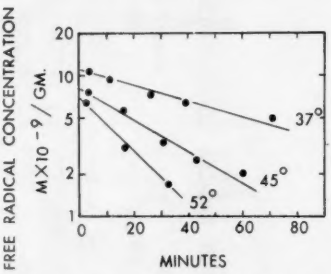

FIG. 4.—Semilog plot showing the change, with time, in the free radical concentration of rat liver slices maintained at the indicated constant temperatures.

temperature, the process being approximately first-order with respect to free radical concentration. As shown in Figure 5, the first-order rate constant rises exponentially with temperature. The heat of activation for the process which limits the loss of free radical, calculated from the data of Figure 5, is about 15–20,000 cal. Temperature effects of this type have been observed in several other tissues; all ESR signals observed in animal tissues (with the exception of those containing melanin, which is a stable free radical[3]) are lost irreversibly when the tissue is boiled for 5 min. This effect, in the case of rat liver, is illustrated in Figure 6.

Oxygen tension has no effect on any of the ESR signals thus far observed in animal tissues. The signals described above were obtained under essentially anaerobic conditions, since the tissue is in a very small volume of medium (about 0.2 ml), which is in turn in contact with air across a minimal area (about 5 mm^2). Explicit evidence for this conclusion is given in Figure 7, which shows that neither shape nor intensity of the signal exhibited by a sample of human liver is affected by saturating the fluid medium with O_2 or N_2 immediately before the ESR determination is made.

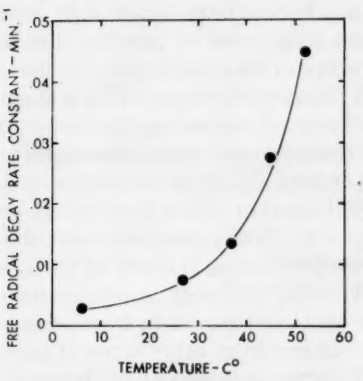

FIG. 5.—The first-order constants for the rate of decline in free radical concentration of rat liver slices at various temperatures, calculated from semilog plots such as those shown in Figure 4.

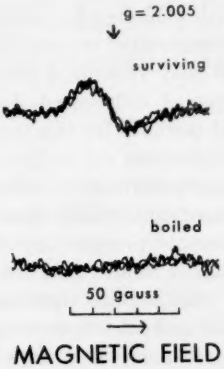

FIG. 6.—ESR signals from surviving rat liver and from the same sample after being boiled for 5 min.

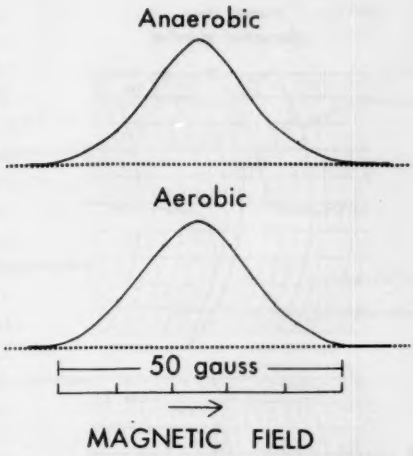

FIG. 7.—Integral signals for 50 mg samples of human liver tissue under aerobic and anaerobic conditions. The free radical concentrations are proportional to the areas under the integral curves.

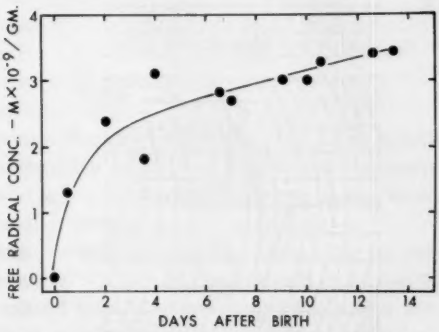

FIG. 8.—Free radical concentrations of samples of liver from litter-mate rats sacrificed at various intervals after birth.

All of the ESR signals described above were observed in tissues from adult animals. We have found, however, that ESR signals are undetectable or noticeably reduced in certain tissues from newborn animals. Figure 8 reports the free radical concentration of liver samples taken from litter-mate rats at intervals after birth. A signal is undetectable in the liver of the newborn rat. Liver from a one-day-old rat exhibits a weak ESR signal, and the free radical concentration increases to a nearly constant value at about the eighth day after birth. Similar effects have been observed in rat kidney and heart tissue.

Additional evidence of a relation between free radical concentration and the physiological status of the tissue has been obtained from some preliminary studies of certain pathological human tissues. A number of human liver samples obtained by biopsy during various surgical procedures have been surveyed for ESR

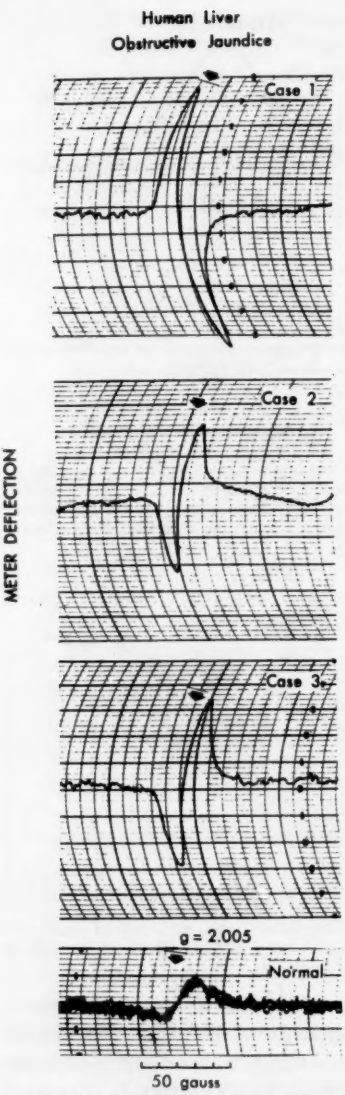

FIG. 9.—ESR signals from 50 mg liver biopsy samples in three cases of extra-hepatic obstructive jaundice compared with a signal from normal human liver. The abscissa and ordinate are as described for Figure 1.

signals. It has been found that liver samples from cases of jaundice due to obstruction of the extra-hepatic bile ducts give a characteristic signal which is about three times as intense as that obtained from normal human liver. Examples of these unusual signals, in comparison with the ESR signal of human liver, are shown in Figure 9. Both signals are irreversibly destroyed by heating at about 40°C; both are enhanced somewhat at temperatures below 20°C and persist in frozen tissue. Liver samples from other types of jaundice (due to cirrhosis and to drugs) do not exhibit an abnormally intense signal. It is possible that this distinction between the ESR signals of liver from cases of obstructive jaundice on the one hand and the signals exhibited by normal liver and by liver from other types of jaundice on the other may provide a basis for a new technique of differential diagnosis. Since present methods for this type of diagnosis are sometimes not subject to unequivocal interpretation, a diagnostic procedure based on the ESR signals may be of considerable practical significance. Clinical trials are now in progress to determine the reliability of differential diagnosis of this and other liver diseases by means of ESR analysis of free radical content.

In our earlier ESR studies of frozen-dried tissues,[1] it was reported that the free radical content of mouse hepatoma was significantly smaller than that of normal mouse liver. We have now re-examined this problem by ESR studies of surviving liver samples. The results, illustrated in Figure 10, show that in contrast with normal liver, free radicals are undetectable in rat and mouse hepatoma. Similarly Figure 11 shows that a biopsy sample of human carcinoma of the colon metastatic to the liver does not exhibit an ESR signal, while tissue from a normal lobe of the same liver exhibits the usual signal. All of the ESR studies of neoplastic tissues up to this time indicate that they are distinguished by relatively

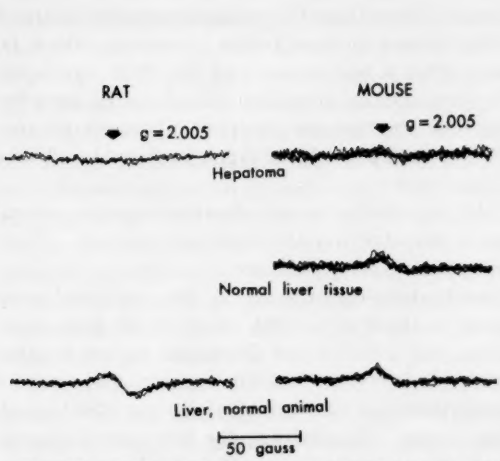

FIG. 10.—ESR signals from 50 mg samples of rat and mouse hepatoma compared with the signals obtained from similar samples of liver tissue from normal animals. In the case of the mouse, the signal from a sample of normal tissue from the hepatoma-bearing liver is also shown. The abscissa and ordinate are as described for Figure 1.

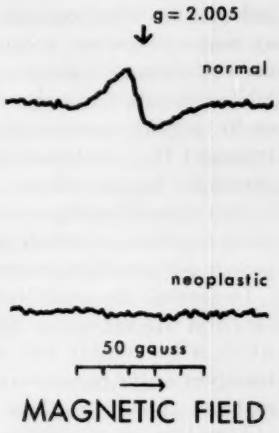

FIG. 11.—ESR signals from 50 mg biopsy samples from a human liver. The upper signal is from a sample obtained from a lobe of the liver containing only normal tissue. The lower signal is from a sample of metastatic carcinoma of the colon occurring in another part of the same liver. The abscissa and ordinate are as described for Figure 1.

low, or wholly undetectable, free radical contents.

Discussion.—The foregoing results show that thermally-unstable ESR signals are commonly observed in surviving mammalian tissue, and that the intensities of these signals are related to the biological origin and physiological state of the tissue. The molecular origin of these signals is, of course, of considerable interest.

In this connection, it is instructive to compare the ESR observations on surviving tissues with our earlier ESR studies on the role of free radicals in biological redox systems. If mitochondria are isolated from liver by techniques which preserve their structural integrity (use of hypertonic sucrose solutions, in particular), they exhibit an appreciable ESR signal at $g = 2.004$, which is about 15–20 gauss wide. The signal is clearly associated with enzymatic redox activity. It is lost irreversibly if the preparation is boiled for a few seconds; its intensity is a function of available concentrations of certain substrates (succinate and fumarate, DPNH, and β-hydroxyburyrate).[6]

Mitochondrial particles that are prepared by somewhat more destructive techniques (especially the use of hypotonic solvents and of extensive washing) do not exhibit an intrinsic ESR signal. However, a strong signal appears when a mixture of succinate and fumarate is added. This signal has a g value of 2.004, a line width of about 15–20 gauss and is irreversibly lost on boiling. It can be shown that the ESR signal exhibited by washed mitochondrial particles in the presence of succinate and fumarate is due to an enzyme-substrate complex of succinic dehydrogenase, which forms an important part of the mitochondrial electron transport chain.[4] These conclusions have been fully confirmed by more recent ESR studies of puri-

fied succinic dehydrogenase systems.[5] Since these free radicals represent forms of an enzyme-substrate complex, they appear in equilibrium systems in which no net oxidation or reduction occurs. This is one reason why the ESR signals exhibited by intact mitochondria, by preparations of washed mitochondrial particles, or by purified succinic dehydrogenase systems are observed when net electron transport (i.e., oxidation) is zero (for example, when oxygen is absent) and may persist for long periods of time.

Less extensive evidence shows that in addition to succinic dehydrogenase several other enzymes commonly present in mitochondria also form free radicals. These include β-hydroxybutyrate dehydrogenase[6] and cytochrome reductase.[3]

In general, the available evidence leads to the expectation that functional mitochondria will exhibit an ESR signal at about $g = 2.004$, about 15–20 gauss wide, which is irreversibly lost on boiling and which is not dependent on net electron transport or the presence of oxygen. It is evident from the experimental evidence reported above that these characteristics are also exhibited by the ESR signals observed in surviving mammalian tissues. In addition, the free radical concentrations characteristic of different tissues generally parallel the known concentrations of mitochondria in these tissues. Thus, the ESR signals from liver and kidney, which are relatively rich in mitochondria, are particularly intense. Heart muscle, which exhibits an appreciable ESR signal, contains a relatively high concentration of mitochondria, while skeletal muscle, which contains relatively few mitochondria, exhibits a barely detectable ESR signal. The increase in free radical concentration observed in rat liver during the first week after birth parallels a similar increase in the concentration of mitochondria and in succinoxidase activity, which has been observed in this tissue by Dawkins.[7] The striking difference between the free radical concentration of normal liver and liver tumor tissue also corresponds to the marked difference in mitochondrial content of normal and neoplastic tissue.

These correlations support the conclusion that the ESR signals observed in surviving mammalian tissues are due to free radicals produced as a result of the enzymatic redox activity of mitochondria. However, in one respect the tissue free radicals appear to differ from those thus far observed in mitochondria and in enzymes isolated from them. Unlike the ESR signals due to mitochondria and to isolated mitochondrial enzymes, the signals exhibited by intact tissues do not become less intense at reduced temperatures but show an opposite effect. This difference is most striking at 0°C. At this temperature, ESR signals are not detectable in mitochondrial particles or in purified succinic dehydrogenase. In contrast, tissue ESR signals rise to a maximum at 0°C and persist in the frozen tissue. There is a similar contrast in the effect of moderately elevated temperatures (i.e., 30–40°C). ESR signals from mitochondrial particles and isolated enzymes are intense and stable over periods of hours at these temperatures. On the other hand, when tissues are maintained at these temperatures, an apparently irreversible loss in signal intensity is observed.

These differences in response to temperature do not necessarily contradict the conclusion that the tissue ESR signals arise in mitochondria. The detailed studies of the succinic dehydrogenase system reported elsewhere[5] show that free radical concentration is dependent not only on enzyme and substrate concentrations but

also on the oxidant/reductant ratio and on the equilibrium constant which governs the interconversion of the normal and free radical forms of the enzyme-substrate complex. It is possible that the effects of temperature on the intensity of tissue ESR signals are due to the influence of temperature on these two parameters. In a complex electron transport system, such as that which is present in intact tissue, the oxidant/reductant ratio relevant to a given enzyme may depend in a quite complicated manner on its own equilibrium constants and on those of other redox enzymes comprising the total chain. In general, the effect of temperature changes on the redox balance of a particular enzyme will reflect *differences* between the temperature effects on the equilibrium constants of individual enzymes that lie above and below it in the electron transport chain. Under these circumstances, decreasing temperature may readily alter the relevant redox balance in such a manner as to increase the free radical concentration.

A possible basis for the effects of moderately elevated temperatures on the free radical concentrations in tissue is suggested by other observations on an isolated enzyme system. It has been found that treatment of purified lactic acid oxidative decarboxylase for 10 minutes at 37°C causes a marked change in the free radical concentration yielded by a given amount of enzyme in the presence of substrate, although specific activity is not affected.[8] The phenomenon is suggestive of a minor effect of temperature on the configuration of the enzyme protein, which could conceivably alter the equilibrium between the free radical and non-free radical forms of the enzyme-substrate complex without appreciably influencing the enzyme's over-all biochemical activity. Such a phenomenon might also account for negative effects of elevated temperature on free radical concentration.

These considerations indicate possible mechanisms which might give rise to the observed effects of temperature on tissue free radical concentrations, and they suggest a line of investigation which may yield the experimental evidence required for an actual explanation of the phenomena.

The wholly empirical observation of decisive differences in free radical concentration related to certain pathological changes in animal and human tissues also suggests certain useful lines of investigation. The distinctive effect of obstructive jaundice on the ESR signal exhibited by liver may on further study provide a clinically useful technique of differential diagnosis. While the remarkable absence of detectable ESR signals in tumor tissue may be only a reflection of the relatively small numbers of mitochondria characteristics of neoplastic tissue, further ESR studies of this phenomenon may provide a useful insight into metabolic differences among tumors and their relation to the effects on antitumor agents. Conceivably, some ESR techniques of diagnostic significance may ultimately result from such studies as well.

In sum, the foregoing ESR observations on surviving mammalian tissues confirm our earlier observations, based on frozen-dried samples, that tissues contain characteristic concentrations of free radicals of metabolic origin. The new observations show also that the ESR signals exhibited by mammalian tissues appear to originate in the redox enzymes associated with mitochondria. The results suggest that ESR determinations of free radical concentrations in tissues may serve to elucidate the metabolic processes characteristic of certain physiological and pathological conditions.

* This work was supported in part by the Office of Naval Research and by research grant C-3983 from the National Cancer Institute, U. S. Public Health Service.

[1] Commoner, B., J. Townsend, and G. E. Pake, *Nature*, **174**, 689 (1954).

[2] Commoner, B., J. J. Heise, and J. Townsend, these PROCEEDINGS, **42**, 710 (1956).

[3] Commoner, B., J. J. Heise, B. B. Lippincott, R. E. Norberg, J. V. Passonneau, and J. Townsend, *Science*, **126**, 57 (1957).

[4] Commoner, B., and T. C. Hollocher, Jr., these PROCEEDINGS, **46**, 405 (1960).

[5] Hollocher, T. C., Jr., and B. Commoner, these PROCEEDINGS, **47**, 1355 (1961).

[6] Hollocher, T. C. Jr. (unpublished observations).

[7] Dawkins, M. J. R., *Proc. Roy. Soc.* (*London*), **B150**, 284 (1959).

[8] Lippincott, B. B., Doctoral Dissertation, Washington University, 1959.

---

*VARIATION IN BASE COMPOSITION OF RIBONUCLEIC ACID IN ESCHERICHIA COLI**

BY MELVIN SANTER, DAVID C. TELLER, AND LIDA SKILNA

DEPARTMENT OF BIOLOGY, HAVERFORD COLLEGE

Communicated by David R. Goddard, July 17, 1961

Santer, Teller, and Andrews[1] have shown that the base ratios of the ribonucleic acid of *Escherichia coli* may be modified by growing this bacterium in different media. These analyses, carried out on the whole RNA of the cell with no attempt to distinguish among various classes of RNA, are supported by a number of experiments dealing with ribosomes and ribosomal-contained RNA of *E. coli*. In these latter experiments modification of RNA has been induced by (1) transferring cells to buffer;[2] (2) suspending cells in a medium containing only an oxidizable carbon source;[3] or(3) growing cells in a phosphate deficient medium until all the phosphate had been exhausted.[4] The change in the RNA has been detected by the release of isotope,[2-4] by observing differences in the ultracentrifuge patterns of the ribosome fraction of cells at various stages in their growth cycle,[5] and by observing the change in ultracentrifuge patterns of cells cultured in different media.[6]

The results presented here show that the base ratio changes induced by changing growth conditions are associated with the ribosome-contained RNA. We have also carried out experiments to determine whether there are changing patterns of RNA synthesis, as measured by P^{32} incorporation into the various nucleotides, during different stages of the growth cycle of *E. coli*. The results of these experiments demonstrate that early log phase cells are producing RNA, associated with the ribosomal fraction, which has a base ratio different from the ratio which is obtained from ribosomal material of late log phase cells.

Materials and Methods.—Growth of *E. coli B* and nucleotide isolations and determinations were carried out as described previously.[1] The ribosome and "soluble" RNA fractions were prepared and separated according to Tissières, Watson, Schlessinger, and Hollingworth,[7] using 0.01 *M* Tris (pH 7.4) buffer with 10^{-2} *M* Mg^{++} and DNAse (1 μg/ml) as the suspending medium. Growth experiments were carried out in two kinds of glucose containing medium. The "normal" phosphate medium (NP) is the standard glucose medium used in previous studies.[1] The low phosphate (LP) medium contained K_2HPO_4 at a concentration of only 2 μg/ml

and 0.1 *M* Tris at pH 7.2. All other ingredients are in the same concentration as in the high phosphate medium.

In all growth experiments the following procedure was used: *E. coli* was grown in 100 ml of nutrient broth-yeast extract (NBYE) broth or glucose salts medium (NP) at 25°C. After 16 hr growth, 100 ml of fresh medium (NBYE and glucose) was added separately to the two kinds of cells and they were allowed to grow for 2 hr at 25°C until there were about 5×10^8 bacteria per ml. The cells were harvested and washed twice at room temperature with sterile distilled water, resuspended in sterile water and inoculated into 40 ml of glucose-LP medium. Cell density was read in the Klett-Summerson colorimeter using the red (660) filter. The incubation flask was a 300-ml Erlenmyer, fitted with a Klett tube extension, so that the incubation mixture could be read in the colorimeter without removing aliquots. Flasks were purchased from Bellco Glass Co., Vineland, N. J. In experiments using radioactive phosphate, P^{32} was added separately to the Klett flask prior to the addition of cells. At the end of the incubation period the cells were harvested at 2°C, washed twice with sterile, cold distilled water and frozen on the inside of a chilled mortar. About 2 gm wet weight of unlabeled cells were added to the mortar as carrier and the mixture was ground with alumina. Subsequently the ribosome and "soluble" RNA fractions were isolated.[7] In experiments using P^{32} about 5 μg/ml DNAse was routinely added to the suspending medium. P^{32}-containing nucleotides were prepared by alkaline hydrolysis of the purified RNA and chromatographed on paper in duplicate,[1] located with an ultraviolet lamp, eluted, dried, and counted.

P^{32} as H_3PO_4 was purchased from Oak Ridge National Laboratory, Oak Ridge, Tenn. DNAse was purchased from Worthington Biochemical Corp., Freehold, N. J.

Results.—Base composition of NBYE-grown and glucose-grown E. coli: In the first series of experiments the base ratios of the ribosome fraction and the "soluble" RNA fractions of late log phase *E. coli* were determined. These data are presented in Table 1. The data clearly show that there are no differences in the base ratio of the "soluble" RNA. The expected differences, based on the results pre-

TABLE 1

NUCLEOTIDE COMPOSITION OF THE RIBONUCLEIC ACID FRACTIONS OF *E. coli* EXPRESSED IN MOLES PER 100 MOLES OF THE FOUR NUCLEOTIDES

(The values represent the mean of twelve to fifteen separate analyses for each nucleotide from four separate experiments. They are presented with the errors expressed as average deviation from the mean of four separate determinations.)

	Glucose-Grown		Nutrient Broth-Yeast-Extract-Grown	
	R	S	R	S
Adenylic acid	27.0 ± 0.1	19.9 ± 0.1	25.4 ± 0.0	20.1 ± 0.2
Cytidylic acid	22.7 ± 0.4	28.0 ± 0.9	21.5 ± 0.3	28.4 ± 0.1
Uridylic acid	18.4 ± 0.0	15.4 ± 0.0	20.4 ± 0.2	14.9 ± 0.2
Guanylic acid	31.5 ± 0.4	33.0 ± 0.0	32.6 ± 0.2	32.9 ± 0.2
Purines/pyrimidines	1.42	1.22	1.38	1.22
6-Am/6-K	0.99	1.00	0.88	1.01
(A + U/G + C)	0.84	0.58	0.85	0.57

6-Am: 6-amino nucleotides (adenylic and cytidylic acids): 6-K: 6-keto nucleotides (guanylic and uridylic acids).
A, G, C, and U stand for adenylic, guanylic, cytidylic, and uridylic acids, respectively.
R: ribosome fraction.
S: "soluble" RNA fraction. Nucleotide composition of the "soluble" RNA expressed in moles per 96 moles of the four major nucleotides. Only two determinations were carried out on "soluble" RNA from glucose-grown cells.

viously gained from whole cell studies, are found in the ribosome fraction. It is interesting to note that our data for the nucleotide composition of the ribosome fraction of the NBYE-grown cells is almost identical to the ratios reported by Spahr and Tissières[8] for ribosomes derived from *E. coli* grown on a medium containing tryptone and yeast extract. The ribosome fraction of *E. coli* grown on glucose has a 6-Amino/6-Keto ratio which is 0.99 while NBYE grown cells have a ratio of 0.88. The "soluble" RNA fractions of both kinds of cells have identical 6-Am/6-K ratios and both ratios are similar to the results of Dunn, Smith, and Spahr.[9]

Base composition of RNA fractions in non-growing cells: It was of interest to examine these two RNA fractions of the cell in non-growing conditions since it had been demonstrated by others that there is considerable breakdown and alteration of RNA during this period. (See review by Mandelstam.[10]) In these experiments late log phase cells were suspended in phosphate buffer for at least 18 hours at refrigerator temperature. At the end of this time period, both RNA containing fractions were analyzed. The data are presented in Table 2 and should be compared to the data in Table 1. It is apparent that the base ratio of the "soluble" RNA remains unchanged. On the other hand, the base ratio of both ribosome fractions are considerably altered from the "normal" ratios obtained from late log phase cells. In each case it is the purine/pyrimidine ratio which reflects the most obvious alteration. This base composition can of course be changed again since it is obvious that these bacteria, on subculture into fresh medium, make RNA whose base ratio (during late log phase) is identical to the values reported in Table 1.

TABLE 2

NUCLEOTIDE COMPOSITION OF RNA FRACTION OF *E. coli* WHICH WAS ALLOWED TO STAND IN BUFFER FOR 18 HR

	Nutrient Broth-Yeast-Extract-Grown Ribosomes	"Soluble"	Glucose-Grown Ribosomes
Adenylic acid	26.5	19.9	26.9
Cytidylic acid	21.8	28.5	25.4
Uridylic acid	17.2	15.0	18.0
Guanylic acid	34.5	32.6	29.4
Purines/pyrimidines	1.56	1.21	1.30
6-Am/6-K	0.94	1.01	1.10
(A + U/G + C)	0.78	0.57	0.82

6-Am: 6-amino nucleotides (adenylic and cytidylic acids); 6-K: 6-keto nucleotides (guanylic and uridylic acids).
A, G, C, and U stand for adenylic, guanylic, cytidylic, and uridylic acids, respectively.

Effect of inorganic phosphate concentration on growth of E. coli: Since we were using two different populations of cells, it was decided to examine some of the growth characteristics of glucose-grown and NBYE-grown *E. coli* when each is placed in fresh glucose medium. Two types of glucose-containing media were employed to study the growth characteristics: one, a low-phosphate (LP) medium (2 μg/ml) and the other, a medium containing the normal concentration of phosphate (NP) (10 gm/liter). The growth curves on both media are presented in Figure 1. The lag phase of glucose-grown cells on glucose-LP medium (Fig. 1) is about 60 min, while the lag phase of NBYE-grown cells on the same medium is about 180 min. On the glucose-NP medium, glucose-grown cells have a 30-min lag phase and NBYE-grown cells on the NP medium have a 60-min lag phase. At the end of the lag phase, glucose-grown cells, whether on high or low phosphate

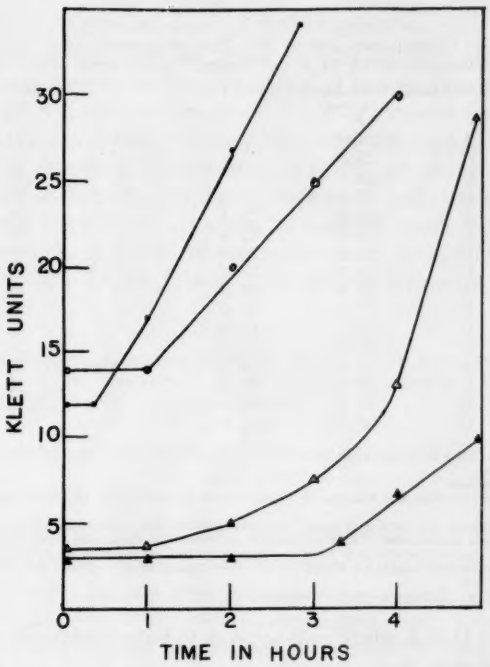

FIG. 1.—Growth curves of *E. coli B* previously grown on nutrient-broth-yeast-extract (NBYE) medium and glucose–normal-phosphate (NP) medium, on glucose–NP medium and glucose–low-phosphate (LP) medium. ● = glucose-grown cells on NP medium; ○ = glucose-grown cells on LP medium; △ = NBYE-grown cells on NP medium; ▲ = NBYE-grown cells on LP medium.

medium, exhibit a constant rate of growth characteristic of the log phase. On the other hand, NBYE-grown cells require some hours to enter their most rapid growth phase although on the NP medium they initiate growth more rapidly than on the LP medium. In view of this phosphate effect, several experiments were carried out to study the rate of incorporation of P^{32} into ribosomal-contained and "soluble" RNA to determine whether a slow growth rate could be correlated with a slow rate of RNA synthesis. At the same time we could determine the base composition of the two kinds of RNA and learn whether there are variations in the base ratio during various stages in the growth cycle.

P^{32} incorporation into ribosome and "soluble" RNA: Washed NBYE-grown and glucose-grown *E. coli* were individually inoculated into the glucose-LP medium containing P^{32}. Cells were incubated for various time periods, harvested, mixed with unlabeled cells as carrier, and the ribosome and "soluble" RNA fractions were analyzed for their P^{32} content. The results of this experiment are presented in Table 3 in terms of per cent radioactivity in each of the nucleotides. This value was calculated by dividing the number of counts in one nucleotide by the total number of counts in all four nucleotides. It is apparent that there is a marked change in the ratio of the ribosome fraction when one compares early log phase and late log phase cells. On the other hand the isotope content of the nucleotides of the

TABLE 3

NUCLEOTIDE RATIOS CALCULATED FROM P^{32} INCORPORATION INTO THE "SOLUBLE" AND RIBOSOMAL RNA OF *E. coli* GROWN ON GLUCOSE MEDIUM

Time of incubation in hr	Nutrient Broth-Yeast-Extract-Grown Cells Per cent R			Glucose-Grown Cells Per cent R		S
1	A	24.0	...	A	24.3	21.3
	C	25.5	...	C	23.6	23.7
	U	26.1	...	U	25.2	23.7
	G	26.5	...	G	26.8	31.2
3	A	27.0	20.4	A	26.2	24.0
	C	23.0	22.8	C	22.3	23.6
	U	25.0	20.6	U	28.0	21.2
	G	24.3	36.2	G	27.8	31.1
6	A	25.6	20.0	A	24.0	21.6
	C	27.1	25.0	C	21.8	24.1
	U	25.1	17.0	U	25.5	22.3
	G	27.2	37.6	G	29.3	31.5
22*	A	24.8	14.0	A	23.8	19.9
	C	17.9	29.0	C	22.5	25.8
	U	18.3	20.7	U	17.2	19.5
	G	38.7	34.8	G	36.7	34.7

A, C, U, and G stand for adenylic, cytidylic, uridylic, and guanylic acids, respectively.
R: ribosome fraction.
S: "soluble" RNA fraction.
Per cent calculated by dividing the number of counts in one nucleotide by the total number of counts in all four nucleotides.
* The discrepancy between the results obtained by radioactivity determinations and actual spectrophotometric analysis of isolated nucleotides (Table 3) may be explained by the larger error involved in P^{32} determinations. Ordinarily, two separate counts were made for each nucleotide with an average deviation of 10% while in the spectrophotometric analyses about 12–15 determinations were made on each nucleotide with an average deviation of 3%.
P^{32} was added as H_3PO_4. Each growth flask received about 2×10^6 cpm.

"soluble" RNA of both kinds of cells appears to have a relatively constant pattern throughout the growth cycle.

The data in Figure 2 demonstrate the rate of incorporation of isotope in glu-

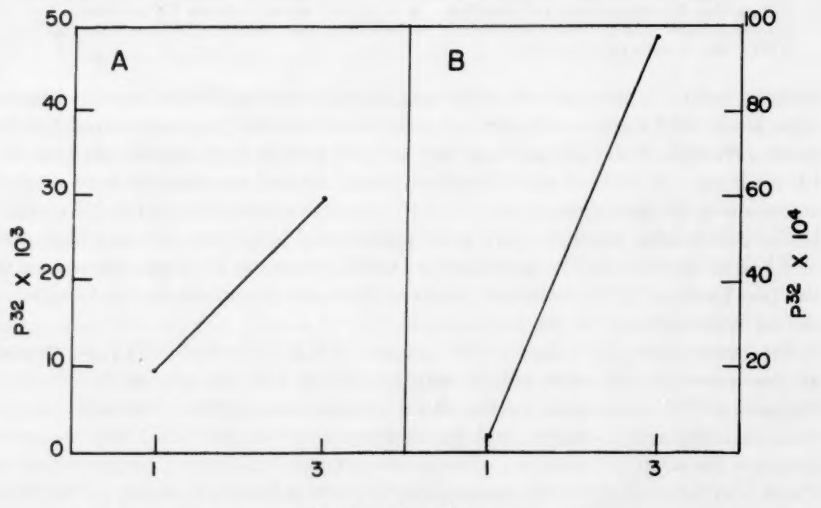

FIG. 2.—P^{32} Incorporated into the RNA of *E. coli* after 1 and 3 hours' growth in glucose-LP medium. The total counts at each time were calculated by adding the total counts in each nucleotide in both the ribosomal contained and "soluble" RNA. *A* = nutrient-broth-yeast-extract-grown *E. coli*; *B* = glucose-grown *E. coli*.

cose-LP medium by cells which were previously grown on NBYE and glucose-NP medium. Paralleling the long lag phase of NBYE-grown cells on the glucose medium is the very slow rate of incorporation of isotope into total RNA. Thus there seems to be a limited synthesis of RNA on transfer to the new medium (Maaloe[11]). At the same time, glucose-grown cells, although exhibiting very little growth during the first hour of incubation (Fig. 1), are incorporating about four times as much P^{32} as NBYE cells during that same period. At the end of 3 hr glucose-grown cells have taken up about 30 times as much P^{32} as NBYE-grown cells. If one examines the ratio of incorporation of isotope into the ribosomal-contained and "soluble" RNA (Table 4), a striking difference is noted between

TABLE 4

P^{32} RATIO OF THE RIBOSOMAL/"SOLUBLE" RNA OF NUTRIENT BROTH-YEAST-EXTRACT- AND GLUCOSE-GROWN *E. coli* IN GLUCOSE MEDIUM

Growth time in hr	NBYE cells	Glucose cells
1	1.26	3.6
3	4.00	8.2
6	5.2	14.8
22	11.6	7.5

NBYE-grown and glucose-grown cells. Glucose-grown cells, within a short time after passing into the log phase, incorporate isotope into both RNA fractions in the expected ratio based on the concentration of the two kinds of RNA in the whole cell. The data of Tissières *et al.*,[7] demonstrated that there is about 8 to 10 times as much RNA in the ribosome fraction as in the "soluble" fraction in log phase *E. coli*. At 3 hr, for example, there is about 8 times as much P^{32} in ribosomal RNA as in "soluble" RNA. On the other hand, the ratio of isotope (ribosomal RNA/"soluble" RNA) in NBYE-grown cells rises more slowly and after 6 hr has not yet reached the maximum which is eventually achieved sometime between the 6th and 22nd hr of growth. In spite of the slow incorporation of isotope by NBYE-grown cells, they are producing ribonucleic acid with an over-all base composition similar to the composition of glucose-grown cells (Table 3, at 1 hr). It might be suggested that the slow increase in P^{32} ratio (ribosome P^{32}/"soluble" P^{32}) in NBYE-grown cells reflects a more rapid synthesis of "soluble" RNA in these cells compared to glucose-grown cells. This is not the case as may be noted from Figure 3. We have plotted the relative increase of isotope in both RNA fractions between 1 and 3 hr growth. In NBYE-grown cells the number of counts in "soluble" RNA doubles approximately during that time period while ribosomal RNA has increased about 4 times. In glucose-grown cells "soluble" RNA has gained 13 times more P^{32} between 1 and 3 hr; however, ribosomal RNA picks up 30 times the amount of P^{32} assimilated at 1 hr.

Discussion.—A number of experiments have demonstrated that environmental factors influence the concentration of RNA in *E. coli*. This bacterium contains a large fraction of its RNA in ribonucleoprotein particles (ribosomes) which, in log phase cells, may constitute about 40 per cent of the dry weight of the cell (Tissières *et al.*[7]). In the stationary phase the concentration of ribosomes decreases to one-fourth the log phase concentration. It is also possible to affect bacterial RNA concentration by altering growth conditions. For example, if *Salmonella typhimurium* is put into a broth medium, from a glucose salts medium, there occurs,

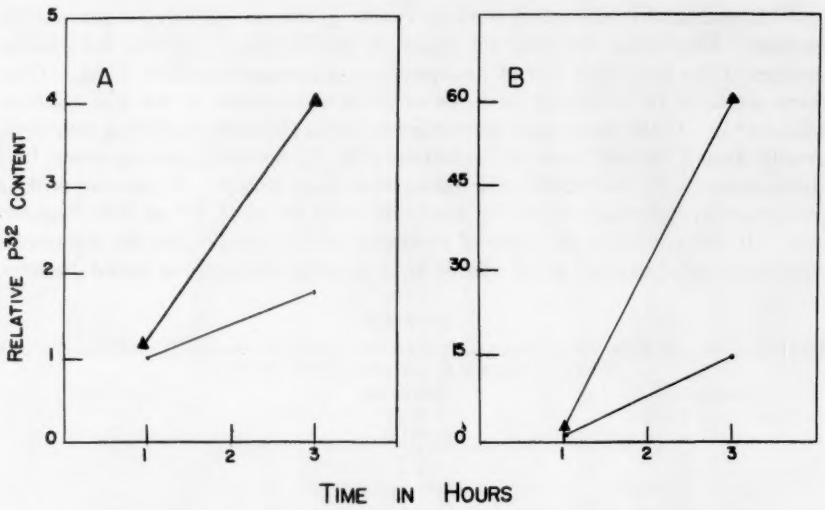

FIG. 3.—Increase in P^{32} content of ribosomal-contained and "soluble" RNA of *E. coli*. *A* = nutrient broth-yeast-extract-grown cells; *B* = glucose-grown cells. ▲ = ribosomal RNA fraction; ● = "soluble" RNA fraction. P^{32} content was obtained by calculating the sum of the radioactivities contained in each nucleotide.

following the transfer, a rapid synthesis of ribosomal materials, apparently independent of generalized protein synthesis, to a level which is required for growth in the new environment. A similar situation holds for *E. coli* and *Aerobacter aerogenes* (Maaloe[11]). Breakdown of RNA may be induced by placing bacteria in a medium where they cannot grow; if cells are maintained in the log phase, however, there seems to be no turnover of RNA.[12, 13]

The experiments reported here reveal a number of additional facts about the properties of RNA in growing and non-growing *E. coli*. The base ratio of ribosomal RNA produced during the early part of the growth cycle is very different from the base ratio of ribosomal RNA made at the end of the log phase. During the early log phase, ribosomal RNA is synthesized from essentially equimolar quantities of all four bases. It is interesting to note that the DNA of *E. coli* contains four bases in essentially equimolar amounts (Sueoka[14]). These results, indicating the presence of a "new" type of RNA detectable in early log phase cells, are similar to the data of Astrachan and Volkin[15] and Nomura, Hall, and Spiegelman[16] for T2-infected *E. coli* where the RNA made during the early stages of infection has a base ratio very similar to the DNA of the infecting phase. However, in the experiments reported here, the production of this "new" RNA is not triggered by the introduction of new DNA into the cell but is produced without genetic change. This finding demonstrates that *E. coli* can produce an RNA similar in composition to its DNA. Hitherto the complete non-equivalence between the total RNA and DNA base ratios of *E. coli* had led to an apparent dilemma. If DNA is specifying the production of RNA there should be some correlation between their respective ratios. The results reported here still do not resolve this problem since there remains to be explained completely the non-complementary nature of the re-

mainder of the RNA of the cell.[14, 17–19] The appearance of a "new" RNA and the changing characteristics of labeling in the RNA of the ribosome fraction during growth suggest that at various times in the growth cycle different cell characteristics manifest themselves which can be the result of altered RNA synthesis and consequently altered protein synthesis. The persistence of this "new" RNA for some hours during the early stages of growth indicates that the cell is primarily producing this material since it would be expected, if there were an equivalent synthesis of RNA of a kind found in ribosomes in late log phase cells, that early log phase cells would show an altered ratio before 3 hr of growth had elapsed (Table 3). During the late log phase the ribosomal-contained RNA now assumes the base composition which was expected from the evidence presented in Table 1. Thus some time between the 6th and 22nd hour of growth the cells began to make RNA of a different base composition.

The base composition of the ribosome fraction of glucose-grown and NBYE-grown *E. coli* (late log phase) are different. The most reasonable assumption, following the analysis by Maaloe,[11] is that the complex nature of the NBYE medium provides a variety of "repressor" substances which, it must be argued on the basis of the experiments reported here, control the synthesis of the RNA ribosomal material itself or RNA which becomes attached to ribosomes. Since it is not clear which RNA has been modified, it would be well to reserve judgment on the obviously relevant question of whether a cell is producing all the ribosomes it is genetically capable of producing at all times and at all stages in the growth cycle. If it proves to be true that all ribosomes are always produced, perhaps with only a quantitative variation, then altered RNA synthesis reported here reflects either this variation or simply the production of nucleic acid which can remain in contact with ribosomes and whose function may be restricted to a role of a controlling element or, more specifically, an information carrier for protein synthesis (Brenner, Jacob, and Meselson[20]). These elements, if present, are there in sufficient number to alter the total base ratio of the ribosome fraction.

The obvious inability of NBYE-grown cells to initiate growth on the low-phosphate-salts medium points to the need for nucleic-acid synthesis in order that growth may occur. This initial reduced ability to make RNA indicates the persistence of a controlling mechanism in NBYE-grown cells which, however, can be overcome more rapidly in a high-phosphate medium. It should be pointed out that the delayed growth of NBYE cells is not due to their inability to oxidize glucose; they oxidize glucose in resting cell suspensions, at the same rate as glucose-grown cells. Therefore NBYE cells can carry out an oxidative metabolism. They are, however, unable to synthesize rapidly ribosomal-contained RNA or ribosomes themselves. The increased rate of RNA synthesis parallels the increased rate of growth.

When *E. coli* cells are allowed to remain in buffer for some time, the ribosomal fraction breaks down in such a way that there is a marked change in the base composition (Table 2). Several explanations may be advanced for this phenomenon, but one in particular seems most attractive. It assumes that the ribosome fraction of *E. coli* is a heterogeneous collection of particles with varying base compositions. If there were some selectivity in the breakdown of ribosomes under the conditions employed here, then a ribosome fraction with an altered base ratio would be recovered. It has been shown that an RNAse exists in the ribosomes of *E. coli*.[21]

The activity of this enzyme might be a contributing factor in altering the base composition.

Under the conditions employed in these experiments the base composition of "soluble" RNA remains essentially constant. If there is some degradation of "soluble" RNA in non-proliferating cells it would appear that all molecules are equally susceptible and consequently no change is induced in the total base composition.

Summary.—The base composition of the RNA of ribosomes of *E. coli* varies during the normal growth cycle. During the lag and early log phase the nucleotide composition of ribosomes resembles the base composition of the DNA of *E. coli*. In late log-phase cells the base composition of ribosomes changes and may be further modified by allowing cells to remain in buffer (non-growing state) for many hours. The growth medium also induces changes in the base composition of ribosomes since nutrient broth-yeast extract (NBYE)-grown and glucose-grown *E. coli* differ in the base composition of their respective ribosome fractions. Upon transfer of cells from the NBYE medium to the glucose medium RNA synthesis is retarded and growth in the new environment parallels the increase in rate of RNA synthesis. The "soluble" RNA appears to have a constant base composition under all the conditions employed in this study.

* This work was supported by grants from the National Science Foundation and from the National Institute of Allergy and Infectious Diseases, National Institutes of Health.

[1] Santer, M., David C. Teller, and W. Andrews, *J. Molec. Biol.*, **2**, 273 (1960).

[2] Mendelsohn, J., and A. Tissières, *Biochim. et Biophys. Acta*, **35**, 248 (1959).

[3] Mandelstam, J., and H. Halvorson, *ibid.*, **40**, 43 (1960).

[4] Horiuchi, T., S. Horiuchi, and D. Mizuno, *ibid.*, **31**, 570 (1959).

[5] McCarthey, B. J., *ibid.*, **39**, 563 (1960).

[6] Dagley, S., and J. Sykes, in *Microsomal Particles and Protein Synthesis*, ed. R. R. Roberts (Washington: Washington Academy of Sciences, 1958), pp. 62–69.

[7] Tissières, A., J. D. Waston, D. Schlessinger, and B. R. Hollingworth, *J. Molec. Biol.*, **1**, 221 (1959).

[8] Spahr, P. F., and A. Tissières, *ibid.*, 237 (1959).

[9] Dunn, D. B., J. D. Smith, and P. F. Spahr, *ibid.*, **2**, 113 (1960).

[10] Mandelstam, J., *Bacteriol. Revs.*, **24**, 289 (1960).

[11] Maaloe, O., in *Microbical Genetics*, ed. W. Hayes and R. C. Clowes (Cambridge, Eng.: Cambridge University Press, 1960), pp. 272–293.

[12] Hershey, A. D., *J. Gen. Physiol.*, **38**, 145 (1954).

[13] Davern, C. I., and M. Meselson, *J. Molec. Biol.*, **2**, 153 (1960).

[14] Sueoka, N., *ibid.*, **3**, 31 (1961).

[15] Astrachan, L., and E. Volkin, *Biochim. et Biophys. Acta*, **29**, 536 (1958).

[16] Nomura, M., B. D. Hall, and S. Spiegelman, *J. Molec. Biol.*, **2**, 306 (1960).

[17] Crick, F. H. C., in *Structure and Function of Genetic Elements*, Brookhaven Symposia in Biology, No. 12 (1959).

[18] Sinsheimer, R., *J. Molec. Biol.*, **1**, 218 (1959).

[19] Sueoka, N., J. Marmur, and P. Doty, *Nature*, **183**, 1429 (1959).

[20] Brenner, S., F. Jacob, and M. Meselson, as quoted by A. Lowoff in *Proc. Roy. Soc.* (*London*), **B154**, 1 (1961).

[21] Elson, D., and M. Tal, *Biochim. et Biophys. Acta*, **36**, 281 (1959).

*IDENTIFICATION OF 5′ LINKED ADENOSINE AS END GROUP OF TMV-RNA**

By T. Sugiyama and H. Fraenkel-Conrat

VIRUS LABORATORY, UNIVERSITY OF CALIFORNIA AT BERKELEY

Communicated by Robley C. Williams, July 8, 1961

The biological activities of nucleic acids seem largely, if not entirely, due to their nucleotide sequences. An obvious experimental approach to elucidation of such sequences is the characterization of the end groups. Recent data suggest that the terminal 5′ linked nucleoside of TMV-RNA is not phosphorylated[1] and thus should appear as a free nucleoside upon decomposition of the RNA by alkali. The detection and quantitation of a single nucleoside liberated from a molecule as large as TMV-RNA (6500 nucleotides) is technically feasible if virus is employed which carries enough of a radioactive label. The presence of 50–100 mc of $C^{14}O_2$ in the atmosphere during most of the propagation period of the virus (12–14 days) in leaves of *N. tabacum* achieves this objective by yielding virus which gives 2–10 $\times$ 10^6 cpm/mg. Less than 1 mg of the RNA of such virus suffices for the estimation of its terminal residues, particularly if carrier nucleosides are added as a guide in isolation of the liberated C^{14} nucleosides.

The evaluation of end group data requires careful consideration of the homogeneity of the preparation. In the case of TMV-RNA, the bulk of the material (50–80 per cent) shows an approximate molecular weight of 2 $\times$ 10^6 and represents the infective molecular species which is under investigation.[2] The rest of the material probably consists largely of fragments of viral RNA, and fragmentation causes the appearance of new end groups. The mode of action of most nucleases, and of alkali, would make one presuppose that most fragments would carry a 3′ (or 2′) terminal phosphate, rather than an unphosphorylated glycol group, and this supposition is supported by data concerning the alkali degradation of P^{32}-RNA.[1] The probability thus appears high that a bona-fide terminal 5′ linked nucleoside can be detected if it is present in TMV-RNA.

The first experiments showed that nucleosides could arise through accidental dephosphorylation of nucleotides. Only after conditions had been established which seemed to reduce dephosphorylation to a non-detectable level could a search for the terminal nucleoside be initiated. This was the case if the alkaline hydrolysate was carefully neutralized with the buffer and the nucleotides were then separated from the nucleosides by means of paper electrophoresis at pH 7.4. The latter could subsequently be separated from one another and further purified by 2-dimensional paper chromatography[3] followed by electrophoresis at pH 3.5. In this manner reproducible results were obtained, as shown on Table 1. It is evident that adenosine is present in about the amount expected for a single terminal residue, and that the other nucleosides occur in lesser amounts varying from 0.04 to 0.3 residues per mole, all after appropriate correction based on the specific radioactivity of the nucleoside and the recovery of the corresponding marker.

It was found of crucial importance that the unlabeled marker nucleosides were added only after the alkaline digestion. If the degradation of C^{14} polynucleotides was carried out in the presence of similar amounts of such markers 0.5 to 1.3 per

TABLE 1

DETERMINATION OF NUCLEOSIDES IN ALKALINE HYDROLYSATES OF C^{14} TMV-RNA*

Condition of alkaline digestion	Amount of RNA hydrolysed ($\times 10^{-4}$ μM)	Carrier nucleoside recovery of 0.1 mg added (%)		C^{14} found in nucleoside cpm	Count corrected for recovery, cpm	Nucleoside found ($\times 10^{-4}$ μM)	Mole nucleoside per mole RNA
Standard conditions† 24 hours' digestion. Carrier nucleosides added after completion of digestion.	1.9	A	19	77	405	1.7	0.9
		G	28	10	36	0.2	0.1
		C	27	3	11	0.1	~0.05
		U	30	11	37	0.3	0.2
48 hours' digestion. Carrier nucleosides added after completion of digestion.	1.9	A	22	94	427	1.8	0.9
		G	25	10	40	0.2	0.1
		C	35	4	11	0.1	~0.05
		U	36	10	28	0.2	0.1
48 hours' digestion. Carrier nucleosides added at 24 hours.	1.9	A	19	107	563	2.4	1.2
		G	25	21	84	0.5	0.3
		C	30	6	20	0.2	0.1
		U	37	18	49	0.4	0.2
24 hours' digestion. Carrier nucleosides added at the beginning of digestion.	1.9	A	20	2458	12300	51	27
		G	12‡	586	4880	30	16‡
		C	30	325	1080	13	7
		U	43	1023	2380	20	10
24 hours' digestion. Traces of C^{12} nucleosides ($\sim 3 \times 10^{-4}$ μM), added at the beginning of digestion. Carrier nucleoside (~0.4 μM) added after the completion of digestion.	1.9	A	21	98	467	2.0	1.0
		G	33	11	33	0.2	0.1
		C	37	4	11	0.1	~0.05
		U	18	4	22	0.2	~0.1

* About 2×10^{-4} μM C^{14}-labeled TMV-RNA was hydrolyzed in 0.1 to 0.4 *N* KOH (OH^-/P = 10 to 40) at 37°C for 18 to 48 hours. Non-labeled adenosine, guanosine, cytidine, and uridine were added as carrier and marker after the hydrolysis, unless otherwise specified. The hydroylsate was chilled in an ice bath and neutralized with ice-cold 2 *M* phosphate buffer (pH 4.5). Nucleosides were separated from nucleotides by paper electrophoresis at pH 7.4 (0.05 *M* phosphate buffer, 1000 volts per 40 cm). In this electrophoretic system, the four nucleosides stay together near the origin and are well separated from the nucleotides which move as a broad band toward the anode. After the run, the nucleosides were eluted from the paper with water, lyophilized and then spotted on Whatmann 3MM paper for two-dimensional chromatography[3] (1st dimension: 71.5 ml ethanol (95%) and 28.5 ml 1 *M* NH_4-CH_3COO (pH 7.5); 2nd dimension: 80 ml saturated $(NH_4)_2SO_4$, 2 ml isopropanol and 18 ml H_2O). The four nucleosides, which were well separated from each other, were eluted from the paper with water and then desalted by adsorbing to Norite A at pH 2.5 (0.1 *N* HCl used to adjust pH), washing with water and then eluting with 0.3 *N* NH_4OH in 50% ethanol. The eluates were dried under low vacuum over $CaCl_2$ and concentrated H_2SO_4, and the nucleosides were further purified by paper electrophoresis at pH 3.5 (0.05 *M* ammonium formate, 1000 volts per 40 cm). Each nucleoside was eluted from the paper, checked for the recovery of the non-labeled carrier by plotting its UV-spectrum, and then dried on a planchet for the counting of its radioactivity. The count actually obtained for each nucleoside was corrected for the recovery of the carrier marker and the amount of C^{14}-labeled nucleoside was then calculated by using the specific count for each nucleoside given in Table 2 (RNA preparation B3).

† After techniques had been established for the isolation of nucleosides, the standard conditions were used in six separate experiments with three samples of RNA prepared from different C^{14} virus preparations. The adenosine found in these experiments was, per mole RNA: 1.0, 0.6, 1.1, 1.4, 1.1, and 0.9 mole, while the other nucleosides ranged from 0.04 to 0.3 mole.

‡ This value is estimated, correcting for accidental loss of part of the solution. A similar relationship of A > G > C, U was obtained in another similar experiment.

cent of the C^{14} appeared in nucleosides (A > G > U, C), thus simulating 20 to 60 5′ linked end groups per mole of RNA.† This phosphate transfer did not occur to a significant extent if the nucleoside concentration was several orders of magnitude lower than that of the nucleotides, as it is the case in the digests of RNA. It appeared that only in *statu nascendi*, and thus possibly at the 2′,3′ cyclic state, did nucleotides undergo such interchange with nucleosides in alkaline solution, since incubation of digests for an additional 24-hr period with added unlabeled nucleosides did not produce greater amounts of nucleosides than observed under the standard conditions. The control of this experiment, in which marker nucleosides were absent, demonstrated that no detectable traces of nucleosides arose through hydrolysis of nucleotides under the conditions of alkaline degradation of the RNA (see Table 1).

Another measure of the phosphate transfer consisted in hydrolysing unlabeled RNA in the presence of varying amounts of C^{14}-labeled nucleosides (about 1 to 120 mole per mole RNA) and determining the label appearing in the nucleotide fraction. This corresponded to only about 1 per cent of the added nucleosides.

Previous studies of alkaline digests of P^{32}-labeled RNA had shown that no detectable amounts of nucleoside diphosphates were formed, thus proving that there was no terminal 5′ phosphate on the other end of the chain.[1] This conclusion was corroborated by the present experiments with C^{14}-RNA, which also yielded less than 0.4 mole per mole of any diphosphate, after due correction for the recovery of internal markers. Figure 1 represents a schematic presentation of our present state of knowledge concerning the chemical structure of TMV-RNA.

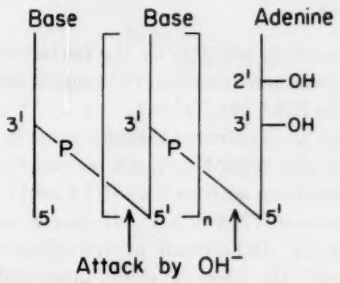

FIG. 1.—*Release of adenosine from TMV-RNA by alkaline degradation.* TMV-RNA is symbolized in conventional manner. Base stands for adenine, guanine, cytosine or uracil. n = approximately 6500.

The same amount of about one mole of adenosine per mole was obtained with the RNA derived from three separate preparations of C^{14}-TMV. In all three cases, similar marked differences were observed in the specific extent of labeling of the four nucleosides or nucleotides (see Table 2). The same difference was also observed when the bases were examined. Since the plants were held in an enclosed airspace containing $C^{14}O_2$ for most of the period of virus propagation and accumulation (12–14 days), no such differences had been anticipated. A related question is that pertaining to the uniformity of labeling throughout the length of the RNA chain. For only if this is uniform is one justified in using the average specific activity of adenosine in calculating the number of terminal adenosine residues per

TABLE 2

SPECIFIC RADIOACTIVITY OF NUCLEOTIDES, NUCLEOSIDES AND BASES IN C^{14}-LABELED TMV-RNA*

RNA preparation	Component	Specific Radioactivity ($\times 10^3$ cpm/μM) A	G	C	U
A	3′(2′)-nucleotide	12.5	6.6	3.8	5.9
	5′-nucleotide	11.3	7.2	4.3	6.8
	nucleoside	11.1	7.6	3.8	6.6
A	Base	3.6	2.0	0.7	1.3
B2	3′(2′)-nucleotide	28.3	19.8	9.9	15.4
B3	3′(2′)-nucleotide	23.9	16.4	8.1	12.2

* The 3′(2′) nucleotides were obtained by KOH hydrolysis of the RNA, the 5′-nucleotides by digestion with purified snake venom phosphodiesterase kindly supplied by M. Laskowski. The nucleotides were separated by electrophoresis at pH 3.5 (0.05 *M* ammonium formate). The nucleosides were obtained by digestion with crude snake venom, and separated by two-dimensional chromatography as described in Table 1. The bases were obtained by digestion with $HClO_4$, and separated by one-dimensional chromatography (65 ml isopropanol, 16.7 ml concentrated HCl, and 18.3 ml H_2O).

TABLE 3

LABELING IN TERMINAL AND RESIDUAL PARTS OF THE RNA CHAIN*

Portion of RNA chain	Specific Count ($\times 10^3$ cpm/μM) AMP	GMP	CMP	UMP
Terminal (18%)	2.63	2.25	1.10	2.08
Residual	2.59	1.84	0.92	1.48
Unfractionated	2.83	1.98	0.99	1.54

* 10 mg of TMV containing about 0.1 mg of C^{14}-labeled TMV was heated at 60°C for 1 min with gentle stirring in 0.04% sodium dodecyl sulfate solution at pH 8.0. The mixture was diluted 6-fold with ice-cold water and centrifuged at 30,000 rpm for 2 hr. The pellet was resuspended in water and incubated with 0.01 mg of pancreatic ribonuclease at pH 7 (overnight at 37°C). The mixture was centrifuged at 40,000 rpm for 2 hr. The supernatant showed a U.V. spectrum indicating that it was largely RNA and contained about 18% of the RNA of the whole virus. Both supernatant and pellet, resuspended in H_2O, were deproteinized by phenol extraction, and the deproteinized RNA was digested with KOH to give the 3′(2′)nucleotides, which were separated and analyzed as described in Table 2. It was found important that the unlabeled virus used as carrier in such experiments be prepared in exactly the same manner as the labeled virus.

mole. Experiments designed to test this by the partial degradation of TMV from one end through limited detergent treatment[4, 5] suggest similar labeling in terminal and residual portions of the RNA (see Table 3).

The finding of adenosine as the terminal residue must be considered in relation to the fact that adenosine is also regarded as the terminal residue of Transfer-RNA. Thus, a 1-per cent contamination with such an RNA could account for the adenosine observed in alkaline digests of TMV-RNA. However, since Transfer-RNA is reported to yield guanosine 3′5′ diphosphate in equivalent amounts to the adenosine upon alkaline degradation[6, 7] the absence of any detectable diphosphates from the digests appears to rule out the presence of as much as 0.3 per cent of Transfer-RNA in TMV-RNA. The conclusion, therefore, appears justified that TMV-RNA, at least as isolated, terminates in an adenosine residue, unphosphorylated at the 2′ and 3′ positions.

The authors wish to express their thanks to C. A. Dekker and P. Whitfeld for their helpful suggestions and counsel throughout this work.

* Supported by a grant from the National Science Foundation, G-9745.

† Preliminary data obtained by P. Whitfeld with alkali treatment of a ribonuclease digest of C^{14} TMV-RNA containing unlabeled nucleosides suggest that the phosphate exchange occurs also at the level of oligonucleotides.

[1] Fraenkel-Conrat, H., and B. Singer, in preparation for press.

[2] Gierer, A., *Nature*, **179,** 1297 (1957).

[3] Felix, F., J. L. Potter, and M. Laskowski, *J. Biol. Chem.*, **235,** 1150 (1960).

[4] Hart, R. G., *Biochim. Biophys. Acta*, **28,** 457 (1958).

[5] Gordon, M. P., B. Singer, and H. Fraenkel-Conrat, *J. Biol. Chem.*, **235**, 1014 (1960).

[6] Zillig, Z., D. Schachtschabel, and W. Krone, *Hoppe-Seyler's Z. physiol. Chem.*, **318**, 100 (1960).

[7] Singer, M. G., and G. L. Cantoni, *Biochim. Biophys. Acta*, **39**, 182 (1960).

---

*REACTION OF CARCINOGENS WITH ACRIDINE**

BY A. SZENT-GYÖRGYI AND JANE MCLAUGHLIN

INSTITUTE FOR MUSCLE RESEARCH, MARINE BIOLOGICAL LABORATORY, WOODS HOLE, MASSACHUSETTS

Communicated July 24, 1961

Only a very small number of the known substances is strongly carcinogenic. This indicates that carcinogenicity is linked to different qualities which all must be present to produce cancer. The various chemical reactions or qualities brought into relation with carcinogenicity reflect one or more of these factors. None of them seems to comprise all involved parameters. At the same time, none of the reactions proposed is strictly characteristic and is thus given also by substances which are not carcinogenic. This is true, also, for the "black reaction" with iodine, as described earlier by Isenberg *et al.*[1, 2]

In spite of these discrepancies the chemical behavior of carcinogens is not without interest, giving, possibly, a clue to one or the other parameter of carcinogenicity. It is in this relation that we want to report reactions with acridine.

TABLE 1

	Color with acridine	Carcinogenicity
Methylcholanthrene	+++	+++
1,2-Benzyprene	−	0
3,4-Benzpyrene	+++	+++
Pyrene	+	0
4-Dimethylaminostilbene	+++	++
Stilbene	−	0
2-Aminofluorene	++	++
4-Aminofluorene	−	0
Fluorene	−	0
Anthracene	−	0
9,10-Dimethylanthracene	+	0
Benzanthracene	+	?
10-Methyl benzanthracene	+	+
9,10-Dimethylbenzanthracene	+++	+++
Phenanthrene	−	0
1,4-Dimethylphenanthrene	++	0
1,10-Phenanthroline	+	0
Phenothiazine	+	0
Biphenyl	−	0
p-Terphenyl	−	0
Triphenylene	−	0
2-Aminobiphenyl	−	0
4-Aminobiphenyl	++	+
Picene	−	0
Chrysene	−	0
Naphthalene	−	0
1-Naphthol	−	0
2-Naphthol	−	0
α-Naphthylamine	+	?
β-Naphthylamine	++	?
Indole	+	?

Acridine has a strong absorption band in the nearest *UV*. If its 0.1 *M* chloroform solution is dried down on filter paper in presence of an equimolar quantity of a classical carcinogen, a strong yellow color appears. Since the color obtained with various carcinogens is identical, evidently, it is not due to a charge transfer absorption but corresponds to a red shift in the absorption of acridine. The results on this line are summed up in Table 1. To our knowledge, no similar reaction has yet been described. An X-ray analysis of the acridine compounds seems to be rewarding.

* This research was sponsored by The Commonwealth Fund and Grant No. G-5836 from the National Science Foundation.

[1] Szent-Györgyi, A., I. Isenberg, and S. L. Baird, Jr., these PROCEEDINGS, **46**, 1445 (1960).

[2] Owing to the courtesy of Charles B. Huggins, the author was able to complete the earlier list, relating to the reaction with iodine, by three more substances. 9,10-dimethylanthracene (not carcinogenic) gave a strong black reaction with iodine, but only after the evaporation of the solvent, indicating a low affinity to the halogen. With trinitrobenzene the substance gives a deep red charge transfer color. 1,4-dimethylphenanthrene (not carcinogenic) gave no black reaction and showed only an orange color with TNB. 4-dimethylaminostilbene (strongly carcinogenic) gave a strong reaction with iodine even in presence of the solvent (chloroform) and gave a deep blue color with TNB.

---

*METALS AND CHARGE TRANSFER**

BY ALBERT SZENT-GYÖRGYI

INSTITUTE FOR MUSCLE RESEARCH, MARINE BIOLOGICAL LABORATORY, WOODS HOLE, MASSACHUSETTS

Communicated July 24, 1961

It is likely[1] that charge transfer plays a major part in biology. For charge transfer to occur, the two interacting molecules must be in a very close proximity which allows orbitals to overlap. This demands exact fit which may be difficult to achieve with the rather complex biomolecules. So, a search for factors facilitating charge transfer seems justified.

It has been noted earlier that the transfer of electrons between *o*-phenylene diamine and 1,2-naphthoquinone is facilitated by Mg ions.[2] This was interpreted to mean that the metal ion formed a bidentate chelate with acceptor and donor, thus forming a bridge between the two molecules over which the electrons could pass. The metal may have facilitated the electron transfer in various ways: by holding the reactants together, decreasing the activation energies and readjusting energy levels, forming a unique electronic system with the reactants, and favoring a "local charge transfer"[3] which does not demand the exact fitting of the two molecules.

A similar example was found, lately, in the interaction of quinone and aromatic amines. If a 0.01 *M* methanol solution of 1,2-naphthoquinone-SO_3Na is mixed with $^1/_5$ vol. of a 0.1 *M* methanol solution of *p*-aminobenzoic acid, or sulphanilamide, procaine, aniline, N-ethylaniline, or N,N-diethylaniline,[4] a slow reaction takes place which leads, eventually, to the formation of azides and declares itself to the eye by the slow formation of a dark color. If an equivalent quantity of Zn acetate

or chloride is added, dissolved in methanol, the coloration is greatly speeded up, leading, in the case of *p*-aminobenzoic acid, to the formation of a dark red crystalline precipitate.[5] It seems likely that the reaction is initiated by a charge transfer which is facilitated by the Zn ions, which form a bidentate chelate with the quinone and coordinate the amine. Mg acts similarly, though weaker. Mn^{2+}, Cu^{+}, Fe^{2+}, or Co^{2+} act similarly to Zn.

What lends special interest to Zn is not only its participation in many enzymic processes but also the fact that it has no two, well-defined, valency states and thus could not mediate charge transfer by shuttling between the reactants, and being alternately oxidized and reduced.

Histidine and histamine gave a similar reaction with naphthoquinone in the presence of Zn. This can be shown in an aqueous medium (in which amines react too fast with quinone to allow a clear demonstration of the action of the metals). The reaction of histidine may be of interest because energy transmission, in certain proteins,[6] was connected with the presence of this amino acid. Imidazole gave no similar reaction with quinone, indicating a specific influence of the side chain. Metallic links between DNA and proteins have been postulated by K. S. Kirby,[7] while G. Wald[8] gave evidence for the participation of histidine in visual excitation.

* This research was sponsored by Grant No. G-5836 from the National Science Foundation and a grant from The Commonwealth Fund.

[1] Szent-Györgyi, A., *Introduction to a Submolecular Biology* (New York: Academic Press, 1960), pp. 54–95.

[2] Szent-Györgyi, A., *Bioenergetics* (New York: Academic Press, 1957), p. 71.

[3] Szent-Györgyi, A., I. Isenberg, and J. McLaughlin, these PROCEEDINGS, **47,** 1089 (1961).

[4] The rate of reaction of anilines is in the order aniline > ethylaniline > diethylaniline. Since the ionization potential is decreased by the ethyl substitution, the decreased rate has to be ascribed to the steric hindrance introduced by the ethyl group, which interferes with complex formation. The P value (energy of the highest filled orbital, kindly calculated by G. Karreman by the LCAO approximation) is 0.544 for aniline, 0.504 for ethylaniline, and 0.461 for diethylaniline. The P value is a linear function of the ionization potential.

[5] Demonstrated at a conference on "The application of spectroscopy of a radiofrequency to biology and structural chemistry," Brussels, April 6–7, 1961 (Organized and printed by the Royal Belgian Academy).

[6] Ehrenberg, A., and H. Theorell, *Acta Chemica Scandinavica,* **9,** 1193 (1955).

[7] Kirby, K. S., *Biochem. J.*, **66,** 495 (1957); **70,** 260 (1958).

[8] Wald, G., *Exptl. Cell Research, Suppl. 5*, 389 (1958).

*THE ENZYMATIC SYNTHESIS OF RNA: NEAREST-NEIGHBOR BASE FREQUENCIES**

By Samuel B. Weiss and Tokumasa Nakamoto

ARGONNE CANCER RESEARCH HOSPITAL† AND DEPARTMENT OF BIOCHEMISTRY, UNIVERSITY OF CHICAGO

Communicated by Charles Huggins, July 31, 1961

RNA[1] polymerase activity, first detected in mammalian cell-free preparations,[2, 3] has now been described in a number of bacterial extracts and plant tissues.[4–7] The reaction catalyzed by this enzyme shows an absolute requirement for all four ribonucleoside triphosphates and DNA and may be represented by the following equation:

$$\begin{matrix} n\text{ATP} \\ + \\ n\text{GTP} \\ + \\ n\text{CTP} \\ + \\ n\text{UTP} \end{matrix} \xrightleftharpoons{\text{DNA}} \begin{bmatrix} \text{Ap} \\ \text{Gp} \\ \text{Cp} \\ \text{Up} \end{bmatrix}_n 4n\text{PP}.$$

The requirement for a deoxypolynucleotide primer raised the question of the role played by this polymer in RNA synthesis. A recent report from this laboratory demonstrated that the base composition of RNA, prepared with a partially purified extract from *Micrococcus lysodeikticus*, was similar to and dependent upon the composition of the primer.[8] Similar results have been obtained by Stevens[9] and Furth *et al.*[10, 11] with extracts prepared from *Escherichia coli*.

Cellular RNA similar in base composition to DNA has been identified in various organisms by a number of investigators.[12, 13] Recently, Hall and Spiegelman have shown that the RNA which appears after T2 phage infection of *E. coli* forms complexes with denatured phage DNA.[14] Such complexes are believed to occur only between strands of complementary base sequences and point out the complementary relationship between the deoxy- and ribopolynucleotides. The existence of similar DNA and RNA molecules in nature has added impetus to the idea that genetic information is transmitted to other cellular sites by so-called "messenger-RNA."[15, 16] The discovery of a DNA-dependent RNA polymerase has stimulated speculation that this enzyme may be responsible for the synthesis of this specific-RNA. So far, no direct experimental proof has been offered to support these speculations.

Weiss and Nakamoto have presented preliminary evidence indicating that the relative position of ribonucleotides in enzymatically prepared RNA is determined by the primer used for the reaction.[8] This information, along with the similar base composition found, suggests, but does not prove, that synthesis occurs with replication of the nucleotide sequences of the primer. Absolute and unequivocal proof of replication can only be supplied by determining the sequential arrangement of bases in both primer and RNA product. In the absence of methods adequate to perform such analysis, a complete nearest-neighbor frequency study for the 16 possible nucleotide pairs in RNA has been determined for RNA's prepared with

different primers. In view of the elegant studies reported recently by Josse, Kaiser, and Kornberg,[17] it is possible to compare our nearest-neighbor pairs with the results published for DNA's that have been similarly characterized. We have also carried out a series of CsCl density-gradient experiments designed to determine the complementary relationship of the RNA formed during reaction with respect to the primer employed, and these results are reported in the following paper.

Materials and Methods.—ATP^{32}, CTP^{32}, and UTP^{32} were prepared as previously described.[3] GTP^{32} was prepared by the method of Tener.[18] Each of these labeled substrates contained P^{32} in the innermost phosphate only. RNA polymerase was obtained from extracts of *M. lysodeikticus*, and preparations ranging from 100- to 200-fold purification were used. *E. coli* DNA was a gift from Dr. A. Rich; T2 DNA was a gift from Dr. L. Grossman; calf thymus DNA was purchased from the Sigma Chemical Company, 3500 DeKalb Street, St. Louis 18, Missouri; and *M. lysodeikticus* DNA was prepared from lysozyme-treated cells as described by Lehman and co-workers.[19]

The reaction mixture for the preparation of P^{32}-labeled RNA contained 3 μmole of $MnCl_2$, 100 μmole Tris-PO_4 buffer of pH 7.4, 0.10 mg of a DNA primer, 1 μmole each of ATP, UTP, CTP, and GTP, only one of which was radioactive (specific activity of 1 to 10×10^6 cpm per μmole), and a purified extract from *M. lysodeikticus* in a total volume of 1.0 ml. Sufficient enzyme was used so that a minimum of 100,000 cpm was incorporated into RNA. For each DNA used, four similar reactions were prepared except that each reaction contained a different labeled substrate. After 30 min at 25°, the reaction was stopped with cold 5 per cent TCA and iced, and the precipitate was collected. The acid-insoluble material was washed three times by dissolving in 0.10 *M* NaOH and reprecipitating with TCA, and once again with ethanol-ether (3:1). One mg of carrier RNA was added, and the residue was extracted twice in 1 ml of 10 per cent NaCl, pH 8, for 30 min at 100°. Two volumes of cold ethanol were added to the combined extracts, and the precipitate was collected after standing at 0° overnight. The nucleic acid fraction was dissolved in 1 ml of water, 0.10 ml of a 20 per cent potassium acetate solution (adjusted to pH 5) was added, and reprecipitation was with ethanol. This procedure was repeated until the ethanol supernatant gave a constant amount of radioactivity. The precipitate was dried under vacuum for 30 min, hydrolyzed in 0.3 *M* KOH for 18 hr at 37°, and acidified with $HClO_4$, and the acid-soluble fraction was subjected to paper electrophoresis as described elsewhere.[3] The 2′-, 3′-nucleoside monophosphates were identified under ultraviolet light, eluted, and assayed for radioactivity.

Results.—During alkaline hydrolysis of RNA, the phosphate esterified to the 5′ position of one ribonucleotide is transferred to the 2′,3′ position of the adjacent nucleotide. P^{32}-RNA, enzymatically synthesized with one ribonucleoside 5′ (pyro)-triphosphate labeled in the ester phosphate only, gives rise to four labeled 2′,3′-nucleoside monophosphates when subjected to this type of hydrolysis. Quantitative determination of the amount of isotope contained in each mononucleotide may be used as a measure of the relative frequency with which the labeled nucleotide occurs next to a given neighbor in the RNA chain. In the synthesis of RNA, if four labeled nucleotides are used separately, in four different reactions, the isotope content of the hydrolyzed mononucleotides can be used to determine the frequencies

TABLE 1

P^{32} CONTENT OF MONONUCLEOTIDES ISOLATED FROM ENZYMATICALLY SYNTHESIZED P^{32}-RNA PRIMED BY *M. lysodeikticus* DNA

Isolated 2',3'-ribonucleotide	Reaction No. 1 ATP^{32}			Reaction No. 2 UTP^{32}			Reaction No. 3 GTP^{32}			Reaction No. 4 CTP^{32}		
	Sequence	Cpm	Fraction	Sequence	Cpm	Fraction	Sequence	Cpm	Fraction	Sequence	Cpm	Fraction
Up	UpA	960	0.065	UpU	947	0.108	UpG	3,834	0.151	UpC	8,124	0.185
Ap	ApA	1,612	0.109	ApU	1,411	0.161	ApG	3,237	0.128	ApC	6,667	0.152
Cp	CpA	5,895	0.397	CpU	3,249	0.371	CpG	10,335	0.406	CpC	13,548	0.310
Gp	GpA	6,360	0.429	GpU	3,145	0.360	GpG	8,041	0.315	GpC	15,447	0.353
Sum	..	14,827	1.000	..	8,752	1.000	..	25,447	1.000	..	43,786	1.000

TABLE 2

P^{32} CONTENT OF MONONUCLEOTIDES ISOLATED FROM ENZYMATICALLY SYNTHESIZED P^{32}-RNA PRIMED BY T2 DNA

Isolated 2',3'-ribonucleotide	Reaction No. 1 ATP^{32}			Reaction No. 2 UTP^{32}			Reaction No. 3 GTP^{32}			Reaction No. 4 CTP^{32}		
	Sequence	Cpm	Fraction	Sequence	Cpm	Fraction	Sequence	Cpm	Fraction	Sequence	Cpm	Fraction
Up	UpA	3,735	0.258	UpU	3,724	0.340	UpG	6,001	0.350	UpC	8,576	0.343
Ap	ApA	5,400	0.373	ApU	3,544	0.324	ApG	5,098	0.298	ApC	6,818	0.273
Cp	CpA	2,760	0.190	CpU	1,878	0.171	CpG	2,856	0.166	CpC	4,336	0.173
Gp	GpA	2,580	0.179	GpU	1,811	0.165	GpG	3,170	0.186	GpC	5,275	0.211
Sum	..	14,475	1.000	..	10,957	1.000	..	17,125	1.000	..	25,005	1.000

of the 16 possible nearest-neighbor base sequences. For a detailed description of nearest-neighbor sequence determination, the reader is referred to Josse and coworkers.[17] The method used here for calculating these values is essentially as reported by these investigators and may be simply described as follows:

Fractional base value × *base-incorporating factor* = *relative frequency.*

For a given reaction, the isotope content found for each mononucleotide was converted to the decimal fraction of the total to give the fractional base values (Table 1). To obtain nearest-neighbor frequencies, the fractional values must be multiplied by a factor which represents the relative amount of each ribonucleotide incorporated into RNA. Since the relative amount of each ribonucleotide incorporated is determined by the base composition of the primer,[8] the molar proportion of adenine, thymine, guanine, and cytosine of the particular DNA employed in each reaction were used as the base-incorporating factors. The DNA base compositions given in Table V of the paper by Josse, Kaiser, and Kornberg[17] were used, since it was felt that these values might be more accurate than previously reported determinations of the chemical composition for deoxyribonucleic acid.

DNA from *M. lysodeikticus* contains a relatively high guanine and cytosine content while T2 phage DNA is rich in adenine

and thymine. Table 1 and Table 2 show the counts and fractional values determined for the various 2′,3′-mononucleotides formed by alkaline hydrolysis of P^{32}-RNA when synthesized in the presence of these distinctly different primers. When the fractional values are multiplied by the appropriate base-incorporating factors (0.147, 0.145, 0.354, and 0.354 for *M. lysodeikticus* DNA and 0.319, 0.318, 0.184, and 0.179 for T2 DNA in the reactions containing ATP^{32}, UTP^{32}, GTP^{32}, and CTP^{32}, respectively), the nearest-neighbor frequencies shown in Table 3 and Table 4 are obtained.

TABLE 3

COMPARISON OF NEAREST-NEIGHBOR FREQUENCIES OF RNA WITH DNA FOR PRIMER *M. lysodeikticus* DNA

Reaction no.	Labeled triphosphate	Isolated 2′,3′-nucleoside Monophosphate							
		Up (Tp)*		Ap		Cp		Gp	
1	ATP^{32}	UpA	(TpA)	ApA		CpA		GpA	
		0.010	(0.011)	0.016	(0.019)	0.058	(0.052)	0.063	(0.065)
2	UTP^{32}	UpU	(TpU)	ApU	(ApT)	CpU	(CpT)	GpU	(GpT)
	($dTTP^{32}$)	0.016	(0.017)	0.023	(0.022)	0.054	(0.050)	0.052	(0.056)
3	GTP^{32}	UpG	(TpG)	ApG		CpG		GpG	
		0.053	(0.054)	0.045	(0.049)	0.143	(0.139)	0.112	(0.112)
4	CTP^{32}	UpC	(TpC)	ApC		CpC		GpC	
		0.065	(0.063)	0.054	(0.054)	0.110	(0.113)	0.125	(0.121)

* The values in parentheses represent the nucleotide pairs and nearest-neighbor frequencies reported by Josse *et al.*[17] for *M. lysodeikticus* DNA.

TABLE 4

COMPARISON OF NEAREST-NEIGHBOR FREQUENCIES OF RNA WITH DNA FOR PRIMER T2 DNA

Reaction no.	Labeled triphosphate	Isolated 2′,3′-nucleoside Monophosphates							
		Up (Tp)*		Ap		Cp		Gp	
1	ATP^{32}	UpA	(TpA)	ApA		CpA		GpA	
		0.082	(0.089)	0.119	(0.111)	0.061	(0.061)	0.057	(0.059)
2	UTP^{32}	UpU	(TpU)	ApU	(ApT)	CpU	(CpT)	GpU	(GpT)
	($dTTP^{32}$)	0.108	(0.106)	0.103	(0.104)	0.054	(0.054)	0.052	(0.051)
3	GTP^{32}	UpG	(TpG)	ApG		CpG		GpG	
		0.064	(0.063)	0.055	(0.057)	0.031	(0.030)	0.034	(0.036)
4	CTP^{32}	UpC	(TpC)	ApC		CpC		GpC	
		0.061	(0.057)	0.049	(0.048)	0.031	(0.034)	0.038	(0.040)

* The values in parentheses represent the nucleotide pairs and nearest-neighbor frequencies reported by Josse *et al.*[17] for T2 DNA.

A comparison of the figures of similar base-pairs found in RNA with those reported for DNA (values in parentheses) shows that the frequency of the 16 nucleotide pairs for primer and product is remarkably close. In all instances where the base-pair frequencies are relatively high or low for a given DNA, the same variation is detected in the base-pairs for the synthesized RNA.

E. coli and calf thymus DNA have base compositions which are somewhat alike. The nearest neighbor frequencies for both these DNA's are also fairly similar except in one or two instances, e.g., the base-pairs CpG and GpC. When the nucleotide pairs of the RNA's formed with these two primers are examined, we find that the frequencies are in good agreement with the values reported for DNA (Table 5). In those few instances where there are marked differences in the base-pair frequencies of the primers, there are also similar differences in the RNA synthesized. Thus, when differences in the nearest-neighbor sequences of two primers exist,

TABLE 5

COMPARISON OF NEAREST-NEIGHBOR FREQUENCIES FOR RNA AND DNA

Nearest-neighbor sequence*	Calf Thymus		*E. coli*	
	Primer DNA†	Synthesized RNA	Primer DNA†	Synthesized RNA
ApA, UpU	0.089, 0.087	0.093, 0.082	0.071, 0.076	0.075, 0.079
CpA, UpG	0.080, 0.076	0.082, 0.070	0.071, 0.071	0.071, 0.068
GpA, UpC	0.064, 0.067	0.062, 0.061	0.055, 0.056	0.059, 0.056
CpU, ApG	0.067, 0.072	0.072, 0.067	0.055, 0.055	0.051, 0.051
GpU, ApC	0.056, 0.052	0.058, 0.053	0.055, 0.054	0.054, 0.058
GpG, CpC	0.050, 0.054	0.061, 0.055	0.056, 0.056	0.057, 0.058
UpA	0.053	0.051	0.051	0.044
ApU	0.073	0.068	0.068	0.070
CpG	0.016	0.016	0.067	0.073
GpC	0.044	0.048	0.083	0.077

* The nucleotide pairs listed are for RNA and are the same for DNA except that T (thymine) would be substituted for U (uridine).

† The nearest-neighbor frequencies for calf thymus and *E. coli* DNA have been reported by Josse *et al.*[17]

the corresponding differences in the RNA products can be readily detected.

Discussion and Summary.—A thorough understanding of the enzymatic mechanism for the synthesis of RNA by DNA-dependent enzymes is important for obvious reasons. The implications of this reaction as a possible step in transmitting genetic information has already been mentioned. The results tabulated in this paper, together with the similar base compositions of DNA and RNA previously determined, provide further evidence for the sequential assembly of ribonucleotides along a DNA template. The data are consistent with the idea that the arrangement of bases along such a template would occur by hydrogen-bonding of the appropriate base-pairs.

RNA polymerase can be primed by heat-denatured DNA as well as native DNA.[20] No definitive answer can be given to the problem whether one or both strands of DNA determine the base sequence and composition of the enzymatically synthesized RNA. In theory, according to the Watson and Crick base-pairing hypothesis,[21] opposing strands of DNA need not have the same base composition, but they may do so on a purely statistical basis. The similar base ratios found for RNA and its primer DNA and the similarity in nearest-neighbor frequencies are consistent with two possibilities: (1) the strands are different and both prime, or (2) the strands are alike in compositions and base sequence and one or both may prime. In the latter case, the results offer no information on the mechanism of priming.

Although the nearest-neighbor frequencies determined in these experiments suggest that the sequential arrangement of nucleotides in RNA is probably the same as that found in the primer, the above results by themselves cannot be considered unequivocal evidence for faithful replication of the base sequences found in DNA. For this reason, we have carried out CsCl density-gradient studies which will be reported in the subsequent paper[22] and which provide more conclusive evidence that the RNA strands synthesized are complementary in base sequence to the deoxypolynucleotide primer. The term complementary is defined as a specific fit of portions of primer and product by appropriate base interactions.

* This investigation was supported by funds from the Argonne Cancer Research Hospital and from the Joseph and Helen Regenstein Foundation.

† Operated by the University of Chicago for the U.S. Atomic Energy Commission.

[1] The abbreviations used in this report are: RNA and DNA for ribo- and deoxyribonucleic

acid; CTP^{32}, ATP^{32}, UTP^{32}, and GTP^{32} for the triphosphates of cytidine, adenosine, uridine, and guanosine labeled with P^{32} in the ester phosphate; Cp, Ap, Up, and Gp for the 2′,3′-nucleoside monophosphates of the bases listed above; PP for inorganic pyrophosphate; Tris, tris-(hydroxymethyl)-aminomethane; TCA, trichloroacetic acid; cpm, counts per minute.

[2] Weiss, S. B., and L. Gladstone, *J. Am. Chem. Soc.*, **81**, 4118 (1959).

[3] Weiss, S. B., these PROCEEDINGS, **46**, 1020 (1960).

[4] Stevens, A., *Biochem. and Biophys. Research Communs.*, **3**, 92 (1960).

[5] Hurwitz, J., A. Bresler, and R. Diringer, *Biochem. and Biophys. Research Communs.*, **3**, 15 (1960).

[6] Weiss, S. B., and T. Nakamoto, *J. Biol. Chem.*, **236**, PC18 (1961).

[7] Huang, R. C., N. Maheshwari, and J. Bonner, *Biochem. and Biophys. Research Communs.*, **3**, 15 (1960).

[8] Weiss, S. B., and T. Nakamoto, these PROCEEDINGS, **47**, 694 (1961).

[9] Stevens, A., *J. Biol. Chem.*, **236**, PC43 (1961).

[10] Furth, J. J., J. Hurwitz, and M. Goldmann, *Biochem. and Biophys. Research Communs.*, **4**, 362 (1961).

[11] *Ibid.*, 431 (1961).

[12] Volkin, E., and L. Astrachan, *Virology*, **2**, 149 (1956).

[13] Yčas, M., and W. S. Vincent, these PROCEEDINGS, **46**, 804 (1960).

[14] Hall, B. D., and S. Spiegelman, these PROCEEDINGS, **47**, 137 (1961).

[15] Brenner, S., F. Jacob, and M. Meselson, *Nature*, **190**, 576 (1961).

[16] Gros, F., H. Hiatt, W. Gilbert, C. G. Kurland, R. W. Rissebrough, and J. D. Watson, *Nature*, **190**, 581 (1961).

[17] Josse, J., A. D. Kaiser, and A. Kornberg, *J. Biol. Chem.*, **236**, 864 (1961).

[18] Tener, G. M., *J. Am. Chem. Soc.*, **83**, 159 (1961).

[19] Lehman, I. R., S. B. Zimmerman, J. Adler, M. J. Bessman, E. S. Simms, and A. Kornberg, these PROCEEDINGS, **44**, 1191 (1958).

[20] Weiss, S. B., *Federation Proc.* (in press).

[21] Watson, J. D., and F. H. C. Crick, *Nature*, **171**, 737, 964 (1953).

[22] Geiduschek, E. P., T. Nakamoto, and S. B. Weiss, these PROCEEDINGS, **47**, 1405 (1961).

---

*THE ENZYMATIC SYNTHESIS OF RNA: COMPLEMENTARY INTERACTION WITH DNA**

BY E. PETER GEIDUSCHEK, TOKUMASA NAKAMOTO, AND SAMUEL B. WEISS

COMMITTEE ON BIOPHYSICS, ARGONNE CANCER RESEARCH HOSPITAL† AND DEPARTMENT OF BIOCHEMISTRY, UNIVERSITY OF CHICAGO

Communicated by Charles Huggins, July 31, 1961

The chemical properties of the polynucleotides synthesized by the DNA-primed RNA polymerase have been described in two previous communications.[1, 2] It has been shown that the average composition and the average nearest-neighbor frequencies of enzymatically synthesized RNA and DNA primer are identical. In view of this information and of the results communicated here, we have named the product of this reaction "Complementary RNA" (C-RNA).[3] It is our working hypothesis that C-RNA is structurally and functionally similar to "messenger" RNA,[9, 10] and that the biosynthesis of C-RNA is an initial step in that sequence of reactions in which DNA asserts the organism's potentialities for protein synthesis. Consequently, it is of considerable interest to discover whether higher-order DNA nucleotide *sequence* is translated with any degree of fidelity in RNA and to describe

in greater detail the manner in which the DNA template is utilized during RNA synthesis. In this communication, we describe the results of experiments along these lines.

Materials and Methods.—DNA: T2 DNA was isolated from bacteriophage by phenol extraction.[12] *Pseudomonas fluorescens* DNA, used as a density reference marker in analytical CsCl gradient centrifugation, and *Escherichia coli* DNA were prepared by a method described elsewhere.[13] DNA from testes of the sea urchin *Strongylocentrotus drobachiensis* was isolated according to the method of Simmons.[14] Bacteriophage T2 DNA, labeled with tritium, was prepared as follows: *E. coli* were grown as described by Kozloff.[15] At late log phase, T2 phage and H^3-labeled adenine were introduced into the medium, and aeration was continued for 4 hr. $MgSO_4$ to 0.005 *M* and 1 μg/ml crystalline pancreatic DNAase I were added. After incubation at 37°C for 1 hr, the entire culture was filtered through celite, and phage was purified from the filtrate.[16] DNA was prepared from the phage by phenol extraction.[12]

The synthesis of C-RNA on a bacteriophage T2 DNA template was carried out as described in the preceding communication.[2] The total volume of the reaction mixture was adjusted to allow incorporation of 50 to 100 mμmoles of labeled substrate into RNA in the presence of 150 to 300 mμmoles of primer DNA-P. The specific activity of labeled nucleotides was reduced to conform with the requirements of the centrifugation experiments.

Isolation of DNA and C-RNA for CsCl gradient centrifugation: Procedure A. The enzymatic synthesis of RNA was terminated by adding an equal volume of 90% redistilled phenol, and shaking 30 min. The phenol extraction was repeated. The aqueous layer containing RNA and DNA was then extracted two to three times with ether to remove dissolved phenol, and residual ether was removed with a stream of N_2. NaCl was added to 0.2 *M*, and CTAB[17, 18] to a final concentration of 1 mg/ml. A precipitate containing DNA and RNA formed immediately. The mixture was allowed to stand for 15–20 min and centrifuged. The precipitate was then washed twice with 0.2 *M* NaCl, and finally dissolved in a small volume of 2 *M* CsCl. All the above steps were carried out at room temperature. Under these conditions, we found that 90% or more of the enzymatically prepared RNA-P^{32} was recovered and that it contained 10 to 20% TCA-soluble nucleotides. The recovery of DNA was less complete, some loss from the aqueous phase occurring in the phenol extraction. However, we did not find it necessary to recover any of that material for the experiments reported here.

Procedure B. Phenol extraction was performed as above. The entire aqueous phase was then reduced under vacuum, adjusted to 7.9 molal CsCl, 0.01 *M* Versene, pH 6.5 in a final volume of 3 ml, and centrifuged at 16°C, 35,000 rpm, for 48 hr. The material which accumulates at the bottom of the tube in the CsCl gradient contains the bulk of the RNA, well separated from DNA. From this fraction, RNA was precipitated as follows: to 0.7 ml CsCl solution, 0.4 ml 0.01 *M* Tris, pH 7 was added, followed by 2.2 ml ice-cold ethanol. The turbid suspension was left standing at room temperature for 20 min, centrifuged, and washed twice with 70% ethanol (1 molal in CsCl). The RNA was then dissolved in the solvent appropriate to the experiment in question.

CsCl density gradient centrifugation in a bucket rotor: Solutions of DNA and RNA in 7.9–8.4 molal CsCl were centrifuged in SW 39 rotors at 35,000 rpm. Three ml of CsCl solution were placed in 5-ml lusteroid centrifuge tubes and overlayered with 2 ml of light liquid paraffin. For the experiments shown in Figures 4 and 5, temperature was controlled (in a Spinco model E analytical ultracentrifuge) within ±0.1°C. For the experiments shown in Figure 2 and 3, the temperature was near 0°C. but was not measured. Centrifuge runs were terminated after 65 to 90 hr, and fractions were collected in a manner similar to that described elsewhere.[19] Each fraction was assayed for acid-precipitable counts and absorbance at 260 mμ.

Analytical methods: Acid-precipitable RNA-P^{32} was determined as described previously.[2] Acid-precipitable DNA-H^3 was determined as follows: nucleic acids, together with exactly 2 mg carrier yeast RNA, were precipitated in 5% TCA and centrifuged, and the supernatant fluid was removed. The residue was dissolved in one drop of concentrated NH_4OH, quantitatively transferred to a planchet, dried, and measured in a windowless gas flow counter.

Properties of RNA synthesized on a phage T2 DNA template: The ultraviolet absorption spectrum of one preparation of T2-C-RNA prepared as above is shown in Figure 1. It has λ_{max} at 258 mμ and λ_{min} at 232 mμ. This material is macromolecular and very heterogeneous, having an

average sedimentation constant $s_{20,w}$ of 5.5*s*, measured at $c = 0.0017\%$ in 0.1 *M* NaCl, 0.01*M* Tris, pH 7. (By comparison, the "messenger" RNA of *E. coli* has a sedimentation constant of $8s^{20}$.) Accordingly, whatever the molecular configuration of C-RNA, this sample must have a much lower average molecular weight than the T2 phage DNA used as a template. We do not know whether this reflects an intrinsic property of RNA polymerase acting *in vitro* or whether it is merely due to degradation by enzymes contaminating the partially purified RNA polymerase.

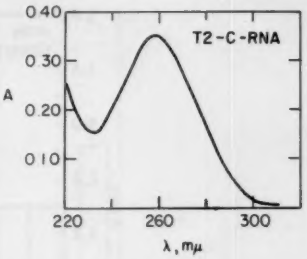

FIG. 1.—Ultraviolet absorption spectrum of T2-C-RNA in 0.01 *M* Tris, pH 7. Absorbances measured in 0.7-ml capacity cuvettes on Beckman DU spectrophotometer.

Results and Discussion.—(1) *Does C-RNA remain attached to the DNA template?* The answer to this question is given by two experiments which show that labeled RNA and DNA are almost completely separated from each other in a CsCl density gradient. In Figure 2, the CsCl gradient centrifugation of the nucleic acids extracted from a T2-C-RNA-P^{32} synthesis is analyzed. It is evident that RNA-P^{32} has accumulated at the bottom of the centrifuge tube and that only a small peak of RNA-P^{32} (less than 3% of the total) can be detected near that portion of the solution which, judged by absorbance measurements, contains the DNA. Figure 3 shows the corresponding experiment in which unlabeled C-RNA has been synthesized on a template of phage T2 DNA-H^3. As in Figure 2, the peak of optical density at the bottom of the tube is due to C-RNA, but there is no sign of a complex with tritiated DNA. The two experiments show that the two nucleic acids are almost completely separated from each other. At present, it is not possible to decide whether the small fraction of C-RNA associated with the DNA band represents C-RNA trapped on the DNA template or whether it is simply due to incomplete disaggregation at some stage of the preparation.

Only two steps have intervened between the RNA synthesis and the gradient centrifugation: phenol extraction at 25°C and precipitation with ethanol or CTAB. As used here, neither step involves even slightly denaturing conditions. Thus, if a complex between the bulk of the C-RNA and its DNA template has been disrupted, we can say with certainty *either* that it is very much more labile than the DNA double helix *or* that it involves a third component (e.g., protein) which is removed during the phenol extraction and nucleic acid precipitation.

(2) *Can DNA-C-RNA complexes be formed?* We have closely followed the elegant method of Hall and Spiegelman[11] in answering this question. Figure 4*a* shows that when T2-DNA and T2-C-RNA are heat-denatured and then "annealed" at 40°C, DNA-C-RNA complexes do form. On the other hand, when the heat-denatured DNA and C-RNA are maintained at "quenching" conditions, almost no DNA-C-RNA complex forms. In other words, the concentration of nucleic acids in this experiment is evidently not high enough to give nonspecific aggregates that are stable to gradient centrifugation (Fig. 4*b*).

The complex formation shown in Figure 4*a* is remarkable. At the concentration of RNA (approximately 100 γ/ml) and DNA (approximately 200 γ/ml) employed in the denaturation and annealing, DNA-RNA complex formation occurs to the complete exclusion of DNA renaturation. That is, in the competition between the

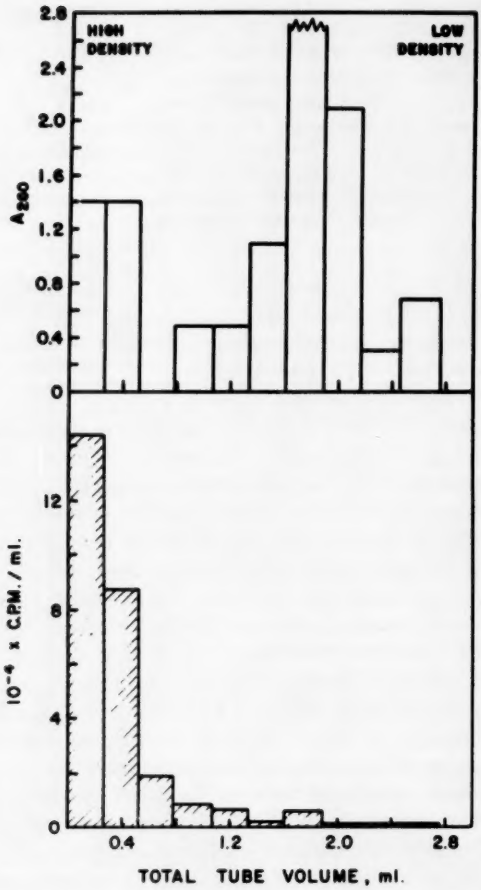

FIG. 2.—Distribution of P^{32}-labeled T2-C-RNA and template T2 DNA in a CsCl density gradient. The volume is calculated from the bottom of the centrifuge tube. For the absorbance measurements, fractions 1 and 2 were combined, and fraction 3 was not measured. *Preparation of RNA and DNA:* Method A (see *Materials and Methods*). *Centrifugation:* 35,000 rpm, 96 hr, near 0°C, 8.4 molal CsCl. *Analysis:* Each fraction is diluted to 0.8 ml and the absorbance measured at 260 mμ. An aliquot is then taken for measurement of TCA-insoluble radioactivity. The concentration of 260 mμ absorbing material and label in the original fraction is calculated from the known volumes, and shown as A_{260} and C.P.M./ml respectively.

two types of equilibria

$$\text{T2-C-RNA} + \text{heated T2-DNA} \rightleftarrows \text{DNA-C-RNA}$$

and $$\text{heated T2-DNA} + \text{heated T2-DNA} \rightleftarrows \text{DNA-DNA (helical)},$$

the former is greatly favored. Upon CsCl gradient centrifugation, the entire DNA band is vacated and a new, considerably denser, band due to DNA-C-RNA complexes appears.

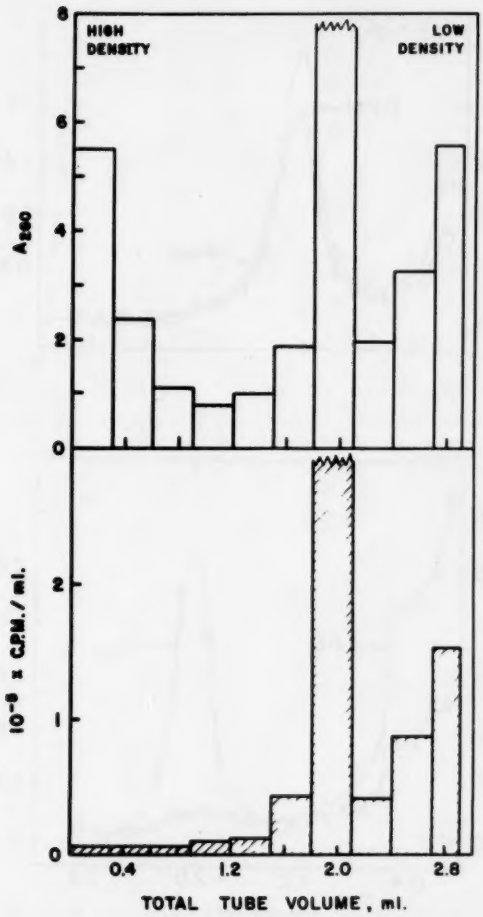

FIG. 3.—Distribution of unlabeled T2-C-RNA and template T2-DNA-H^3 in a CsCl density gradient. Preparation of nucleic acids, centrifugation, and analysis as described in Figure 2.

(3) *Is the DNA-C-RNA complex specific?* T2-C-RNA has been isolated by density gradient centrifugation and separately annealed with denatured T2 DNA (35 mole % GC), sea urchin DNA (Strongylocentrotus, 38 mole % GC), and *E. coli* DNA (51 mole % GC). In this experiment, both DNA (approximately 90 γ/ml) and RNA (*ca.* 10 γ/ml) were more dilute in the annealing mixture, so that complexation was less extensive than observed in the previous experiment. The results are shown in Figure 5. T2 and sea urchin DNA are very close in average base composition. Nevertheless, under conditions in which complex formation between T2 DNA and T2-C-RNA is clearly demonstrable, none occurs between sea urchin or *E. coli* DNA and T2-C-RNA. In fact, no interaction between T2-C-RNA and the heterologous sea urchin DNA occurs at the higher concentration of the

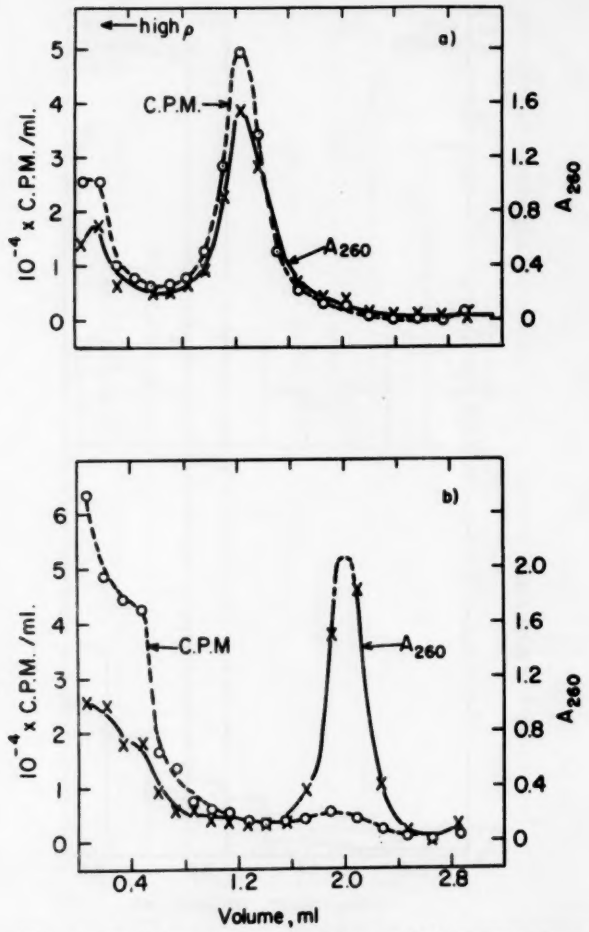

FIG. 4.—Conditions for the Formation of DNA-C-RNA Complexes.

(*a*) Distribution of a heated and annealed mixture of P^{32}-labeled T2-C-RNA and T2-DNA in a CsCl density gradient. ×: A_{260}. ○: C.P.M. *Preparation of RNA:* Method B. *Denaturation and annealing:* 0.07 μmoles T2-C-RNA-P and 0.1 μmoles T2-DNA-P in 0.22 ml 2 *M* CsCl are heated to 100°C for 10 min, quenched, and equilibrated 12 hr at 40.1°C. The mixture is then made up to 3 ml of 8.4 molal CsCl, 0.01 *M* Tris, pH 7. *Centrifugation:* 35,600 rpm, 75 hr, 25°C. *Analysis:* as in Figure 2.

(*b*) Distribution of a heated and quenched mixture of P^{32}-labeled T2-C-RNA and T2 DNA. ×: A_{260}. ○: C.P.M./ml. *Denaturation and quenching:* 0.07 μmoles T2-C-RNA-P and 0.1 μmoles T2-DNA-P in 0.22 ml 2 *M* CsCl, heated to 100°C for 10 min, quenched and maintained at 0°C for 12 hr. The mixture is then made up to 3 ml of 8.4 molal CsCl, 0.01 *M* Tris pH 7. *Centrifugation and analysis:* as in (*a*).

experiment discussed in the previous section, and shown in Figure 4 (data are not presented here).

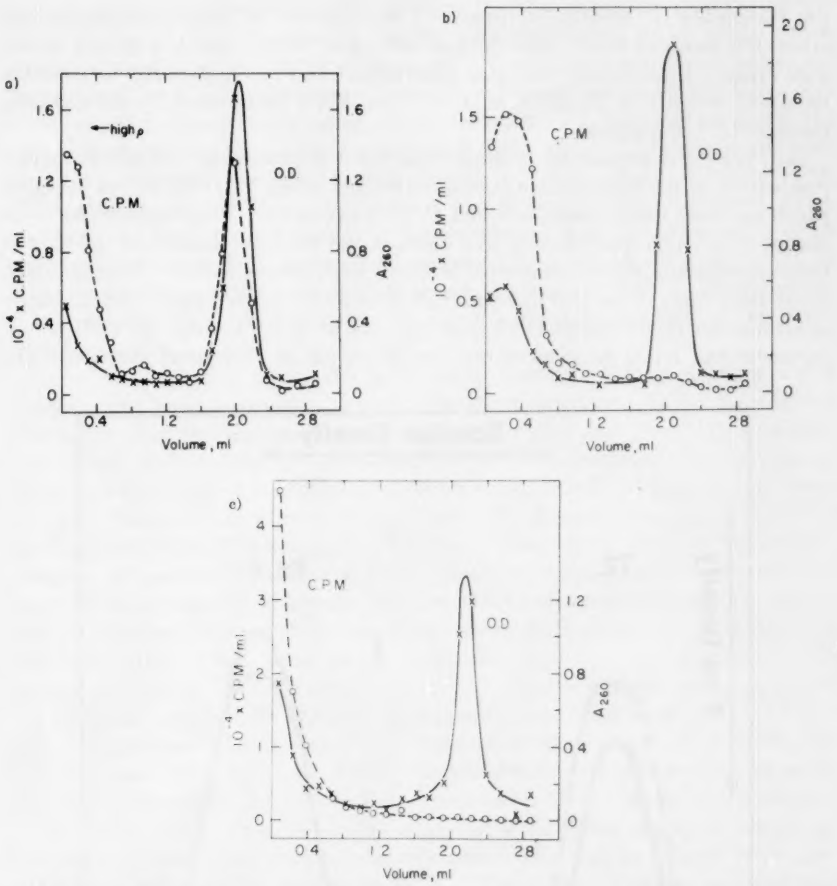

FIG. 5.—The specificity of DNA-C-RNA complexes. Distribution of heated and annealed mixtures of P^{32}-labeled T2-C-RNA with:

(*a*) T2-DNA (35 mole % GC).
(*b*) Sea urchin DNA (38 mole % GC).
(*c*) *E. coli* DNA (51 mole % GC) in a CsCl density gradient. ×: A_{260}. ○: C.P.M./ml.
Preparation of RNA: Method B.

Denaturation and annealing: (*a*) 0.02 μmoles T2-C-RNA-P; 0.12 μmoles T2 DNA-P; (*b*) 0.02 μmoles T2-C-RNA-P 0.10 μmoles sea urchin DNA-P; (*c*) 0.02 μmoles T2-C-RNA-P 0.10 μmoles *E. coli* DNA-P; each in 0.35 ml of 0.6 *M* CsCl. Samples are heated in boiling water for 10 min, quenched, and equilibrated 10 hr at 37°C. Each mixture is then made up to 3 ml of 8.4 molal CsCl, 0.01 *M* Tris pH 7.
Centrifugation: 35,600 rpm; 77 hr; 25°C; 0.01 *M* Tris.

(4) *Is the DNA-C-RNA complex unique?* It appears from the experiments shown in Figures 4*a* and 5*a* that the density of DNA-C-RNA complexes depends on the experimental conditions of the denaturation and annealing and specifically, in these two experiments, on the concentrations of both components. When complex formation is incomplete, the DNA-C-RNA is only slightly heavier than DNA. When complex formation is very extensive, the density of DNA-C-RNA complex

(or complexes) is greatly increased. The evidence of these experiments and others not recorded here is that the composition of DNA-C-RNA may vary over a wide range. Undoubtedly this is, at least in part, due to the disparity between the molecular weights of T2 DNA, and the T2-C-RNA synthesized by the partially purified RNA polymerase.

(5) *Does RNA polymerase priming cause DNA denaturation?* Figure 6 shows a comparison of the buoyant densities of unreacted phage T2 DNA and of T2 DNA which has been used as template in a C-RNA synthesis. There appears to be no change of DNA buoyant density as a result of the RNA synthesis. In the light of these experiments, this result is capable of only two interpretations: (1) phage DNA is not irreversibly denatured by its participation as a C-RNA template, or (2) only a small number of the phage DNA molecules act as C-RNA template, and this experiment has failed to demonstrate the behavior of this small fraction. The

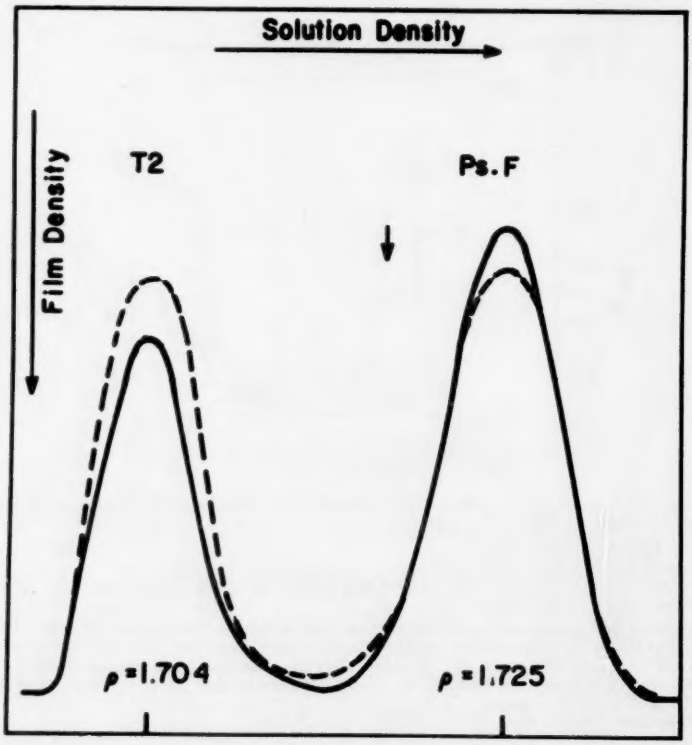

FIG. 6: The CsCl buoyant density of template T2 DNA and T2 DNA which has not taken part in RNA synthesis. *Ps. fluorescens* DNA is used as a density marker. Data are presented in terms of densitometric traces of absorption camera pictures through the region of the DNA "bands." The vertical arrow shows the anticipated location of denatured T2 DNA. The buoyant densities of T2 and *Pseudomonas* DNA are taken from published data.[30, 31]

Centrifugation: 7.7 molal CsCl, 0.01 *M* Tris pH 8, 44,700 rpm, 25°C, 24 hr. 0.60 ml solution are contained in a 12-mm Kel-F cell equipped with a 1° negative prismatic window.

second alternative is rejected on the grounds that the maximum quantity of T2-DNA having changed density (i.e., having been denatured) which could escape detection is not more than 10 % of the total. If, however, only 10 per cent of the molecules of the DNA preparation were active as primer, this could only have come about by 90% primer inactivation during isolation: the inactivation could not entail denaturation. This seems unreasonable, since all the T2 DNA preparations used by us have had comparable priming activities and compare favorably with DNA primers derived from other sources and isolated in many different ways. Furthermore, the RNA synthesis for this experiment was carried out at a DNA concentration lower than, and enzyme concentration close to, saturation. All of these considerations militate against the possibility that less than 10 per cent of the DNA molecules prime all of the C-RNA synthesis while the bulk of the DNA remains inactive.

Comments.—At this point, the relationship between C-RNA and its DNA template has been determined at several levels of structure. It has been shown previously that the average composition of C-RNA's and their DNA primers correspond, [1,21,22] and the preceding communication demonstrated that the nearest-neighbor frequencies of four different C-RNA's and their DNA primers also correspond.[2] These two experiments suggest, but by no means prove, that C-RNA is a faithful copy of its DNA template. There is a tendency for many of the nearest-neighbor frequencies of a DNA to follow patterns consistent with its *average* base composition, so that the differences between DNA's of comparable average nucleotide composition, while evident, are by no means distinctive (ref. 23, Tables VI, VII, and VIII). Only when longer nucleotide sequences are investigated, do species specificities become more clear-cut.[11, 24] In these experiments, therefore, the ability of template T2 DNA to form specific complexes with T2-C-RNA is a test of the presence of entire nucleotide *sequences* in DNA and C-RNA chains that are simultaneously capable of binding to each other in the face of the competing tendency of complementary nucleotide sequences on DNA strands to recombine.[11]

We have evidence also that every strand of a T2 DNA sample is capable of forming such complexes, since in one experiment (Fig. 4*a*) we entirely eliminated material banding at the density of DNA. The simplest interpretation of this finding is that C-RNA molecules exist which are complementary to both strands of T2 DNA and that both DNA strands act as template, either separately or together.[25]

We turn next to a consideration of the manner in which the DNA is utilized in the C-RNA synthesis. Others have shown, as have we, that a double helix in which only a small portion of the nucleotide sequence is maintained in register at all times can rewind in such a manner as to obliterate, for the purposes of the density-gradient experiment, all traces of its unfolding.[26–28] In order to account for the unchanged buoyant density of template DNA (Fig. 6), we must therefore assume that DNA double helices do not have to unwind entirely in serving as RNA templates. In addition, we know from the annealing experiments (Fig. 4*a*) that DNA-C-RNA complexes involving entire C-RNA molecules must be very stable. The clear separation of T2-C-RNA from its template argues against any C-RNA synthetic mechanism involving such intermediates. We are, therefore, left with two alternatives: (1) The template for RNA synthesis is a single polynucleotide

strand of DNA, of which only the small region immediately surrounding the site of terminal nucleotide addition is unwound, or (2) the double helix may act as a template without unwinding.

The similarity of the RNA and DNA syntheses on a DNA template is striking. However, in this study a difference of great importance can be observed. While the *in vitro* DNA template synthesis involves recombination of template and product polynucleotide,[29] the *in vitro* synthesized C-RNA is free of its template. Finally, let us suppose that the mechanism of the *in vivo* formation of messenger RNA is the same as that of C-RNA *in vitro*. In that case, it seems probable that as the assembly of the RNA is completed, the two nucleic acids part and the DNA remains in, or spontaneously returns to, its double helical form.

We should like to express our thanks to S. Spiegelman for his generous advice, to L. M. Kozloff and R. Mackal for gifts of bacteriophage, to J. Moohr for preparing tritium-labeled phage, and to G. Gibson for constructing a fraction collecting device.

* This investigation was supported by funds of the U.S. Public Health Service (grant C-5007), the Argonne Cancer Research Hospital, and the Joseph and Helen Regenstein Foundation.

† Operated by the University of Chicago for the U.S. Atomic Energy Commission.

[1] Weiss, S. B., and T. Nakamoto, these PROCEEDINGS, **47,** 694 (1961).

[2] *Ibid.*, **47,** 1400 (1961).

[3] A number of different enzymes (polynucleotide phosphorylase, RNA polymerase, polyribonucleotide synthetase) from various sources have now been reported for the synthesis of RNA.[4–6] Each of these reactions has different properties, and the products formed, although exhibiting characteristic polynucleotide linkages, are not the same. Furthermore, in recent years, a distinction between RNA molecules has been made by various investigators based upon their cellular origin and biological properties, e.g., soluble RNA,[7] amino acyl RNA,[8] and their chemical composition, e.g., "messenger" RNA.[9, 10] In view of this, we have tentatively assigned the name of "complementary RNA" to the product of the reaction catalyzed by RNA polymerase, in order to designate a specific type of RNA, that is, one which is formed from a DNA template, contains a similar base composition and nearest-neighbor frequency to that of the primer, and exhibits the type of complementary properties with its primer first described by Hall and Spiegelman.[11]

[4] Grunberg-Manago, M., and S. Ochoa, *J. Am. Chem. Soc.*, **77,** 3165 (1955).

[5] Weiss, S. B., these PROCEEDINGS, **46,** 1020 (1960).

[6] Reddi, K. K., paper presented at the 98th Annual Meeting of the National Academy of Sciences (1961).

[7] Hoagland, M. B., P. C. Zamecnik, and M. L. Stephenson, *Biochim. et Biophys. Acta*, **24,** 215 (1957).

[8] Berg, P., F. H. Bergmann, E. J. Ofengand, and M. Dieckmann, *J. Biol. Chem.*, **236,** 1726 (1961).

[9] Volkin, E., and L. Astrachan, *Virology*, **2,** 149 (1956).

[10] Jacob, F., and J. Monod, *J. Molec. Biol.* **3,** 318 (1961).

[11] Hall, B. D., and S. Spiegelman, these PROCEEDINGS, **47,** 137 (1961).

[12] Mandell, J. D., and A. D. Hershey, *Anal. Bicchem.*, **1,** 66 (1960).

[13] Hamaguchi, K., and E. P. Geiduschek, manuscript in preparation.

[14] Simmons, N., as quoted by V. L. Stevens and E. L. Duggan, *J. Am. Chem. Soc.*, **79,** 5703 (1957).

[15] Kozloff, L. M., and M. Lute, *Biochim. Bicphys. Acta*, **37,** 420 (1960).

[16] Soller, A., *Virology*, **13,** 267 (1961).

[17] Abbreviations: C-RNA, complementary (biosynthetic) RNA; T2-C-RNA, complementary RNA synthesized on a bacteriophage T2 DNA template; DNA-C-RNA, a complex between DNA and complementary RNA; CTAB, cetyltrimethylammonium bromide; TCA, trichloracetic acid; G, guanine; C, cytosine; Tris, tris-(hydroxymethyl)-aminomethane; A_{260}, absorbance at 260 mμ; s, svedberg unit.

[18] Jones, A. S., *Biochim. Biophys. Acta*, **10**, 607 (1953).

[19] Bolton, E. T., R. J. Britten, D. B. Cowie, B. J. McCarthy, K. McQuillen, and R. B. Roberts, *Carnegie Institution of Washington Year Book 1958-59*, p. 259.

[20] Gros, F., H. Hiatt, W. Gilbert, C. G. Kurland, R. W. Risebrough, and J. D. Watson, *Nature*, **190**, 581 (1961).

[21] Stevens, A., *J. Biol. Chem.*, **236**, PC43 (1961).

[22] Furth, J. J., J. Hurwitz, and M. Goldman, *Biochem. Biophys. Res. Comm.*, **4**, 362 (1961).

[23] Josse, J., A. D. Kaiser, and A. Kornberg, *J. Biol. Chem.*, **236**, 864 (1961).

[24] Shapiro, H. S., and E. Chargaff, *Biochim. Biophys. Acta*, **26**, 608 (1957).

[25] One other, less plausible possibility exists which, however, cannot be excluded. It is that the DNA-C-RNA complexes of Figure 4*a* consist of networks, each involving many DNA and RNA chains. In such a network, DNA-C-RNA complexes might involve one type of DNA strand *only*, while the complementary DNA strand is carried along solely because of its ability to form intermittent DNA-DNA complexes.

[26] Geiduschek, E. P., *Fed. Proc.*, **20**, 353 (1961).

[27] Marmur, J., and L. Grossman, these PROCEEDINGS, **47**, 778 (1961).

[28] Geiduschek, E. P., these PROCEEDINGS, **47**, 950 (1961).

[29] Baldwin, R. L., R. B. Inman, and R. G. Wake, *Fed. Proc.*, **20**, 354 (1961).

[30] Rolfe, R., and M. Meselson, these PROCEEDINGS, **45**, 1039 (1959).

[31] Fleischman, J. B., *J. Molec. Biol.*, **2**, 226 (1960).

*STUDIES ON THE KINETICS OF PROTEIN SYNTHESIS IN YEAST**

BY R. J. YOUNG,† H. K. KIHARA, AND H. O. HALVORSON

DEPARTMENT OF BACTERIOLOGY, UNIVERSITY OF WISCONSIN

Communicated by R. H. Burris, July 17, 1961

It is now generally agreed that ribosomal particles are the primary site of protein synthesis. In yeast, this evidence is supported by studies on the incorporation of amino acids *in vivo*[1, 2] and *in vitro*[3] and by the finding on ribosomes of bound protein[4] and enzymes[5] which are presumably newly synthesized protein. One question raised by these findings is what percentage of the ribosomal protein is represented by newly synthesized polypeptides and what is the relationship between this material and the structural proteins of the ribosome? In an attempt to further characterize the nascent ribosomal protein, this material was isolated and compared with the structural protein of the ribosomes. These two classes of protein differed not only in their composition and properties but also in the kinetics of synthesis. The nascent protein has a transient existence on the ribosome and the kinetics of its turnover is sufficient to account for the over-all rate of protein synthesis.

Methods.—A diploid yeast (*Saccharomyces dobzanskii* × *Saccharomyces fragilis*) was used in these experiments. Unless otherwise specified, all cultures were grown in a sulfur-low, synthetic medium prepared by adding to one liter of water: NH_4Cl, 6.4 gm; K_2HPO_4, 17.4 gm; succinic acid, 11.6 gm; $CaCl_2$, 0.2 gm; $MgCl_2$, 0.2 gm; $(NH_4)_2SO_4$, 5 mg; sulfur-free trace elements; and vitamin mixture. The cultures were grown at 30° in shaken Erlenmeyer flasks. Under the conditions employed, the generation time was about 190 min.

For the kinetic studies on S^{34} and C^{14} amino acid incorporation, yeast cells were grown in the above medium until the optical density had reached a level of about

0.20–0.30 as measured in a Beckman spectrophotometer at 600 mμ in a 10 mm cell. The sulfur content of the medium is sufficient to provide exponential growth to optical density levels above 1. For the S^{35} experiments, carrier-free $H_2S^{35}O_4$ was added at a level of 7.5 mC per 100 ml of culture. At intervals, samples were withdrawn immediately into tubes containing 10% TCA or poured into beakers containing crushed, frozen medium.[6] In both cases, further incorporation was immediately arrested. The samples were then fractionated as described in the text. Ribosomes were prepared as previously described.[5]

Protein was measured by the method of Lowry *et al.*[7] using crystalline serum albumin as the standard. For radioactivity experiments, aliquots of the various fractions were evaporated to dryness on stainless steel planchets and counted in a gas flow counter, and their radioactivities were corrected to infinite thinness.

Materials.—Cacodylic acid was obtained from the Fisher Scientific Company. Diisopropylfluorophosphate was obtained from Dr. R. M. Bock and the amino acids from the California Corporation for Biochemical Research. Deionized glass-distilled water was used for all experiments. Carrier-free $H_2S^{35}O_4$ was obtained from the Oak Ridge National Laboratory. Totally labeled amino acids were prepared by growing *Hydrogenomonas facilis* on $C^{14}O_2$ (52.6 per cent isotope excess) and preparing an acid hydrolysate of the proteins as described by Roberts *et al.*[8]

Results.—Kinetics of $S^{35}O_4^{=}$ incorporation: As a preliminary step to the study of ribosomal incorporation, an investigation was undertaken on the kinetics of incorporation of $S^{35}O_4^{=}$ into exponentially growing yeast. At intervals, 2.0 ml aliquots were removed by means of a hypodermic syringe and squirted into tubes containing 5 ml of crushed, frozen medium. The cells were then washed with ice water and precipitated and washed with 10 per cent TCA containing 1 *M* $(NH_4)_2SO_4$. The pellet was resuspended and an aliquot extracted several times with hot TCA. The extracted pellet was solubilized with 5 *N* NH_4OH and counted as a measure of the incorporation into the protein fraction. The results are shown in Figure 1. As can be seen, the total uptake of radioactivity has not reached a steady state by 600 sec. The cold TCA-soluble fraction was treated with Ba^{++} to remove the sulfate; the remaining radioactivity was found almost exclusively in S-containing amino acids. The rate of incorporation into this fraction is much more rapid than that of the growth rate and follows kinetics expected of that of a precursor material.[8] The initial rate of incorporation into proteins is only about 20–25 per cent of that of the labeling of the cold TCA-soluble pool. Of interest was the finding that the rate of incorporation into the hot TCA-soluble fraction, which includes the soluble RNA complexes, was slower than that of the rate of labeling of the protein fraction.

The rate of incorporation of $S^{35}O_4^{--}$ into the hot TCA-insoluble fraction was followed at shorter intervals by pipetting aliquots directly into tubes containing hot TCA and nonradioactive substrate. As is shown in Figure 2, the rate of incorporation into this fraction is linear over the initial 90 sec of incubation. The rate of incorporation extrapolates back to the addition of the isotope, and thus the delay in incorporation is less than 5 sec and is probably on the order of 1–2 sec.

Incorporation of C^{14} amino acids into ribosomes and soluble proteins: The kinetics of incorporation of totally labeled C^{14} amino acids into ribosomal and soluble proteins of exponentially growing yeast were studied by the following experiments.

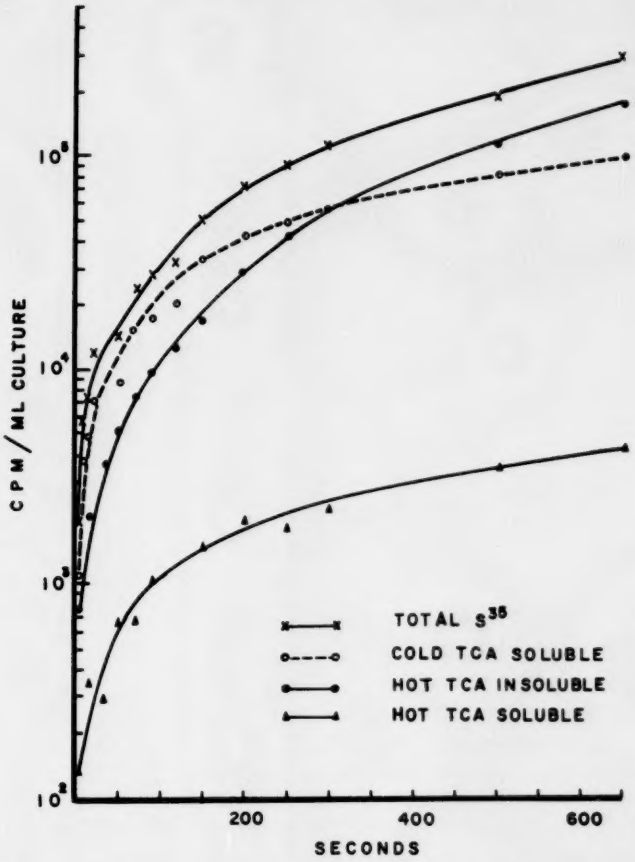

FIG. 1.—Kinetics of $S^{35}O_4^{=}$ incorporation into growing yeast. At the indicated times, aliquots were removed, washed, and fractionated as indicated in the text.

At intervals after addition of the isotope, samples were poured on ice chilled to $-20°$. The cells were collected by centrifugation, washed twice with cold water, and resuspended in cold 6×10^{-4} *M* Mg cacodylate buffer, pH 7.2. The cells were broken in a French press and the ribosomal and supernatant fractions collected as described elsewhere.[5, 6] The soluble protein fraction was precipitated from the supernatant with hot TCA; the precipitate was washed with an aqueous solution of unlabeled amino acids and finally solubilized with 5 *N* NH_4OH. The results are shown in Figure 3. The rate of incorporation into the ribosome fraction is about 4 × that of the soluble proteins. At 80 sec, excess unlabeled amino acids were added. Within 10 sec, all incorporation into the ribosome fractions was terminated and the specific activity of the ribosome dropped to a constant level after 120 sec. This decrease is paralleled by a net increase in the soluble protein

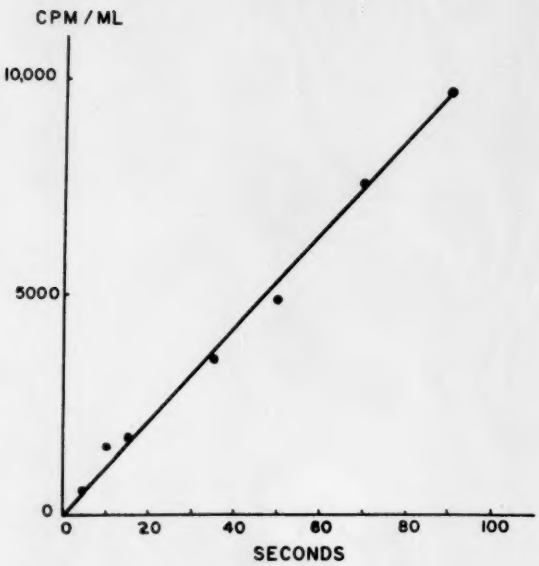

FIG. 2.—Time course of $S^{35}O_4^=$ incorporation into yeast proteins. $S^{35}O_4^=$ was added to a growing culture of yeast. At intervals, 2 ml aliquots were removed and pipetted into tubes containing boiling 10 per cent TCA and unlabeled sulfate, methionine, and cysteine. The pellets were washed twice with 10 per cent TCA, solubilized with 5 *N* NH_4OH and counted for radioactivity.

fraction. From the pool size and kinetics of decrease, approximately 10 sec or less of synthesis is associated with the ribosome fraction.

The nondisplaceable fraction presumably represents the newly synthesized structural protein of the ribosome. As is described by Yin and Bock[9] and shown below, about 95 per cent of the protein of ribosomes is insoluble at neutral pH and apparently serves as a structural protein. The kinetics of structural protein synthesis can thus be measured by following the formation of polypeptides which are not displaced from ribosomes by treatment for 120 sec with unlabeled amino acids. As indicated by the center curve of Figure 3, approximately 50 per cent of the radioactivity is associated with this nondisplaceable fraction.

Fractionation of yeast ribosomes: The use of C^{14}-labeled amino acids to study the turnover rate of protein bound to ribosomes is difficult because of delays in its exchange with the large pool of free amino acids in yeast. This problem is less serious with $S^{35}O_4^{--}$, as the pool of precursor S in yeast can be specifically reduced by growing in a medium with a reduced concentration of sulfur. Preliminary to the experiments on incorporation of $S^{35}O_4^{--}$, the distribution of S in ribosomes was analyzed.

Yeast cells were grown in a synthetic medium containing $S^{35}O_4^{--}$ (1.628×10^6 cpm/mg S). The cells were washed several times, resuspended in cacodylic buffer, and broken in French press. After removal of the debris, the supernatant was spun for 90 min at 40,000 rpm in the angle head rotor (40) of the Spinco Model L

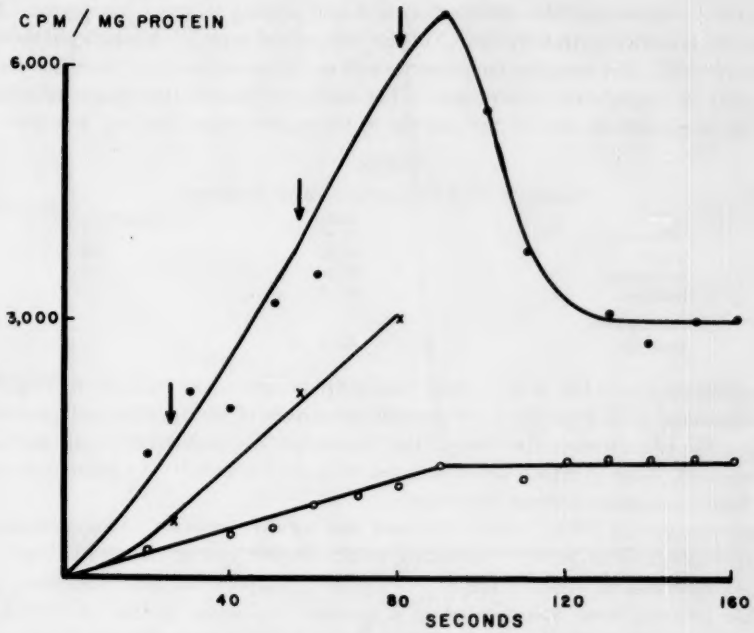

FIG. 3.—Kinetics of the incorporation of C^{14} labeled amino acids into ribosomes and soluble proteins. C^{14}-labeled *Hydrogenomonas* protein hydrolysate (4.4×10^6 cpm/ml; 54 μg. total N) was added to a growing culture of yeast (600 ml). The total free amino acid pool in this culture is about 1,500 μg. Since only a small fraction of the labeled amino acids are assimilated during the short incubation period, the free amino acid pool is not significantly altered by the added amino acids. At intervals, 40 ml aliquots were removed and treated as described in the text. At 30 and 60 seconds, 40 ml aliquots were transferred to separate flasks containing unlabeled amino acids and incubated for an additional 120 seconds. At 80 seconds, an enzymic digest of casein was added to a final concentration of 1 per cent. The specific activity of C^{14} in supernatant protein (○), total ribosomes (●), and nondisplaceable fraction of ribosomes (×) were determined as described in the text.

centrifuge. The supernatant was retained for further analysis. The ribosome fraction was repeatedly layered (3 times) on a sucrose density gradient (5–20%) and centrifuged in the swinging bucket rotor (SW 25) for 4 hr at 23,000 rpm until a constant specific activity was obtained.[5] An aliquot of the purified ribosomes was degraded with 30 μg/ml ribonuclease in 1 M urea.[9] To prevent possible protease action during digestion, 1 μmole/ml of diisopropylfluorophosphate was added before the addition of ribonuclease. The reaction mixture was allowed to stand for 1 hr. at 37° and then kept overnight at 4° to allow complete precipitation of the structural protein. The precipitate was washed three times with water, dissolved in 8 M urea and 1 per cent Dupanol, and reprecipitated by dialysis against water. The final protein was again resuspended in urea and Dupanol. The soluble protein of the cell as well as the protein solubilized from the ribosomes was precipitated with hot TCA, dissolved in 5 N NH_4OH, reprecipitated with TCA, and finally washed with alcohol and ether before assay.

Table 1 summarizes the distribution of S and protein in yeast ribosomes. The ribosome protein is primarily (96%) of the "structural type." A minor component is soluble (4%) and contains enzymes[5] as well as the same classes of proteins[4] found normally in the soluble supernatant. The sulfur content of the ribosomal soluble protein is similar to that of the protein of the supernatant fraction, whereas the

TABLE 1

COMPOSITION OF S^{35}-LABELED YEAST RIBOSOMES

Ribosomes	Sulfur (% wt.)	Protein in fraction (%)
Total	0.32	100
Structural	0.30	96
Soluble	0.53	4
Supernatant Protein	0.63	..

structural protein is low in S. These results are in agreement with the finding that the ribosomal soluble proteins are nascent precursors of the supernatant proteins.[4] During the ribonuclease digestion of the ribosomes, low molecular weight peptides are released, some of which are associated with nucleotides.[10] An examination of this fraction is under current investigation.

Incorporation of $S^{35}O_4^{--}$ into ribosomes and soluble proteins: Measurement of the incorporation of $S^{35}O_4^{--}$ appeared to be the method of choice for studying protein synthesis in yeast. The kinetics of S^{35} incorporation into ribosomes and soluble proteins were investigated in a manner analogous to that described in Figure 3 for work with C^{14}-labeled amino acids. The results are shown in Figure 4. The ribosome fraction was labeled at a rate, which in parallel experiments was 6 times faster than that of the soluble proteins. Upon addition of methionine, cysteine, and unlabeled sulfate, the specific radioactivity of the ribosome fraction drops 85 per cent within 10 sec. These findings suggest that the majority of the acid-stable S of ribosomes formed in a short period from $S^{35}O_4^{--}$ is associated with nascent rather than structural protein.

Addition of unlabeled S to S^{35}-labeled yeast cells: To further characterize the size of the nascent protein fraction in yeast ribosomes, 0.1 M $(NH_4)_2SO_4$, cysteine, and methionine were added to a suspension of S^{35}-labeled yeast cells. At 0, 40, and 160 sec, samples were withdrawn, and soluble protein and ribosomes were collected as previously described. The specific activities of the two fractions recorded in Table 2 show no detectable decrease, whereas following a brief exposure to isotope (Fig. 4), most of the incorporated S^{35} is displaced by unlabeled precursor. These findings further support the conclusion that the nascent protein represent only a small fraction of the total protein of yeast ribosomes.

Discussion.—In yeast ribosomes, Yin and Bock[9] isolated over 90 per cent of the ribosomal protein as strongly aggregating proteins with a predominant molecular

TABLE 2

THE EFFECT OF THE ADDITION OF UNLABELED SO_4^{--} CYSTEINE, AND METHIOHINE ON THE S^{35} CONTENT OF FRACTIONS FROM S^{35}-LABELED YEAST CELLS

Period of displacement (sec)	Protein (cpm/mg protein)	Ribosome (cpm/E_{260}/ml)
0	1.025×10^7	2.24×10^5
40	1.045×10^7	2.37×10^5
160	1.02×10^7	2.39×10^5

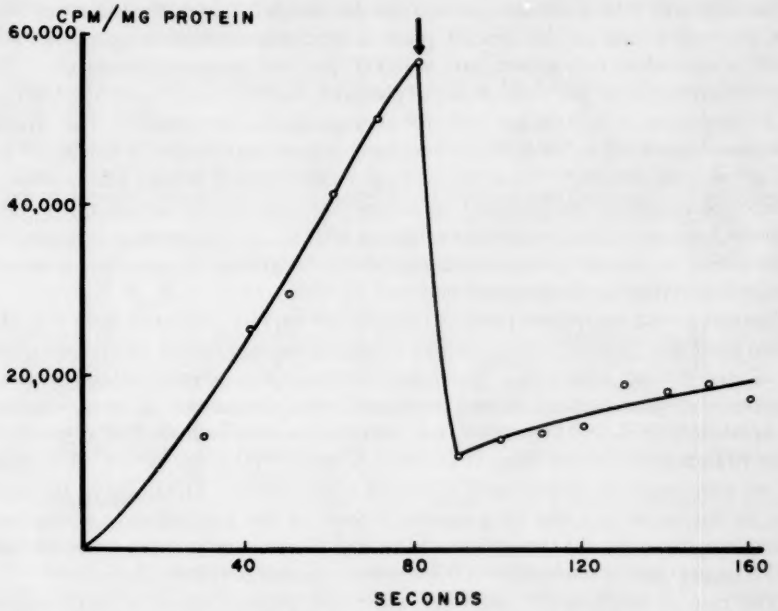

FIG. 4.—Incorporation of $S^{35}O_4^-$ into ribosomes of yeast. Experimental conditions were similar to those of Figure 3 except that $S^{35}O_4^-$ was used. At 80 seconds, unlabeled $(NH_4)_2SO_4$, cysteine, and methionine were added to a final concentration of 0.1 *M* each.

weight of 12,000. These polypeptide chains were low in amino acids containing S and had similar solubility and electrophoretic properties but at least 8 different N-terminal amino acids. These polypeptides aggregate to form complexes of 50,000 molecular weight; 40 such protein units are found per ribosomal particle.

In addition to the insoluble structural protein, a minor fraction of the ribosomal protein can be isolated as soluble heterogeneous protein. The classes of S^{35}-labeled proteins released from ribosomes are identical to the classes of soluble protein present in the cytoplasm.[4] In addition, a number of enzymes including RNAase,[11] β-glucosidase,[5] and triose-phosphate dehydrogenase,[12] have been solubilized from these particles. As described in the present paper, this fraction contains about four per cent of the ribosomal protein and has a S content which is about twice that of the structural protein.

The kinetic studies on incorporation of C^{14} amino acid and S^{35} as SO_4^{--}, support the findings in *E. coli*[6] that the soluble fraction from ribosomes contains the nascent proteins which are precursors of the soluble proteins. Evidence supporting a ribosomal-bound β-glucosidase has already been presented.[5] The ribosomal-soluble fraction represents a molecular weight of about 89,000 per ribosome. The size of the nascent polypeptide chain is probably a fraction of this, since some enzymes such as RNAase[11] are associated only with ribosomes and others such as β-glucosidase have high molecular weights. In addition, peptides have been identified in yeast ribosomes.[10] Some authors[6, 13] have described nascent protein as growing polypeptide chains of about 10,000–20,000 molecular weight.

The turnover rate of nascent protein can be calculated from the following data. The generation time of this diploid yeast in synthetic medium is about 190 min, which is equivalent to a growth rate of 0.0061 per cent increase in mass/sec. The protein content is 47 per cent of the dry weight, which is equivalent to about 3.3×10^7 molecules of protein per cell (10^5 average molecular weight). The number of ribosomes per cell is 5.5×10^5; these have a molecular weight of 4.5×10^6 and are 52 per cent protein.[5] Thus, the average yeast cell each second will increase its number of ribosomes by 33.5 and its polypeptides by 20,100, assuming the polypeptides have an average molecular weight of 10,000. If all the ribosomal particles were active in nascent protein synthesis, then the average time required to synthesize a polypeptide chain would be about 27 sec.

Assuming that completed nascent proteins are rapidly displaced from the ribosomal particles, then only the molecules being synthesized during an average period of 27 sec remain attached. These calculations agree approximately with the kinetics of displacement of isotope from prelabeled ribosomes. A 10-sec exposure to unlabeled $(NH_4)_2SO_4$, cysteine, and methionine was sufficient to displace S^{35} from ribosomes recovered from yeast treated with $S^{35}O_4^{--}$ for 80 sec, while about 40 sec were required to displace C^{14}-labeled amino acids. The delay in the latter may be due to the fact that the precursor S pools are low and reduced under growth in medium low in S; the free amino acid pool of the remaining amino acids are high, and a longer time is required to influence their specific activity.

The rate of synthesis of ribosomal structural protein can also be calculated. Each second, the average yeast cell must synthesize 5,360 polypeptides (average molecular weight of 12,000) to account for new ribosome formation. The rate of amino acid incorporation into structural polypeptide, therefore, is about $1/3$ of that for soluble protein synthesis. Thus, in 90 sec a quantity of ribosomal structural protein is formed equal to the steady-state concentration of nascent protein. This is confirmed in the data of Figure 3, when after 80 sec of labeling with C^{14} amino acids half of the radioactivity was associated with the structural protein. The data of Table 2 indicate that added unlabeled SO_4^{--}, cysteine, and methionine do not displace S^{35} from labeled cells in the steady state. These results provide an explanation for the experiments of Osawa and Hotta,[1] who failed to detect any displacement of C^{14} amino acids from the ribosomal fraction of yeast after 18 min of previous exposure to labeled amino acids. After 18 min, the nascent protein represents only a few per cent of the newly formed ribosomal protein.

Summary.—The kinetics of incorporation of $S^{35}O_4^{--}$ and C^{14} amino acids have been followed in exponentially growing cultures of yeast. Within a few seconds, the isotopes are incorporated into protein, appearing first in the ribosomal fraction as nascent protein. After 80 sec exposure of growing yeast cells to C^{14}-labeled amino acids or $S^{35}O_4^{--}$, the addition of unlabeled amino acids or unlabeled cysteine, methionine, and SO_4^{--} caused a rapid decrease in the concentration of C^{14} or S^{35}, respectively, held by the ribosomes. This response indicated that nascent protein synthesized on the ribosomes is displaced quickly upon completion of its synthesis into the soluble protein pool. Nascent protein represents only a small fraction of the ribosomal protein; however, its turnover rate is sufficient to account for the over-all rate of protein synthesis of the cell.

The methods employed furnish an estimate of the kinetics of synthesis of the structural protein of ribosomes.

We are indebted to R. M. Bock, F. H. Yin, and A. S. L. Hu for their advice and assistance in certain experiments.

* Published with the approval of the Director of the Wisconsin Agricultural Experimental Station. This investigation was supported in part by research grants from the U.S. Air Force Office of Scientific Research of the Air Research and Development Command (AF 49(638)-314), National Institutes of Health (E-1459), and the National Science Foundation (B-7150).

† Present address: Enzyme Institute, University of Wisconsin, Madison, Wisconsin.

[1] Osawa, S., and Y. Hotta, *Biochim. et Biophys. Acta*, **34**, 284 (1959).

[2] Kihara, H. K., R. J. Young, and H. O. Halvorson, *Federation Proc.*, **19**, 347 (1960).

[3] Webster, G. C., *J. Biol. Chem.*, **229**, 535 (1957).

[4] Kihara, H. K., H. O. Halvorson, and R. M. Bock, *Biochim. et Biophys. Acta*, **49**, 212 (1961).

[5] Kihara, H. K., A. S. L. Hu, and H. O. Halvorson, these PROCEEDINGS, **47**, 489 (1961).

[6] McQuillen, K., R. B. Roberts, and R. J. Britten, these PROCEEDINGS, **45**, 1437 (1959).

[7] Lowry, O. H., N. J. Rosebrough, A. L. Farr, and R. J. Randall, *J. Biol. Chem.*, **193**, 265 (1951).

[8] Roberts, R. B., P. H. Abelson, D. B. Cowie, E. T. Bolton, and R. J. Britten, *Studies of Biosynthesis in Escherichia coli*, Publication 607 (1955) of the Carnegie Institution of Washington.

[9] Yin, F. H. and R. M. Bock, in preparation.

[10] Koningsberger, V. V., Chr. O. van der Grinten, and J. Th. G. Overbeek, *Biochim. et Biophys. Acta*, **26**, 483 (1957); Kihara, H K., R. J. Young, and H. O. Halvorson, *Federation Proc.*, **20**, 388 (1961).

[11] Stenesch, J. J., Doctoral Thesis, University of California, Berkeley (1958).

[12] Warren, W., and D. Goldthwait, *Federation Proc.*, **20**, 144 (1961); Hauge, J. G., unpublished results.

[13] Rabinovitz, M., and M. E. Olson, *Exptl. Cell Research*, **10**, 747 (1956); Dintzis, H., H. Borsook, and J. Vinograd, in *Microsomal Particles and Protein Synthesis*, ed. R. B. Roberts (New York: Pergamon Press, 1958 p. 95; Tissieres, A., D. Schlessinger, and F. Gros, these PROCEEDINGS, **46**, 1450 (1960).

---

*BIOCHEMICAL CONTROL OF STOMATAL OPENING IN LEAVES**

BY ISRAEL ZELITCH

BIOCHEMISTRY DEPARTMENT, THE CONNECTICUT AGRICULTURAL EXPERIMENT STATION

Communicated by H. B. Vickery, July 25, 1961

In the course of previous studies on the role of glycolic acid in leaf metabolism, it was found that α-hydroxysulfonates are effective inhibitors of the enzyme glycolic oxidase.[1] Treatment of leaves with these substances resulted in rapid and extensive changes in the products formed during photosynthesis.[2, 3] More recently, visible physiological effects have been observed when tobacco leaves are treated under certain environmental conditions. When slightly wilted leaves were supplied with these glycolic oxidase inhibitors during high water stress, in bright sunlight, the water vapor lost by transpiration decreased with the result that such leaves regained their turgidity more rapidly than control leaves.

Most of the water transpired by leaves apparently escapes through the stomata.[4] The width of the stomatal apertures is controlled by osmotic forces in the kidney-shaped guard cells which surround these openings. When the guard cells are

filled with water and are turgid, the stomata are open; when the guard cells lose water and become flaccid, the stomatal apertures are greatly reduced in size.[5] The readily observable effect of glycolic oxidase inhibitors on the water relations of leaves suggested that these compounds rapidly affect the osmotic pressure within the guard cells and thus control the width of the stomata.

An investigation was therefore made of some biochemical aspects of the control of stomatal opening and the effect of stomatal closure on the transpiration of leaves in light. A standardized system for assaying the extent of stomatal opening in tobacco leaf disks was developed, and with this assay a number of metabolic regulators were tested for their ability to close the stomata. This study was facilitated by a new technique for measuring stomatal apertures quickly and accurately. In addition, the effect of artificially induced closure of stomata on reducing water loss by transpiration without affecting CO_2 assimilation during photosynthesis was studied.

Methods.—Measurement of stomatal apertures: The still unpublished technique described here was devised and shown to me by Joan Tucker, Department of Botany, University of Oxford, to whom I am most grateful. A viscous fluid silicone rubber ("RTV-11," Silicone Products Dept., General Electric Company, Waterford, N. Y.) which has been well stirred and then mixed with a sufficient amount of catalyst ("Silicure T-773") is gently spread with a spatula over the area of the leaf or leaf disk to be examined. Enough catalyst is added so that the fluid polymer is converted into a firm piece of rubber within 2 to 3 min. The silicone rubber, which is then peeled from the leaf surface, provides an accurate impression of the epidermis. The impression is dried briefly in a desiccator and is then painted with a thin film of cellulose acetate solution (commercial colorless nail polish diluted with an equal volume of acetone). When the film has dried, it is stripped off and examined under a microscope fitted with an ocular micrometer at a magnification of 1,000 ×. The epidermal cells, guard cells, and stomatal apertures are clearly visible on the film (Fig. 1).

Preliminary experiments with this method indicated that if a tobacco leaf were kept with its base in water in darkness for 1 hour, although narrow slits could almost always be observed, the apertures never exceeded 1 to 1.5 μ in width. If the tobacco leaf were then placed in sunlight in a humid atmosphere, within about 1 hr more than 90% of the stomatal apertures were 2μ in width or greater, and some apertures as wide as 10–12μ (Fig. 1) have frequently been measured. Based upon this experience, although all of the stomatal apertures measured were recorded, those openings 2μ in width or greater are considered to be "open," and those less than 2μ as "closed." The measurements are made, one in each of 100 microscope fields and, by counting the number of apertures 2μ or larger, the results can be conveniently expressed as "per cent stomata opened." With experience, this procedure requires only a few minutes.

The classification of percentage of stomatal apertures as "open" or "closed" correlates well with the mean stomatal width (Table 1); a mean stomatal width of about 1μ corresponds to 0% "open," and an average width of 4μ is approximately equivalent to 100% of the apertures "open."

The silicone impressions can be stored for many months and fresh films prepared for examination as required. As many as four successive impressions have been made in one day on the same area of a leaf still attached to the plant with no apparent damage.

Standard assay of stomatal closure in tobacco leaf disks: Leaves were taken from greenhouse grown tobacco plants (var. Havana Seed or Connecticut Shade). For stomata to open fully, I have found it to be essential that the plants constantly receive an abundant supply of water. A leaf, 7–12-gm fresh weight, is cut and its base placed in water in darkness for at least 1 hr to insure complete closure (in terms of the assay) of the stomata. A sufficient number of disks, 1.6 cm in diameter, are then cut with a sharp punch from the central region of the leaf, avoiding large veins. Disks chosen at random are placed in pairs right side up in 50-ml beakers. Exactly 3 min after the cutting of the disks commences, 5 ml of water or of the solution to be tested are added to the beaker. The disks are immersed in the fluid, and the beakers are placed in a water bath maintained at 24°. The disks float on the surface and are illuminated from above with

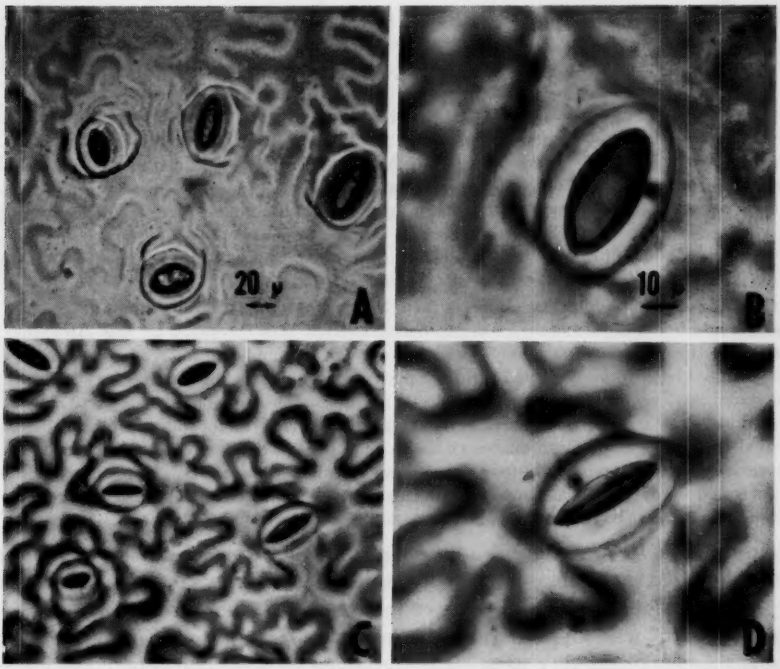

FIG. 1.—Photomicrographs of lower epidermis of tobacco leaf disks prepared from silicone rubber impressions. *A* and *B* are taken from cellulose acetate films prepared from impressions of a leaf disk floated on water under the conditions of the standard assay described under *Methods*. *A* represents a microscopic field viewed at 430 ×, and *B* is the stoma on the extreme right viewed at 1000 ×. *C* and *D* are analogous photomicrographs taken from a tobacco leaf disk floated on a solution of α-hydroxy-2-pyridinemethanesulfonic acid, and illustrate that "closed" stomata, according to the definition given under *Methods*, still have an aperture of 0.5 to 1 μ in width.

TABLE 1

EFFECT OF α-HYDROXYSULFONATES SUPPLIED THROUGH THE BASE OF THE LEAF ON STOMATAL OPENING AND TRANSPIRATION

	Experiment 1: 30 min			Experiment 2: 60 min		
	Leaf in water	Leaf in 0.01 *M* A*	Leaf in 0.01 *M* B*	Leaf in water	Leaf in 0.01 *M* A*	Leaf in 0.01 *M* B*
Initial leaf wt, gm	12.35	13.75	13.75	9.45	10.85	12.50
Wt change of leaf, gm	−0.10	+0.25	+0.80	+0.40	+0.75	+1.05
Fluid change, gm	−1.85	−1.90	−1.75	−3.50	−2.55	−2.70
Transpiration rate, gm H_2O per gm leaf per hr	−0.32	−0.24	−0.14	−0.33	−0.17	−0.13
Per cent stomata "open" zero time	4	0	2	4	12	10
Mean stomatal width zero time, μ	0.5	0.5	1.0	1.1	1.3	1.3
Per cent stomata "open" at end	58	6	14	96	18	12
Mean stomatal width at end, μ	2.0	1.2	1.4	4.3	1.5	1.4

* Compound A is α-hydroxy-2-pyridinemethanesulfonic acid, and B is sodium hydroxymethanesulfonate.

Tobacco plants were permitted to wilt slightly in bright sunlight before the start of the experiment. In each experiment, successive leaves from the same plant were chosen, and stomatal opening was determined from silicone rubber impressions prepared from a small area of the upper surface of each leaf before the leaves were excised at zero time. The leaves were weighed and placed in previously weighed beakers containing water or the solution to be tested. At the end of the experimental period, silicone rubber impressions of the upper surface of the leaves were again prepared, and the leaves and beakers were weighed separately to obtain the transpiration rates.

In Experiment 1, the leaves were maintained in an upright position in 4,700 ft-c of sunlight at 24° and 75% relative humidity for 30 min. In Experiment 2, the leaves were kept at about 3,700 ft-c of sunlight at 32° in high relative humidity for 60 min.

300-watt photoflood lamps that provide 4,000 ft-c at the upper surface. Mirrors placed below the beakers provide about 2,000 ft-c to the lower surface. A fan is fitted to blow air across the beakers so that the temperature of the fluid in contact with the leaf disks remains at about 25°.

At the end of the assay period, 90 min, the disks are blotted and impressions are made of the lower epidermis. Since it was found that stomata of tobacco leaf disks floated on water open at the same rate in the upper and lower epidermis, and there are 2 to 3 times as many stomata in the lower epidermis, it is more convenient to utilize the lower surface for the assay. The "per cent of stomata opened" is estimated by measuring 50 stomatal apertures from impressions made of each of the 2 disks. Control disks placed in water furnish a standard of comparison for test solutions, the stomata of the control disks being generally 80–100% "open." All assay results are expressed as "per cent of stomata closed" in comparison with these controls. This assay provides a measure of the effectiveness of chemical compounds in reducing stomatal opening.

Materials.—Of the α-hydroxysulfonates used, those containing 10 carbon atoms or less, and the bisulfite addition compound of 2,4-dichlorobenzaldehyde were prepared in this laboratory by reaction of the corresponding aldehyde with an excess of sodium bisulfite.[2] The compounds were recrystallized from aqueous alcohol and their purity was established by analysis for sodium. The acetylated hydroxymethanesulfonate, sodium acetoxymethanesulfonate, was prepared as described by Lauer and Langkammerer[6] and gave the correct analysis for sodium and saponification equivalent. The α-hydroxysulfonates with more than 10 carbon atoms, and the pyridine aldehyde derivatives used were purchased from the Aldrich Chemical Company. The plant growth regulators tested were commercial samples; each was recrystallized from an appropriate solvent before use and was found to have the correct melting point.

Results.—Physiological effects of α-hydroxysulfonates on whole leaves: The first indication that inhibitors of glycolic oxidase influence water relations was the observation that wilted leaves recover more quickly when a solution of an α-hydroxysulfonate was supplied through the base of sunlit tobacco leaves. These visible effects on turgidity were easily confirmed by measurements of the increase in weight of treated leaves. When the method for determining stomatal openings became available, it was possible to investigate the effect of α-hydroxysulfonates on stomatal behavior directly (Table 1).

Although most of the water vapor which diffuses from the plant moves through the stomatal apertures because they offer the path of least resistance, there is still a difference of opinion concerning the absolute relationship between stomatal opening and rate of transpiration.[4] From the water budget calculated from the experiments in Table 1, however, under conditions favorable for the opening of closed stomata in tobacco leaves, α-hydroxysulfonates supplied through the base of the leaf inhibited stomatal opening in turgid leaves with a concomitant reduction in transpiration of 25 to 60%. Treated leaves gained in fresh weight and became turgid more rapidly than control leaves. In experiments of 30 min duration, the amount of fluid taken up by an excised leaf was approximately the same whether it was placed in water or α-hydroxysulfonate solution. The stomata in treated leaves did not open as much, and such leaves transpired significantly less water. The action of α-hydroxysulfonates in closing stomata in whole leaves was exerted within 30 min, an observation which is reminiscent of the time scale of glycolic acid accumulation in intact leaves under similar conditions.[2, 3] It should be pointed out, however, that in Table 1 sodium hydroxymethanesulfonate appears to be more effective in reducing transpiration than the pyridine analogue. This is the reverse of the order of the relative reactivity of these two compounds in bringing about the accumulation of glycolic acid in sunlight in whole leaves,[2, 3] an observation which suggests that the guard cells are more responsive to chemical control

than is the mechanism which results in glycolic acid synthesis in the tissues of the whole leaf.

These results clearly demonstrated the feasibility of effectively reducing transpiration by artificially induced stomatal closure in bright sunlight, and stimulated a further investigation of this phenomenon.

Control of Stomatal Opening in Leaf Disks.—Effect of light: The disk technique provided a convenient method of obtaining uniform samples of leaf tissue for studying stomatal opening. When disks from leaves previously kept in the dark for 1 hr in order to close the stomata were floated on water and exposed to 4,000 ft-c of light, the stomata opened fully in about 90 min as shown in Figure 2. For this reason a 90-min period was used routinely in the standard stomatal assay When leaf disks with opened stomata were returned to darkness, the stomata closed within 30 min, and when brought into the light for a second time they opened again at the initial rate.

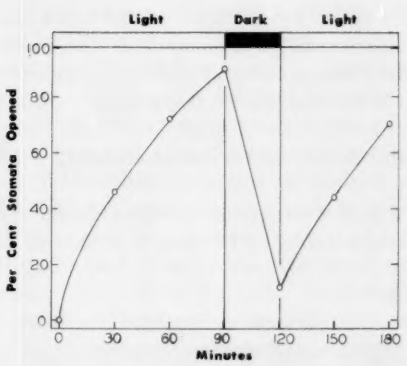

FIG. 2.—Effect of time and light on stomatal opening of tobacco leaf disks. Disks were floated on water under the conditions of the standard assay. During the dark period, the beakers containing the disks were covered with aluminum foil.

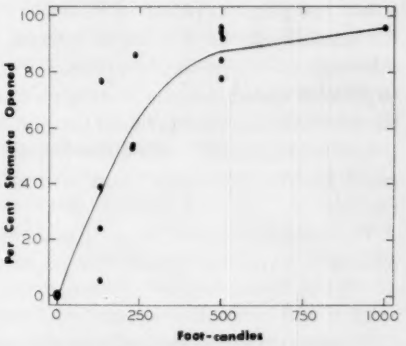

FIG. 3.—Effect of light intensity on stomatal opening of tobacco leaf disks. The various light intensities were obtained by covering the beakers used in the standard assay with various thicknesses of glass cloth. Each point at the same light intensity represents a different experiment with disks cut from another leaf. The results are expressed as percentages of similar observations on control disks kept at 4,000 ft-c.

Under the conditions of the standard assay, the stomata of leaf disks on water remained opened for many hours when provided with continuous light. In one such experiment, after 1.5 hr, 93% of the stomata were found opened; after 3 hr, 85%; after 5 hr, 81%; and after 10 hr, 85%.

The necessity for light in order for the stomata of tobacco leaf disks floating on water to open is striking, and attempts were therefore made to estimate the light intensity required to bring about stomatal opening under the conditions of the standard assay (Fig. 3). At light intensities of about 140 ft-c, leaf disks from different leaves varied in their response. In all experiments, the stomata were opened more than 50% at a light intensity of 250 ft-c, and at 500 ft-c almost maximal opening was achieved. The light intensities required to open stomata in

tobacco leaf disks are accordingly considerably lower than those necessary to obtain maximal rates of CO_2 assimilation in intact leaves.[7]

Disks half in light and half in darkness: I have also studied stomatal opening in tobacco leaf disks which were floated on water under the standard assay conditions except that one-half of each disk was completely shaded from the light from above and below with a light-shield constructed of two thin stainless steel plates. In one such experiment, disks completely in the dark had 0% stomata open at the end of 90 min; disks all in the light had 74% open; disks half in light and half in dark had 85 and 0% of the stomata open in the respective parts. Moreover, it was determined that within a distance of 1 mm from the line separating light from dark on the same disk receiving both treatments simultaneously, the stomata were either completely opened or closed.

Chemical control of stomatal opening in leaf disks: In light, under conditions otherwise favorable for the opening of stomata, a number of compounds were found to prevent closed stomata in tobacco leaf disks from opening (Table 2). In general, the effective compounds found thus far can be divided into several groups: certain α-hydroxysulfonates, which are known to be inhibitors of glycolic oxidase; some plant growth regulators; and several metabolically active metal-chelating compounds.

The results in Table 2 show that there is a great difference in the effect of stomatal closure in leaf disks by α-hydroxysulfonates depending on the length of the carbon

TABLE 2

EFFECTIVENESS OF VARIOUS COMPOUNDS ON STOMATAL CLOSURE OF TOBACCO LEAF DISKS

Compound	Per Cent Stomata Closed* 0.01 *M*	0.0033 *M*	0.001 *M*	0.0001 *M*
Sodium bisulfite	A	A	C	..
Na hydroxymethanesulfonate	C	..	D	..
Na acetoxymethanesulfonate	C	..	D	..
Na α-hydroxyethanesulfonate	C	..	..	..
Disodium sulfoglycolate	D	..	..	..
Na α-hydroxyhexanesulfonate	..	D	D	..
Na α-hydroxyoctanesulfonate	..	A	D	..
Na α-hydroxydecanesulfonate	..	A	A	D
Na α-hydroxyhexadecanesulfonate	..	..	D	..
Na α-hydroxyoctadecanesulfonate	..	..	D	..
Na α-hydroxy-2,4-dichlorobenzenemethanesulfonate	..	..	A	D
α-hydroxy-2-pyridinemethanesulfonic acid	..	A	B	D
α-hydroxy-3-pyridinemethanesulfonic acid	..	..	C	D
α-hydroxy-4-pyridinemethanesulfonic acid	..	..	D	D
Glycolic acid	C	..	..	..
Na 2,4-dichlorophenoxyacetate	..	A	B	D
Indole-3-acetic acid	D	..	..	..
Na 1-naphthaleneacetate	..	..	A	D
β-naphthoxyacetic acid	..	..	A	D
Phenoxyacetic acid	..	..	C	..
Methoxyacetic acid	C	..	..	..
2,4-Dinitrophenol			..	D
Sodium cyanide			C	D
8-Hydroxyquinoline sulfate			A	D
Na dimethyldithiocarbamate			D	D
Disodium ethylenediamine tetraacetate			D	D
Sodium azide			A	D

* A represents 100 to 76% stomatal closure, B is 75 to 51% closure, C is 50 to 26% closure, and D is 25 to 0% closure.

The compounds tested were supplied to tobacco leaf disks as described under *Methods* for the standard assay of stomatal closure.

chain. Of the various straight chain homologues of α-hydroxysulfonates tested, the most effective appeared to be the decanesulfonate.

Among the three substituted pyridine homologues examined, the relative order of decreasing effectiveness is substitution in the 2-, the 3-, and the 4-positions. This latter relationship is similar to unpublished results obtained earlier in this laboratory in experiments carried out on the accumulation of glycolic acid by detached leaves in sunlight.[2, 3] When 5×10^{-3} *M* solutions of each of the α-hydroxysulfonic acid derivatives indicated were supplied through the base of tobacco leaves, the glycolic acid found per gm of leaf at the end of 1 hr was 6.6 μmoles with the 2-, 1.4 μmoles with the 3-, and 1.1 μmoles with the 4-substituted derivative, respectively. Thus in this series, the effectiveness in stomatal closure is in the same order as the ability to block the glycolic oxidase reaction *in vivo*.

There are several reports in the literature on the effect of plant growth regulators on the closing of stomata. Ferri and Levy[8] have indicated that spraying an aqueous solution of β-naphthoxyacetic acid at a concentration of 1.5×10^{-3} *M* on nasturtium leaves, or using this solution to water the soil of potted plants, brought about stomatal closure and reduced transpiration as compared with control plants. Bradbury and Ennis[9] reported that dipping kidney bean leaves in solutions of 2,4-dichlorophenoxyacetate at concentrations ranging from 4×10^{-5} *M* to 4×10^{-3} *M* gave progressively increasing stomatal closure. As shown in Table 2, both of these growth regulators brought about large reductions in stomatal apertures in the standard tobacco leaf disk assay at approximately the same concentrations described by these workers. Naphthaleneacetate was also effective, but indole-3-acetic acid and phenoxyacetic acid were completely ineffective in this assay.

Some commonly used metabolic inhibitors, such as 2,4-dinitrophenol and cyanide, did not influence stomatal closure in the leaf disk assay, while the fungicide and metal-chelating compound 8-hydroxyquinoline sulfate, and the respiratory inhibitor sodium azide were highly effective, preventing stomatal opening at concentrations of 1×10^{-3} *M*.

The adequate reproducibility of the standard leaf disk assay, and its ability to discriminate between inhibitors of stomatal opening is illustrated in greater detail in Figure 4. From such dosage-response curves, it is clear that sodium azide will close 50% of the stomata in disks at a concentration of about 2×10^{-4} *M*, while α-hydroxy-2-pyridinemethanesulfonic acid brings about 50% closure at a concentration of approximately 1×10^{-3} *M*. The slopes of the dosage-response curves for these two compounds are evidently different, thus suggesting that they influence stomatal closure by interfering with different biochemical mechanisms, as might be expected. By comparison, as shown in Figure 4, about 0.68 *M* sucrose is required to prevent the opening of half of the stomata. These results indicate that the osmotic pressure in the guard cells, which is responsible for the increase in water in these cells during stomatal opening, must be approximately 15.2 atmospheres. The molar concentration of sucrose required is thus 680 times as high as the equally effective concentration of α-hydroxy-2-pyridinemethanesulfonic acid and 3,400 times greater than that of sodium azide under the same conditions.

Chemical control of closure of opened stomata: Since a number of the compounds tested could effectively prevent the opening of stomata in leaf disks under standard conditions, it became of interest to determine whether an active compound could

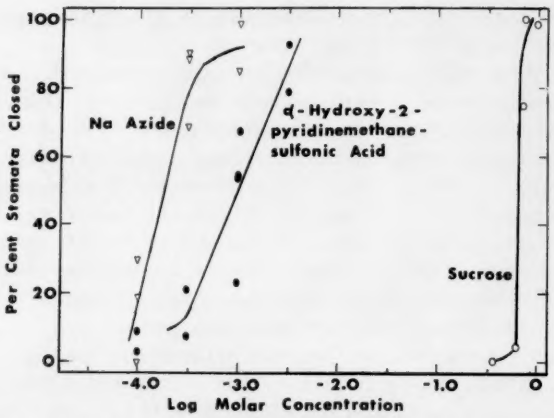

FIG. 4.—Effect of different concentrations of sodium azide, α-hydroxy-2-pyridinemethanesulfonic acid, and sucrose on stomatal closure of tobacco leaf disks. Each replicate point shown at a given concentration represents a different experiment with disks from separate leaves. The data were obtained under the conditions of the standard assay.

also close already opened stomata under environmental conditions otherwise favorable for them to remain open. The experiments shown in Table 3 clearly demonstrate that α-hydroxy-2-pyridinemethanesulfonic acid at a concentration which largely prevents stomatal opening (Fig. 4) also rapidly caused opened stomata to close.

Effect of stomatal closure on transpiration and photosynthesis in whole leaves: In previous experiments with $C^{14}O_2$ in which α-hydroxysulfonates were supplied through the base of the leaf in sunlight, CO_2 assimilation was inhibited about 33%.[3] Similar reductions in photosynthesis have now been observed in experiments in which a CO_2 gas analyzer was used. Such inhibitions probably arise from metabolic effects of these compounds on mesophyll cells and are unrelated to the effect of α-hydroxysulfonates on stomatal closure.

In order to test this view, I have attempted to close stomata by spraying α-hydroxysulfonates on both surfaces of leaves. Under these conditions the guard cells in the epidermis might be more readily influenced than the mesophyll tissue. Results are shown in Table 4. It is clear that completely reproducible stomatal

TABLE 3

CLOSURE OF OPENED STOMATA IN LEAF DISKS

Treatment	Per cent stomata open	Stomata closed as percentage of water control
Experiment 1		
90 min water	99	..
90 min water; 90 min water	82	..
90 min water; 60 min A*	12	86
90 min water; 90 min A*	4	95
Experiment 2		
90 min water; 90 min water	96	..
90 min water; 90 min A*	44	54

* A is 0.001 *M* α-hydroxy-2-pyridinemethanesulfonic acid.

The experiments were carried out under the conditions described in the text for the standard assay with tobacco leaf disks. In some treatments, after the usual 90 min, the disks were blotted and returned for another period as indicated in either water or α-hydroxysulfonate solution.

TABLE 4

EFFECT OF α-HYDROXYSULFONATE SPRAY ON STOMATAL APERTURES, TRANSPIRATION RATE, AND PHOTOSYNTHETIC RATE OF DETACHED TOBACCO LEAVES

Expt. no.	Initial wt of leaf, gm	Fluid sprayed	Mean width of stomata in upper surface at end, μ	Transpiration rate, μmoles H_2O per gm of leaf per hr	Photosynthetic rate, μmoles CO_2 per gm of leaf per hr	Ratio transpiration: photosynthesis
1	11.94	water	4.7	8,670	172	50
	11.87	0.0033 *M* A*	3.9	6,890	168	41
2	10.60	water	3.6	8,610	164	53
	9.33	0.0033 *M* A*	5.0	9,330	186	50
3	12.04	water	3.0	6,940	148	47
	11.50	0.001 *M* B*	2.3	5,510	172	32
4	12.22	water	2.9	5,610	189	30
	10.97	0.0033 *M* B*	1.1	1,110	181	6
5	11.23	water	1.0	8,390	173	49
	14.80	0.001 *M* A*	1.2	5,830	173	34

* Compound A is α-hydroxy-2-pyridinemethanesulfonic acid and compound B is sodium α-hydroxydecanesulfonate.

Adjacent tobacco leaves from the same plant were kept with their bases in water in the dark for 1 hr to insure closure of the stomata before the start of each experiment. Each leaf was then weighed, and a fine mist of the solution indicated was sprayed on both surfaces. The excess liquid was shaken off, and the base of the leaf was then placed in a small previously weighed beaker containing water. The experiments were conducted in a glass chamber, volume 15.5 liters, maintained at about 28° with high relative humidity, and illuminated with approximately 7,000 ft-c provided by 300-watt photoflood lamps immersed in a running water bath.[10] Normal air was always available to the leaf, and for one 5-min period out of every 15 min, an airtight glass cover was placed on the chamber. The air was continuously sampled with the aid of a circulating pump and passed through a Beckman infrared CO_2 analyzer fitted with a recorder, from which the rate of carbon assimilation was determined. At the end of the experiment, 60 min, except for Experiment 5 which lasted 90 min, the leaf and beaker were again weighed to determine the rate of transpiration, and silicone rubber impressions were simultaneously taken of the upper and lower surfaces of the central portion of the lamina in order to determine the stomatal opening.

closure cannot yet be attained by the procedure used with the compounds tested. However, in 3 of the 4 experiments of 60 min duration, significantly more of the stomata of the upper surface of the leaf were closed at the end in treated leaves than in control leaves (Experiments 1, 3, and 4). In these same experiments, stomatal apertures in the lower surfaces of all leaves were unaffected, and the water lost by transpiration in treated leaves was diminished by 20, 20, and 80%, respectively. In spite of the reduction in water loss, there was no significant reduction in CO_2 assimilation, so that the ratio of transpiration to photosynthesis was also lowered. In Experiment 2, there was an 8% increase in transpiration in the treated leaf, but the photosynthetic rate was also higher so that the ratio of transpiration to photosynthesis remained unchanged.

Experiment 5, Table 4, proceeded for 90 min, and although at the end of this period the stomata were "closed" in both the treated and control leaves, the photosynthetic rates were high, being about 20 times as great as the anticipated rate of oxygen uptake in darkness by the same tissue.[3] The treated leaf transpired 30% less water. The rates of CO_2 assimilation in both leaves were approximately equal during the entire 90-min period, and were constant after the first 15 min. Even at high light intensities, the rate of diffusion of CO_2 through the stomatal aperture clearly does not limit the rate of CO_2 assimilation.

Although the ideal α-hydroxysulfonate, or the optimal conditions for supplying it to leaves in order to obtain efficient and specific stomatal closure are still uncertain, the data in Table 4 demonstrate that at high light intensities it should be possible to reduce water loss of leaves without interfering seriously with their CO_2 uptake.

Discussion.—Heath[5] has recently pointed out that although more than a century has elapsed since the first investigation on the mechanism of the opening and closing

of leaf stomata was conducted, the only certainty is that, at least in many species, this process is controlled by the turgor differences between the guard cells and adjacent cells. Now that a simple standard system for controlling and measuring the opening of stomata in leaf disks is available, it should be easier to define more clearly the biochemical events responsible for these rapid turgor changes in the stomatal apparatus.

In the tissue studied here, the requirement for light and the rapidity of its action in bringing about stomatal opening have been most impressive (Figs. 2 and 3). From the results obtained with disks divided into segments receiving either a light or a dark treatment, it must be concluded that whatever may be the substance produced under the influence of light and which changes the turgidity of the guard cell, this substance must be generated either within or closely adjacent to the guard cell it affects.

There appear to be a number of possible ways in which metabolic regulators can influence stomatal closure in the light and bring about the closure normally observed only in the dark or during wilting. The induction of some alternative pathway of carbon metabolism could inhibit the formation of a solute essential for the increased turgidity of the guard cells. The effect of α-hydroxysulfonates in rapidly altering the products formed in photosynthesis in whole leaves,[3] suggests that these compounds operate in this way. The reactions by which chloroplasts in light produce adenosine triphosphate,[11] a substance essential for carbohydrate synthesis, may also be influenced. The effect of light in stimulating stomatal opening could be brought about directly or indirectly by this photosynthetic phosphorylation, and any method of interfering with the synthesis of adenosine triphosphate near the guard cells or of stimulating its breakdown might then cause stomatal closure. Darkness would of course also accomplish this result. The varied kinds of metabolic regulators (Table 2) which close stomata in leaf disks suggest that there are many biochemical approaches available for investigating the mechanism responsible for control of turgidity in the guard cells. This view is supported by the differing slopes in the dosage-response curves of compounds which would be expected to influence stomatal closure by affecting different biochemical pathways (Fig. 4).

With use of the present leaf disk assay, it should be possible to find even more effective compounds that could be applied to plants to control stomatal opening. In addition to the experiments in Table 4, which support the feasibility of reducing transpiration without affecting photosynthesis, the experiments of Moss *et al.*[12] on photosynthesis in corn plants under field conditions are relevant. These workers found that raising the concentration of CO_2 in the atmosphere around the plants diminished the stomatal apertures of corn leaves. At a CO_2 concentration of 575 ppm, for example, compared with plants at 310 ppm of CO_2, they observed a reduction in transpiration of 23% with a concomitant increase in CO_2 assimilation of 36%.

The CO_2 taken up in photosynthesis, in addition to passing through the stomatal aperture, must also diffuse through an aqueous phase of the mesophyll cell wall before it can react. As pointed out by Hill and Whittingham,[13] stomatal diffusion must therefore represent a much greater proportion of the total diffusion path in the case of transpiration, and stomatal control might be expected to result in a greater decrease of loss of water vapor than CO_2 uptake.

The possibility of conserving water normally lost through plant leaves by biochemically reducing stomatal apertures does not seem to have been considered seriously. The rapidity with which many compounds close stomata in leaf disks suggests that practical methods should be sought under which equally efficient control of stomatal apertures can be achieved under field conditions.

Summary.—The effect of α-hydroxysulfonates, inhibitors of glycolic oxidase, supplied to detached tobacco leaves in sunlight in markedly reducing the water lost by transpiration by stomatal closure is reported. This study was aided by a new technique for measuring stomatal apertures without altering the leaf environment by means of silicone rubber impressions made of the leaf surface. A standard assay for measuring the extent of stomatal closure by compounds supplied to tobacco leaf disks in the light is described. With this leaf disk assay, a number of metabolic regulators, including α-hydroxysulfonates, plant growth regulators, and metal-chelating compounds have been found to prevent stomatal opening at concentrations of about 1×10^{-3} M. One of the α-hydroxysulfonates has also been shown to close already opened stomata.

Evidence is presented that by inducing stomatal closure in intact leaves, it is possible to reduce water lost by transpiration at high light intensities without diminishing photosynthetic CO_2 assimilation. These studies offer a new approach to the conservation of water through the biochemical control of leaf stomata.

Grateful acknowledgment is made to Hubert B. Vickery for helpful discussion, to Dale N. Moss for cooperation in use of the CO_2 gas analyzer, and to Maria Borsanyi for skilful technical assistance.

* This investigation was supported in part by a grant from the National Science Foundation and was also aided by a Fellowship from the John Simon Guggenheim Memorial Foundation at the University of Oxford.

[1] Zelitch, I., *J. Biol. Chem.*, **224**, 251 (1957).

[2] *Ibid.*, **233**, 1299 (1958).

[3] *Ibid.*, **234**, 3077 (1959).

[4] Kramer, P. J., in *Plant Physiology*, ed. F. C. Steward (New York and London: Academic Press, 1959), vol. 2, p. 607.

[5] Heath, O. V. S., *ibid.*, p. 193.

[6] Lauer, W. M., and C. M. Langkammerer, *J. Am. Chem. Soc.*, **57**, 2360 (1935).

[7] Burnside, C. A., and R. H. Böhning, *Plant Physiol.*, **32**, 61 (1957).

[8] Ferri, M. G., and A. Levy, *Contrib. Boyce Thompson Inst.*, **15**, 283 (1948).

[9] Bradbury, D., and W. B. Ennis, Jr., *Am. J. Bot.*, **39**, 324 (1952).

[10] Rawlins, S., and D. N. Moss, *Agron. J.*, submitted for publication.

[11] Arnon, D. I., M. B. Allen, and F. R. Whatley, *Biochim. et Biophys. Acta*, **20**, 449 (1956).

[12] Moss, D. N., R. B. Musgrave, and E. R. Lemon, *Crop Science*, **1**, 83 (1961).

[13] Hill, R., and C. P. Whittingham, *Photosynthesis* (London and New York: Methuen and Co. and John Wiley and Sons, 1956), p. 12.

THE PROTON IRRADIATION OF METHANE, AMMONIA, AND WATER AT 77°K

By Rainer Berger

CONVAIR SCIENTIFIC RESEARCH DEPARTMENT, SAN DIEGO

Communicated by Harold C. Urey, July 14, 1961

It has been shown by Miller[1] that significant amounts of organic compounds such as amino acids could have been formed on the primitive earth by electric discharges passing through gas mixtures. The question arises as to whether the synthesis of organic material could have occurred even before the earth existed, and furthermore, if organic molecules are presently being synthesized in space on comets, icy meteors, and perhaps interstellar dust. Lederberg has pointed out that this is probable.[2] The production of the lower hydrocarbons from methane using electrons as a source of energy has been demonstrated by Glasel.[3] It was of interest to see if more complex organic compounds could be synthesized in frozen mixtures of gases using Whipple's comet model.[4] Papazian had suggested the bombardment of water, methane, and ammonia at 77°K with electrons.[5] For this experiment protons were chosen to supply the energy, because 85 per cent of cosmic radiation is composed of these particles.[6]

Experimental.—As a model environment, a glass irradiation chamber was constructed which admitted radiation through an aluminum window. The reactants could be condensed on a cold finger in the path of the incident radiation. The chamber had provisions for connection to a high vacuum system allowing the transfer of reactants and products.

The target mixture contained 721 mg of methane, 768 mg of ammonia, and 800 mg of water. Protons with an energy of 12 Mev at a flux rate of 0.5 μA/sec were obtained from the 60-inch cyclotron of the Crocker Laboratory of the University of California at Berkeley. The irradiation time was 200 sec at 77°K.

The methane used was Phillips research grade which was analyzed by a mass spectrometer and found to contain 99.53% of methane, 0.28% nitrogen, 0.08% carbon dioxide, 0.05% propane, 0.05% ethane, and 0.01% *n*-butane. The ammonia was Matheson anhydrous grade which was purified by condensation at 77°K and subsequent fractionation. The water used was triple distilled. A blank without irradiation gave no products.

After the bombardment the volatile compounds of the reaction mixture were collected in a flask. All nonvolatile substance was dissolved in 10 ml of distilled water. Within the next 24 hrs the radioactivity of the solution had decayed to less than 10 mr/hr. Both the volatile and aqueous fractions were analyzed by gas chromatography in a Perkin-Elmer 154 Vapor Fractometer. Besides a number of very small peaks, only one major unknown peak was observed. Comparison of the unknown with a sample of known acetone indicated the presence of acetone in both the volatile and aqueous fractions. In order to ensure the identity of acetone sufficiently, analyses were carried out using two different adsorbants, Carbowax 1500 and polyoxyethylene sorbitan monostearate. The retention time of acetone was 2.6 min utilizing a 2 inch-long Carbowax 1500 column at 64°, 20 lb of helium pressure, and 8 V of detector voltage. In the case of a 2 in. long poly-

oxyethylene sorbitan monostearate column at 44°, 20 lb of helium pressure and 8 V detector voltage the retention time was 1.9 min. The total amount of acetone produced was 9 mg as calculated by peak height analysis. This corresponds to a yield of approximately 1% on methane.

After concentration of the solution, the total weight of solids was determined to be 1.1 mg. The following structures were excluded by the appropriate spot tests; amino acids, certain amines, indoles, imidazoles, guanidines, and sugars.[7] Ultraviolet absorption at 260 mμ suggested purine or pyrimidine compounds which was supported by positive tests with bromophenol-blue/silver nitrate and mercuric nitrate reagents. However, extensive ultraviolet spectrophotometry, ultraviolet absorption photography,[8] and infrared measurements were inconclusive—indicating that these compounds were either absent or present in amounts below the limit of detectability.

The Ehrlich reagent gave a bright yellow spot suggesting ureides. In addition, fluorescence in the ultraviolet at 360 mμ and a positive bromophenol-blue/silver nitrate test[9] pointed to a conjugated —NH—CO— system. Chromatography in 86% *n*-butanol/14% water (v/v) showed that both the unknown and a sample of known urea run alongside had an R_f value of 0.32. Similarly, in 100% ethanol the R_f value was 0.28.

Infrared spectrography of an eluted urea spot did not give the correct spectrum for urea. Rather, the spectra of eluted sections of an evenly divided chromatogram strip run in 100% ethanol were those of acetamide (maxima at 3,200, 1,670, 1,380, and 1,140 cm^{-1}). By blanketing the infrared absorption of acetamide present in the urea sample with that of acetamide, the correct spectrum for urea was obtained (maxima at 3,350, 1,610, 1,450, and 1,140 cm^{-1}). In another sample of unknown, urea was hydrolyzed by the enzyme urease which confirmed the presence of urea again since this enzyme reacts only with urea.[10] The remaining substance was treated with xanthydrol which yielded the correct derivative of acetamide, N-xanthydryl acetamide, whose mixed melting point was not depressed at 238–241°.[11]

The over-all utilization of carbon was about 1.1% and the energy yield G was 1.39 molecules formed per 100 electron volt.

Discussion.—It has been demonstrated experimentally that urea, acetamide, and acetone are obtained by radiation synthesis under conditions likely to be encountered in space. The number of proton impacts per cm^2 in the experiment approaches the order of magnitude of those sustained by a comet of the age of the solar system.[12]

Hydrolysis of urea yields ammonia and carbon dioxide which may possibly be a source of the carbon dioxide observed in the spectra of comets. This implies that the reducing atmosphere of the primitive earth may have contained significant amounts of carbon dioxide. Urea is known to form clathrates with straight-chain hydrocarbons which would tend to stabilize such hydrocarbons against the influence of radiation and might prevent isomerization into branched chains.

Acetamide when hydrolyzed will yield acetic acid and ammonia. Acetic acid has long been recognized as an important intermediate in biogenetic processes.

In the photochemical decomposition of acetone a whole variety of compounds have been observed such as carbon monoxide, ketene, and ketones (e.g. $CH_3COCOCH_3$, $CH_3COCH_2CH_3$, $CH_3COCH_2CH_2COCH_3$, and $CH_3COCHCOCH_3$).[13]

Carbon monoxide, which is found on comets may possibly be derived in part from the radical decomposition of acetone. An observation that acetone and water will yield reducing sugars on prolonged exposure to intense sunlight[14] needs confirmation as well as a report on the occurrence of different hydrates of acetone.[15] One of these hydrates of acetone with a composition of $C_3H_6O \cdot 17\ H_2O$ has been shown to exist by Quist and Frank only recently.[16] The formation of hydrates of small organic molecules in space is of considerable astronomical interest and has been discussed by Miller.[17]

The author wishes to express his appreciation to H. C. Urey and S. L. Miller for many invaluable discussions and to B. Jones and the crew of the Crocker Laboratory for their kind assistance.

[1] Miller, S. L., *Science*, **117**, 528 (1953); Miller, S. L., *J. Am. Chem. Soc.*, **77**, 2351 (1955); Miller, S. L., *Biochim. et Biophys. Acta*, **23**, 480 (1957).

[2] Lederberg, J., in *Science in Space* (New York: McGraw-Hill Book Co., 1961), chap. 9.

[3] Glasel, J. A., these PROCEEDINGS, **47**, 174 (1961).

[4] Whipple, F. L., *Astrophys. J.*, **111**, No. 2 (1950).

[5] Papazian, H. A., (private communication).

[6] Simpson, J. A., in *Science in Space* (New York; McGraw-Hill Book Co., 1961), chap. 9.

[7] Feigl, F., *Spot Tests in Organic Analysis* (Princeton, New Jersey: Elsevier Pub. Co., 1956); Smith, I., *Chromatographic Techniques* (New York: Interscience, 1960); Block, R. J., E. L. Durrum, and G. Zweig, in *Paper Chromatography* (New York: Academic Press, 1958).

[8] Markham, R., and J. D. Smith, *Biochem. J.*, **45**, 294 (1949).

[9] Trofimenko, S., and J. W. Sease, *Anal. Chem.*, **30**, 1432 (1958).

[10] Sumner, J. B., *The Enzymes* (New York: Academic Press, 1951), p. 886.

[11] Phillips, R. F., and B. M. Pitt, *J. Am. Chem. Soc.*, **65**, 1355 (1943).

[12] The author is indebted to Professor H. C. Urey for suggesting this comparison.

[13] Noyes, W. A., and L. M. Dorfman, *J. Chem. Phys.*, **16**, 788 (1948).

[14] Dhar, N. R., and R. P. Sanyal, *J. Phys. Chem.*, **29**, 928 (1925).

[15] Varenne, E., and L. Godefroy, *C.R. Acad. Sci. (Paris)*, **138**, 991 (1904).

[16] Quist, A. S., and Frank, H. S., *J. Phys. Chem.*, **65**, 5601 (1961).

[17] Miller, S. L. (to be published).

---

*THE STAGE OF THE GENOME-PLASMON INTERACTION IN THE RESTORATION OF FERTILITY TO CYTOPLASMICALLY POLLEN-STERILE MAIZE**

BY JANSON G. BUCHERT†

THE CONNECTICUT AGRICULTURAL EXPERIMENT STATION, NEW HAVEN

Communicated by Donald F. Jones, July 28, 1961

The expression of various characters in many organisms is known to depend upon genome-plasmon interactions, but information on the time and location of these interactions is meager. In phenomena such as the killer trait in *Paramecium*,[1] the production of a normal cytochrome system in *Saccharomyces*,[2] the modified slow-growth (*poky*) character in *Neurospora*,[3] and certain phenomena described by Michaelis,[4] the interaction appears to be continuous; however, in many other cases the interaction possibly takes place in only certain tissues (or cells) and at only certain stages during the development of the organism. In view of the great

deal of work which has been done in the area of developmental genetics, time and place of interaction could be important factors in development. That time and location of a genome-plasmon interaction could also influence the heredity of nuclear genes would not be so readily anticipated. Time and place of such an interaction, their effect upon pollen development, and their effect upon the inheritance pattern of a chromosome segment have revealed themselves during a study of the restoration of fertility to cytoplasmically induced pollen-sterile maize.

In the process of combining a sterility-inducing plasmon and its restorer(s) (chromogenes capable of restoring fertility to plants with this plasmon) with various inbred nuclear genotypes during the course of seven years (1950–1956) at the Connecticut Agricultural Experiment Station, there occasionally appeared backcross progenies which contained all fertile plants. These progenies resulted from crosses which, according to Mendelian segregation, should have given rise to segregating families, for the male parents were theoretically heterozygous for a restorer gene(s). In view of the fact that the progenies of hundreds of similar crosses were grown during this period, that only from ten to eighteen representatives of an individual progeny were grown, and that many different genic ratios are possible, it was thought that these nonsegregating rows represented extreme variations due to chance, or were the expression of a complex genic system.[5] The writer's attention was called to the problem by H. T. Stinson when in 1956 a few progenies, all with similar genic material, had only fertile plants where segregation was expected. A pedigree search involving all relatives of all the nonsegregating cultures since 1949 was undertaken by the writer. When the search was completed and all the crosses and their resulting progenies were organized in pedigree fashion, it immediately became evident that many of the families with this behavior could be placed into one group. The pedigree of the progenies of the group displayed a somewhat consistent behavior pattern, and all entries fell into place fairly well. The study of this group revealed the phenomena presented below.

Table 1 shows the relationship and observations of some of the families in the group. The families have been listed according to the year grown, and in generation sequence. Specific families have been given numbers (in parentheses) so that they can be identified in subsequent crosses. The first entry listed reveals the source of restoration. Since [*ms*$_2$]A158 (see Table 1 for key) is sterile, the seven fertile segregates in the progeny must have resulted from the action of a gene(s) introduced by Ky21. When one of these fertile plants was backcrossed to the sterile line, instead of segregation, only fertile plants were recorded. While it is conceivable that some sterile plants were present but not recorded, the behavior of subsequent generations makes this unlikely.

All subsequent generations seem to follow the same pattern. Whenever an [*ms*$_2$]-sterile was pollinated by a plant of the type [*ms*$_2$]Rf heterozygous for the restorer(s), only fertile plants resulted. The one sterile plant in the progeny of [*ms*]A73^4 × [*ms*$_2$]RfA158^4(5), which appears to be an exception, could have been due to any one of a number of nonpertinent factors, and shall be tentatively disregarded. Likewise when selfed, such heterozygous plants produced only fertile progeny; that is, except the progeny of [*ms*$_2$]RfA158^4(5) selfed. One of the three sterile plants in this culture was definitely "off type," indicating that it was an outcross. Since outcrosses usually do not occur singly, the other two may have

TABLE 1

STEPS IN THE CONVERSION OF A158 TO ITS RESTORED-STERILE COUNTERPART, AND OBSERVATIONS OF THE FAMILIES*

	Family no.	No. of ears	Year grown	Observations
[ms_2]A158^4 × (Ky21 × A158)	(1)	2	1951	7+, 5−
[ms_2]A158^5 × [ms_2]RfA158^1(1)	(2)	1	1952	MAP
[ms_2]A158^6 × [ms_2]RfA158^2(2)	(3)	3	1953	MAP about normal
[ms_2]A158^7 × [ms_2]RfA158^3(3)	(4)	?	1954	All MAP
			1957	All 29+
[ms_2]RfA158^3(3) × [ms^+]A158	(5)	3	1957	23+, 4−
			1958	21+, 17−
[ms_2]RfA158^4(4) × [ms_2]RfA158^4(5)	(6)	1	1955	All 19+
[ms_2]RfA158^4(5) selfed		3	1955	17+, 3−?
[ms_2]RfA158^4(5) × [ms^+]A158	(7)	3	1955	11+, 5−
			1957	30+, 24−
[ms_2]A73^4 × [ms_2]RfA158^4(4)	..	1	1955	+
[ms_2]A73^4 × [ms_2]RfA158^4(5)	..	3	1955	Remainder +, 1−
[ms_2]A374^4 × [ms_2]RfA158^4(4)	..	3	1955	All +
[ms_2]A374^4 × [ms_2]RfA158^4(5)	..	4	1955	All +
[ms_2]M14D^7 × [ms_2]RfA158^4(4)	..	?	1955	All +
[ms_2]M14D^7 × [ms_2]RfA158^4(5)	(8)	1	1955	All +
[ms_2]RfA158^4-S$_1$(6) selfed	(9)	1	1956	All +
			1957	All 35+
[ms_2]RfA158^4-S$_1$(6) selfed	(10)	1	1956	All +
			1957	All 42+
[ms_2]RfA158^5(7) selfed	(11)	1	1956	All +
			1957	All 68+

* Crosses and observations made prior to 1957 were made by D. F. Jones. MAP = many anthers extruded, pollen; + = fertile; − = sterile; [ms^+] = normal plasmatype; [ms_2] = sterility-inducing plasmatype (sometimes referred to as "S"); Rf (not italicized) = restorers present but genotype not known; Ky21, A158, A73, A374, and M14D = residual genotypes (inbreds). (Superscripts designate the number of backcrosses to the inbred.)

had that origin also. When heterozygous restored-sterile plants were pollinated by the inbred ("reciprocal" cross), however, the two families segregated.

These data suggested the operation of a type of male gametophytic selection which insures fertilization by pollen grains carrying the restoring allele(s). To investigate this problem further, samples of remnant seed of the previously grown families were planted again in 1957. Observations of these samples (Table 1) were similar to those made by D. F. Jones. Many plants in each culture were used in making one or two of the three types of "crosses": [ms_2] × [ms_2]Rf, [ms_2]Rf × [ms^+]A158, and [ms_2]Rf selfed. Portions of the tassels of many plants were taken and preserved for later analysis.

Offspring of the crosses made the previous year were planted and observed in 1958. Whenever an [ms_2]RfA158 plant (heterozygous for the restorer(s)) was used as a male, no segregation occurred; while in crosses where these were not used as the male segregation always resulted. The presence of an equal number ($P = 1.0$ and 0.9–0.8) of fertiles and steriles in the segregating families clearly demonstrates that the difference between the steriles and fertiles in these progenies was brought about by a single gene (Rf^2) introduced by Ky21. As determined by microscopic examination of anther contents, the amount of normal pollen produced by randomly chosen plants which were theoretically heterozygous for the restorer was about 50% of that produced by the normal counterpart ([ms^+]A158) on the same day.

It appears, then, that all the pollen grains bringing about fertilization had the restorer. Consequently the inheritance pattern can be explained by assuming that

only pollen grains with Rf^2 function, while those with the alternate allele (rf^2) abort. The hypothesis was tested as follows: (1) Anthers from plants in families resulting from a self-pollinated plant of the type [ms_2]Rf^2rf^2A158 were checked for degree of normal-pollen production. It was found that half of the plants in such families produced pollen 50% of which was aborted, while about an equal number (P = 0.3–0.2) of plants exhibited no such abortion of pollen. This is to be expected if each viable pollen grain of the parent carried Rf^2 and only half the egg nuclei contained the restoring allele. The plants in these "F_2" families exhibiting no abortion would, therefore, be Rf^2Rf^2, while those with 50% abortion would be the heterozygous offspring. (2) When these "F_2" plants with about normal pollen production were used as females in crosses with [ms^+]A158 the progenies contained only fertile plants; in contrast, when the segregates with 50% pollen abortion were used in similar crosses with [ms^+]A158, the progenies gave a 1:1 sterile-to-fertile ratio. This would also be expected if indeed the plants with no abortion were Rf^2Rf^2, and those with the excess abortion were heterozygous for the restorer.

These observations seem to establish firmly the idea expressed in the foregoing hypothesis.

Apparently, then, the mechanism of selection is the interaction of the [ms_2] plasmagene and the Rf^2 chromogene: the abortion is due to the presence of the [ms_2] factor, and the normal pollen grains produced by plants carrying [ms_2] are not aborted because of a type of epistatic effect of Rf^2 upon [ms_2]. To test this further, Rf^2 was combined with two other types of cytoplasm: [ms_1], another type of sterility-inducing plasmon; and [ms^+]. Plants heterozygous for the restorer gene with these types of plasmon exhibited no selection for Rf^2.

Since the restoration process takes place only in those spores with Rf^2, it can be concluded that there is no way for a sufficient amount of the essential product of the restoring gene to get into the cytoplasm of the spores which abort. This condition could only result if the critical restoring action takes place at a place and time when the cytoplasms of the different spores are separated by a barrier to the transfusion of the essential substance. Such circumstances only exist in the microspore or maturing pollen grain, i.e., after the formation of the crosswalls during microsporogenesis, the onset of the gametophytic generation. Further, also the critical time of production of the primary diffusible gene product must occur after the barrier is formed. This is because all other conditions necessary for the completion of the restoration process exist in both types of spores, for the residual genotype is the same in each spore.

Knowing the approximate time of critical restoring action helps to establish also the time when the critical step in the abortion mechanism occurs in [ms_2]-steriles. Several steps must precede this critical stage: among them, the synthesis of the primary diffusible chromogene product; and the more direct restoration process. Since the critical times for these two steps occur after microsporogenesis, the critical stage determining the abortion must occur only a short time before the deterioration can be seen, i.e., in the early stages of spore maturation.

The type of nuclear-cytoplasmic interaction, and consequently the inheritance pattern and degree of pollen abortion, encountered with the [ms_2] plasmatype is different than that encountered with the [ms_1] type (sometimes referred to as "T"). Plants with [ms_1] which are heterozygous for the restorers may produce as

much pollen as their normal counterparts,[5] and the restorers (Rf_1[1] and Rf_2[1]) segregate (by progeny observation) normally.[6, 7]

* This paper is a part of a dissertation presented for the degree of Doctor of Philosophy at Yale University.

† Present address: Eastern States Farmers Exchange, West Springfield, Massachusetts.

[1] Beale, G. H., *The Genetics of Paramecium aurelia* (Cambridge University Press, 1954).

[2] Ephrussi, B., *Nucleo-cytoplasmic Relations in Microörganisms* (Oxford: Clarendon Press, 1953).

[3] Mitchell, M. B., and H. K. Mitchell, *J. Gen. Microbiol.*, **14**, 84–89 (1956).

[4] Michaelis, P., *Adv. in Genetics*, **6**, 288–401 (1954).

[5] Jones, D. F., H. T. Stinson, and U. Khoo, *Connecticut Agr. Expt. Sta. Bull.* 610 (1957).

[6] Jones, D. F., *Genetics*, **36**, 557 (1951).

[7] Duvick, D. N., *ibid.*, **41**, 544–565 (1956).

---

*ENZYME COMPLEMENTATION IN MIXED EXTRACTS OF MUTANTS FROM THE SALMONELLA HISTIDINE B LOCUS**

By John C. Loper

DEPARTMENT OF BIOLOGY, THE JOHNS HOPKINS UNIVERSITY†

Communicated by Herman M. Kalckar, July 7, 1961

Imidazoleglycerol phosphate dehydrase, the enzyme in the pathway of histidine biosynthesis (see Table 1) which converts imidazoleglycerol phosphate (IGP) to

TABLE 1

TERMINAL STEPS IN HISTIDINE BIOSYNTHESIS

	Reaction	Related *Salmonella* gene
(1)	IGP $\xrightarrow{\text{IGP dehydrase}^3}$ IAP + H_2O	*his B*
(2)	IAP + L-glutamate $\xrightleftarrow{\text{IAP transaminase}^4}$ HLP + α-ketoglutarate	*his C*
(3)	HLP + H_2O $\xrightarrow{\text{HLP phosphatase}^5}$ Histidinol + PO_4	
(4)	Histidinol + 2DPN$^+$ + H_2O $\xrightarrow{\text{Histidinol dehydrogenase}^6}$ Histidine + 2DPNH + $2H^+$	*his D*

These reactions, based upon observations in *Neurospora*, in *E. coli*, and in yeast, also occur in *Salmonella*.[1] Genetic[2, 8] and biochemical studies[1] have correlated 3 of the reactions with the genes indicated; no specific gene was correlated with reaction (3). Abbreviations used are: IGP (imidazoleglycerol phosphate); IAP (imidazoleacetol phosphate); HLP (histidinol phosphate), DPN and DPNH (diphosphopyridine nucleotide and reduced diphosphopyridine nucleotide, respectively).

imidazoleacetol phosphate (IAP), has been correlated with the *his B* genetic locus in *Salmonella typhimurium*.[1] This locus is complex in that tests by abortive transduction have indicated four subgroups with the capacity for genetic complementation.[2] This paper reports that complementation also occurs between cell extracts, i.e., that dehydrase activity appears in mixtures of extracts from appropriate dehydraseless *his B* mutants. Biochemical and immunochemical data thus far obtained indicate that this complementation is effected through interaction of protein components. The capacity, or lack of the capacity, of *his B* mutants to yield IGP dehydrase activity in extract mixtures correlates well with the genetic com-

plementation pattern, and in turn suggests that protein interaction may be the mechanism for genetic complementation at this locus.

Also reported here are observations suggesting that the *his B* locus governs the enzyme histidinol phosphate phosphatase (HLP phosphatase, reaction (3), Table 1), as well as IGP dehydrase.

Materials.—N-α-formyl-L-histidine, L-histidinol phosphate (HLP), imidazoleglycerol phosphate (IGP), and imidazoleacetol phosphate (IAP) were provided by Bruce N. Ames. Formylhistidine was also synthesized by the procedure of Fischer and Cone.[9] Additional IGP was synthesized according to Ames,[3] using a modification he had suggested (personal communication). Natural IGP was obtained by extraction from the culture media of a *his B* mutant. Solutions of IGP were standardized on the basis of the extinction coefficient for imidazoleformaldehyde, obtained upon periodate oxidation of IGP.[3] Natural or synthetic IGP could be used interchangeably in enzyme assays.

Bacterial strains and nomenclature: The wild type and mutant stocks of *S. typhimurium*, strains LT-2 and LT-7, employed in this study have been described in detail.[8] In addition, *his-705*, which originated spontaneously from strain LT-2 containing phase 1 H antigen suppressor, was provided by B. A. D. Stocker. The complementation pattern of individual *B* mutants is indicated by use of lower case letters *a*, *b*, *c*, and *d* in their genetic designation. Mutants failing to complement by abortive transduction with other mutants of more than one complementation unit are indicated by multiple letters. Thus mutant *Bcd-102* can form abortive colonies in transduction crosses with *Ba* and *Bb* mutants, but does not with other *Bc* or *Bd* mutants. Mutant *Babcd-29* shows no complementation by abortive transduction with any *B* mutant. Mutants *Ba(bc)-12*, *-14*, and *-24* are *Ba* mutants which only weakly complement *Bb* and *Bc*. The parentheses indicate this "position effect."[2] The genetic characterizations of mutants *-425*, *-429*, *-448*, and *-705*, previously unpublished, were established in Hartman's laboratory.

Methods.—Cell culture and harvest conditions: Stocks were maintained on Bacto-Nutrient Agar slants at 4°. Growth incubations were all performed at 37°, with aeration. Mutants were routinely inoculated into nutrient broth bubbler tubes, cultured approximately 12 hours and then sub-inoculated into the E medium of Vogel and Bonner[10] made 2.0×10^{-2} *M* with respect to glycerol and 1.0×10^{-4} *M* with respect to L-histidine. These preparations were incubated for 12 to 18 hours, and a 1/100 dilution was then made into similar E-glycerol medium made 3.0×10^{-5} *M* with respect to formylhistidine.[1] These final cultures, varying in volumes from 100 ml to several liters in some cases, were grown for 18 to 19 hours with vigorous aeration. Cells were harvested by Sharples or Lourdes continuous-flow centrifugation, or by centrifugation in bottles. Assays of cell titer and percentage prototrophs at the time of harvesting were determined by optical density, and by serial dilution and plating upon nutrient and minimal agar plates. Cells were generally washed once with 0.85% saline and were suspended in a standard buffer of 1.0×10^{-1} *M* triethanolamine-HCl (TEA-HCl), pH 7.5, made 1.0×10^{-2} *M* with respect to 2-mercaptoethanol (MET) and 1.0×10^{-3} *M* with respect to ethylenediamine-tetraacetate (EDTA). They were then frozen and stored at −60° until used.

Preparation of cell extracts: Suspensions of approximately 3×10^{11} cells/ml were disrupted in the standard buffer in a Raytheon 10-kc oscillator. Small volumes were contained in Lourdes 6 DT tubes or in collodion-treated lusteroid tubes held in water during sonication; volumes of 6 to 20 ml were added directly to the oscillator cup. Varying times of sonication at 0.9 to 1.0 amperes were employed. Disrupted suspensions were subsequently centrifuged at 21,000 *g* for 10 min, and the lighter portion of the pellet obtained was resuspended and centrifuged an additional 10 min at 26,000 *g*. Supernatant fluids were then combined and dialyzed or subjected to other purification steps. Dialysis of 2 to 10 ml portions of the supernatant fluids was performed against the standard buffer for 4 hours at 4°. Two or three changes of 300 to 1000 ml of buffer were used for the dialysis, depending on the volume of extract. All preparations were stored at −60°.

Assays: Protein concentrations were determined by the method of Lowry *et al.*[11] using amorphous insulin (Lot W-3255, Eli Lilly and Co.) as a standard. Interference in determinations caused by the buffer was circumvented by adding a constant amount of buffer in all assays. Spectrophotometric assays of IGP dehydrase and HLP phosphatase were performed as described by Ames

et al.[1] The former assay is based upon the absorption of the product, IAP, in alkali. In the latter, an ascorbic-molybdate mixture is used to determine the PO_4 liberated. In each case, one unit of enzyme is that amount which catalyzes the formation of one micromole of reaction product per hour under defined conditions. The addition of sodium arsenate (5.2×10^{-3} *M*) to the dehydrase assay buffer retarded undesirable IGP and IAP phosphatase activity with no apparent effect upon the dehydrase reaction. Qualitative assays for the presence or absence of IGP dehydrase activity in mixtures of *B* mutant extracts were accomplished by paper chromatography of reaction products using a solvent of *n*-propanol-1 *N* acetic acid (3:1). IAP and imidazoleacetol (*IA*) were identified on the basis of their Rf, color after sulfanilic acid diazotization, and their reduction of copper sulfate.[12]

Immunochemical procedures: As reported by Ames and Garry,[13] mutant cells grown on formylhistidine in the manner described are relatively free of histidine repression. Wild type levels of histidine biosynthetic enzymes are characteristically the same when cells are grown with or without formylhistidine. The same enzymes in mutant cultures are elevated from 10- to more than 30-fold the wild type level. The advantage of this phenomenon was applied in obtaining preparations of enzyme antigen for the immunization of rabbits. Extracts of derepressed *his C-86*, obtained as described, were purified an additional 5-fold with respect to both IGP dehydrase and HLP phosphatase by protamine, streptomycin, and ammonium sulfate fractionations. The resulting solutions had, for both enzymes, specific activities of greater than 300-fold the levels characteristic of crude extracts of wild type bacteria. These preparations were administered to rabbits intramuscularly over a 2-month period[14] according to the procedure of Cohn.[15]

Immune sera were cross-absorbed with protein extracts from the nonreverting mutant, *his B-22*. Precipitin reactions were studied by mixing varying proportions of antigen and antiserum in 0.9 per cent saline. The mixtures were centrifuged after incubating from 6 to 24 hrs at 4° and precipitates were suspended in the standard buffer. Both these and the supernatant solutions were assayed for both enzyme activities and compared with assays from parallel tubes using nonimmune serum. Agar gel diffusion experiments were conducted according to Ouchterlony.[16]

Results.—Activities of dehydrase in B mutants: Derepressed, dehydrase-deficient mutants contain less than 20 per cent of wild type dehydrase activity. This low level of dehydrase in mutant extracts is less than 1 per cent of the high level observed in other histidineless mutants following relief of repression.

Extracts were prepared from 38 mutants genetically characterized as *his B*. All were shown to be lacking dehydrase by the chromatographic assay, a procedure which readily demonstrates activity in extracts of wild type cells. Spectrophotometric examination of extracts of 17 mutants showed that all were completely deficient in dehydrase activity within the limits of the assay method (less than 1 per cent of the elevated level just described).

HLP phosphatase activities among B mutants: During the purification of IGP dehydrase, HLP phosphatase activity showed a tendency to accompany the dehydrase enzyme. The *B* mutants were accordingly surveyed for HLP phosphatase activity as well. Results are shown in Table 2. In all mutants genetically determined as *Bc*, and in all multiple-unit mutants involving the *Bc* unit, the HLP phosphatase activity is approximately at the level of the wild type activity, or is lower. In contrast, significantly elevated levels of HLP phosphatese were observed in mutants of the *Ba*, *Bb* and *Bd* complementation units. These specific activities are generally 10- to 100-fold higher than for *Bc* mutants.

Included in the category of *B* mutants low or deficient in HLP phosphatase are the three *Ba*(*bc*) mutants showing a genetic position effect extending over *Bb* and *Bc*.

Dehydrase complementation in extract: General surveys for dehydrase complementation between mutants were made by preparing a number of dialyzed extracts

TABLE 2

LEVELS OF HISTIDINOL PHOSPHATE PHOSPHATASE IN EXTRACTS OF *his* B MUTANTS

Mutant number	Genetic designation	Per cent prototrophs	HLP phosphatase u/mg
Wild type	+	100.	0.75
86	*C*	0.23	18.9
20	*Ba*	...	10.6
79	*Ba*	3.8	8.7
12	*Ba[bc]*	<0.1	0.3
14	*Ba[bc]*	<0.001	0.15
24	*Ba[bc]*	<0.001	0.4
53	*Bb*	<0.1	14.7
61	*Bb*	<0.001	8.5
206	*Bb*	<0.001	7.5
56	*Bc*	leaky	1.1
59	*Bc*	<0.001	0.8
116	*Bc*	0.48	0.01
136	*Bc*	0.1	1.5
167	*Bc*	<0.001	0.5
429	*Bc[abd]*	6.0	1.4
40	*Bd*	0.01	13.6
47	*Bd*	<0.001	7.0
65	*Bd[abc]*	...	12.0
143	*Bd*	<0.001	6.6
213	*Bd*	2.8	7.4
217	*Bd*	0.1	9.9
229	*Bd*	0.8	19.3
238	*Bd*	0.5	11.5
241	*Bd*	0.3	8.5
257	*Bd*	<0.001	8.3
289	*Bd*	4.0	23.6
102	*Bcd*	2.0	0.5
234	*Bbcd*	0.4	0.8
118	*Babc(d)*	<0.01	0.5
243	*Babc(d)*	1.2	1.2
21	*Babcd*	...	0.5
22	*Babcd*	0.01	0.06
29	*Babcd*	<0.002	0.2
138	*Babcd*	<0.001	0.9
262	*Babcd*	<0.002	1.3
425	*Babcd*	<0.01	0.7
448	*HBabc(d)*	0.05	0.04
705	*Babcd*	<0.001	0.8
57	*EFAHBCDG*	<0.01	0.01

at protein concentrations of 15 to 30 mg/ml. Equal volumes were mixed in small tubes, diluted 1:1 with the assay buffer and preincubated 20 minutes at 37°. Aliquots were then incubated for 30 minutes or longer at 37° in the same assay mixture made 5.2×10^{-3} *M* with respect to arsenate and 4.4×10^{3} *M* with respect to IGP. After incubation, aliquots were chromatographed and assayed for IAP and IA as described. Appearance of these compounds was taken as evidence of functional dehydrase complementation. The extracts were also run singly as controls.

The results of such surveys are presented in Table 3. Entries of 0 indicate a lack of detectable dehydrase activity; complementation is indicated by a +. The table has been supplemented in two instances by information not checked by chromatography but obtained spectrophotometrically. These complementations, *his-79* (×) *-47* and *his-61* (×) *-47*, are indicated by (+) in the table. The symbol * (combination *his-143* (×) *-206*) represents one case in which no activity was detected chromatographically although earlier spectrophotometric evidence for complementation exists. Three questionably positive complementations, not resolved under the conditions used, are identified by question marks.

TABLE 3

DEHYDRASE COMPLEMENTATION IN MIXED EXTRACTS OF DEHYDRASELESS MUTANTS

Mutant number	Genetic designation	Assayed singly															
20	*Ba*	0	*20*														
79	*Ba*	0	0	*79*													
12	*Ba*[*bc*]	0	0	0	*12*												
14	*Ba*[*bc*]	0				*14*											
24	*Ba*[*bc*]	0					*24*										
53	*Bb*	0	+	+	0	0	*53*										
61	*Bb*	0	+	+				*61*									
206	*Bb*	0	+	+	0		0	0	*206*								
59	*Bc*	0					0			*59*							
116	*Bc*	0	0	0	0		0		0		*116*						
167	*Bc*	0	0	0				0	0		0	*167*					
429	*Bc*	0	0										*429*				
40	*Bd*	0	+	+	0		+		+		0			*40*			
47	*Bd*	0	+	[+]			+	[+]	?						*47*		
65	*Bd*	0	0	0	0		+	+	+		0	0	0	0		*65*	
143	*Bd*	0	0	0	0		0		*								
213	*Bd*	0	+				+										
217	*Bd*	0	+				+										
229	*Bd*	0	+			0	+										
238	*Bd*	0	+				+										
241	*Bd*	0	?				+										
257	*Bd*	0	?				+										
289	*Bd*	0	+				+							0			
102	*Bcd*	0	0						0					0			
234	*Bbcd*	0	0						0					0			
118	*Babc*[*d*]	0	0						0					0			
243	*Babc*[*d*]	0					0										
21	*Babcd*	0															
22	*Babcd*	0	0		0				0							0	
29	*Babcd*	0	0														
138	*Babcd*	0															
262	*Babcd*	0					0							0			
425	*Babcd*	0	0											0			
448	*HBabc*[*d*]	0	0														
705	*Babcd*	0	0													0	
57	*EFAHBCDG*	0	0						0								

Dialyzed extracts of mutants were combined in pairs in assay buffer and incubated at 37° in the presence of 4.4×10^{-3} *M* imidazoleglycerol phosphate. A "+" indicates chromatographic evidence of imidazoleacetol phosphate (IAP) formation; a "0" indicates no evidence of IAP formation. Other symbols and additional details are described in the text.

In no case examined does a mutant complement in extract with another of the same complementation unit as determined by genetic tests. This is true, for example, of *Ba* (×) *Ba* mixtures and also of representative *Ba* (×) *Babcd* mixtures.

Only mutants possessing elevated HLP phosphatase activity have successfully complemented in extract. Moreover, this capacity is present for mutants of all three complementation units where the HLP phosphatase activity is characteristically high. Both *Ba* mutants complement with any of the three *Bb* mutants. *Ba-20* or *Bb-53* have been shown to complement in extract with a majority of the *Bd* mutants. In contrast to the *in vivo* experiments, no mutant genetically involving the *Bc* complementation unit has been shown to complement in extracts. The failure to complement in mixtures appears characteristic of multiple-complementation unit mutants which involve *Bc* as well as for specific *Bc* mutants.

Efforts at the purification and characterization of these complementing components have just begun, but preliminary data give some indication as to their nature.[14] The capacity to complement in extract appears to be nondialyzable. Dialyzed extracts were routinely used in complementation survey experiments,

and representative complementing and noncomplementing mutants showed the same pattern if the dialysis step was omitted. Extracts of representative *Ba*, *Bb*, and *Bd* mutants are heat labile. Preheating of either extract for a few minutes at 100° prevents the appearance of dehydrase activity upon mixing with a normally complementing, unheated extract. Extracts thus far examined have been shown also to maintain their capacity to complement after removal of nucleic acid with streptomycin and after pH and ammonium sulfate fractionation. Studies of a representative *Ba* (×) *Bb* mixture indicate that a few minutes preincubation in the presence of $MnCl_2$ and mercaptoethanol, at concentrations which activate wild type enzyme, results in a higher restored activity.[14]

Immunochemical studies: It should be noted that the preparations used to elicit antibody formation contained both IGP dehydrase and HLP phosphatase at comparably elevated specific activities. The antisera obtained in this procedure react to affect to an equal extent both enzyme activities. Over a wide range of ratios of enzyme units to 1 ml of antiserum, the antiserum partially inactivates and partially precipitates in an active form both enzymes in a parallel manner. Data from a typical experiment are shown in Table 4. A mutant *C-86* extract prepara-

TABLE 4

EFFECT OF DEHYDRASE-HLP PHOSPHATASE ANTISERUM UPON DEHYDRASE AND HLP PHOSPHATASE ENZYME ACTIVITIES

Nonimmune serum	Dehydrase	HLP phosphatase
Supernatant fraction (no. ppt. as formed)	73.4	100.
Antiserum	(Values in nonimmune serum as 100%)	
Supernatant fraction	6.6	c.4.0
Precipitate	45.0	44.3
Per cent inactivation due to antibody treatment	48.4	51.7

tion containing both enzyme activities was incubated in tubes containing either antiserum or nonimmune serum. The nonimmune serum contained the same concentration of *his B-22* protein used for absorption of the antisera. Tubes were centrifuged after 6 hours incubation at 4°, and both precipitates and supernatant solutions were assayed. The per cent recoveries in nonimmune serum control tubes are given. Results of enzyme recovery after antibody treatment are expressed as per cent of enzyme activity remaining in the nonimmune serum control. HLP phosphatase activity in the antiserum supernatant fraction is given as an approximation due to the high blank involved.

A survey of mutants for the quantitative demonstration of cross-reacting material (CRM) was made difficult by this partial inactivation characteristic. Ouchterlony's diffusion technique was therefore utilized in qualitative examinations of mutant extracts for the presence of CRM. Aliquots of crude dialyzed protein solutions of from 15 to 30 mg/ml were placed in the outer wells surrounding a well containing cross-absorbed antiserum. Nonimmune serum was added to one well in the series as a standard control against nonspecific precipitation. *His B-22* protein, the absorbing antigen preparation, was similarly employed.

Typical results are depicted in Figure 1. Several faint precipitation bands occur between the antiserum and most of the antigen-containing wells, including well number 3 containing *his B-22* protein. These bands indicate that the antiserum is not monospecific. In addition to these bands, a single strong reaction band

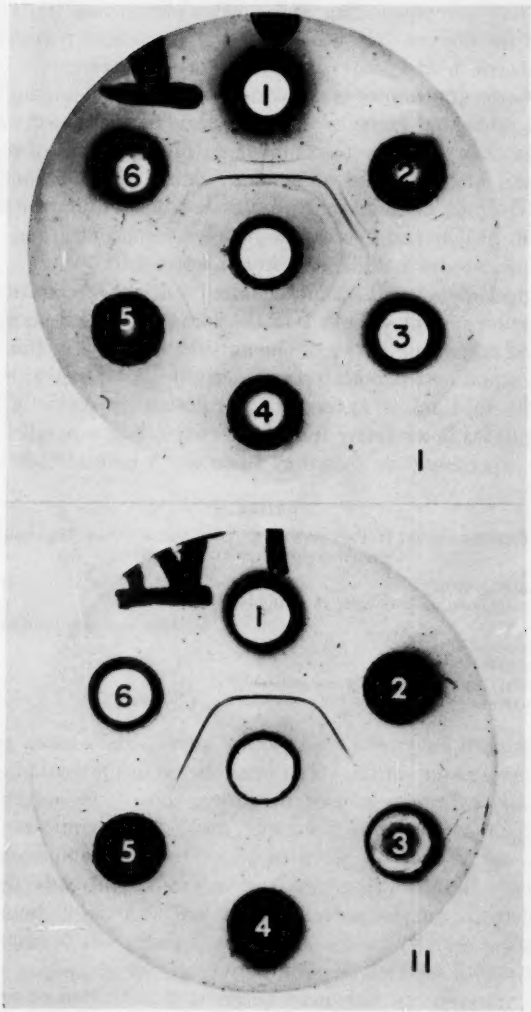

FIG. 1.—Antiserum absorbed with *his Babcd-22* was added to the center well of each plate. Mutant extracts were added to the surrounding wells as indicated in the tabulation below. *C-86* extract contained active IGP dehydrase and HLP phosphatase; extract of the stable mutant *Babcd-22* lacks both of these activities. (Multisite mutant *Babcd-22* appears to be a genetic deletion of the entire *B* locus).

Gel	Well Number					
Number	1	2	3	4	5	6
I	*C-86*	Ba-79	Babcd-22	Bcd-102	Bc-116	Bd-143
II	*C-86*	Bb-53	Babcd-22	Ba(bc)-12	Bcd-102	Bd-217

appears between the center well and well number 1 to which was added a preparation containing dehydrase and HLP phosphatase activity. No evidence of this band

can be seen opposite well number 3. This same reaction band can also be distinguished among the several bands obtained when testing unabsorbed antisera. Several of the mutants tested gave precipitation bands which coalesced with this major enzyme-antibody band. A summary of these findings, including other diffusion gels not photographed, is found in Table 5.

TABLE 5

RESULTS OF IMMUNOLOGICAL AGAR DIFFUSION TESTS OF *his B* MUTANTS

Mutant number	Genetic designation	Coalescing precipitation band	Mutant number	Genetic designation	Coalescing precipitation band
86	*C*	+	*213*	*Bd*	+
20	*Ba*	+	*217*	*Bd*	+
79	*Ba*	+	*229*	*Bd*	+
12	*Ba(bc)*	−	*238*	*Bd*	+
24	*Ba(bc)*	−	*289*	*Bd*	+
53	*Bb*	+	*102*	*Bcd*	−
61	*Bb*	+	*234*	*Bbcd*	−
206	*Bb*	+	*118*	*Babc(d)*	−
116	*Bc*	−	*22*	*Babcd*	−
167	*Bc*	−	*29*	*Babcd*	−
429	*Bc(abd)*	−	*138*	*Babcd*	−
40	*Bd*	+	*448*	*HBabc(d)*	−
47	*Bd*	+	*705*	*Babcd*	−
65	*Bd(abc)*	+	*57*	*EFAHBCDG*	−
143	*Bd*	−	nonimmune serum		−

Antiserum used affected both IGP dehydrase and HLP phosphatase activities. A "+" or "−" indicates presence or absence of the coalescing precipitation band. See test for details.

Discussion.—The lack of dehydrase activity in individual *B* mutants, characteristic patterns for dehydrase complementation, and the restriction of elevated HLP phosphatase activity to mutants not involving *Bc* correlate with the genetic classification of the mutants. The only differences from the genetic data (see Fig. 2 in ref. 2) thus far are in the capacities for complementation in extract between *Bb-53* and *Ba* mutants, and between *Bb* mutants and *Bd-65*, capacities not expected to be so efficient in view of these two mutants' position effects.[2] Also, mutant *-289*, originally designated *Babcd*, appears to be *Bd* by abortive transduction tests performed as a recheck following demonstration of its enzyme capacities in cell extracts (Hartman, personal communication).

The conclusion that IGP is converted to IAP in a single enzymatic step is derived from several lines of evidence. Immunological and fractionation studies indicate the presence of a single protein species.[14, 13] Secondly, genetic data indicate the existence of a number of *B* mutants which give no abortive colonies over 2, 3, or 4 complementation units but which appear by recombination data to be mutant at single sites located in different parts of the *B* gene.[2, 8] In all cases where these mutants were tested for complementation in mixed extracts with potentially complementing *Ba*, *Bb*, or *Bd* preparations, no dehydrase activity was restored. Furthermore, no compounds other than IGP and IAP, and their dephosphorylated derivatives, were detected in reaction mixtures, nor did IGP disappear in any tests where IAP failed to accumulate.

An increasing number of examples of genetic complementation among mutants lacking a specific enzymatic activity are being reported (see ref. 17). Woodward has described adenylosuccinase complementation *in vitro* using either crude extracts[13] or partially purified protein components from *Neurospora* mutants.[19]

The work of Yanofsky and co-workers[20] on *Escherichia coli* tryptophan synthetase provides a precedent for such enzyme protein studies in bacteria. In that system, complementation results from interaction of two separable and distinct protein components.

Highly purified preparations of the complementing components for IGP dehydrase have not been obtained. However, in view of the nondialyzable nature of these components, their heat lability, and their other features as mentioned above, they too are believed to be protein or polypeptide units. The similarity of patterns among mutants for both genetic complementation[2] and complementation in extract suggests that both phenomena may occur through interaction of these protein components.

One mechanism for this interaction would attribute complementation to a reassortment of distinct polypeptide enzyme subunits, corresponding to *Ba*, *Bb*, *Bd*, and a *Bc* "matrix" polypeptide unit. This possibility cannot be eliminated by present data, but the assumptions required for its application to available data are numerous and complex. A more attractive scheme ascribes complementation to the cooperation of total intact molecules elicited by the entire *B* locus. Thus the active dehydrase enzyme, following complementation interactions, is viewed as a polymer of altered protein molecules structurally similar to the wild type. Each type of the basic unit is synthesized under the control of a single functional *B* locus in each of two different mutant chromosomes. Indeed, the active normal wild-type enzyme may itself be a polymer, comprised of identical units. The sedimentation behavior of normal IGP dehydrase has been studied recently using sucrose gradient centrifugation.[21] The enzyme aggregates to form a more rapidly sedimenting component in the presence of divalent cations, or in the presence of mercaptoethanol. These factors, which enhance complementation in extract mixtures, are known to activate the normal dehydrase enzyme.[1] Mutations leading to alterations of the *Bc* portion of the enzyme protein, and perhaps at other regions, as with mutant *Bd-143*, may result in rapid denaturation of the protein upon extraction. Such behavior would account for the observation with some mutants of complementation *in vivo* and the failure to detect complementation in mixed extracts.

The indications that genetic control of HLP phosphatase may reside in the dehydrase locus are compatible with other evidence relating these two enzymes. It was seen that antiserum precipitates both enzyme activities in parallel fashion in tube reactions, and yields only one precipitation band when directed against both activities in agar diffusion tests. Comparison of Tables 2 and 5 shows that only mutants containing high HLP phosphatase activity give precipitation bands with antisera to HLP phosphatase and IGP dehydrase. In all cases, however, these same mutants are the ones showing the capacity to provide dehydrase activity by complementation in extracts (Table 3). Thus by this immunological evidence the two enzyme activities appear to reside in similar molecules. Significantly, both enzyme activities have been reported to band together by DEAE chromatography[13, 14] and by sucrose gradient centrifugation.[21] It is not known if the two enzyme activities reside in identical molecules or on separate but highly similar molecules, and a number of biochemical and physical comparisons have not yet been accomplished.

As a unifying hypothesis, it is suggested that the *his B* locus in *Salmonella* does control the formation of a bifunctional protein, capable of both IGP dehydrase and HLP phosphatase activities. This protein would be active as HLP phosphatase under certain conditions, and in a different state of polymerization would be capable of dehydrase activity. Regardless of the relevancy of these speculations, further investigations concerning dehydrase mutant proteins and the complementation process should give an increased understanding of enzyme structure and function.

Summary.—Thirty-eight mutants of the genetically complex *his B* locus, grown under conditions which derepress the formation of histidine synthetic enzymes, were examined for IGP dehydrase and HLP phosphatase. All were deficient in the former enzyme, but only mutants involving the *Bc* genetic complementation unit failed to exhibit elevated HLP phosphatase activity in extract. Extracts of mutants genetically classified in any of the other three complementation units, not involving *Bc*, have elevated HLP phosphatase. When cell extracts representing any two of these three complementation units were mixed, IGP dehydrase activity could generally be observed, although this enzyme activity was missing in the unmixed extracts.

Imidazoleglycerol phosphate dehydration is apparently catalyzed by a single enzyme; the phenomenon of enzyme complementation in extract mixtures seems to be the result of interaction of structurally similar protein molecules formed under control of the mutant genes. Immunochemical studies of mutant extracts using IGP dehydrase and HLP phosphatase antisera support this scheme. Indications are that both IGP dehydrase and HLP phosphatase activities are controlled by the single *his B* locus, and reside in quite similar protein molecules.

The author is indebted to Philip E. Hartman for his guidance throughout this problem, and special gratitude is extended to Bruce N. Ames for his helpful suggestions.

* Work reported here was supported by Grants E-1650 and 2G-57 of the National Institute of Allergy and Infectious Diseases, U. S. Public Health Service.

† Present address, Department of Pharmacology, St. Louis University School of Medicine, St. Louis 4, Missouri.

[1] Ames, B. N., B. Garry, and L. A. Herzenberg, *J. Gen. Microbiol.*, **22**, 369 (1960).

[2] Hartman, P. E., Z. Hartman, and D. Šerman, *ibid.*, 354 (1960).

[3] Ames, B. N., *J. Biol. Chem.*, **228**, 131 (1957).

[4] Ames, B. N., and B. L. Horecker, *J. Biol. Chem.*, **220**, 113 (1956).

[5] Ames, B. N., *J. Biol. Chem.*, **226**, 583 (1957).

[6] Adams, E., *J. Biol. Chem.*, **217**, 325 (1955).

[7] Hartman, P. E., in *Genetic Studies with Bacteria*, Pub. 612 (1956) of the Carnegie Institution of Washington, D. C., p. 35.

[8] Hartman, P. E., J. C. Loper, and D. Šerman, *J. Gen. Microbiol.*, **22**, 323 (1960).

[9] Fischer, E., and L. H. Cone, *Ann.*, **363**, 116 (1908).

[10] Vogel, H. J., and D. M. Bonner, *J. Biol. Chem.*, **218**, 97 (1956).

[11] Lowry, O. H., N. J. Rosebrough, A. L. Farr, and R. J. Randall, *J. Biol. Chem.*, **193**, 265 (1951).

[12] Ames, B. N., and H. K. Mitchell, *J. Biol. Chem.*, **212**, 687 (1955).

[13] Ames, B. N., and B. Garry, these PROCEEDINGS, **45**, 1453 (1959).

[14] Loper, J. C., "Gene-Enzyme Relationships in Histidine Biosynthesis in *Salmonella*," Ph.D. Dissertation, The Johns Hopkins University (1960).

[15] Cohn, M., *Methods in Med. Research*, **5**, 271 (1952).

[16] Ouchterlony, O., *Acta Pathol. Microbiol. Scand.*, **32**, 231 (1953).

[17] Fincham, J. R. S., *Advances in Enzymol.*, **22**, 1 (1960).

[18] Woodward, D. O., these PROCEEDINGS, **45**, 846 (1959).
[19] Woodward, D. O., *Quart. Rev. Biol.*, **35**, 313 (1960).
[20] Yanofsky, C., *Bacteriol. Rev.*, **24**, 221 (1960).
[21] Martin, R. G., and B. N. Ames, *J. Biol. Chem.*, **236**, 1372 (1961).

DENSITY DIFFERENCES BETWEEN GENETIC MARKERS IN PNEUMOCOCCAL TRANSFORMING PRINCIPLE

BY RONALD ROLFE* AND HARRIETT EPHRUSSI-TAYLOR

GATES AND CRELLIN LABORATORIES OF CHEMISTRY,† NORMAN W. CHURCH LABORATORY OF CHEMICAL BIOLOGY, CALIFORNIA INSTITUTE OF TECHNOLOGY, PASADENA, AND LABORATOIRE DE GÉNÉTIQUE PHYSIOLOGIQUE DU C.N.R.S., GIF-SUR-YVETTE, FRANCE

Communicated by Linus Pauling, July 3, 1961

It is known that DNA carries genetic information, and it is commonly assumed that the identity and linear order of the genes are determined by the linear sequence of nucleotides in DNA. However, little is known about the detailed relationship (or "code") between the DNA and proteins of a given species. A linkage group of genes may correspond to a unique nucleotide sequence, or it is possible that a large number of different nucleotide sequences could in principle carry the same genetic information.

The DNA of a given bacterial species is restricted by some mechanism within narrow limits of nucleotide composition, relative to the observed range of compositions for the various species.[1, 2] To explain the wide differences in nucleotide composition between DNA's from species that presumably have considerable genetic information in common, codes have been proposed in which A is formally equivalent to C, and G is equivalent to T, so that the AT and GC pairs are interchangeable.[3, 4] Given such a code, mistakes in replication could lead to changes in nucleotide composition with no change in genetic information, and DNA molecules containing a given genetic marker would have a range of possible nucleotide compositions equal to that for the total DNA. Differences in nucleotide composition between molecules containing different genetic markers, and the nucleotide compositional heterogeneity of the DNA, should be consistent with the predictions of a random model for the occurrence of fluctuations in nucleotide composition around some equilibrium value.[5]

In the experiments to be described, the nucleotide compositions of DNA molecules containing specific genetic markers have been investigated, taking advantage of the fact that the buoyant density of a DNA molecule depends upon its nucleotide composition,[1, 2] and that the biological activity of transforming principle may be determined after isolation from a CsCl density gradient.

Materials and Methods.—Pneumococcal DNA containing the genetic markers streptomycin resistance (S^r), optochin resistance (Q^r), bryamycin resistance (B^r), and aminopterin resistance [$A^r(136)$] in various combinations was studied. A bacterial lysate containing about 20 μg of DNA was centrifuged in CsCl solution of density 1.70 g cm^{-3}, buffered at pH 8.5 with 0.01 M *tris*-(hydroxymethyl)-aminoethanol, and containing 0.001 M sodium versenate. After 48 hr at 35,000 rpm in the Sw39 head of the Spinco preparative ultracentrifuge, the CsCl solution was fractionated by making a small pinhole in the bottom of the lusteroid centrifuge tube and collect-

ing the effluent drops individually. The relationship between CsCl solution density and drop number was established by refractive index measurements[6] of individual drops (Fig. 1). The drops were assayed for biological activity as follows: One milliliter of a culture of receptor strain R36A, grown to maximal competence and chilled, was added to a cold test tube containing 0.01 ml of the CsCl drop to be assayed. The mixture was incubated 20 minutes at 37°C, chilled, and

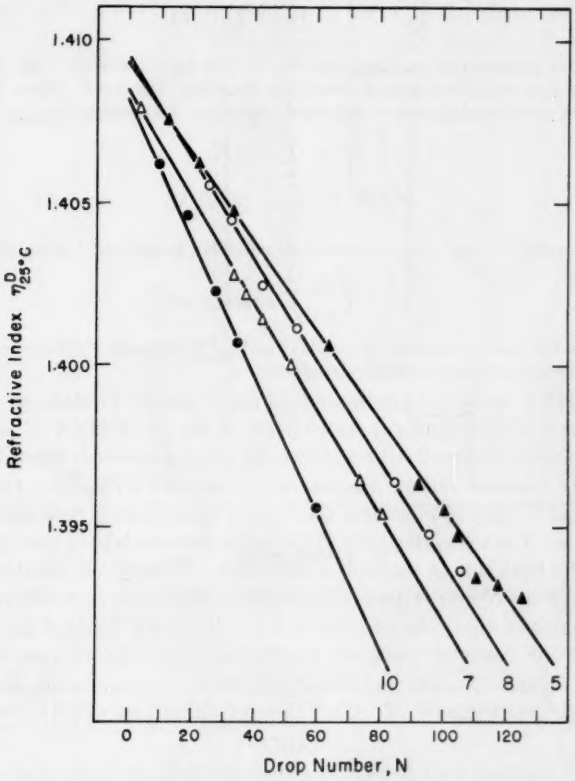

FIG. 1.—The relationship between CsCl drop number and refractive index, for the various experiments. Refractive indices for sodium D light at 25°C. $\eta_D^{25°C}$ for effluent CsCl drops are plotted against drop number. The values are correct to within an additive amount which was constant for a given experiment. Data from experiments 5, 7, 8, and 10 are presented.

plated on blood agar after appropriate dilution. The plates were incubated 2 hr at 37°C, to allow expression of phenotype, overlayered with an equal volume of antbiotic-containing agar, to select the transformants, and colonies were counted 24 to 36 hr later. Antibiotics used were dihydrostreptomycin (200 μg/ml), bryamycin[7] (1.5 μg/ml), optochin (5 μg/ml), or aminopterin (0.75×10^{-5} *M*). Reaction of the cells with the DNA is restricted to 10 min, which is the duration of competence of the receptor strain under the culture conditions used.

The number of transformants for a given marker in the assay system was proportional to the DNA concentration, in the range employed in these experiments. Ratios of numbers of transformants for the different markers found in replicate cultures were constant for a given medium and DNA preparation, and were independent of DNA concentration. However, these ratios were not completely independent of CsCl and other ion concentrations in the medium and it was

found necessary to employ a standard amount of the CsCl solution in the assay culture. Differences in CsCl concentration of the drops from opposite ends of the density gradient were insufficient to modify the transformation ratios.

Density-gradient distributions of transforming activity for the different genetic markers have been plotted according to the following expression:

$$F(N) = \mathrm{T}(N)/\sum_N T(N) \tag{1}$$

where $F(N)$ is the frequency of transformation for the Nth drop, and $T(N)$ is the absolute number of transformants for the given marker obtainable from the Nth drop. Mean drop number $\bar{N}$ and variance σ^2 were determined for each density-gradient distribution using the formulae

$$\bar{N} = \sum_N NF(N) \tag{2}$$

$$\sigma^2 = \sum_N (N - \bar{N})^2 F(N) \tag{3}$$

Variances expressed in drops^2 were converted to variances in gm^2 cm^{-6} using the relationship

$$\bar{\sigma}^2 = \left(\frac{d\rho}{dN}\right)^2 \sigma^2 \,\mathrm{gm}^2\,\mathrm{cm}^{-6} \tag{4}$$

where $d\rho/dN$ is the density gradient. In units of gm^2 cm^{-6}, variances are characteristic for a given DNA sample, independent of the density gradient.

Results.—DNA molecules containing different genetic markers occupy different portions of the density-gradient distribution of the total DNA of pneumococcus. This can be seen in Figure 2, which shows the density-gradient analysis of a sample of genetically marked DNA, simultaneously labeled with P^{32}. Comparing the distributions of P^{32} and of biological activity for streptomycin resistance, we observe that the marker S^r is associated with DNA molecules which have an average buoyant density greater than that of the bulk of the DNA. In addition, the density-gradient distributions of the S^r and B^r marked molecules differ from each other, and are considerably narrower than the distribution for the total DNA. Density-gradient distributions for pairs of unlinked genetic markers were compared in several experiments (Figs. 2–5), and significant differences in mean drop number $\bar{N}$ were detected for all pairs except (S^r, A^r). Density differences (Table 1) between pairs

TABLE 1

TABULATED PARAMETERS* FOR DENSITY-GRADIENT DISTRIBUTIONS OF GENETICALLY MARKED PNEUMOCOCCAL DNA

Expt.	$d\rho/dN$ gm cm^{-3} drop^{-1} $\times 10^3$	Marker	N_m drop number ± 0.01	$\bar{\sigma}_m^2$ gm^2 cm^{-6} $\times 10^6$	$-\Delta\rho(S^r, m)$ gm cm^{-3} $\times 10^4$: $\frac{d \log T_{S^r}/T_m}{d\rho}$	$(N_m - N_{S^r}) \times d\rho/dN$	$-\frac{d \ln T_{S^r}/T_m}{d\rho}\bar{\sigma}_m^2$
5	1.37	S^r	76.706	3.1	...	...	...
		Q^r	77.086	2.9	80	5.2	5.5
10	2.10	S^r	42.818	3.1	...	...	...
		Q^r	42.994	3.3	57	3.8	4.2
		A^r	42.809	3.1	57	4.0	4.2
8	1.54	S^r	70.866	3.7	...	...	...
		B^r	71.512	4.7	123	10	10.6
		P^{32}	71.906	5.5	...	...	...
7	1.63	S^r	58.153	7.2	...	...	...
		B^r	58.905	6.3	141	12.2	22

* The following are tabulated: $d\rho/dN$ gm m^{-3} drop^{-1}: the gradient of CsCl-solution density ρ with drop number N; $\bar{N}_m$: mean drop number for the distribution of biological activity for the genetic marker m; $\bar{\sigma}_m^2$ gm^2 cm^{-6}: variance of the distribution of biological activity for the marker m; T_{S^r}/T_m (N): ratio of the number of transformants for the marker S^r to the number of transformants for the marker m obtainable from the Nth drop; $\Delta\rho(S^r, m)$ gm cm^{-3}: the difference in mean buoyant density between DNA molecules containing the marker m and those containing the marker S^r.

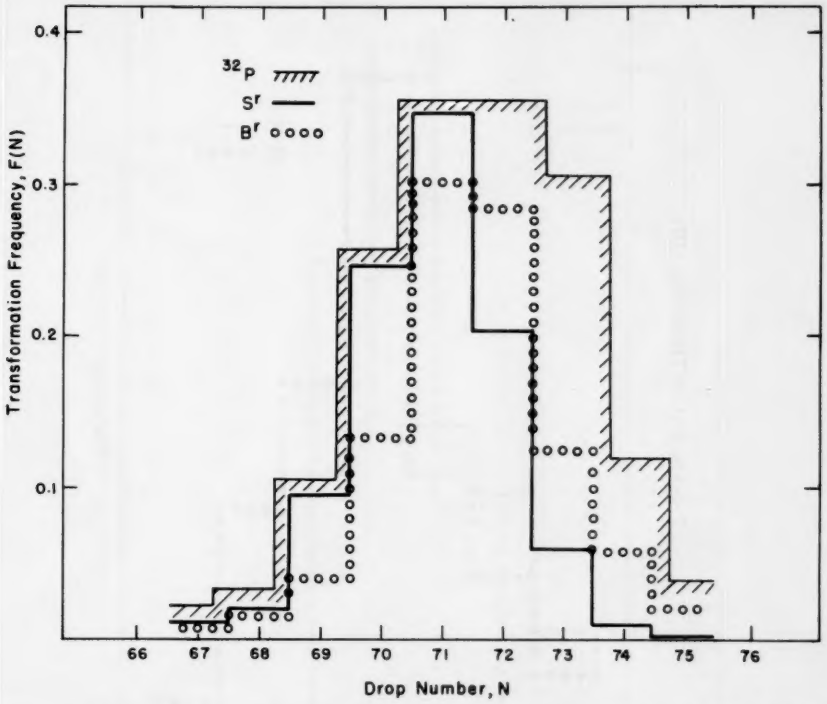

FIG. 2.—Equilibrium density gradient distributions for genetically marked, ^{32}P containing pneumococcal DNA. *D. pneumoniae* carrying the genetic markers for streptomycin resistance S^r, and bryamycin resistant B^r, was grown in a medium containing ^{32}P. Genetically marked DNA labeled to the extent of one ^{32}P atom per 10 molecules was isolated from these organisms and studied in the CsCl density gradient. Distributions of radioactivity and of biological activity for each marker were determined. For the markers S^r and B^r transformation frequency $F(N)$ is plotted against effluent drop number N. For ^{32}P activity, the fraction of total counts multiplied by the factor 1.55 is plotted against N.

of markers $\Delta\rho(A,B)$ were determined from differences in mean drop number $\Delta\bar{N}(A,B)$ and the density gradient $d\rho/dN$ using the relationship

$$\Delta\rho(A,B) = \Delta N(A,B)\left(\frac{d\rho}{dN}\right) \tag{5}$$

For the markers S^r, Q^r and A^r, the density gradient distributions of biological activity are unimodal and not grossly asymmetrical.[8] Due to differences in drop size, the values of $d\rho/dN$ and the width of the marker distributions measured in drops differed in different experiments. However, as can be seen in Table 1, the variances of the distributions for the different markers in a single experiment, and for the same marker in different experiments, were closely similar when expressed in $gm^2\ cm^{-6}$.[9]

If the DNA molecules containing a given genetic marker are homogeneous in density and molecular weight, their density-gradient distribution will be gaussian. Gaussian character cannot be judged directly from the few observed points for

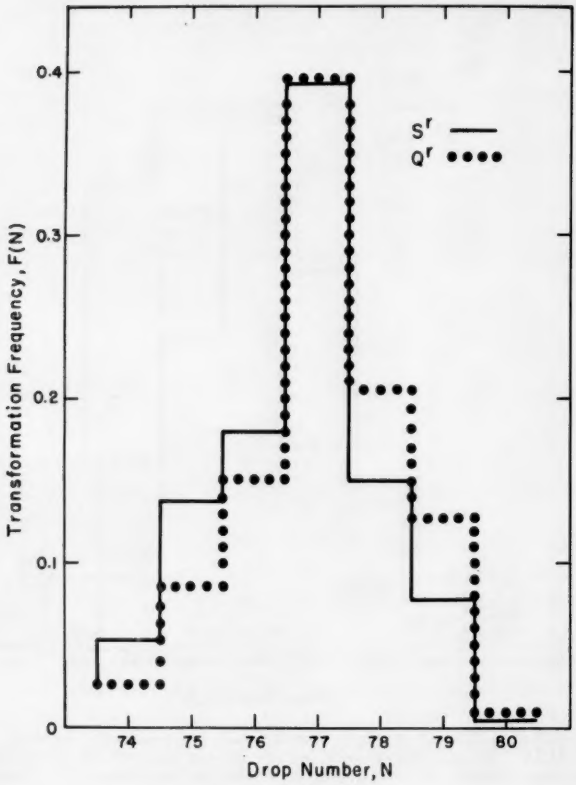

FIG. 3.

each marker distribution. However, a study of ratios of numbers of transformants for pairs of genetic markers (T_A/T_B), as a function of drop number N, suggests that the density-gradient distributions may be gaussian.

Assume that the density-gradient distributions for the genetic markers A,B are gaussian with equal variances. If ρ is solution density, $C_i(\rho)$ is the concentration at ρ of molecules carrying the marker i, and ρ_i is the buoyant density of these molecules, we can write

$$C_i(\rho) = C_i(\rho_i) \exp\left(- \frac{(\rho - \rho_i)^2}{2\bar{\sigma}_i^2} \right) \tag{6}$$

$$\bar{\sigma}_i^2 = \bar{\sigma}^2; \; i = A,B$$

Then the logarithm of the ratio C_A/C_B should be a linear function of solution density ρ

$$\ln \frac{C_A}{C_B}(\rho) = \alpha\rho + \beta;$$

$$\alpha = \frac{\Delta\rho(A,B)}{\bar{\sigma}^2}, \tag{7}$$

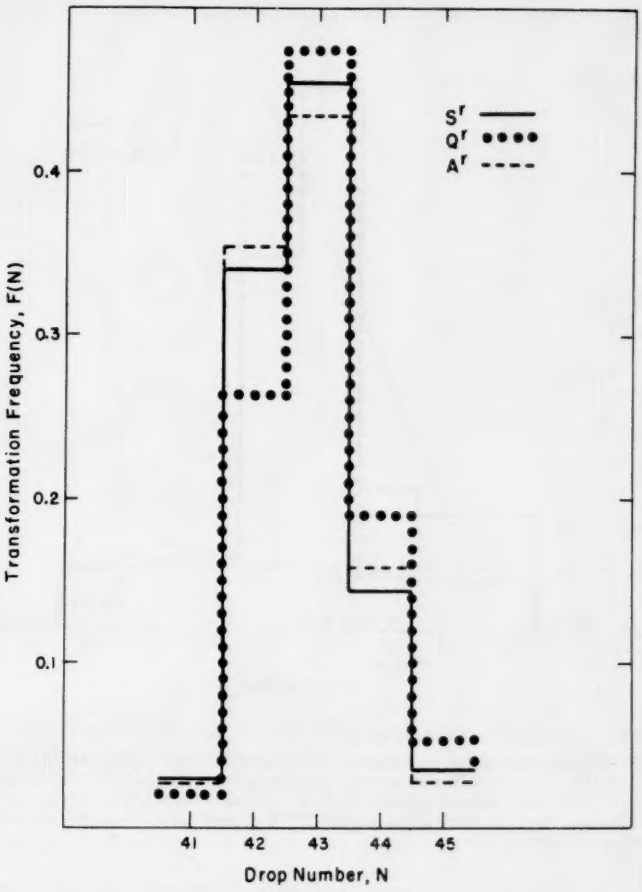

FIG. 4.

$$\beta = \frac{\rho_B^2 - \rho_A^2}{\bar{\sigma}^2} + \ln \frac{C_A(\rho_A)}{C_B(\rho_B)}$$

Plots of log (T_A/T_B) versus drop number N for the various pairs of genetic markers are fairly linear (Figs. 6–8). Since we may write

$$\ln (C_A/C_B) = 2.3 \log (T_A/T_B) + \text{constant} \tag{8}$$

the density difference $\Delta\rho(A,B)$ may be calculated from the slope $[d \log(T_A/T_B)]/dN$, the density gradient $d\rho/dN$, and the variance $\bar{\sigma}^2$ according to the expression

$$\Delta\rho(A,B) = \frac{2.3 \dfrac{d \log (T_A/T_B)}{dN}}{d\rho/dN} \bar{\sigma}^2 \tag{9}$$

Density differences between markers calculated on the assumption that the distri-

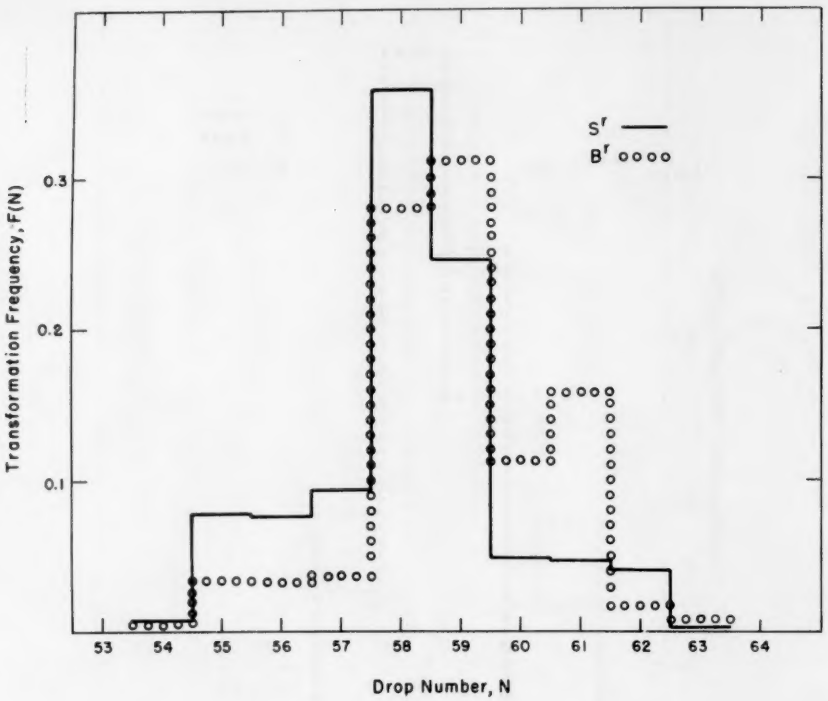

FIG. 5.

FIGS. 3–5.—Equilibrium density gradient distributions of transforming activity for the genetic markers S^r, Q^r, B^r. For the different genetic markers in experiments 5, 10, and 7, transformation frequency $F(N)$ is plotted against drop number N. In experiment 10, a mixture of two kinds of DNA was studied: (1) A purified DNA marked with A^r and (2) a DNA marked with S^r and Q^r isolated from a bacterial lysate.

butions are gaussian (Table 1) agree well with differences calculated according to equation (5).

It has been shown that the DNA of pneumococcus contains classes of DNA molecules associated with different genetic markers. These classes differ in mean buoyant density, but are nearly identical with respect to the variance of their density gradient distributions $\bar{\sigma}^2$ (marker). If we assume that the DNA of pneumococcus consists *entirely* of such classes of molecules, we may use the variance $\bar{\sigma}^2$ (marker) to calculate lower bounds for the number average molecular weight[10] M_n and for the density heterogeneity[11] σ_D of the DNA. The true values of these parameters will exceed the calculated lower bounds only to the extent that molecules containing a specific genetic marker are themselves heterogeneous in density.

Thus we may write

$$M_n \text{ (total DNA)} = M_n \text{ (marker molecules)} \geqslant \frac{35}{\bar{\sigma}^2\text{(marker)}} \tag{10}$$

$$\bar{\sigma}^2{}_T > \bar{\sigma}^2{}_D \geqslant \bar{\sigma}^2{}_T - \bar{\sigma}^2 \text{ (marker) gm}^2 \text{ cm}^{-6} \tag{11}$$

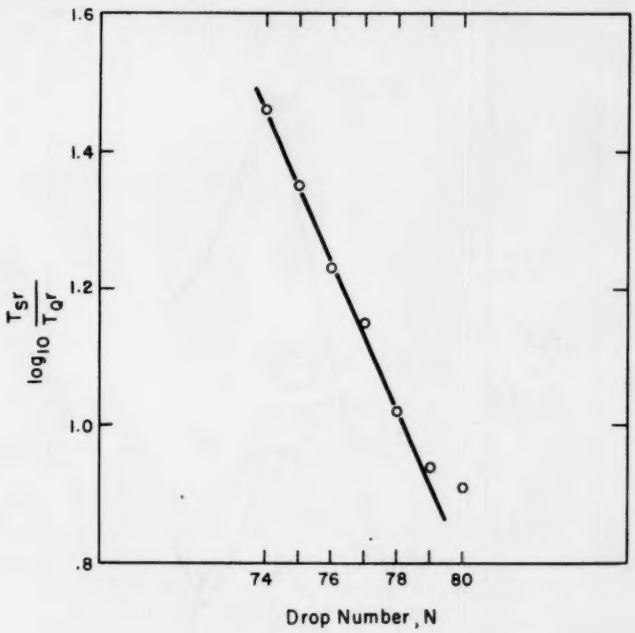

FIG. 6 (EXPT. 5).

where $\bar{\sigma}^2{}_D$ is the contribution of density heterogeneity to the total variance of the DNA $\bar{\sigma}^2{}_T$. Taking the observed value $\bar{\sigma}^2$ (marker) $= 3 \times 10^{-6}$ gm^2 cm^{-6} we obtain

$$M_n \geqslant 9 \times 10^6$$

corrected to the sodium salt of DNA, but neglecting solvation effects.[12] Using values of $\bar{\sigma}^2{}_T$ (P^{32}) and $\bar{\sigma}^2$ (S^r) from experiment 8 (Table 1) and substituting in formula 11, we obtain

$$2.35 \times 10^{-3} > \bar{\sigma}_D \geqslant 1.34 \times 10^{-3} \text{ gm cm}^{-3}$$

Taking the density differences between DNA molecules containing different genetic markers as entirely due to differences in nucleotide composition, we use the relationship[2]

$$\rho_{25°C} = 1.658 + 0.100\, GC \text{ gm cm}^{-3} \qquad (12)$$

where $\rho_{25°C}$ is the buoyant density in CsCl at 25°C and GC is the mole fraction of guanine-cytosine, to calculate the compositional differences between molecules containing the markers S^r, B^r, A^r, and Q^r. Similarly, we estimate the nucleotide compositional heterogeneity of the DNA from its heterogeneity in density.

Assuming a molecular weight of 9×10^6, molecules containing the marker S^r have 12,000 nucleotide pairs; they have 50 more GC pairs than molecules marked with Q^r, 120 more than those marked with B^r, and differ in nucleotide composition from molecules containing A^r by less than 10 GC pairs. For randomly constructed

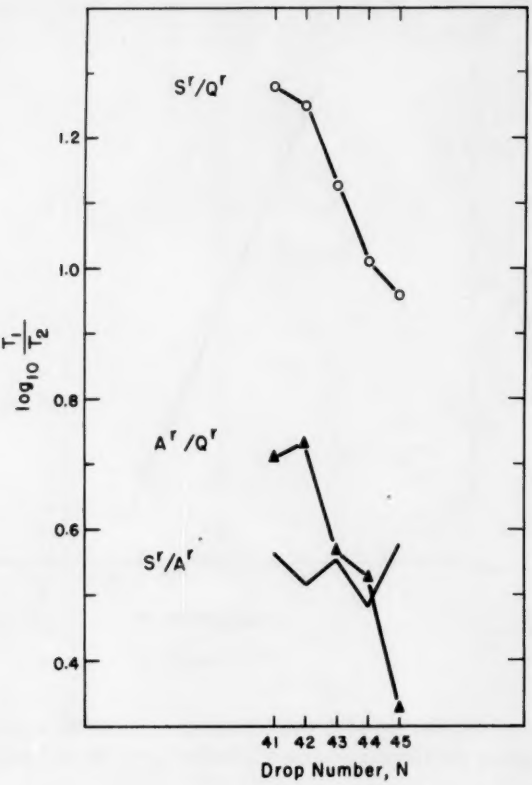

FIG. 7 (EXPT. 10).

molecules of this size (similar results also hold if M_n is greater than 9×10^6) let us write[13]

$$n = 12{,}000 \text{ nucleotide pairs}$$
$$\text{probability of } GC = 1 - (\text{probability of } AT) = 0.4 = p$$
$$\text{standard deviation} = [np\,(1-p)]^{1/2} = 53\ GC \text{ pairs/molecule}$$

The standard deviation of 53 *GC* pairs for the random model is much less than a lower bound for the standard deviation calculated from the observed lower bound for the density heterogeneity of the DNA

$$2.34 \text{ per cent } GC > \text{S.D. } (GC) = 10\ \sigma_D$$
$$\geqslant 1.34 \text{ per cent } GC \text{ or } 160\ GC \text{ pairs per molecule.}$$

With respect to their own mean, the nucleotide compositions found for the markers studied have a standard deviation of only 64 guanine-cytosine pairs; however it is interesting that the observed compositions for the markers all lie on the guanine-cytosine-rich side of the total DNA distribution, with a mean composition differing from that of the total DNA by 150 *GC* pairs, or 1.3 per cent

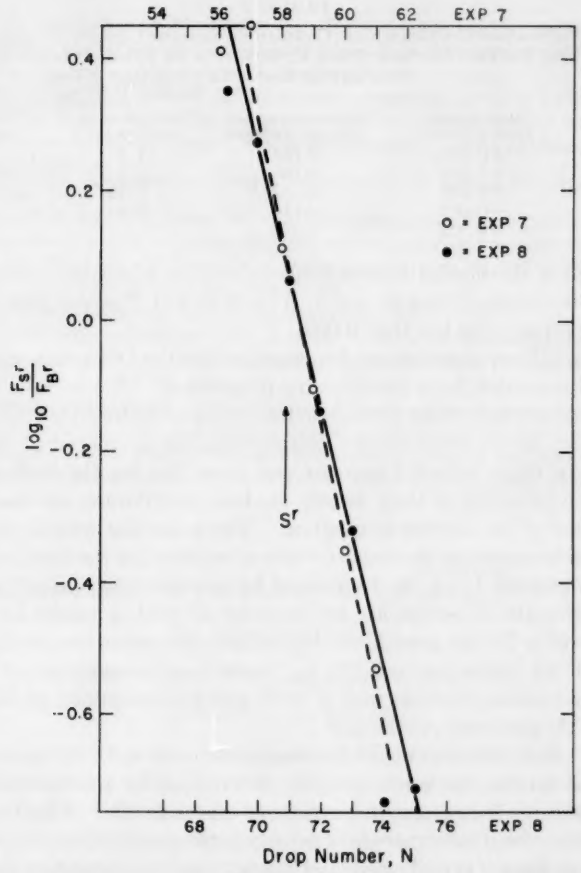

FIG. 8 (EXPTS. 7 AND 8).

FIGS. 6–8.—Logarithmic plots of ratios of numbers of transformants for pairs of genetic markers versus drop number for experiments 5, 10, 7, and 8.

guanine-cytosine. Let us assume that (1) the DNA molecules of pneumococcus that carry genetic information have the same mean composition as the bulk of the DNA and (2) the four markers studied represent a random sample of the total marker population. Using these assumptions, let us calculate P, the probability of observing the compositions found for the various genetic markers. There are two alternative ways of making the calculation, corresponding to two alternative ways of expressing the deviations of observed compositions for the markers from the mean composition for the DNA. The deviations (Table 2) may be expressed in terms of (1) the standard deviation observed for the distribution of nucleotide compositions among the DNA molecules (160 guanine-cytosine pairs per molecule), or in terms of (2) the calculated standard deviation for randomly constructed molecules (53 guanine-cytosine pairs per molecule). In each case P is the proba-

TABLE 2

NUCLEOTIDE COMPOSITIONS OF MOLECULES CONTAINING SPECIFIC GENETIC MARKERS IN PNEUMOCOCCAL DNA; DEVIATIONS FROM MEAN COMPOSITION OF TOTAL PNEUMOCOCCAL DNA

	Deviation from Mean DNA Composition in Units of		Standard Deviation for the Distribution of Nucleotide Compositions	
Genetic marker	Mole fraction, guanine-cytosine	Guanine-cytosine, pairs per molecule	Observed in the total DNA	Calculated from a random model
S^r	+0.016	+190	1.2	3.6
A^r	+0.016	+190	1.2	3.6
B^r	+0.006	+ 70	0.45	1.3
Q^r	+0.012	+140	0.9	2.6
Mean	+0.013	+150	...	...

bility that all of the marker compositions exceed the population mean by at least X standard deviations; thus in case 1, $X = 0.45$ and P is less than 0.013 and in case 2, $X = 1.3$ and P is less than 0.0001.

Discussion.—These experiments demonstrate that the DNA molecules carrying a specific genetic marker have the following properties.

(1) They are more homogeneous in buoyant density than the bulk of the DNA.

(2) They have a mean density characteristic for the marker;[14] it differs from that for other unlinked markers and from that for the bulk of the DNA.

(3) The variances of their density gradient distribution are essentially independent of the marker in question. The molecular weights obtained from the variances are in the range of values reported for the best preparations of pneumococcal DNA, as determined by sedimentation velocity studies.[11]

The experimental observations are inconsistent with a model for DNA composition in which (1) the genetic markers of pneumococcus are evenly distributed among its DNA molecules and (2) the nucleotide composition of a particular molecule is a random variable with a fixed, species-determined probability of occurrence for the guanine-cytosine pair.

It appears likely that the nucleotide composition of a DNA molecule containing a specific genetic marker is uniquely determined by the compositions of the genes of a definite linkage group comprising this molecule. This hypothesis will require modification if the existence of density heterogeneity in molecules containing the bryamycin marker is confirmed, and if in addition it can be shown that unlinked genes for the B^r phenotype are not present in the DNA. Finally it would be interesting to examine the nucleotide compositions of molecules containing other genetic markers of pneumococcus, to investigate the possibility that genetic information is confined to a special, guanine-cytosine rich fraction of the total DNA.

The authors are indebted to Professor Jean Weigle for helpful criticism of the manuscript.

* Postdoctoral Fellow of the U. S. Public Health Service.

† Contribution No. 2719.

[1] Sueoka, N., Marmur, J., and Doty, P., *Nature*, **183**, 1429 (1959).

[2] Rolfe, R., and Meselson, M., these PROCEEDINGS, **45**, 1039 (1959).

[3] Sinsheimer, R. L., *J. Molec. Biol.*, **1**, 218 (1959).

[4] Crick, F. H. C., in *Structure and Function of Genetic Elements*, Brookhaven Symposia in Biology, No. 12 (1959).

[5] Sueoka, N., *J. Molec. Biol.*, **3**, 31 (1961).

[6] Weigle, J., Meselson, M., and Paigen, K., *J. Molec. Biol.*, **1**, 379 (1959).

[7] Kindly supplied by the Bristol Drug Company.

[8] Distributions for the marker B^r differed importantly from those for the other markers. The variance of the B^r distribution was significantly larger than that for S^r in experiment 8, and in

experiment 7, the distribution for B^r was bimodal. These observations may result from gross differences in drop size, but if they are not experimental artifacts, they suggest that molecules containing the B^r marker are not homogeneous in buoyant density.

[9] A partially purified pneumococcal DNA preparation was used instead of a bacterial lysate in experiment 7. The large values of the variances for the marker distributions may be due to a small quantity of low molecular weight DNA in the preparation. The agreement between the values of $\frac{d \log Ts^r/T_{B^r}}{d\rho}$ in experiments 7 and 8 indicates that the bulk of the DNA was of a size comparable to that of the DNA studied in the other experiments. The slightly increased value for $\sigma^2(S^\lambda)$ in experiment 8 may be due to molecular scissions associated with P^{32} decay.

[10] Meselson, M., Stahl, F., and Vinograd, J., these PROCEEDINGS, **43**, 581 (1957).

[11] Sueoka, N., these PROCEEDINGS, **45**, 1480 (1959).

[12] Hearst, J., Thesis, California Institute of Technology, 1961.

[13] The nucleotide composition of the DNA from the strain of pneumococcus used is 0.40 mole fraction guanine-cytosine, both by chromatographic analysis (R. Litman personal communication) and buoyant density ($\rho_{25°C}$ = 1.698 gm cm^{-3}).

[14] A given genetic marker may be introduced into different strains of pneumococcus by transformation. Experiments in progress in these laboratories suggest that (1) the characteristic density of a marker is the same in different strains of pneumococcus, and (2) independent occurrences of a given marker in different strains of pneumococcus have the same characteristic density.

---

*SECOND-GENERATION HYBRIDS OF THE SPECIES OF TARICHA**

BY VICTOR C. TWITTY

DEPARTMENT OF BIOLOGICAL SCIENCES, STANFORD UNIVERSITY

Communicated July 27, 1961

In 1953 I began a long-term program of field experiments on the biology and speciation of the western newt, *Taricha*. This was the outgrowth of the earlier discovery of new forms of this genus[1] and their subsequent use for combined genetic and embryological experiments designed especially to analyze the developmental basis of species differences in larval pigmentation.[2–4] It was immediately apparent from the success of artificial cross-fertilizations that hybrid viability is widely characteristic of the genus, and this has since been confirmed for all possible interspecific combinations. However, we had not yet developed satisfactory methods for culturing newts to maturity in the laboratory, and one of the original incentives of the field program was to entrust to nature the responsibility of rearing artificially produced hybrids to maturity for tests of their fertility and for further genetic studies. To this end we began the release of large numbers of young hybrids at a field station in the coastal mountains of northwestern Sonoma County. It was also recognized at the outset that the hybrid populations might yield information of considerable interest concerning such matters as the inheritance of behavioral differences and the possible introduction of new genes into the native population through introgressive hybridization, but these features will be touched upon only incidentally in the present account.

PLANTING PROGRAM AND HYBRID RECAPTURES

The nature of the planting program has been outlined, and the site of the study described and pictured, in earlier publications.[5–7] As I have just indicated, the

purposes of establishing hybrid populations in nature are manifold, but in this paper we are primarily concerned with their use for tests of fertility and for genetic analysis of the characteristics distinguishing the species of *Taricha*. Reference will be confined principally to results with two hybrid combinations involving three of the species and subspecies of *Taricha*, namely, *T. rivularis*, *T. torosa torosa*, and *T. t. sierrae*. Using *rivularis*, the species native to the study area, as the maternal form for both combinations, its eggs have been fertilized in large numbers by sperm of *torosa* and *sierrae* and the resulting hybrids released at hatching in a $1^1/_2$-mile stretch of Pepperwood Creek, a tributary of the Wheatfield Fork of the Gualala River. Between 1953 and 1958 an estimated 100,000 young larvae of each combination were planted in rock-strewn portions of the stream bed to afford them maximal protection from fish and other predators. Larval mortality through predation is very high, however, as it undoubtedly is in native *rivularis* itself, and during the past three years we have resorted to rearing hybrid larvae through metamorphosis in the laboratory before releasing them in sheltered places at the stream side.

The first mature hybrid to be recovered, a *rivularis-torosa* male, was captured in the experimental stream during the breeding season of 1959, six years after the first planting of hybrid larvae. The following season 5 *rivularis-torosa* males and 10 *rivularis-sierrae* males were taken, and in 1961 the recaptures again increased substantially, to a total of 57 for the season; among these were the first mature females to be recovered. There were 8 of the latter, 5 *rivularis-torosa* and 3 *rivularis-sierrae*, and of the 49 males 13 were *rivularis-torosa* and 36 were *rivularis-sierrae*. If the numbers of hybrids returning as adults to the stream continue to increase at this rate during coming years, as we believe they will, the prospects of ultimately establishing sizable hybrid populations in the experimental stream are quite promising.

The long lapse of time between release of the hybrids as larvae and their first recapture as mature adults is not entirely unexpected. Although there is no very accurate information concerning the period required by the species of *Taricha* to reach sexual maturity, Chandler[8] has estimated that it is 4 or 5 years in *T. granulosa* and I suspect it is fully as long if not longer in the other three forms. *Granulosa* is aquatic in habit during much of the year, whereas the other species spend the dry months underground where opportunities for maximal feeding and growth may well be more restricted. In any event, there is no reason to believe that the hybrids suffer any disadvantage in rate of growth and attainment of sexual maturity in comparison with the parental species; among the animals that we have reared in the laboratory the hybrids seem to grow fully as rapidly as the parental forms.

I do not yet know why hybrid females have been slower than the males in reentering the stream as adults. There is, however, one recently established fact that may have a bearing on the question. Miller and Robbins,[9] on the basis of differences in the degree of maturity of the gonads in adult populations of *T. t. torosa*, postulated that in this species breeding may occur at intervals of more than one year. From studies on homing behavior[6, 7] that we have conducted concurrently with the hybridization program, we have learned that in *rivularis* a substantial percentage of the males enter the stream for breeding during immediately successive years; it is not uncommon to recover during a given season over one-half of the males marked by partial limb amputations during the preceding season. Until recently we had used only adults of this sex for marking experiments, but dur-

ing the 1960 season we marked by toe clipping all of the 1231 females encountered in the course of our daily patrols of the experimental stream. The following year, 1961, we recorded only 9 of these marked females in the stream during the entire season. This suggests indeed that females enter the water for breeding at less frequent yearly intervals than do males, and it is quite possible that this difference between the sexes in the timing of the breeding cycle may well account at least in part for the delayed recapture of hybrid females.

A full characterization of the *rivularis-torosa* and *rivularis-sierrae* adults is beyond the scope of the present paper, but it may be said that they are readily distinguishable from one another and from the native *rivularis*. *Rivularis-torosa* adults are considerably lighter in dorsal coloration than those of *rivularis* and in fact are rather strikingly similar in general appearance to adults of the paternal form, *torosa*. They are immediately distinguishable from the latter, however, by the pigmentation of the iris. In *torosa* the iris is profusely pigmented with brightly colored chromatophores, whereas in adult *rivularis* the eye is invariably a dark chocolate brown; the hybrid iris is intermediate in coloration, never as dark as in *rivularis* but definitely less brightly pigmented than in *torosa*. The iris of *rivularis-sierrae* hybrids is of the same intermediate character, in keeping with the fact that *sierrae*, like *torosa*, has a brightly colored eye, but otherwise the hybrids of this combination have a strong superficial resemblance to adults of the maternal species, *rivularis*. As in the latter, the skin is dark, almost black, above and reddish below. On closer examination, however, one finds that whereas in *rivularis* there is heavy encroachment of the dark dorsal pigmentation onto the ventral surfaces of the limbs, and usually a black band extending downward over the cloacal lips, these characteristics are lacking in the *rivularis-sierrae* hybrids. Thus when we are collecting in the stream, the *rivularis-torosa* hybrids can usually be distinguished from *rivularis* at a glance, by their lighter dorsal coloration, and examination of the iris serves merely as a secondary confirmation of their identity. *Rivularis-sierrae* hybrids might often escape recognition if it were not for our practice of removing from the water and examining virtually all dark-colored adults—the very great majority of which prove to be *rivularis*, of course—for the presence or absence of cloacal bands and melanization of the under surfaces of the limbs. Incidentally, once a hybrid is captured it is marked by coded toe-clipping so that when released again it will not be counted twice during either the same or subsequent years. A few of the hybrids are of course lost permanently, through sacrifice for use in the artificial fertilizations to be described later.

The *rivularis-torosa* hybrids are also usually distinguishable from those of *rivularis-sierrae* by their somewhat heavier body conformation and greater total length: an average of 182 mm for 7 *rivularis-torosa* males that were measured compared with 163 mm for 10 *rivularis-sierrae* males. Both of these averages are within the range of variation in body length of all three parental species, but no detailed size comparisons will be attempted until larger populations of hybrids are available for measurements.

All of the hybrids were in breeding condition at the time of capture in the stream, and each animal that was sacrificed proved to have sperm-filled vasa deferentia or mature ovarian eggs. In fact, many were in amplexus with *rivularis* adults of the opposite sex when captured, and in the section to follow it will be seen that these

matings often culminate in effective insemination and ovulation.

Although it does not relate directly to the main theme of the present paper, parenthetical reference is made at this point to an incidental feature of the hybrid recaptures bearing on another phase of our studies with *Taricha*. When we first began the planting of hybrid larvae we were faced with the question whether at maturity they could be expected to return to the point of release, or perhaps instead to random locations in the experimental or even other streams in the area. This led to marking experiments, with adults of the native *rivularis* population, which have since clearly demonstrated that newts do indeed return regularly each year to the same segment of the breeding stream.[6, 7] This is accomplished through a true homing ability that enables the adults to return to the original site even after transfer to distant locations. However, since our marking experiments were all performed with adult animals we have had no way of knowing whether identification with a given segment of the breeding stream is "imprinted" at the time of first entry as mature adults, or much earlier, either during larval life or at the time they leave the water as newly metamorphosed juveniles. Fortunately, our records of the recapture of adult hybrids give us some information bearing directly on this problem.

In planting the hybrid larvae different sections of the experimental stream were chosen for the release of the *rivularis-torosa* and *rivularis-sierrae* series. The former were placed in the upstream portion of the $1^1/_2$-mile stretch and the latter in the downstream segment. And of the 73 adult hybrids that have been recaptured all except 4 have been taken in the appropriate portions of the stream; that is, in the segments where they had been released as larvae. The four exceptions were *rivularis-torosa* hybrids, and even these were only a relatively short distance "out of bounds." It thus seems probable that association with specific breeding sites becomes fixed in larval or early juvenile life, and not at maturity when adults enter the stream for their first breeding experience.

Rivularis-granulosa hybrids: In addition to the very large population of *rivularis* in the breeding stream there is a small population of *T. granulosa*. When our planting program was first conceived and initiated, it was decided to exclude hybrid combinations involving this species because of the following considerations and assumptions.

For reasons that need not be recounted here[5, 10], *granulosa* seems to stand somewhat apart from the other three forms with respect to closeness of evolutionary or systematic affinities, and accordingly the prospects of fertility in hybrids involving *granulosa* seemed somewhat less promising than in combinations using only *rivularis*, *torosa*, and *sierrae*. There is also the consideration that *granulosa* is often sympatric with the other three (as it is in the experimental stream), "while the latter themselves are never known to occur together with one another in the same immediate vicinity. It is accordingly plausible to conjecture that more effective, and perhaps more deep-seated reproductive barriers or isolating mechanisms may have become established between *granulosus* and the other species than those that may exist between the latter three forms themselves."[5]

In 1958, however, a male was found in the experimental stream whose coloration and other characteristics immediately suggested that it was a *rivularis-granulosa* hybrid. The male proved to be fertile when its sperm was used for an artificial

backcross to *rivularis*, and the pigmentary features of the larval offspring seemed to support fully our identification of its parentage. Further confirmation was added when we compared the backcross offspring with those obtained by fertilizing *rivularis* eggs with sperm from an artificially produced *rivularis-granulosa* male that had been reared to sexual maturity in the laboratory.

I am sure that the incidence of natural hybridization between *rivularis* and *granulosa* is very low, since this specimen is the only one that has been encountered among the literally scores of thousands of *rivularis* and *granulosa* adults that we have examined in Pepperwood and other creeks during intensive collection and study over the course of many years. Each breeding season we observe isolated instances of interspecific amplexus, between *granulosa* and *rivularis* adults, but I am convinced that these merely reflect the highly aggressive and somewhat promiscuous sexual proclivities of male newts and that the matings almost never culminate in insemination.

However, the knowledge that hybrids of this combination are fertile has now stimulated us to include them in our planting program, and we are looking forward to the eventual recapture of *rivularis-granulosa* hybrids in numbers sufficient for genetic studies similar to those described below for the other species combinations. Certain striking differences between *granulosa* and *rivularis*, such as in egg size and the manner of egg deposition (singly in *granulosa*, in clusters in *rivularis*) will heighten the interest afforded by behavioral comparisons and genetic analysis with this particular combination.

BACKCROSS AND F_2 GENERATIONS

In this section I shall deal with the viability and development of second-generation hybrids, including the segregation of genetic characteristics that distinguish the parental *Taricha* species, by description of several selected but representative series. The series chosen involve in all cases the use of F_1 hybrids recaptured as mature adults from the experimental stream. One reason for this restriction is that greater interest attaches itself to the hybrid combinations on which the planting program is based; another is that the hybrids recaptured in nature have proved to be larger and sturdier specimens than those reared in the laboratory and accordingly may be presumed to offer optimal material for evaluation of hybrid fertility and of viability of the F_2 offspring. It may be stated, however, that the results with several series of laboratory-grown hybrids (see references 18 and 19), both males and females, are consistent with those to be described for the "stream hybrids."

In presenting the results with each combination of species the general plan will be to describe first the backcross series, in which only one parent is of hybrid constitution, followed by an account of the F_2 series, in which both parents are F_1 hybrids. Exceptions to this are necessary, however, in series with divided paternity; that is, when some of the eggs of a given hybrid female have been fertilized by sperm of a parental species and others by sperm from a hybrid male. In such cases direct comparison requires joint description of the backcross and F_2 offspring.

Species Combination.—T. rivularis and T. t. torosa. Rivularis ♀ × *rivularis-torosa* ♂*:* One hundred ninety seven eggs taken from the oviducts of spawning *rivularis* females were treated with a sperm suspension prepared from a single

rivularis-torosa male hybrid. Nine days later, after removal of unfertilized and damaged eggs, 155 embryos were found to have developed to the early tailbud stage. At hatching there were 134 survivors, and at the next count, 4 months after fertilization, the series consisted of 108 larvae. At approximately 8 months, after all members of the series had completed metamorphosis, 87 were still alive and vigorous.

One naturally wishes to inquire whether in this series, as in others to be described, the percentages of fertilization and of subsequent viability have any import in relation to the question of hybrid fertility; that is, to the possibility that the observed developmental failures are attributable to genetic defects in the gametes produced by the hybrid parents. This is a matter that can be fully resolved only by cytological studies, but I wish to emphasize at the outset that in evaluating the failures a large allowance must be made for strictly environmental hazards. This can be most simply expressed, perhaps, by explaining that the results in the present series, both with respect to the percentage of fertilization and to subsequent survival through embryonic and larval stages, can be appraised as "good" in comparison with any typical series produced by artificial fertilization. Even in homospermic series, i.e., when the eggs and sperm are of the same species, the percentage of successful fertilization is by no means always predictable or high and, in fact, may sometimes be markedly lower than in the present backcross series. Abnormalities of early development, of various grades and appearing at different embryonic stages, are also not infrequent following artificial fertilization, possibly because of the mere physical handling of the eggs during the procedure. Attrition in backcross series during larval stages is also seemingly no greater than in the parental species or their F_1 hybrids, and again is almost certainly attributable mainly to environmental factors. Particularly when they are grown in mass cultures, as is necessary when dealing with larvae in the large numbers handled by us each year, only the utmost care can prevent losses through such causes as fouling of the water.

Further evidence that failures of fertilization and development in the backcross series are not attributable primarily to genetic factors comes from a series of eggs spawned naturally by *rivularis* females after they had mated with *rivularis-torosa* hybrid males in a wire-mesh enclosure constructed in the bed of a small stream. Eight egg clusters totaling 74 eggs deposited on stones in the manner characteristic of *rivularis* were carefully removed and their development observed. Without exception all of the eggs were fertilized and developed normally to the hatching stage, at which time an examination of their pigmentary and other characteristics established their hybrid paternity.

This complete success in the development of eggs fertilized and deposited under natural conditions does not of course in itself prove that there was no meiotic breakdown whatever in the male hybrid parent. In fact, preliminary cytological studies by H. G. Callan of St. Andrews University, Scotland, on the testes of a few male *Taricha* hybrids shipped to him by me showed that meiotic irregularities do indeed occur in some spermatocytes. This suggests that such cells may not differentiate into functional spermatozoa or that, if they do, the chromosomal aberrations are not serious enough to interfere with the normal development of eggs fertilized by them. I shall return to the question of meiotic breakdown and its possible consequences later in the paper, but this somewhat parenthetical reference

to the natural backcross series will give the reader a better perspective in evaluating the results of the artificial crosses on which our study is principally based.

Segregation of larval pigment patterns: *Torosa* and *rivularis* differ strikingly in their patterns of larval pigmentation, and the possibility of analyzing the inheritance of these distinguishing characteristics lends added interest to the F_2 series.

The contrasting pigment patterns of *torosa* and *rivularis* are shown in Figures 1 and 2. In *torosa* most of the melanophores are compacted into a dorsal band on each side, whereas in *rivularis* they are widely and uniformly dispersed over the flanks. When a *rivularis* egg is fertilized by a *torosa* sperm, the resulting arrangement of the melanophores (Fig. 3) shows features of both parental patterns, although the well-defined dorsal band imparts a closer resemblance to the *torosa* pattern.

When, as in the backcross combination immediately under consideration, *rivularis* eggs are fertilized by sperm from one of these hybrids after it has grown to maturity, the resulting larvae display pigment patterns ranging between those characteristic of the *rivularis* and *hybrid* parents. Examples of the two extremes and of a pattern intermediate to them are shown in Figure 4. The larva at the top (*a*) presents a pattern essentially indistinguishable from that of the hybrid *rivularis-torosa* parent, and the larva at the bottom (*c*) similarly duplicates in appearance the maternal *rivularis* pattern. Between these two photographs is one of a third larva (*b*) illustrating a melanophore pattern essentially intermediate in character to the parental extremes.

Using the categories illustrated by these three photographs the 134 larvae of this series were scored at hatching with the following results:

Hybrid-type pattern	Intermediate pattern	*Rivularis*-type pattern
40	58	36

The series referred to above, resulting from natural mating between *rivularis* females and *rivularis-torosa* hybrid males, gave corresponding scores of 27, 19, and 28, when scored on the same basis. In a third and larger series of the same backcross combination, comprising 284 larvae at hatching, the scores for the three categories were 72, 121, and 191, respectively. When the scores of all three series are combined, the totals are 139, 198, and 255.

It will of course be understood that in scoring the pigment patterns not all cases fall neatly into one or another of the three categories. There is some variation in pigment pattern among larvae assigned to any given category, and within an entire series there is probably an almost continuous spectrum of patterns ranging between those completely typical of the *rivularis* parent at one extreme and of the hybrid parent at the other. Scoring judgments are thus necessarily somewhat arbitrary and probably not even entirely consistent, either within a single series or especially between different series scored at different times. This may in fact account partly for the somewhat different segregation ratios in the three series cited, no two of which were made during the same year. The fact remains, however, that the scoring standards were reasonably strict, and in no cases did the pigment patterns assigned to given categories deviate very substantially from those shown in the photographs (Fig. 4) that illustrate the three basic categories employed.

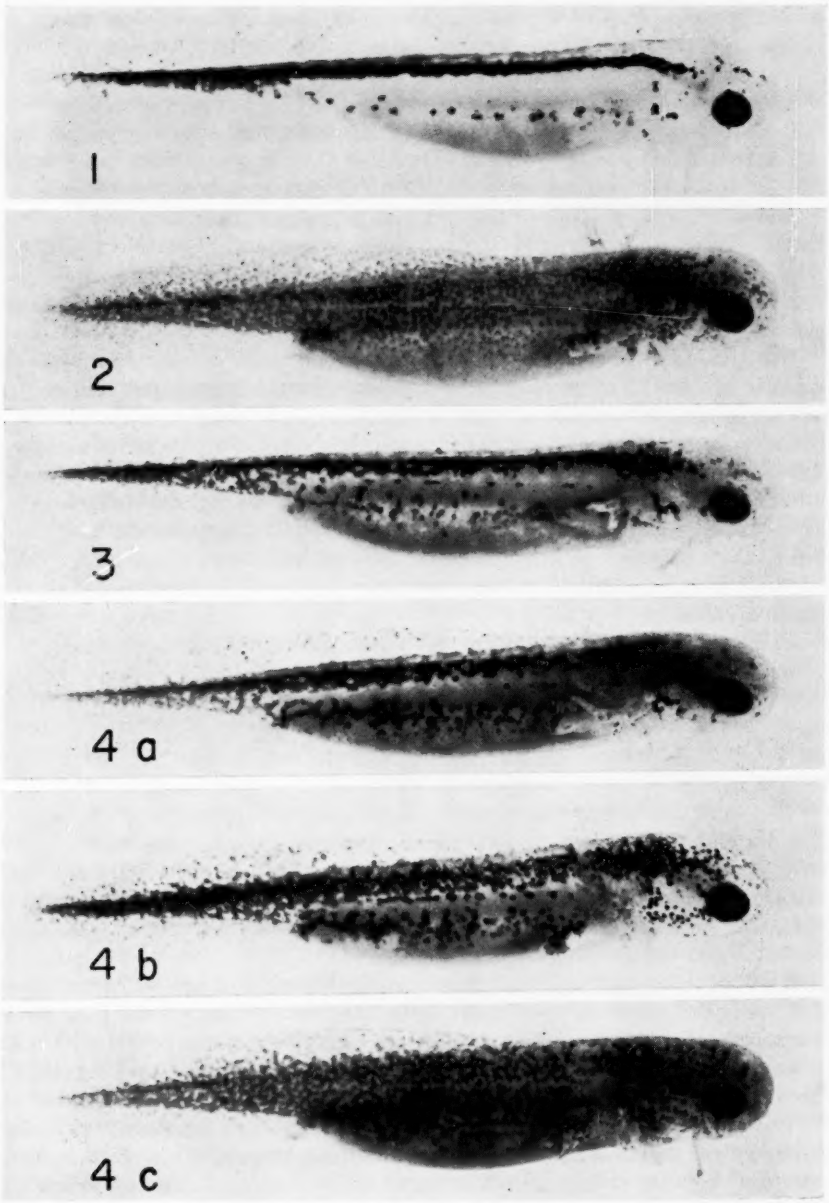

FIGS. 1 and 2.—Young larvae of *torosa* and *rivularis*, respectively.

FIG. 3.—*Rivularis* ♀ × *torosa* ♂ hybrid.

FIG. 4.—Offspring of *rivularis* ♀ × *rivularis-torosa* ♂ backcross, illustrating segregation of pigment patterns closely similar to those of the hybrid (*a*) and *rivularis* (*c*) parents, and (*b*) a pattern intermediate to these two.

One point of obvious interest in connection with the observed segregation ratios is their implication concerning the number of genes responsible for the differences in the larval pigment patterns of *rivularis* and *torosa*. Although I shall not venture specific estimates, it seems evident that the number of genes or gene blocks involved cannot be large and in all probability is quite small. This would seem to follow from the high percentages in all backcross series of patterns essentially identical to one parental extreme or the other, that is, to the typical *rivularis* pattern or to the typical hybrid pattern. If many genes were participating the probabilities are presumably small that either of these two contrasting patterns would emerge in such high ratios among the backcross offspring. In this connection, although it is merely a special example of the same type of evidence, it may be illustrative to point out that these contrasting patterns characteristically appear among even very small numbers or samples of backcross offspring. I have already referred more than once to the series resulting from natural mating of *rivularis* females with *rivularis-torosa* male hybrids. Within almost every one of the eight egg clusters deposited by the females, typical hybrid- and *rivularis*-type patterns were sharply represented. As I have already indicated, this situation merely repeats what might be expected from the ratios revealed by the scoring of entire backcross series, but when equally clear-cut segregation is found within a single cluster of 8 to 10 eggs, one is somehow led even more forcibly to the conclusion that the conspicuously different larval pigmentation of *rivularis* and *torosa* is based on only a few gene differences.

Segregation of other characters distinguishing rivularis and torosa larvae: In addition to the contrasting pigment patterns, *rivularis* and *torosa* larvae differ with respect to the condition of the *balancer*, which is always present in *torosa* and absent or rudimentary in *rivularis;* and in the development of the *dorsal fin*, which extends less far anteriorly on the trunk in *rivularis* than in *torosa*. In F_1 hybrids the balancer is always present, although reduced in size compared with the normal *torosa* organ, and the dorsal fin is likewise intermediate in its degree of development.[2] In the backcross offspring segregation is again clearly evident, with the balancer and fin ranging in development between the extremes typical of the *rivularis* and hybrid parents. Thus the balancer is sometimes completely lacking, as it usually is in normal *rivularis*, or it may attain the size typical of this organ in *rivularis-torosa* F_1 hybrids. Likewise the dorsal fin may be reduced as in *rivularis* or may extend further anteriorly, nearer the base of the head, as in the hybrid parent. Scoring of these strictly quantitative differences is more difficult and arbitrary than when dealing with pigment patterns, and except for noting the presence or absence of the balancer we have usually not attempted detailed examination of these characters. Of the 74 larvae resulting from the natural backcross mating, the balancer was absent in 16 and present in varying sizes in the remaining 58.

As was probably to be expected, the three characteristics disinguishing *rivularis* and *torosa* larvae appear to segregate independently of one another. Although our records have not been analyzed exhaustively in this regard, they reveal numerous instances in which virtually all possible combinations of pigment pattern, balancer development, and fin-size are represented in individual members of the backcross series. Thus a larva with a hybrid-type pigment pattern may either possess or lack a balancer, and its dorsal fin may or may not be reduced in extent. Similarly, a *rivularis*-type pigment pattern may be associated with a well-developed balancer

and fin, whereas neither of the latter is typical of normal *rivularis* itself.

Segregation of Post-Metamorphic Characters.—Eye color: The iris of both *rivularis* and *torosa* larvae is conspicuously pigmented with brightly colored chromatophores. In *torosa* these persist and are augmented following metamorphosis (Fig. 5), but

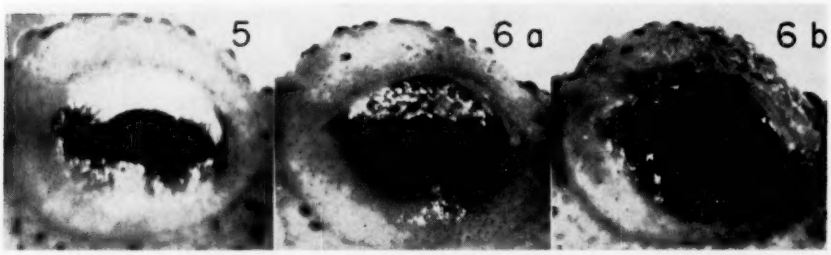

FIG. 5.—Postmetamorphic pigmentation of the normal *torosa* iris.

FIG. 6.—Iris-types segregating among *rivularis-torosa* ♀ × *rivularis* ♂ backcross offspring: *a*, hybrid-type iris; *b*, iris identical to that of the completely dark *rivularis* eye except for the presence of a very few brightly colored pigment cells.

in *rivularis* their disappearance during larval transformation leaves the adult eye a dark-chocolate brown that distinguishes this species infallibly from *torosa* as well as from the other *Taricha* species. This change in the *rivularis* iris at metamorphosis has been described and analyzed experimentally in very interesting studies by Barden[11, 12]. In F_1 *rivularis-torosa* hybrids the iris is intermediate in character, neither as brightly pigmented as in *torosa* nor as dark as in *rivularis*. Among backcross offspring the pigmentation of the iris following transformation again tends to span the range between the conditions typical of the *rivularis* and hybrid parents. At one extreme the brightly colored chromatophores, although rarely completely absent, not infrequently number less than a dozen (Fig. 6b), while at the other they are present in the relative profusion characteristic of an F_1 hybrid iris (Fig. 6a).

Limb pigmentation: In *rivularis* the blanket of pigment that darkens the dorsal body skin at metamorphosis envelops also a considerable area of the under surfaces of the limbs, whereas on the *torosa* appendages this ventral encroachment does not occur to any comparable degree.[10] Extension of melanin pigment to the under surface of the limb appears to be a recessive character, since it does not materialize in F_1 *rivularis-torosa* hybrids. When the latter are backcrossed to *rivularis*, however, both parental extremes emerge among the metamorphosed offspring. Of 24 members of a backcross series that were scored for this character, pigment was well represented on the under surfaces of the limbs in 7 cases and lacking in the remaining 17.

General body color: In *rivularis* the dorsal pigment is quite dark, almost black, and the belly color is a distinctive tomato red. In *torosa* the back and sides are usually medium to dark brown, and the ventral surfaces typically light yellow or orange, often with a greenish cast. As mentioned in an earlier section, the skin colors of *rivularis-torosa* hybrids recaptured in the experimental stream were usually similar to those of normal *torosa*, although the hues of the belly pigment tended to be somewhat warmer. In the hybrids of this same combination that were reared

in the laboratory, the dorsal skin color was for unknown reasons more variable, and was usually somewhat darker than in the "stream hybrids."

Shades of pigmentation are difficult at best to designate and categorize, and accordingly our attempts to score the body colors of backcross offspring have not proved to be entirely satisfactory. However, as in the cases of the better-defined pigmentary characters treated above, clear evidence of segregation of general body color is present in the F_2 series. For example, in the series of 24 backcross hybrids mentioned above in connection with iris color, the dorsal pigmentation was scored as "dark" in 9 cases, "medium" in 10, and "light" in 5. The contrast between the two extremes was quite striking, with the darkest individuals approximating *rivularis* in intensity of melanization. There was also considerable range in belly color, extending in a few cases to the distinctive *rivularis*-red that is never realized in first-generation hybrids.

There appears to be no "linkage" between larval and postmetamorphic pigmentary characteristics. For example, larvae with a *rivularis*-type pigment pattern are no more prone to develop at metamorphosis the dark-colored iris and intense melanization of the dorsal body skin characteristic of normal *rivularis* than are larvae with a banded, hybrid-type, pigment pattern.

Torosa ♀ × *Rivularis-Torosa* ♂.—In virtually all of our artificial backcrosses involving hybrids of *rivularis* and the two subspecies of *torosa*, *rivularis* has been used as the maternal species, largely because spawning females of *torosa* and *sierrae* are not available in nature at our field station where the experiments are performed. The only exception is the present series, in which sperm of a *rivularis-torosa* male were used to fertilize the eggs of *torosa* females brought from near Palo Alto for the purpose. Incidentally, the paternity in this series is identical to that in the series described at length in the preceding section, since both series were made in immediate succession using the same sperm suspension.

To provide a background for the description of this series, reference must first be made to the cross in which *torosa* eggs are fertilized by *rivularis* sperm. In the reciprocal of this cross, as we have already seen (Fig. 3), the larval pigment clearly reflects the participation of genes contributed by both gametes. Although the *torosa* features are somewhat more conspicuous, even the *torosa*-like band of the hybrid is less sharply defined than in *torosa* itself, and the relatively generous complement of melanophores lower on the flank is obviously referable to the *rivularis* component of the hybrid genome. However, when the parentage is reversed, i.e., when *torosa* eggs are fertilized by *rivularis* sperm, the operation of *rivularis* genes is much less clear.

This is especially true in the young larval stages when pigment pattern first becomes well defined, at which time one would in fact be at a loss to distinguish the pigmentation of most hybrids from that of normal *torosa* controls. Later in hybrid development the *rivularis* parentage becomes more evident, as the dorsal band loses some of its compactness and the number of melanophores on the flank and fin increase, but it is nevertheless clear that factors associated with the *torosa* egg reinforce the dominance exercised by this species in the genetic control of hybrid pigment pattern.[13] As would be predicted from this situation, it was found that *torosa* eggs fertilized by hybrid sperm yielded pigment patterns in which there was in the large majority of cases little manifestation of the *rivularis* genes contributed by

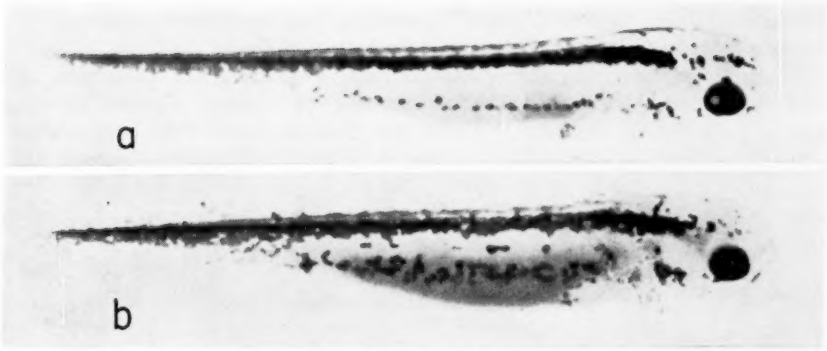

FIG. 7.—*Torosa* ♀ × *rivularis-torosa* ♂ backcross offspring. Pigmentation of the large majority typified by *a*, is hardly distinguishable from that of normal *torosa* larvae; *b*, typifies a small minority showing the effects of *rivularis* genes contributed by the male hybrid parent.

the male parent (Fig. 7). (Further reference to the question of *torosa* dominance in the control of pigment pattern will be made in connection with the description of F_2 crosses using *rivularis-torosa* females.)

The backcross series consisted of 158 eggs, of which 130 were developing normally in tailbud stages; 67 of these were alive following metamorphosis about 6 months later. At the latter stage, when they were compared with the *rivularis* ♀ × *rivularis-torosa* ♂ backcross animals of the same age, the differences between the two series in body color and iris pigmentation were in keeping with the different ratios of *torosa* and *rivularis* genes represented in the two backcross combinations. That is, the amount of brightly colored iris pigment, although again variable, was on the average much greater in the present series, and the dorsal body coloration was considerably lighter.

Rivularis-Torosa ♀ × *Rivularis* ♂; *and Rivularis-Torosa* ♀ × *Rivularis-Torosa* ♂.—Four *rivularis-torosa* female hybrids recaptured as mature adults in the experimental stream during the 1961 breeding season were subjected to pituitary implantation and later sacrificed for artificial fertilization of the oviducal eggs. I shall deal first with the female (SH ♀ 2) yielding the largest series of viable offspring, and subsequently refer in lesser detail to the results with the other three.

At the time this hybrid female was captured in the stream she was in amplexus with a native *rivularis* male. She was placed in a container at the field laboratory for observation and on the second morning was found to have deposited 12 eggs. No further spawning ensued and two days later she was implanted with a pituitary gland from an adult *rivularis* female.

All of the eggs spawned prior to implantation developed normally, and their *rivularis* paternity became clearly evident when their pigmentary patterns were examined at hatching. These ranged from the banded condition highly suggestive of F_1 *rivularis-torosa* hybrids to the uniformly dispersed pigmentation of the paternal *rivularis*. Examples of these are seen in Figure 8, which may be compared with the very similar patterns (Fig. 4) segregating in the reciprocal combination described earlier (*rivularis* ♀ × *rivularis-torosa* ♂).

Three days after pituitary implantation, when "stripping" revealed that ovula-

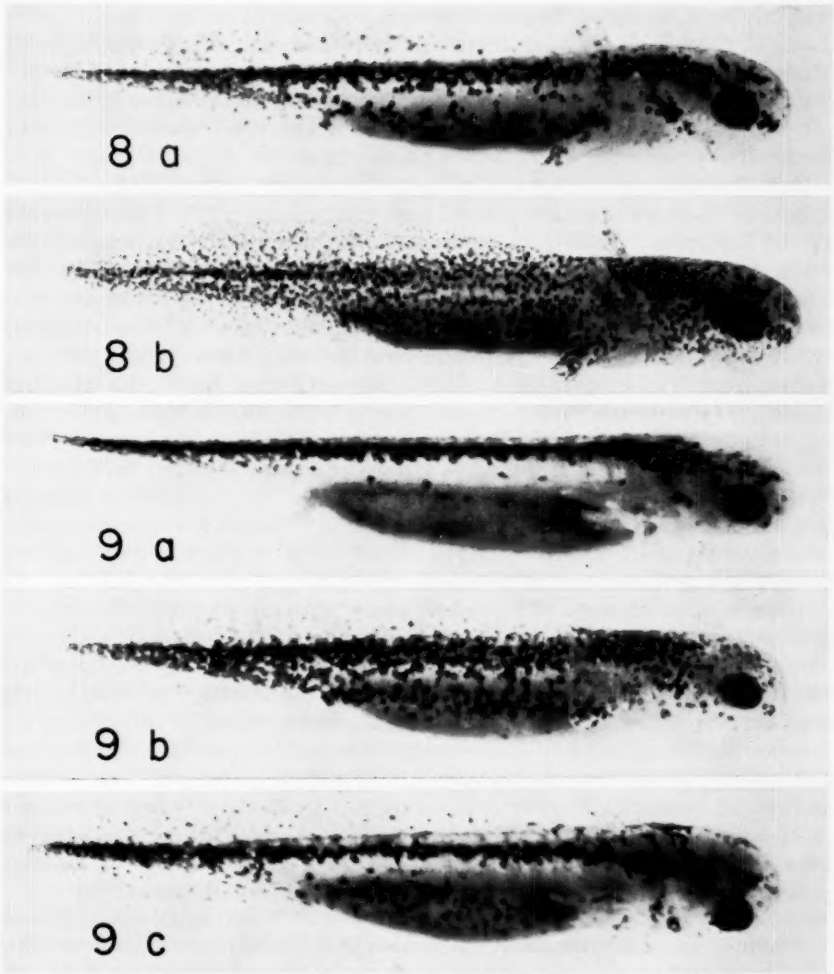

FIGS. 8 and 9.—Backcross and F_2 offspring of the same *rivularis-torosa* female hybrid.
FIG. 8.—Backcross larvae developing from eggs spawned naturally after insemination by a *rivularis* male: *a* and *b*, pigment patterns similar to those of the hybrid and *rivularis* parents, respectively. FIG. 9.—F_2 larvae developing from eggs fertilized artificially with sperm from a *rivularis-torosa* male hybrid: *a*, *torosa*-type pigment pattern; *b*, member of the series most closely approaching the *rivularis*-type pigment pattern; *c*, illustrating the independent segregation of the strong banding characteristic of *torosa*, and the presence of melanophores scattered freely over the embryonic yolk-mass as found in *rivularis*.

tion was in progress, the female was sacrificed and the oviducal eggs fertilized by sperm from a *rivularis-torosa* male hybrid.

Of a total of 76 eggs all except a very few were fertilized and underwent completely normal cleavage and development. Sixty-one survived beyond the hatching stage and at the time of writing, a few months later, the series still numbers 59 vigorous larvae in advanced stages.

In this series, unlike all the preceding ones, both parents are of hybrid constitution, and accordingly we have the possibility of restoring among some of the F_2 offspring the original gene combinations not merely of one parental species but of both. In pigmentation, for example, we might then hope to recover both *torosa* and *rivularis* patterns, perhaps in equal numbers, with the intermediate patterns symmetrically distributed between these two extremes.

This of course involves the assumption that the genes of the two species participate on equal terms in the control of pigmentation, and we have seen from the F_1 and backcross hybrids that the evidence on this is not entirely consistent. When *rivularis* eggs are fertilized by *torosa* sperm, the resulting pattern, although more suggestive of *torosa*, nevertheless retains unmistakable aspects of the *rivularis*-type pigmentation. In the reciprocal cross, this "blending" is less evident. When the hybrids first become pigmented most of them are hardly distinguishable, if at all, from larval *torosa* of the same age. One can perhaps resolve this difference between the reciprocal hybrids by postulating maternal effects exerted by the *torosa* egg cytoplasm, referable ultimately to genic action on the cytoplasm prior to ovulation and fertilization. The results of Dalton[14] (see also Twitty[15]) with *Taricha* "haploid hybrids" (enucleated eggs of one species fertilized by sperm of another) indicate that early cytoplasmic history does indeed condition the expression of genetic pigment pattern, and it is conceivable that this genic imprinting on the cytoplasm is stronger in *torosa* than in *rivularis*.

These considerations, to which I shall return later, are offered here as a background that may give some perspective in evaluating the results of the F_2 series immediately under consideration. Whatever the interpretation may be, the actual fact is that the pigment patterns segregating among the offspring are rather heavily weighted toward the *torosa* end of the *torosa-rivularis* spectrum.

In scoring the patterns five categories, again necessarily somewhat arbitrary, were established. At the two extremes are the contrasting patterns of normal *torosa* and normal *rivularis*. Midway between these is the pattern typical of *rivularis* ♀ × *torosa* ♂ F_1 hybrids, while the remaining two bridge the gaps between the *torosa* and hybrid patterns on the one hand, and between the hybrid and *rivularis* patterns on the other. These categories, and the scores for each, are as follows:

Torosa-type	Intermediate	Hybrid-type	Intermediate	*Rivularis*-type
15	20	15	11	0

One will note that whereas 15 were scored as *torosa*-type, not one was scored as *rivularis*-type. The closest approach in this series to the *rivularis* pattern is shown in Figure 9b; although the flank is rather profusely pigmented in this case, it is by no means as evenly or fully blanketed with melanophores as in *rivularis* itself. In those classed as *torosa*-type, on the other hand, the approximation of the normal *torosa* pattern is almost complete. Of the 15 in this category, 4, like the one shown in Figure 9a, were barely distinguishable from *torosa* and the resemblance shown by the remaining 11 was only slightly less striking. If pooled with a group of normal larvae of this species it is doubtful that they could be singled out without the most careful scrutiny. However, there are usually a few slight discrepancies, particularly the somewhat more dispersed arrangement of melanophores on the head, and

not long after the stage shown in the photograph an increase in the complement of these cells on the fin bears further evidence that complete segregation of *torosa* pigment genes is approached but perhaps never fully realized in the F_2 offspring.

This reference to increasing deviation of the *torosa*-type pattern from the normal *torosa* pattern as development continues should not be construed to imply that the early similarities are ephemeral in nature. In advanced larval stages the dorsal bands of the *torosa*-type individuals have somewhat fewer cells and are hence less compact than those of normal *torosa* larvae, but the basic resemblance to the *torosa* pattern is still as intact as ever. This applies equally to the series as a whole, within which all of the pattern types represented at hatching were still recognizable when the series was scored six weeks after the beginning of feeding.

The implications of this skewed distribution of pigmentary types in the F_2 generation are not entirely apparent to me, and undoubtedly can best be left to evaluation by readers with more training and experience in such matters. The results would be interpretable on the assumption that the *torosa* pattern is dominant to that of *rivularis*, but, as we have seen, the evidence from the F_1 hybrids concerning the extent of this dominance and its possible basis is not clear or consistent. If we postulate, as was suggested above, that the greater dominance of the *torosa* pattern in *torosa* ♀ × *rivularis* ♂ hybrids compared with *rivularis* ♀ × *torosa* ♂ hybrids is referable to factors associated with the *torosa* cytoplasm, then it would seem to follow that this dominance should diminish or possibly disappear in the F_2 generation, since the cytoplasm of the oocyte is now "generated" under the joint control of both *rivularis* and *torosa* genes. Unless we assume that even under these conditions the *torosa* alleles still play a somewhat dominant role in preconditioning the cytoplasm, it is difficult to grasp readily the reasons why *rivularis*-type pigment patterns are represented so weakly and infrequently among the F_2 segregants. However, as already emphasized, I have mentioned these considerations mainly to help define the problem for more expert evaluation of the results, and not in any confidence that I have discerned or properly construed all of the evidence inherent in the facts as presented.

In addition to the main difference between the *torosa* and *rivularis* pigment patterns, namely banded versus diffuse arrangement of the melanophores, there is a secondary difference that merits special reference here. In young larval *torosa* the few cells that escape incorporation into the bands never descend beyond the ventral margins of the developing somites, whereas in *rivularis* the blanket of melanophores extends well below this level of the flank. By surgical exchange of neural crest between embryos of the two species it has been shown [3, 16] that in *torosa* there is a barrier of unknown nature along the dorsal margin of the embryonic yolk mass that blocks the further dispersal of the migrating melanoblasts. Experiments of DeLanney[17] indicate that this barrier resides in the flank mesoderm.

In an early paper,[15] dealing primarily with the general problem of genetic controls in amphibian development, incidental reference was made to the question whether this feature of *torosa* pigmentation is inherited independently of banding itself or is somehow a concomitant of the latter. The answer is seemingly supplied by the present series, which includes occasional individuals possessing strong banding together with ventral complements of melanophores scattered freely over the yolk mass (Fig. 9c).

In no case in this series did the balancer attain the full size characteristic of normal *torosa*, but it was nevertheless well developed in the majority (48). In 4 cases, although present, it was quite vestigial, and in 9 it was completely absent.

Two other F_2 series of this same combination yielded a substantially smaller percentage of viable offspring, but otherwise the results were closely similar to those already described and for the most part require no separate treatment. For convenience I shall refer to the two series by their protocol designations, SH ♀ 6 and SH ♀ 8.

The female of Series 6 yielded 99 oviducal eggs. Fifty-seven of these were treated with a sperm suspension from a *rivularis-torosa* hybrid male, and the remainder with sperm from a normal *rivularis* male. Of the former, a substantial number later showed various degrees of abnormality in the early cleavage pattern. At the tailbud stage there were 28 survivors, and these were still developing normally at the hatching stage. The distribution of pigment pattern types was again heavily weighted toward the *torosa* side of the spectrum. Of the 42 eggs fertilized by *rivularis* sperm, a somewhat smaller fraction showed abnormal cleavage, but at the hatching stage the percentage of normal survivors was roughly the same (23 out of 42, compared with 28 out of 57). As was to be expected, the pigmentation of these larvae reflected the heavier contribution of *rivularis* genes by the male parent than in the series fertilized by hybrid sperm.

Before this female was sacrificed to obtain the oviducal eggs for artificial fertilization, she had already deposited 13 eggs that proved to be fertilized. It is of considerable interest that earlier, at the time the female was captured in the stream, she was in amplexus with a *rivularis-sierrae* hybrid male. Since the population of hybrid adults thus far established throughout planting efforts is still small, a mating encounter between a hybrid male and a hybrid female, whether of the same or different interspecific combination, is statistically an improbable event. We had considered it unlikely that in this instance the female, if inseminated at all at the time of capture, had been inseminated by the hybrid male clasping her at the moment. It is not unusual for male newts to clasp females after previous insemination by another male, or even after she has begun to ovulate.

All 13 eggs deposited by the female before she was sacrificed were in early cleavage stages the following day, although cleavage was abnormal in two of them. Of the latter, one became arrested at the blastula stage and the second, although continuing to develop, was microcephalic; the other 11 were completely normal at hatching. Thus a much higher percentage of eggs developed successfully than in either of the two groups from the same female that were later fertilized artificially. I mention this comparison because of its implication that normally spawned eggs may give a more reliable measure of the true degree of hybrid fertility than do those subjected to the hazards of artificial fertilization, and perhaps it is in this light that the lower percentages of viability in the other two series from this female can best be evaluated.

When the eleven normal members of the series were scored at hatching the character of the pigment patterns definitely supported the possibility mentioned above that the female had been inseminated by the hybrid *rivularis-sierrae* male clasping her at the time of capture. Compared with the series in which the eggs were fertilized artificially by *rivularis* sperm, the percentage of banded offspring was much

higher and the percentage approaching or approximating the diffuse *rivularis*-type pigmentation conspicuously lower. This is in keeping with the fact that *sierrae* larvae, like those of *torosa*, also have a banded pigmentation, even though the bands are less sharply defined than in the latter. However, this conclusion concerning the paternity of the series can best be left as tentative, since to support it fully one would need to make direct comparisons with larvae known definitely to be of the parentage that we have postulated.

The second of the two females now under consideration, SH ♀ 8, was in amplexus with a *rivularis* male when captured, but apparently had not been inseminated; when implanted with a pituitary gland, she later spawned 10 unfertilized eggs before being sacrificed to obtain eggs from her oviducts. There were 109 of the latter, and treatment with sperm from a *rivularis-torosa* male yielded a series numbering 60 embryos at the neurula stage and 40 survivors at the time of hatching. Several eggs were not fertilized or cleaved abnormally, whether because of inherent genetic defects or the hazards of artificial fertilization.

The distribution of pigment pattern types was about the same as in Series 2 and 6. Excellent dorsal bands, hardly distinguishable from those of normal *torosa*, were present in several cases, and again there were no larvae in which the *rivularis*-type pigment pattern was fully realized. Figure 10 shows four selected members of the series, grading from the best example of *torosa*-type pigmentation to the one that most nearly approached the pattern characteristic of *rivularis*. Balancers of various sizes, but never as large as in normal torosa, were present in 30 cases; absent in the remaining 10.

Finally, reference may be made to the one remaining stream-captured *rivularis-torosa* female (SH ♀ 7) whose eggs were artificially fertilized by sperm from a male of this same hybrid constitution. As we have seen, the percentages of viable offspring yielded by the other *rivularis-torosa* females, although variable, were in all cases substantial. In the present instance, however, the results were very poor, possibly because of attendant circumstances that will be mentioned shortly.

Sacrifice of the female following pituitary implantation yielded 90 oviducal eggs of which 56 were treated with a *rivularis-torosa* sperm suspension. In 23 of these cleavage was normal or essentially so, while the others were either unfertilized or cleaved abnormally. A week later, after the series had been transported from the field station to my laboratory at Stanford, it was found that all except a few of the embryos had died. There was some fouling of the water, possibly because the damaged and unfertilized eggs had not been removed from the dish, and I am inclined to believe that this accounts at least in part for the low survival. The other eggs from this female, fertilized by sperm of normal *rivularis*, met a similar fate, with only 3 surviving to the tailbud stage and 1 to hatching.

As in the case of two of the other hybrid females, this animal had deposited several eggs shortly before she was sacrificed. Of a total of 18, 12 of these eggs cleaved normally, 5 abnormally, and 1 was unfertilized. It was evident as early as the young tailbud stage that some of the embryos were becoming necrotic, and by hatching all except one had died. The eggs of this group had been deposited in a compact jelly cluster, and it is again probable that death was caused at least in part by the spread of infection. However, we have no sure means of distinguishing

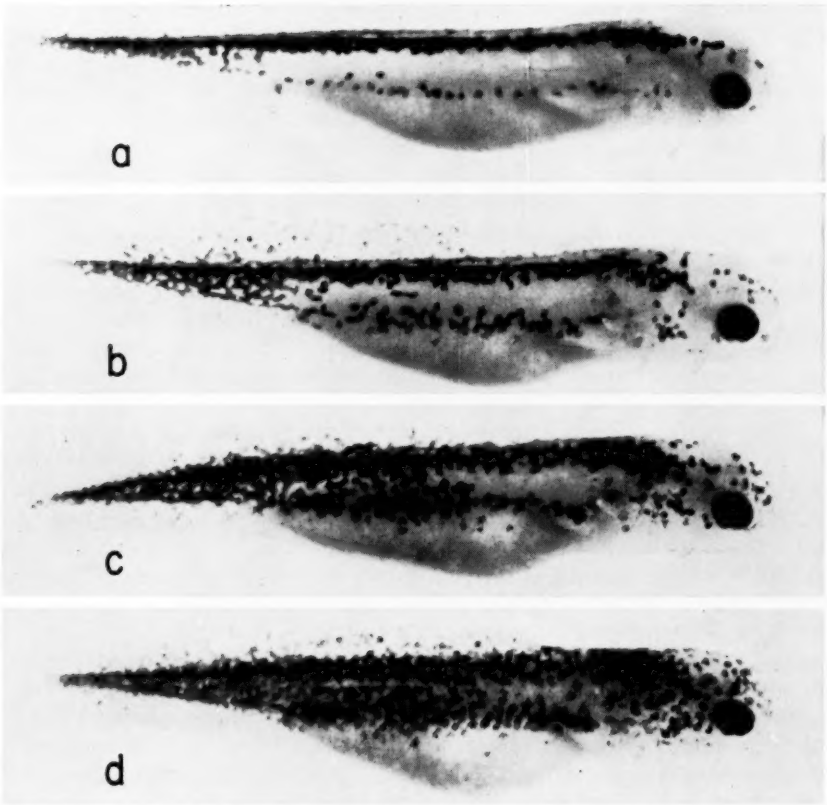

FIG. 10.—Members of a *rivularis-torosa* F_2 series selected to illustrate the spectrum of pigment patterns ranging from *torosa*-type (*a*) through intermediate types (*b* and *c*) to one (*d*) that approaches the *rivularis*-type pattern.

between the effects of environmental and genetic factors in evaluating this series, and speculation as to its significance is accordingly not profitable.

Taken at their face value the results with the four hybrid females described in this section of the paper would seem to indicate that hybrid fertility varies in degree with the individual, ranging from almost if not entirely complete fertility in some females to almost complete hybrid breakdown in others.[18] It is my personal conviction, based largely on the generally more successful development of eggs that are spawned naturally, that environmental factors account in considerable measure for many of the developmental failures encountered and that with further study we shall be able to confirm this. Especial interest will be attached to the results of natural matings and spawnings, when hybrids of both sexes are placed together within enclosures constructed in the breeding stream. This will be undertaken on an extensive scale during future breeding seasons, when we hope that hybrid females will be recaptured in increasing numbers.

Species Combination.—T. rivularis and T. t. sierrae: Since the results with this

combination of species are generally consistent with those already described for the various *rivularis-torosa* series, and involve almost identical issues, their presentation can be accomplished in much briefer compass.

As already indicated, *sierrae* shares many basic characteristics with *torosa*. Both species possess fully developed balancers; the larval pigmentation differs principally in that the dorsal bands of *sierrae* are less compactly formed and the flank melanophores somewhat more scattered and numerous; and in postmetamorphic stages both have a brightly pigmented iris and relatively little melanin pigmentation on the ventral surfaces of the limbs.

Rivularis ♀ × *rivularis-sierrae* ♂: Four series of artificial fertilizations totaling over a thousand eggs have been performed in this backcross combination, but since the results of one of these, SH ♂ 13, are thoroughly representative and our records of it somewhat more complete, I shall confine the description to this particular series.

One hundred fifty-three *rivularis* eggs were treated with a sperm suspension prepared from a *rivularis-sierrae* hybrid male. These yielded 127 normal embryos at the tailbud stage and 124 larvae at hatching. Of the latter, 71 survived through metamorphosis, and the mortality during the intervening period was almost certainly attributable primarily to the ordinary hazards of mass culture during the several months spanned by the larval period.

Larval pigment pattern: As in the backcross series involving *rivularis-torosa* hybrids, the pigment patterns emerging among the present series range between those typical of the F_1 hybrids and the *rivularis* parents. As would have been predicted, however, the contrast between these two patterns is not as great as in the former backcross; banding is not as perfect in *sierrae* as in *torosa*, and hence the banding is correspondingly less pronounced in F_1 *rivularis-sierrae* hybrids than in those of *rivularis-torosa*. The pigment pattern typical of young *sierrae* is illustrated in Figure 11 together with that of an F_1 *rivularis-sierrae* hybrid (Fig. 12). When the pigment patterns of the 124 members of the backcross series were scored at hatching, 48 were classified as "hybrid-type," 27 as "*rivularis*-type," and 49 as "intermediate" to these two.

Thus, just as in the *rivularis-torosa* backcross series, the high recovery of hybrid and *rivularis* patterns among the offspring again strongly suggests that the differences in larval pigment pattern distinguishing the species of *Taricha* derive from mutations affecting a small number of genes.

Balancer. In this same series the balancer was absent in 45 cases; present as a minute vestige on only one side in 5; paired but weakly developed in 36; and represented in the larger size typical of F_1 hybrids in 38.

Postmetamorphic characters. As in the *rivularis-torosa* backcrosses, the number of brightly colored chromatophores in the iris following transformation ranged from the relative profusion typical of F_1 hybrids to a very sparse representation approximating the completely darkened condition of the *rivularis* eye. Of 23 specimens scored several months following larval transformation, the iris pigmentation was essentially hybrid-type in 9, almost entirely black in 7, and intermediate in character in the reminaing 7.

Melanin pigmentation extended onto the ventral surface of the limb with much greater frequency in this series than in the corresponding *rivularis-torosa* back-

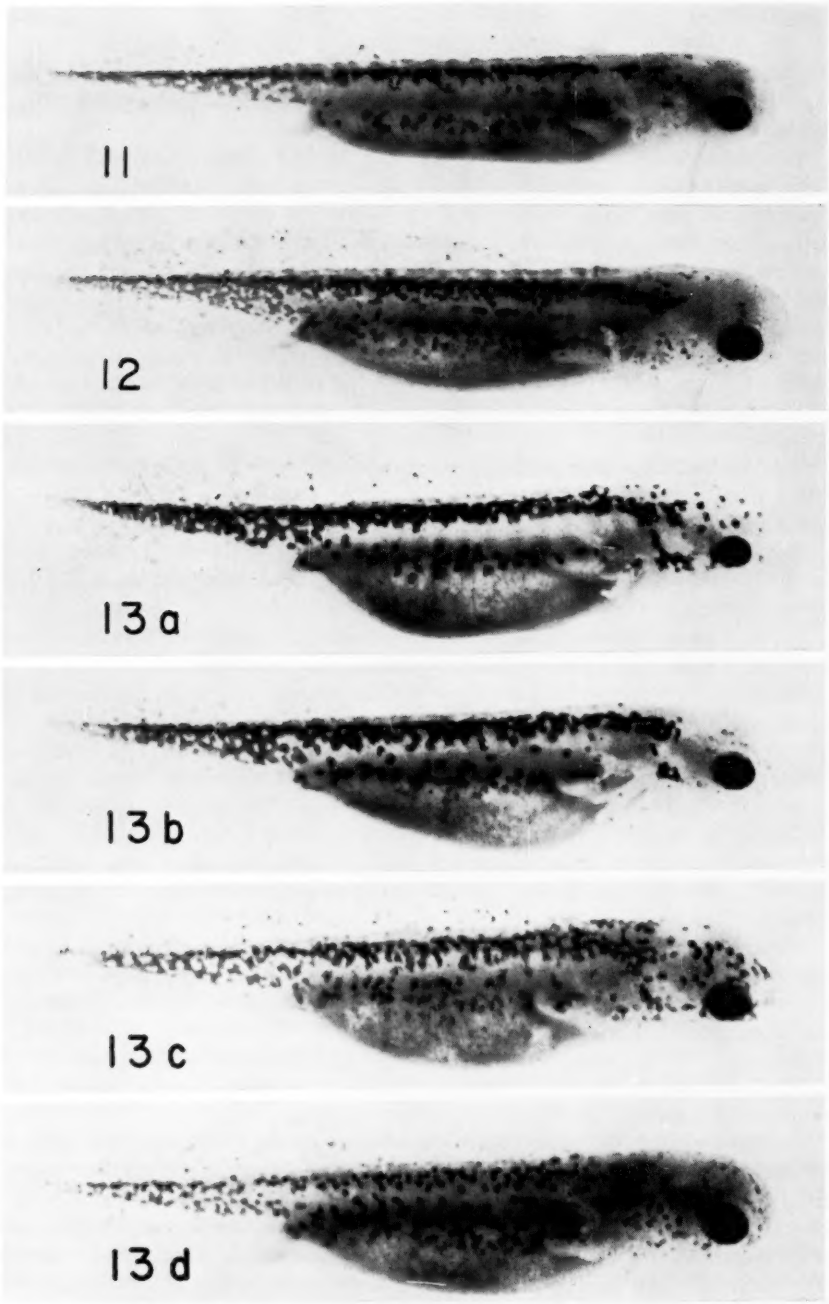

FIG. 11.—Normal *sierrae* larva.
FIG. 12.—*Rivularis* ♀ × *sierrae* ♂ hybrid larva. FIG. 13.—Members of a *rivularis-sierrae* F_2 series selected to illustrate segregation of *sierrae*-type (*a*), *rivularis*-type (*d*), and intermediate-type (*b* and *c*) pigment patterns.

cross series described earlier. However, subsequent examination showed that this condition was also fairly common in a laboratory-reared series of F_1 *rivularis-sierrae* hybrids of about the same age. This is somewhat unexpected since it is not characteristic of the mature *rivularis-sierrae* hybrids that we have recaptured in the experimental stream. The answer may lie in the report by Riemer[10] that although melanization of the under surface of the limb is not generally characteristic of *sierrae* it sometimes is found among populations from the region of the State of California (Butte and Plumas counties) where we collect material for our experiments. Since the *sierrae* males used for the artificial fertilizations are selected at random, specimens bearing this particular feature may well have introduced it into our hybrid stocks in individual series.

General body color was uniformly dark above and pink to red below in all members of the backcross series. In these respects they would be difficult to distinguish from F_1 *rivularis-sierrae* hybrids, which in turn are very similar in coloration to normal *rivularis* except for iris pigment and the degree of melanization on the under surface of the limbs.

Rivularis-sierrae ♀ × *rivularis-sierrae* ♂: The eggs of two stream-captured *rivularis-sierrae* females have been used for artificial fertilization by *rivularis-sierrae* sperm. Both females were in amplexus with *rivularis* males at the time of capture, and the subsequent deposition by one of these of a few fertilized eggs showed that she had been inseminated. Following pituitary implantation the two were sacrificed together and the oviducal eggs treated with the same sperm suspension. Excluding a few damaged by handling during artificial fertilization, one female yielded 37 eggs and the other 65; in both cases some mature eggs remained in the ovaries at the time of sacrifice.

Of the 37 eggs taken from the first female, cleavage was classified as normal or essentially so in 23, abnormal in 10, and 4 were unfertilized. At hatching, there were 24 survivors of which 4 showed varying degrees of abnormality or retardation. Survival in the other series was lower. Of the 65 eggs, cleavage was classified as abnormal in 35, and 4 were unfertilized. Twelve days later, after discarding abnormal embryos including some arrested in blastula stages, there were 21 survivors in early tailbud stages and 16 of these continued to develop normally thereafter; the remaining five were microcephalic or retarded.

When the normal survivors were scored at hatching for segregation of pigment patterns, using the same five categories employed for the corresponding *rivularis-torosa* series, the combined scores of the two groups were as follows:

Sierrae-type	Intermediate	Hybrid-type	Intermediate	*Rivularis*-type
3	8	11	12	2

If one compares these scores with the corresponding ones for the *rivularis-torosa* series given earlier, it will be noted that the distribution of pigmentary types is more symmetrical in the present series. The majority of the cases are about equally divided between the three middle categories, with both the *sierrae* and *rivularis* extremes poorly represented. Thus the partial dominance of *torosa* over *rivularis* genes in the control of pigment pattern does not seem to be shared by the genes of the subspecies, *t. sierrae*. This may well be related to the somewhat weaker tendency toward banding in *sierrae* as compared to *torosa*.

Figure 13 shows four young larvae illustrating the spectrum of patterns segregating among offspring of one of the two *rivularis-sierrae* females. The two extremes, *a* and *d*, were scored as *sierrae*- and *rivularis*-type patterns, respectively, although actually neither is completely typical of the patterns of the original parental species. There are more melanophores on the fin in *a* than would be present in *sierrae* at this stage (compare with Fig. 11), and the flank in *d* is not quite as fully or evenly blanketed with pigmentation as in normal *rivularis*. The resemblance in both cases is nevertheless strong, and again demonstrates that in F_2 hybrids of the species of *Taricha* it is possible to approach very closely the reconstitution of gene combinations responsible for highly distinctive differences between the original parental species.

Of the 36 larvae scored at hatching, 32 were still alive and vigorous in advanced larval stages at the time of writing a few months later. I mention this in order to emphasize that once the development of F_2 offspring is successfully launched their viability tends to continue unimpaired, except for the occasional mortalities that beset any group of larvae reared in laboratory culture.

Failures in early stages, at the time of fertilization and shortly thereafter, are of course another matter. As mentioned in the account of the *rivularis-torosa* series, one probably must assume from the high incidence of unsuccessful development in some series, including the present ones, that hybridization of the *Taricha* species is followed by variable degrees of true genetic breakdown.[19] At the moment, however, I feel that judgments on this issue can best be postponed until we have the opportunity during coming breeding seasons to establish the incidence of developmental failures among eggs of hybrid females that have mated and spawned naturally.

Evidence from cytological studies on the hybrid gonads will of course be equally if not more pertinent. Another approach, already initiated, will be the examination of tailtip preparations from the second generation larvae for any evidence of aneuploidy resulting from meiotic irregularities during gamete formation by the F_1 parents. My assistant, David Grant, has stained tailtips from numerous members of the *rivularis-torosa* and *rivularis-sierrae* F_2 series described in this paper, but the time-consuming and difficult task of studying these preparations for determination of chromosome numbers has only begun. Cursory examination reveals no obvious instances of aneupoidy, and H. G. Callan (personal communication) informs me that on the basis of his extensive experience with European newt hybrids the occurrence of viable aneuploids is somewhat improbable. If they are formed at all in our F_2 series, it is not unlikely that they are represented primarily among the embryos that are weeded out by failures of development before reaching the hatching stage at which tailtip preparations can first be made.

Discussion.—I have described in this paper the results of genetic tests with artificially produced F_1 interspecific *Taricha* hybrids that had grown to maturity in nature after release as young larvae. In view of the limited fertility of interspecific and even intraspecific hybrids of the widely studied European newts, the fertility of the *Taricha* hybrids has proved to be greater, and the development of their offspring more successful, than had actually been anticipated.

Lantz[20] and others have shown that female hybrids of the closely allied *Triturus cristatus* and *T. marmoratus* are fertile, but failure of chromosome pairing and

spermatid degeneration lead to infertility of the males.[21, 22] Spurway and Callan[23] have recently described an interspecific cross between *T. vulgaris* and *T. helveticus* that yielded a female who proved fertile when backcrossed to *helveticus*, but cytological study of one of the male hybrids revealed meiotic irregularities in a high proportion of the spermatocytes. These abnormalities are similar in kind but more extreme than in the hybrids of the subspecies of *T. cristatus* that have been studied so intensively and fruitfully by these same authors.[24, 25] In general they find reduced chromosome pairing in all the hybrid combinations studied, and marked variability in vigor as well as a high larval and metamorphic mortality among the backcross and F_2 offspring. Of especial interest is their conclusion that chromosomal translocations have been importantly involved in newt speciation. Cytological studies of the type they have made on meiosis during spermatogenesis and more recently on the lampbrush chromosomes of the oocytes[26] must be extended to *Taricha* if we are to evaluate fully the implications of our results with respect to hybrid fertility and the systematic affinities within the genus. In the meantime, however, it seems evident that the evolutionary separation of distinct species and subspecies of Californian newts has thus far led to less profound genetic isolation or incompatibility than exists between species and races of European *Triturus*. Although interbreeding in nature between the species of *Taricha* appears to be extremely rare, artificially produced hybrids are highly viable, and of the several combinations that have been tested for hybrid fertility, most of the individuals have yielded very successful series of backcross and F_2 offspring. The incidence of developmental failures in the second generation has been much lower following natural matings and spawning of the F_2 hybrids, and it is believed that hazards of artificial fertilization account in part for the variable success among some of the individual series described.

Altogether, our results suggest that, to a greater extent than in European *Triturus*, the species of *Taricha* have arisen and their integrity has been preserved more through the establishment of effective reproductive barriers[27, 28] (believed to be primarily ethological) than by the subsequent or concomitant differentiation of basically incompatible genomes. However, the evidence from the backcross and F_2 series strongly suggests, and cytological studies will almost certainly confirm, that there is indeed some true genetic breakdown in the F_1 hybrids and to this extent our studies support and justify the taxonomic recognition of *torosa*, *rivularis*, and *granulosa* as distinct forms worthy of full specific status. "Abnormality of meiosis in at least one sex is the minimum condition for making (or recognizing) specific distinction between two parent forms."[23]

Even though incomplete, hybrid fertility is great enough to add considerable interest to the future of our hybrid planting program. It is already established that the hybrids will mate effectively in nature with the native maternal species, *rivularis*, and if accomplished on a sufficient scale this backcrossing might lead to significant modification of the native gene pool.[29] In view of the slowness with which generations of Californian newts succeed one another, as well as the present uncertainty concerning the size of the hybrid population that we can hope to establish, I am not overly sanguine about the prospects of an early or far-reaching impact of this introgressive hybridization, but it is obviously a feature that will bear watching if the program can be perpetuated over a sufficient number of years.

The species of *Taricha* lend themselves better than most amphibians to the study of segregation ratios in second-generation offspring because of the striking differences that distinguish the early developmental stages of the parental forms. Differences in early larval pigmentation are especially distinctive, such as the sharp dorsal bands in *torosa* contrasted to the uniformly dispersed blanket of melanophores on the flank of *rivularis*. When F_1 *rivularis-torosa* hybrids are backcrossed to *rivularis*, the high incidence among the offspring of patterns characteristic of the hybrid and *rivularis* parents immediately suggests that the number of genes responsible for the differences between the larval pigmentation of *torosa* and *rivularis* must be quite small. Scoring of other characters, such as the size or presence of the larval organ known as the "balancer," and the coloration of the eye and skin in postmetamorphic stages, indicate that these differences as well have arisen through mutations affecting relatively small numbers of genes. Spurway,[25] in discussing the results that she and Callan have obtained with European newt hybrids, refers to the reconstruction of the parental species within two generations, "suggesting selection for genotypes carrying the most allelomorphs from the same species. This selection is so strong that a species can be reconstructed, apparently without any allelomorph exchange, in two generations from the interspecific mating. . . . This pseudolinkage would be expected as a result of the parental gametes differing by translocation." In our second generation *Taricha* hybrids the various characters have seemed to segregate quite independently of one another, but we have admittedly not analyzed our data in sufficient detail to establish that their redistribution is completely random.

The possible dominance of *torosa* over *rivularis* alleles in the control of pigmentation, as suggested by the high frequency of *torosa*-type patterns among F_2 *rivularis-torosa* offspring, was discussed in the descriptive section of the paper and merits no further comment here.

In earlier, strictly embryological, studies[4, 16] with the species of *Taricha* I have analyzed in considerable detail the developmental basis of the striking difference between larval pigmentation in *torosa* and *rivularis*. After leaving the neural crest the embryonic melanophores at first assume a scattered distribution over the flank in both species. In *rivularis* this distribution is permanent, but in *torosa* the melanoblasts soon withdraw dorsally to become compacted into paired bands high on the back. This dorsal reaggregation of previously dispersed melanophores is a genetically fixed predisposition of *torosa* pigment cells, expressing itself equally well when *torosa* crest is grafted to the mid-dorsal line of *rivularis* hosts. Its manifestation is dependent, however, on conditions that are not species specific, namely upon influences exerted primarily by the underlying somites over which the melanoblasts have initially spread. If before departure of the melanoblasts from the neural crest the somites are inverted surgically, the melanophores later aggregate at the lower (originally upper) margins of the inverted somites instead of dorsally as in normal development.

This identification of the melanoblast itself as the principal target of genetic factors differentiating *torosa* and *rivularis* pigmentary behavior thus serves to complement the results of the present study, in pointing to the mode and site of action of the genes segregating in the second-generation offspring of *torosa-rivularis* hybrids.

Conclusions.—*Taricha rivularis* × *T. torosa torosa* and *T. rivularis* × *T. t. sierrae* F_1 hybrids produced in large numbers by artificial cross-fertilization and released as larvae or newly metamorphosed juveniles in a selected experimental stream have been recaptured as mature adults and used for tests of their fertility and for genetic analysis of the characteristics distinguishing the species of *Taricha*.

Fertility of the hybrids and viability of the second-generation offspring were high in most of the backcross and F_2 series, indicating that the evolutionary separation of the forms of *Taricha*, and the preservation of their integrity through ethological and other mechanisms of reproductive isolation, have been achieved without the differentiation of basically incompatible genomes. This fact, together with the observation that the F_1 hybrids will mate voluntarily and effectively with the native *rivuliris* adults, suggests that our planting program may lead eventually to modification of the local gene pool through introgressive hybridization.

Segregation ratios in the second-generation offspring indicate that the characteristics distinguishing the species of *Taricha*, such as larval pigment pattern, presence or absence of the "balancer," color of the adult skin and iris, etc., are each referable to mutations affecting a very limited number of genes. These various characters appear to segregate independently of one another; there is little if any discernible tendency toward the reconstitution of the parental species through backcrossing or interbreeding of the F_1 adults.

Inheritance of the characters studied is mostly on a "blending" basis, although there is evidence of partial dominance of *torosa* over *rivularis* alleles in the control of larval pigment pattern.

This paper is DEDICATED TO THE MEMORY OF ROSS G. HARRISON as an inadequate token of my admiration and affection for him.

I wish to acknowledge the invaluable aid given by several graduate students and assistants, particularly James Duncan, Oscar Anderson, David Grant, and Herbert Little who have been associated with the project during the recent period when the results of the hybrid planting program have first begun to materialize. I am also heavily obligated to Roy and Ruth Hedgpeth and to the subsequent owners of the ranch where my field station is situated, as well as to members of the Radtkey family who operate the ranch, for many privileges and courtesies extended to me.

* This study was supported by grants from the Program of Systematic Biology, National Science Foundation.

[1] Twitty, V. C., *Copeia*, No. 2, 66 (1942).

[2] Twitty, V. C., *J. Expll. Zool.*, **74**, 239 (1936).

[3] Twitty, V. C., and D. Bodenstein, *ibid.*, **81**, 357 (1939).

[4] Twitty, V. C., *ibid.*, **100**, 141 (1945).

[5] Twitty, V. C., *ibid.*, **129**, 129 (1955).

[6] Twitty, V. C., *Science*, **130**, 1735 (1959).

[7] Twitty, V. C., *Vertebrate Speciation: A Symposium* (Austin: University of Texas Press, 1961).

[8] Chandler, A. C., *Oreg. State Coll. Agr. Expt. Sta. Bull.*, **152**, 1 (1918).

[9] Miller, M. R., and M. E. Robbins, *J. Expll. Zool.*, **125**, 415 (1954).

[10] Riemer, W. J., *Univ. Calif. Publ. Zool.*, **56**, 301 (1948).

[11] Barden, R. B., *J. Expll. Zool.*, **90**, 475 (1942).

[12] Barden, R. B., *ibid.*, **92**, 171 (1943).

[13] Comparison of postmetamorphic specimens shows that at this stage *rivularis* ♀ × *torosa* ♂ and *torosa* ♀ × *rivularis* ♂ hybrids are very similar in pigmentation. The former are somewhat darker on the average, with few individuals that would be classified as "light," but approximately

the same range of coloration exists in each group. The iris pigmentation is essentially identical in both.

[14] Dalton, H. C., *J. Exptl. Zool.*, **103,** 169 (1946).

[15] Twitty, V. C., *Biol. Symposia,* **6,** 291 (1942).

[16] Twitty, V. C., *Symp. Soc. Growth and Devel.*, **9,** 133 (1949).

[17] DeLanney, L. E., *J. Exptl. Zool.*, **87,** 323 (1941).

[18] The results with laboratory-reared females are consistent with this interpretation. Hybrids grown in the laboratory become sexually mature at a considerably smaller body size, and the number of eggs in the ovaries is correspondingly smaller. Six *rivularis-torosa* females implanted with pituitary glands yielded a total of 148 oviducal eggs that were treated with *rivularis* sperm suspensions. As with the stream-capture females, the percentages of fertilization and normal cleavages were variable. In the best series, 28 out of 30 eggs developed completely normally to the hatching stage (18 survived metamorphosis); while at the other extreme most of the 33 eggs yielded by one female cleaved abnormally and only 4 developed successfully to hatching. Altogether, 63 of the 148 eggs reached hatching and 31 survived through metamorphosis.

[19] As in the case of *rivularis-torosa* females, the results with laboratory-reared hybrids are consistent with those using stream-captured animals. Seven *rivularis-sierrae* females grown in the laboratory yielded a total of 179 eggs that were treated with sperm from *rivularis* males. Seventy-six of these developed to hatching and 38 through metamorphosis. In the best series, 24 out of 26 eggs developed to hatching and 13 through metamorphosis, while in the poorest series the same number of eggs (26) produced only one survivor to the tailbud stage and none to hatching.

[20] Lantz, L. A., *Proc. Zool. Soc. London,* **117,** 247 (1947).

[21] White, M. J. D., *J. Exptl. Zool.*, **102,** 179 (1946).

[22] Lantz, L. A., and H. G. Callan, *J. Genet.*, **52,** 165 (1954).

[23] Spurway, H., and H. G. Callan, *ibid.*, **57,** 84 (1960).

[24] Callan, H. G., and H. Spurway, *ibid.*, **50,** 235 (1951).

[25] Spurway, H., *Soc. Exp. Biol., Symp.*, **7,** 200 (1953).

[26] Callan, H. G., and L. Loyd, *Phil. Trans. Roy. Soc. London, Ser. B,* **243,** 135 (1960).

[27] Mayr, E., *Systematics and the Origin of Species* (New York: Columbia University Press, 1942).

[28] Dobzhansky, Th., *Genetics and the Origin of Species* (New York: Columbia University Press, 1953).

[29] Stebbins, G. L., *Proc. Am. Phil. Soc.*, **103,** 231 (1959).

ORGANIZATION OF THE SALIVARY-GLAND CHROMOSOME AS REVEALED BY THE PATTERN OF INCORPORATION OF H^3-THYMIDINE, †*

BY PHILIP S. WOODS,[‡] H. GAY, AND A. ŞENGÜN[§]

BROOKHAVEN NATIONAL LABORATORY, UPTON, NEW YORK, AND CARNEGIE INSTITUTION OF WASHINGTON, COLD SPRING HARBOR, NEW YORK

Communicated by Berwind P. Kaufmann, June 27, 1961

The salivary-gland chromosome of the fully developed dipteran larva is generally regarded as an aggregation of closely appressed subsidiary strands or chromonemata.[1] This pattern of organization is presumably determined by the uncoiling, growth, and replication of the four chromonemata derived from the mitotic-type progenitor chromosomes. The basic number, four, is established by the pairing and synapsis of homologues, each containing two microscopically separable chromonemata.[2] Assumedly this basic number increases, in the salivary-gland chromosome of *Drosophila melanogaster*, to an eventual total of approximately 2048 or

4096 during larval life as a result of a series of successive endomitotic replications. Evidence in support of this numerical increase has been obtained from measurements of the deoxyribonucleic acid (DNA) content of the chromosomes at different stages of their development,[3] and from counts and measurements of the strands as seen in electron micrographs of chromosomes of third-instar larvae.[4]

Despite the wealth of evidence favoring the concept of multistranded or polytene salivary-gland-chromosome structure, other interpretations have been advanced. One group of theories rests on the belief that the cross striations or bands seen in squash preparations represent surface manifestations of a pair of coiled threads,[5] or segments of such threads that have become disrupted in the course of ontogeny.[6] Another group of theories is based on the assumption that the salivary-gland chromosome retains its basic quadripartite structure throughout development but that hypertrophy of the chromonemata and modification of the component chromomeres lead to the appearance of alternating band and interband regions.[7]

What seems to be needed at this point is evidence about the fate of individual chromonemata in the course of chromosome growth. Methods of autoradiography offer promise of meeting the requirement. The pattern of incorporation of tritium-labeled thymidine into the newly synthesized DNA of growing salivary-gland chromosomes of *D. melanogaster* has therefore been tested. The results lend further support to the theory that the giant chromosomes are multistranded or polytene, and that the strands are highly stable entities.

Materials and Methods.—Two series of experiments were undertaken with larvae of the Swedish-B wild-type strain of *D. melanogaster* grown at 15–17°C. In the first, young larvae were obtained from hatching eggs and placed in a small container on a radioactive medium that had been heat-sterilized for a few minutes. This medium consisted of 0.63 gm of the standard cornmeal-molasses-agar mixture,[8] 0.08 gm of yeast, and 28.4 μg of H^3-thymidine (Schwarz Laboratories, Inc.). The thymidine had a specific activity of 244 mc/mM; the total amount of isotope in the medium was 28.6 μc. The duration of the treatment was either 24 hr, 49 hr, or the entire larval life. After the 24- and 49-hr treatments, the larvae were transferred to a nonlabeled medium and kept there until they were preparing to pupate, when the salivary glands were removed.

In the second set of experiments, young larvae were treated for either 1, 3, 6, or 12 hr on a labeled medium, similar to that described above but containing H^3-thymidine with a specific activity of 1600 mc/mM. The larvae either were transferred directly to the radioactive medium upon hatching or were placed on a nonlabeled medium for 24, 72, or 120 hr before transfer to the labeled medium (Fig. 1). After the radioactive treatment, all larvae again were transferred to the standard (nonradioactive) cornmeal-molasses-agar mixture and kept until late third instar, when the salivary glands were removed.

To prepare the material for autoradiography, the salivary glands were fixed in 45% acetic acid. Squash preparations were made and frozen on "dry ice" to facilitate removal of the cover slips. Cellular materials adhering to the slides were then hydrolyzed in 1 *N* HCl at 60° for 10 min and stained by the Feulgen method for localization of DNA. Stripping film was applied, and autoradiographs were prepared as described by Taylor.[9] The phase contrast microscope was used to facilitate observation of fine structure, especially of the interband regions.

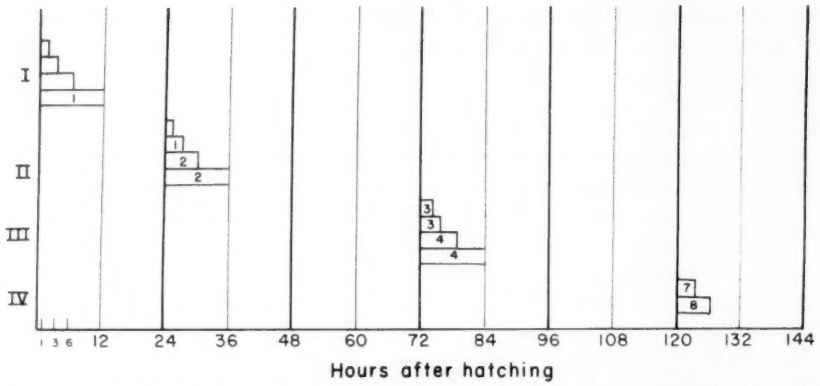

FIG. 1.—Diagrammatic representation of experimental procedure for treatment of *Drosophila* larvae by exposure to food containing tritiated thymidine. Bars indicate beginning and duration of treatments. Larval cultures were maintained at 17°C. Figures within bars represent the approximate numbers of grains observed across the width of any chromosomal band in autoradiographs of late-third-instar salivary-gland squash preparations. I, II, III, IV refer to different experiments.

Results.—Incorporation of H^3-thymidine in salivary-gland chromosomes may be considered with respect to their linear and their lateral organization. In terms of linear distribution, the radioactive materials appear to be restricted to the banded regions, where, to judge by the Feulgen test, the DNA is located. The preparation illustrated in Figure 2 was obtained from a larva that had been allowed to feed continuously throughout its life (11 days) on the H^3-thymidine-containing medium. In this preparation, radioactive material seemed to be restricted primarily to the heavier bands. The preparations illustrated in Figures 3 and 4 were obtained from larvae that had been treated for 49 hr on the labeled medium before growth for 9 days on unlabeled medium. Again, radioactivity appeared primarily in the banded regions.

With respect to lateral distribution, it is apparent that the spread of radioactivity across the breadth of the chromosome was dependent partly on the length of time the young developing larvae were permitted to ingest the labeled DNA precursor and partly on the stage of development of the larvae when they received the radioactive food. When larvae were fed H^3-thymidine either continuously throughout life or during the first 49 hr, the label extended across the entire chromosome (Figs. 2, 3, and 4). When the larvae were fed on labeled medium during the first 24 hr of life, only isolated silver grains appeared at any given locus along the chromosome (Figs. 5, 6, and 7). When larvae were treated for shorter periods (12 hr or less), but at later stages of development, the label again extended across the entire chromosome. This point is illustrated in Figure 1. The numbers in the rectangles represent approximate numbers of silver grains appearing across the width of the chromosome at any band. It can also be noted from this diagram that the rate of incorporation of H^3-thymidine in the developing chromosome is not constant. The rate evidently increases with increasing larval age.

Closer study of the autoradiographs of preparations from larvae treated for 24 hr with H^3-thymidine, or for shorter periods of time during the first days of larval life,

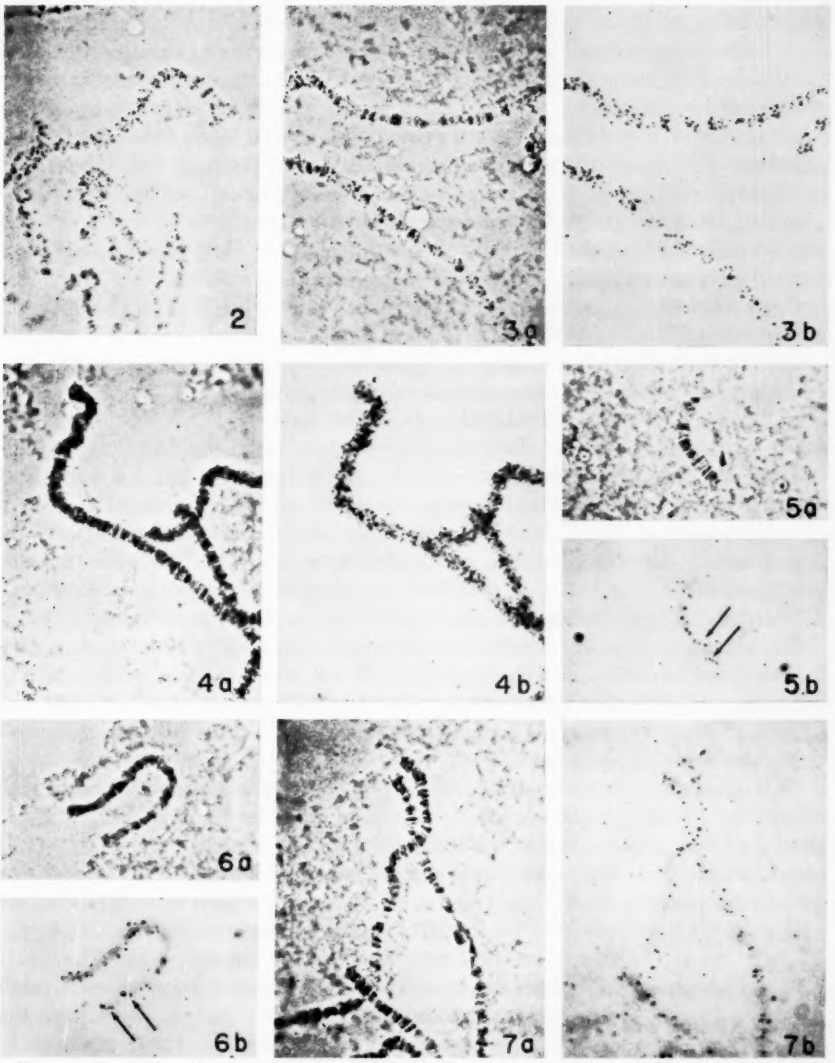

FIGS. 2–7.—Autoradiographs of salivary-gland chromosomes of late-third-instar *Drosophila* larvae that had been placed on food containing H^3-thymidine immediately after hatching. Glands were squashed in 45% acetic acid and stained by the Feulgen reaction. Stripping film was exposed for 82 days, except that illustrated in Figure 2, which was exposed for 30 days.

FIG. 2.—Autoradiograph of a chromosome from a larva fed continuously (11 days) on H^3-thymidine food.

FIG. 3.—Well-stretched chromosome (*a*) and its autoradiograph (*b*) from a larva fed for 49 hr on H^3-thymidine food and then for 9 days on the standard mixture.

FIG. 4.—Chromosome (*a*) and autoradiograph (*b*) of a larva treated for 49 hours with radioactive food and then transferred to unlabeled medium.

FIG. 5.—Small portion of a chromosome (*a*) and its autoradiograph (*b*) from a larva treated for 24 hr with H^3-thymidine food. Arrows indicate two short rows of dots.

FIG. 6.—A chromosome (*a*) and its autoradiograph (*b*) from a larva fed H^3-thymidine for 24 hr. Arrows indicate two short rows of dots.

FIG. 7.—Chromosome (*a*) and its autoradiograph (*b*) from a larva treated for 24 hr.

revealed that often the isolated silver grains were oriented in short but continuous rows (especially clear in Figs. 5*b*, 6*b*, and 7*b*). These rows of radioactivity traversed a number of bands and extended either parallel with or at a small angle to the longitudinal axis of the chromosome. Those that formed a small angle occurred often as pairs of diagonals and seemed to follow the natural twist of the chromosome, as indicated by the arrows in Figures 5*b* and 6*b*. It was also apparent that portions of the length of a chromosome were unlabeled, weakly labeled, or labeled in such a way that the silver grains did not form rows. The fact that some parts were unlabeled indicates that the autoradiographs of other parts were really due to disintegrating tritium atoms and not to false images caused by pressure.

Interpretation and Discussion.—These studies are consistent with the earlier contentions of Taylor, Woods, and Hughes[10] that DNA occurs in the form of a unit extending throughout the length of the chromosome, and that once it has been formed during replication the unit remains intact through succeeding replications (except for possible interstrand exchanges, to be discussed later). In the present study, the longitudinal rows of radioactivity, detected when the H^3-thymidine feeding period was limited to the first 24 hr of larval life, can be interpreted as evidence that new DNA is laid down as part of a unit that extends throughout the length of the chromosome and occupies only a small part of the cross-sectional area of the chromosome. It cannot, of course, be determined whether the unit is composed of a single strand of DNA molecules connected end to end or a bundle of such DNA strands lying parallel with one another, or whether it is composed of many DNA molecules attached perpendicularly along a backbone strand of some non-DNA-containing material, such as protein. In any event the mature chromosome might be an aggregation of these units. The fact that the pattern of incorporation of H^3-thymidine is maintained through 9 or 10 replication cycles also reflects the extreme stability of the units contributing to the structure of the chromosomes.

In the preparations that exhibit rows of radioactivity, the rows are always relatively short, usually traversing no more than about 15 or 20 bands. Inability to trace the silver grains along the full length of any single strand is probably due to a number of factors. The low initial energy (0.018 Mev) of the beta particle emitted by tritium is an important consideration. In material of unit density, 90% of the beta particles have a range of 1.2 microns or less.[11] The vertical diameter of these strongly squashed chromosomes was measured as approximately 2 microns. It is evident that most of the silver grains appearing in an autoradiograph must result from disintegrations close to the upper surface of the chromosome; those deeper in the chromosome would not be recorded. The natural twisting characteristic of the chromosomes would limit to short linear distances the proximity of a given strand to the stripping film. Another possibility is that portions of a labeled strand exchange with corresponding portions of an unlabeled strand, so that after a number of replications labeled segments become far removed from their original positions. Such exchanges have been frequently observed in sister chromosomes of plant root-tip cells, when sufficient time has been allowed for the cells to undergo a second division after brief treatment with H^3-thymidine.[10, 12] It may also be that the strands do not replicate simultaneously at all points along their length. Recent studies suggest that such asynchronous replication is of common occurrence in many materials.[13]

The results of this study also lend further support to the concept that the giant

chromosomes form as a result of a series of endomitotic replications of component strands. Salivary-gland chromosomes increase in volume many hundreds of times during development, and it is clear that part of this increase is due to the formation of new DNA. The question of how the new DNA is laid down in the developing chromosome is of prime importance. The fact that rows of radioactivity are seen in the fully developed chromosomes of larvae receiving short and early treatment would indicate that the DNA is laid down as a strand which persists. Because of the nature of the experiment, this conclusion can be applied only for the DNA that is first synthesized. DNA synthesized later in development might conceivably be laid down as a simple accumulation on the four original chromonemata, as Kodani[7] has proposed, but this interpretation is difficult to accept in the light of the present findings. The fact that the rate of incorporation of H^3-thymidine is not constant, but rises in the developing chromosomes, suggests that DNA is not laid down as a simple accumulation on pre-existing nonduplicating strands. Labeled DNA appears to increase geometrically in these chromosomes, as might be expected if the strands replicate according to the present concept of endomitosis. The hypotheses of Hovanitz[5] and Kosswig and Şengün[6] apparently are incorrect: according to their interpretations, the label (in the short- and early-treatment experiments) should appear randomly across the entire width of the chromosomes.

When the period of time afforded for ingestion of H^3-thymidine is extended to 49 hr (Figs. 3 and 4 compared with Figs. 5, 6, and 7), the silver grains increase greatly in number and extend completely across the chromosome. It might appear on first appraisal, in conformity with the tenets of the polytene hypothesis, that replication of chromonemata proceeds at an extraordinarily rapid pace during the second day of larval life. An evaluation in quantitative terms indicates, however, that this is not necessarily the case. If the four original chromonemata were replicated in the presence of H^3-thymidine, the four new strands could be expected to contain radioactive DNA whereas the original four remained unlabeled. A second replication involving the incorporation of H^3-thymidine would account for eight additional labeled chromonemata, if all were duplicated, producing at the end of two endomitotic cycles a ratio of three labeled strands to one unlabeled. A third cycle would increase this ratio from three-to-one to seven-to-one. Such chromosomes would appear "filled" with radioactive strands. When the organization of these chromosomes is considered in terms of multiplication of intertwined chromonemata, moreover, it is not surprising to find little difference in appearance between autoradiographs of chromosomes exposed to H^3-thymidine for only 2 days (Figs. 3 and 4) and those of chromosomes exposed throughout the full 11 days of larval life (Fig. 2). In fact, this point is most clearly emphasized by the observation that the autoradiographs of chromosomes labeled for only a few hours late in larval development (3 to 6 hr during the sixth day of the third-instar period) were completely filled with radioactive strands, because the chromosome at this stage presumably has many duplicating strands.

Linear as well as lateral patterns of chromosomal organization were analyzed. Silver grains were detected in the stripping film above the characteristic banded regions of the salivary-gland chromosomes, but not above regions that were unequivocally interbands. This finding leads to the conclusion (in essential conformity with earlier studies utilizing the Feulgen reaction, digestion with deoxyribonuclease,

ultraviolet absorption, form birefringence, X-ray absorption and microinterferometry, and microincineration) that DNA is not distributed uniformly along the strands, but is concentrated strongly in regions that correspond with the bands and less concentrated or lacking in regions that correspond with the interbands. It should be stressed, however, that autoradiography, like Feulgen stainability and the other methods for detection of DNA, indicates only relative concentration, so that areas in which radioactivity was not detected might show indications of its presence if the exposure time were longer. The question of whether any DNA occurs in the interbands remains to be answered.

Summary.—Methods of autoradiography, involving incorporation of H^3-thymidine in the salivary-gland chromosomes of young developing larvae of *D. melanogaster*, have been used to determine lateral and linear patterns of organization in fully developed chromosomes. The findings are consistent with the view (1) that DNA occurs as a unit, which traverses the bands and extends along the full length of the chromosome; (2) that the unit occupies only a small part of the cross-sectional area of the chromosome and therefore constitutes a single strand among many; (3) that this entity remains intact during succeeding replications (except for possible interstrand exchanges); and (4) that DNA may not be distributed uniformly along the strands, because radioactivity appears to be concentrated primarily in regions that correspond to the bands.

The authors gratefully acknowledge the counsel and encouragement of Dr. Berwind P. Kaufmann throughout the course of this work.

* Research carried out at Brookhaven National Laboratory, Upton, New York, under the auspices of the United States Atomic Energy Commission, and at the Carnegie Institution of Washington, Cold Spring Harbor, New York (with the support of USPHS research grant RG-149)

† A brief statement of the findings were reported on p. 383 of *Carnegie Institution of Washington Year Book 56*, (1957), and on p. 72 of Abstracts for the 10th International Congress of Cell Biology Paris, France, September, 1960.

‡ Present address: Department of Biology, University of Delaware, Newark, Delaware.

§ Fellow of the Carnegie Institution of Washington, 1957. Permanent address: Zooloji Enstitüsü, Fen Fakültesi, Bayazit, Istanbul, Turkey.

[1] Supporting evidence has been summarized by Alfert, M., *Intern. Rev. Cytol.*, **3**, 131–169 (1954); Beermann, W., *Chromosoma*, **5**, 139–198 (1952); Gay, H., *Dissertation Abstr.*, **15**, 899–900 (1955); Kaufmann, B. P., H. Gay, and M. R. McDonald, *Intern. Rev. Cytol.*, **9**, 77–127 (1960).

[2] Kaufmann, B. P., *J. Morphol.*, **56**, 125–155 (1934) reported that somatic pairing in *D. melanogaster* involves lateral approximation of longitudinally split chromosomes, which then become closely appressed or intertwined.

[3] Kurnick, N. B., and I. H. Herskowitz, *J. Cellular Comp. Physiol.*, **39**, 281–299 (1952); Swift, H., and E. M. Rasch, *J. Histochem. and Cytochem.*, **2**, 456–458 (1954).

[4] Gay, H., *J. Biophys. Biochem. Cytol.*, 2 Suppl., 407–414 (1956); Kaufmann, B. P., H. Gay, and M. R. McDonald, *Intern. Rev. Cytol.*, **9**, 77–127 (1960). Larger numbers have been reported in salivary-gland chromosomes of *Chironomus* by W. Beermann and G. F. Bahr, *Exptl. Cell Research*, **6**, 195–201 (1954).

[5] Hovanitz, W., these PROCEEDINGS, **42**, 609–613 (1956).

[6] This interpretation has been supported most vigorously in recent years by C. Kosswig and A. Şengün (e.g., Şengün, A., *Rev. Fac. Sci. Univ. Istanbul, Ser. B*, **16**, 1–44 (1951)).

[7] Kodani, M., *J. Hered.*, **33**, 114–133 (1942); Goldschmidt, R., and M. Kodani, *Am. Naturalist*, **76**, 529–551 (1942).

[8] The formula is given in *Drosophila Guide*, by M. Demerec and B. P. Kaufmann, 7th ed. (Washington, D. C., Carnegie Institution of Washington, 1961).

[9] Taylor, J. H., in *Physical Techniques in Biological Research*, (New York: Academic Press, 1956).

[10] Taylor, J. H., P. S. Woods, and W. L. Hughes, these PROCEEDINGS, **43**, 122–128 (1957).

[11] Fitzgerald, P. J., M. L. Eidinoff, J. E. Knoll, and E. B. Simmel, *Science*, **114**, 494–498 (1951).

[12] Taylor, J. H., *Genetics*, **43**, 515–529 (1958).

[13] Lima-de-Faria, A., *J. Biophys. Biochem. Cytol.*, **6**, 457–466 (1959); Taylor, J. H., *J. Biophys. Biochem. Cytol.*, **7**, 455–463 (1960); Pelc, S. R., and F. L. La Cour, in *The Cell Nucleus* (New York: Academic Press, 1960); Wimber, D., *Exptl. Cell Research*, **23**, 402–407 (1961).

ON THE SUPERSOLVABILITY OF BICYCLIC GROUPS

BY JESSE DOUGLAS

THE CITY COLLEGE OF THE CITY UNIVERSITY OF NEW YORK

Communicated July 12, 1961

1. By a *bicyclic* group G, we mean a finite group each of whose elements is expressible in the form A^xB^y where A,B are fixed elements of G. In other words, $G = \{A\}\{B\} = \{B\}\{A\}$, where $\{A\}$, $\{B\}$ denote the cyclic groups generated by A,B respectively. In case $\{A\} \cap \{B\} = \{1\}$, the bicyclic group will be termed *exact*.

A finite group G is called *supersolvable*[1] when it has a chief (or principal) series whose indices are all prime numbers, i.e.,

$$G = G_0 > G_1 > \ldots > G_{i-1} > G_i > \ldots > G_n = \{1\},$$

G_i invariant in G, $G_{i-1}:G_i$ (the index of G_i in G_{i-1}) a prime for $1 \leqq i \leqq n$. The group $\{1\}$ will also be considered supersolvable.

B. Huppert has proved that every bicyclic group is supersolvable.[2] He also mentions an unpublished proof by N. Itô. The following quite elementary proof, which is a by-product of the author's work on exact bicyclic groups,[3] may be of interest.

2. First, it is obvious that any homomorphic image of a bicyclic group is bicyclic. Equivalently stated, the factor group G/N of a bicyclic group G with respect to any normal (invariant) subgroup N is also bicyclic. The supersolvability of G will then follow by induction if we can prove that every bicyclic group $\neq \{1\}$ contains a normal subgroup of prime order, N_p. For, if the chain

$$G' = G_0' > G_1' > G_2' > \ldots > G_n' = \{1\}$$

exhibits the supersolvability of $G' = G/N_p$, then the counter-images in G with the identity adjoined, namely,

$$G = G_0 > G_1 > G_2 > \ldots > G_n = N_p > \{1\},$$

exhibit the supersolvability of G. This is because the properties of invariance in the entire group, and the primality (indeed, the numerical values) of the indices $G_i':G_{i-1}'$ are preserved in the passage from G' to G by the inverse of the natural homomorphism of G into G'. Of course, the primality of the last index, $N_p:\{1\}$, is essential.

In turn, the existence of N_p will follow if we show that every bicyclic group $G \neq$

$\{1\}$ contains a *cyclic* normal subgroup $N_c \neq \{1\}$. For let N' denote any subgroup of N_c, and suppose N'' conjugate to N' in G. Then N'' is a subgroup of N_c having the same order as N', hence $N'' = N'$, since a finite cyclic group has no more than one subgroup of any given order. This proves the invariance in any finite group G of every subgroup of an invariant cyclic subgroup. Now the cyclic group $N_c \neq \{1\}$ has a subgroup of order p, where p is any prime divisor of the order of N_c; this subgroup is our N_p.

In case G is not exact, the subgroup $\{A\} \cap \{B\}$, being cyclic, normal (indeed, central), and $\neq \{1\}$, furnishes immediately the required subgroup N_c. We need therefore consider only the exact case.

Accordingly, our goal will be reached when we prove the following

THEOREM. *If* $G = \{A\}\{B\} = \{B\}\{A\}$ *is an exact bicyclic group* $\neq \{1\}$, *then either* $\{A\}$ *or* $\{B\}$ *contains a subgroup* $N \neq \{1\}$ *invariant in* G.

We may remark that the existence of the normal cyclic subgroup N, under the title of "A-nucleus" or "B-nucleus," has been established in our cited notes[3] as part of our general theory of exact bicyclic groups. However, the derivation presented here is simpler and self-contained.

3. Let m,n denote the orders of the generating elements A,B respectively. Since A,B occur symmetrically in the structure of G, we may suppose $m \geqq n$. We may also suppose $n > 1$, since otherwise $B = 1$, and G reduces to the cyclic group $\{A\} \neq \{1\}$, for which the stated theorem is trivial.

Our theorem depends on the following

LEMMA. *If* $G = \{A\}\{B\} = \{B\}\{A\}$ *is an exact bicyclic group* $\neq \{1\}$, *and* $m \geqq n > 1$, *then* $\{A\}$ *contains an element* $A^s \neq 1$ *whose transform by* B *is again a power of* A: $B^{-1}A^sB = A^t$.

Proof: For each value of $x = 0,1,2, \ldots, m-1$, there are values of y,z such that

$$B^{-1}A^x = A^yB^z. \tag{1}$$

We may assume $0 \leqq y \leqq m-1, 0 \leqq z \leqq n-1$, then y and z are uniquely determined because of the exactness of G.

Now z can never take the value 0. For then (1) implies $A^{x-y} = B \neq 1$, contrary to the exactness hypothesis: $\{A\} \cap \{B\} = \{1\}$. Accordingly, formula (1) sets up a mapping of the set

$$[x] = [0,1,2, \ldots, m-1] \tag{2}$$

into the set

$$[z] = [1,2, \ldots, n-1]. \tag{3}$$

Since the set $[x]$ contains m different elements, and the set $[z]$ only $n-1$, which is *less* than m, it must happen that two different values of x give the same value of z; i.e.

$$B^{-1}A^x = A^yB^z, \qquad B^{-1}A^{x'} = A^{y'}B^z, \qquad x \neq x'. \tag{4}$$

By multiplying the first of these equations with the inverse of the second, we get

$$B^{-1}A^{x-x'}B = A^{y-y'}. \tag{5}$$

Here $A^{x-x'} \neq 1$, otherwise $A^x = A^{x'}$, which is impossible, since $x \neq x'$. With this remark, formula (5) establishes our lemma.

4. The proof of the theorem stated in section 2 now follows immediately. The set of all elements A^s such that $B^{-1}A^sB = A^t$ for some t evidently forms a group N, as we see by multiplying together any two relations of this form. By the lemma, $N \neq \{1\}$. The elements A^t form a group N' conjugate to N in G. But, since N and N', as conjugate groups, have the same order, and each is a subgroup of the cyclic group A, it follows that $N' = N$, i.e., $B^{-1}NB = N$.

Thus N is invariant under conjugation by B. As subgroup of $\{A\}$, N is obviously invariant under conjugation by A; hence, N is invariant under conjugation by A^xB^y for all x,y; i.e., N is invariant in G.

This completes the proof of the theorem of section 2, and therewith the supersolvability of G.

[1] This concept was introduced by G. Zappa, "Sui gruppi supersolubili," *Rend. Sem. Math. Univ. Roma* (4), **2**, 323–330 (1937).

[2] Huppert, B., "Über das Produkt von paarweise vertauschbaren zyklischen Gruppen," *Math. Zeitschr.*, **58**, 243–264 (1953), p. 257.

[3] Douglas, J., "On finite groups with two independent generators," these PROCEEDINGS, **37**, 604–610, 677–691, 749–760, 808–813 (1951).

A SIMPLIFIED PROOF OF VON NEUMANN'S COORDINATIZATION THEOREM

BY ISRAEL HALPERIN

QUEEN'S UNIVERSITY AT KINGSTON, ONTARIO

Communicated by Einar Hille, July 3, 1961

1. *Introduction.*—In 1936–37, von Neumann proved the following result: Suppose L is a complemented modular lattice possessing a homogeneous basis $a_1, \ldots, a_n$ with n finite and ≥ 4. Then there exists a regular associative ring S with unit such that L is lattice-isomorphic to $L(S^n)$, where S^n denotes the set of vectors $(\alpha^1, \ldots, \alpha^n)$ with all α^i in S and $L(S^n)$ denotes the set of finitely generated submodules of S^n, ordered by set inclusion (submodule means left submodule with S as ring of scalars).[1]

Von Neumann defines S to be the auxiliary ring of L-numbers (α is in S means: $\alpha = (\alpha_{ij})$ for a certain family of lattice elements α_{ij}, each a relative complement of a_j in $a_i + a_j$). Then, by induction on m ($m = 1, \ldots, n$), von Neumann shows:

$$\text{The sublattice } [0, a_1 + \ldots + a_m] \text{ is isomorphic to } L(S^m). \tag{1}$$

Von Neumann's proof of (1) employs powerful and involved technique. We now point out that for $m = 1$, (1) is an immediate consequence of the regularity of S; for $m = 2,3$, (1) can be verified by straightforward calculations; and what is surprising, for $m > 3$, the validity of (1) can be deduced from its validity for $m = 3$ by simple lattice calculations.

Our simplification[2] of the proof of (1) covers extensions of von Neumann's

theorem to the case $n = 3$ supplemented by a Desarguesian[3] (or Moufang[4] or even weaker[5]) condition. With minor changes, it yields at once an extension wider than that of Jónsson:[6] Jónsson assumes that L has a basis $a_1, \ldots, a_n$ with each a_i perspective to a subelement $\bar{a}_i$ of a_1 and $\bar{a}_i = a_1$ for $i = 2,3,4$, (or for $i = 2,3$ together with a supplementary condition). With non-Desarguesian hypotheses on L, the associative law for multiplication and the left distributive law may fail to hold in S.

For the special case that L is an $n - 1$ dimensional projective geometry and the a_i are points (then the only idempotents in S are 0,1), this gives a direct and rather transparent demonstration of the classical coordinatization theorem for projective geometry.

We sketch below our simplified proof of von Neumann's original theorem ($n \geqslant 4$). A detailed discussion will be given elsewhere.

2. *Notation.*—$A^i \equiv a_1 + \ldots + a_i$, $A^0 \equiv 0$, $A_j{}^i \equiv a_1 + \ldots + a_{j-1} + a_{j+1} + \ldots + a_i$. An x is called an i-element if $x \leqslant A^i$ and $xA^{i-1} = 0$. If $v = (\alpha^1, \ldots, \alpha^n)$ with $\alpha^j = 0$ for $j > i$ and with $\alpha^i =$ idempotent and $\alpha^i\alpha^j = \alpha^j$ for $j < i$, then v is called an i-vector. $M(w, \ldots)$ denotes the submodule generated by the vectors $w, \ldots$. If α is in S, the reach of α into a_j, written $(\alpha)_j{}^r$, means $(\alpha_{ij} + a_i)a_j$ for any $i \neq j$.

Suppose x is an i-element. We choose an idempotent $e \equiv e(x)$ with $(e)_i{}^r = (x + A^{i-1})a_i$. For $j < i$, we define x^j to be $(x + A_j{}^{i-1})(a_i + a_j)$ and we choose any β^j in S with $(\beta^j)_{ij} \geqslant x^j$. Then $v(x)$ is defined to be the i-vector $(-e\beta^1, \ldots, -e\beta^{i-1}, e, 0, \ldots, 0)$. $M(v(x))$ is determined uniquely by x although $v(x)$ depends on the choice of $e(x)$.

If x is an arbitrary element in L, we choose a base-decomposition $x = x_1 + \ldots + x_n$ with each x_i an i-element and so obtain a submodule $M(x) \equiv M(v(x_1), \ldots, v(x_n))$. This $M(x)$ is determined uniquely by the particular choice of $x_1, \ldots, x_n$, but it is not yet clear that it is the same for all base-decompositions of the given x.

3. *Statement of the Problem.*—It is easy to show that every element in $L(S^n)$ occurs among the $M(v(x_1), \ldots, v(x_n))$ as x varies over L. The correspondence $x \to M(x)$ is therefore a lattice isomorphism of L onto $L(S^n)$ if the following statement holds: whenever x, y have base-decompositions $x_1 + \ldots + x_n$, $y_1 + \ldots + y_n$ respectively, then

$$x \leqslant y \quad \text{implies} \quad M(v(x_1), \ldots, v(x_n)) \leqslant M(v(y_1), \ldots, v(y_n)), \tag{2}$$

$$M(v(x_1), \ldots, v(x_n)) \leqslant M(v(y_1), \ldots, v(y_n)) \quad \text{implies} \quad x \leqslant y. \tag{3}$$

4. *Reduction of the Problem.*—In (2) and (3), we need only consider the case: $x = x_m$ for some $m \leqslant n$ and $y_j = 0$ for $j > m$. Then we may assume that $e(x_m) = e(y_m)$ since (i) $x_m \leqslant y_m$ implies that $v(x_m) = e(x_m)v(y_m)$ and (ii) $ee(y_m) = e$(idempotent) implies that $ev(y_m) = v(x_m)$ for some m-element $x_m \leqslant y_m$. Finally, we may even assume $e(x_m) = e(y_m) = 1$.

This settles the case $m = 1$. If $m \geqslant 2$, it is sufficient to verify (2), (3) when $y_j \neq 0$ for precisely one $j < m$ and we may even suppose that the exceptional j is $m - 1$. Thus we need only show that if

$$v(x_m) = (-\alpha^{m,1}, \ldots, -\alpha^{m,m-1}, 1, 0, \ldots, 0),$$

$$v(y_m) = (-\beta^{m,1}, \ldots, -\beta^{m,m-1}, 1, 0, \ldots, 0),$$

and $$v(y_{m-1}) = (-\gamma^{m-1,1}, \ldots, -\gamma^{m-1,m-2}, f, 0, 0, \ldots, 0),$$

then,

$$x_m \leqslant y_{m-1} + y_m \quad \text{implies} \quad v(x_m) = v(y_m) + \delta v(y_{m-1}) \quad \text{for some } \delta \text{ in } S, \tag{4}$$

and $$v(x_m) = v(y_m) + \delta v(y_{m-1}) \text{ for some } \delta \text{ in } S \quad \text{implies} \quad x_m \leqslant y_{m-1} + y_m. \tag{5}$$

5. *The Case $m = 2$.*—The relation $v(x_2) = v(y_2) + \delta v(y_1)$ is equivalent in turn to each of: (i) $\beta^{2,1} - \alpha^{2,1}$ is in the left ideal of f, (ii) $(\beta^{2,1} - \alpha^{2,1})_1{}^r \leqslant (f)_1^r$, (iii) $((\beta^{2,1})_{2,1} + (\alpha^{2,1})_{2,1})a_1 \leqslant y_1$, (iv) $(x_2 + y_2)a_1 \leqslant y_1$, and (v) $x_2 \leqslant y_1 + y_2$. This settles the case $m = 2$.

6. *Deduction of* (4) *from* (5).—Assume $x_m \leqslant y_{m-1} + y_m$. Then, by an argument like that of paragraph 5, $\beta^{m,m-1} - \alpha^{m,m-1} = \delta f$ for some δ. If now we assume (5) holds, we obtain with this δ: $v(y_m) + \delta v(y_{m-1}) = v(\bar{x}_m)$ for some $\bar{x}_m \leqslant y_{m-1} + y_m$. Then,

$$x_m + A^{m-2} = \bar{x}_m + A^{m-2};$$

so, $$x_m = (y_{m-1} + y_m)(x_m + A^{m-2}) = \bar{x}_m,$$

and hence (4) holds.

7. *Reduction of* (5) *to the Case $m = 3$.*—To complete the proof, we need only prove (5) for the case $m \geqslant 3$.

If $m > 3$ and $v(x_m) = v(y_m) + \delta v(y_{m-1})$ we choose any $j \leqslant m - 2$ and "project" into $[0, a_j + a_{m-1} + a_m]$. Now if (5) is assumed for the special case $m = 3$ we can obtain

$$x_m \leqslant A_j^{m-2} + y_{m-1} + y_m \quad \text{for all } j \leqslant m - 2;$$

hence $x_m \leqslant y_{m-1} + y_m$, proving (5). So we need only prove (5) for the case $m = 3$.

8. *Proof of* (5) *for the Case $m = 3$.*—Suppose $v(x_3) = v(y_3) + \delta v(y_2)$. Then, by an argument like that of paragraph 5: $x_3 \leqslant a_1 + y_2 + y_3$. If now we assume (5) holds for the special case $m = 3, f = 1$, we have also

$$x_3 \leqslant (f_{21}a_2 + y_2) + y_3,$$

and so, $$x_3 \leqslant (a_1 + y_2 + y_3)(f_{21}a_2 + y_2 + y_3) = y_2 + y_3.$$

So we need only prove (5) for the case $m = 3, f = 1$. Now we have

$$(\beta^{3,2} - \alpha^{3,2})(-\gamma^{2,1}) = \beta^{3,1} - \alpha^{3,1},$$

$$(\beta^{3,2}\gamma^{2,1} + \beta^{3,1})_{3,1} = (\alpha^{3,2}\gamma^{2,1} + \alpha^{3,1})_{3,1}.$$

If we calculate the right and left sides of the last equality using the ternary relation[7]

$$(\beta\gamma + \delta)_{3,1} = (\gamma_{2,1} + (\delta_{3,1} + a_2)(\beta_{3,2} + a_1))(a_3 + a_1),$$

we obtain $y_2 + y_3$ and $y_2 + x_3$ respectively. Hence, $x_3 \leqslant y_2 + y_3$, verifying (5). This completes the proof of von Neumann's theorem.

[1] See von Neumann, *Continuous Geometry* (Princeton University Press, 1960), part 2, chapters 1–14, especially Theorem 14.1 on page 208, or Fryer, K. D., and I. Halperin, "On the coordinatization theorem of J. von Neumann," *Can. Journ. of Math.*, **7**, 432–444 (1955), or Amemiya, I., "On the representation of complemented modular lattices," *Journ. Math. Soc. Jap.*, **9**, 263–279 (1957).

[2] For simplifications in the construction of *S*, see Fryer, K. D., and I. Halperin, "Coordinates in geometry," *Trans. Roy. Soc. Can.*, **48**, Ser. 3, 11–26 (1954).

[3] Fryer, K. D., and I. Halperin, "The von Neumann coordinatization theorem for complemented modular lattices," *Acta Sci. Szeged*, **17**, 203–249 (1956).

[4] Fryer, K. D., and I. Halperin, "On the construction of coordinates for non-Desarguesian complemented modular lattices," *Proc. Roy. Neth. Acad. (Amsterdam)*, **61**, 142–161 (1958); Amemiya, I., and I. Halperin, "On the coordinatization of complemented modular lattices," *Proc. Roy. Neth. Acad. (Amsterdam)*, **62**, 72–78 (1959) and "Complemented modular lattices derived from non-associative rings," *Acta Sci. Szeged*, **20**, 181–201 (1959).

[5] Baer, R., "Homogeneity of projective planes," *Amer. J. Math.*, **64**, 137–152 (1942); Fryer, K. D., "Coordinates in non-Desarguesian complemented modular lattices," *Proceedings of Symposia in Pure Mathematics, volume II; Lattice Theory* (Providence: American Mathematical Society, 1961), pp. 71–77.

[6] Jónsson, Bjarni, "Representations of complemented modular lattices," *Trans. Amer. Math. Soc.*, **97**, 64–94 (1960).

[7] See (5.2.2) in ref. 3 above.

---

*COLICINE V**

BY JOHN J. HUTTON AND WALTHER F. GOEBEL

THE ROCKEFELLER INSTITUTE

Communicated July 12, 1961

Nearly a decade ago this laboratory began an investigation on the nature of colicines—antibacterial agents of remarkable potency which are elaborated by certain *Enterobacteriaceae* and which kill other microorganisms of the same species. These agents were first described by Gratia in 1925[1] who observed that cell-free filtrates of a virulent strain of colon bacillus with which he was working contained an agent, "principle V," which killed a sensitive host strain "coli ϕ." Gratia observed that his principle was thermostable and that it diffused through cellophane membranes. He pointed out that the agent bore a remarkable similarity to bacteriophage, yet differed in that it would not reduplicate upon serial passage.

A resurgence of interest in the colicines took place in the mid-forties, largely through the work of Frédéricq,[2] to whom most of our modern knowledge concerning the distribution, specificity, and tenuous relationship of the colicines to the bacteriophages can be attributed.[3] Extensive as our knowledge is in this regard, our understanding of their chemical nature has remained singularly enigmatic despite the efforts of a number of investigators.[4]

Several years ago we in this laboratory described the isolation of one of the colicines—colicine K.[5] This substance proved to be a lipocarbohydrate-protein complex, identical with the somatic O antigen of the microorganism from which it was derived. The material had exceedingly potent antibacterial properties. It was antigenic in rabbits and the antisera specifically precipitated the colicine and neutralized its antibacterial properties as well.[6] Although the colicines and bacteriophages show striking resemblances,[2] we were unable to demonstrate any serological relationship between our colicine K and the coli-dysentery phage T6, the virus to which this colicine is presumed to be related.

We have now isolated another and different colicine—colicine V. We chose to

study this substance not only because it was the first of the colicines to be described, the "principle V" of Gratia, but, if it is indeed readily dialyzable as he has said,[1] it should prove to be a far less complicated molecule than colicine K.

A colicine V producing bacillus, termed *E. coli* K357, was kindly sent us by Pierre Frédéricq of the University of Liège. Six variants were obtained from this microorganism which differed in colonial morphology. One of these, designated as *E. coli* K357 L-T, was selected for study because it liberated more colicine in the culture medium than did the others.

When this microorganism was grown at pH 7.0 in a medium containing only dialyzable constituents,[7] it elaborated some 400–800 units per ml of colicine V. After concentrating the cell-free medium *in vacuo* followed by dialysis, there was obtained by freeze drying the nondialyzable residue, a grayish-white, friable, amorphous powder. This substance, "crude colicine V," had striking antibacterial properties. A solution containing 1 to 2 μg per ml, when tested by a technique described in a former communication,[7] completely inhibited the growth of the test organism *E. coli* ϕ.

Purification of the colicine was effected by precipitating it at low ionic strength (0.02 *M* sodium acetate) with ethanol at 0°C. The substance which precipitated between 30 and 60 per cent ethanol concentration proved to be the colicine. The latter was further purified by passing a solution (1.6 gm in 100 ml of 0.05 *M* Tris buffer at pH 8.0) through a short column of DEAE cellulose (4 gm compressed in a column 1.9 × 10 cm). The last traces of pigment were thus removed without incurring an appreciable loss of the colicine.

Chemical Properties.—Purified colicine V is obtained as a white, water-soluble, amorphous substance. Its analysis is as follows: carbon, 49.95%; hydrogen, 7.75%; phosphorus, 2.02%; nitrogen, 3.80%; and acetyl, 5.90%. The material gives strong biuret and Folin tests indicating the presence of protein. On acid hydrolysis it yields 43 per cent of reducing sugars calculated as glucose and 11.3 per cent of a chloroform-soluble lipid. Colicine V is not precipitated by trichloroacetic or picric acids, nor does it precipitate with the salts of heavy metals, such as copper, uranium, lead, or silver. A solution of colicine V, when heated at 100°C with an equal volume of saturated picric acid yields a precipitate; presumably the complex is dissociated into its component parts and the protein component is precipitated as an insoluble picrate. Finally, it should be stated that we were unable to confirm Gratia's observation that colicine V is dialyzable. Our substance does not diffuse through cellophane membranes.

Toxic Properties of Colicine V.—Colicine V exhibits toxic properties both for bacteria and for mammals. A solution containing 1.5 μg of colicine per ml completely inhibits the growth of the test organism *E. coli* ϕ. *E. coli* B is also sensitive to colicine V, but it requires a concentration of 3 μg per ml to inhibit the growth of this bacillus. When colicine V is injected intraperitoneally into mice, it is found that the $L.D._{50}$ for the Collins-Nelson Rockefeller Institute strain of white mice is 0.90 mg. The intradermal injection of rabbits with 1 mg of colicine in saline occasionally results in death of the animal, but as a rule there occurs only a marked systemic reaction, accompanied by malaise and fever. There is a great deal of edema at the site of injection and usually within 24 hours a marked necrotic area appears.

Immunological Properties of Colicine V.—Colicine V is a potent antigen. The sera of rabbits which have received an intradermal injection followed by one or two courses of intravenous injections of minute quantities (200–500 μg), invariably show the presence of precipitating antibodies. The antisera also agglutinate at high dilutions (1:6400) the bacillus from which the colicine is obtained. These same sera neutralize the antibacterial properties of colicine V, so that the colicine is no longer capable of killing the sensitive organism *E. coli* ϕ. As a rule, 0.2 ml of a potent serum is sufficient to neutralize the antibacterial activity of 100 μg of colicine V.

A study of the immunological cross reactions of colicine V in colicine K antiserum and vice versa, has revealed that neither colicine is neutralized or precipitated by the heterologous serum. Furthermore, colicine V antisera do not agglutinate the colicine K producing bacillus *E. coli* K235, nor do colicine K antisera agglutinate the colicine V producing microorganism. The antigenic mosaics of the two bacilli appear to be quite unrelated.

Summary.—Colicine V had been isolated as an electrophoretically homogeneous substance. Chemical analyses indicate that it is a lipocarbohydrate-protein complex which is typical of many *Enterobacteriaceae*. Colicine V is toxic both for bacteria and for mammals. It is an excellent antigen and it elicits in rabbits antibodies which both precipitate and neutralize the colicine and which agglutinate the parent colicinogenic microorganism. Despite their close chemical similarity, colicine K and colicine V exhibit no cross serological relationships whatsoever.

This work is being continued in our laboratory. The isolation and characterization of still other colicines will be reported in subsequent communications.

* The work presented in this communication was supported in part by a grant from the Department of Health, Education and Welfare, U.S. Public Health Service, National Institutes of Health, Bethesda, Maryland.

[1] Gratia, A., *Compt. rend. soc. biol.* (Paris), **93,** 1040 (1925). Gratia, A., *Ann. ist. Pasteur*, **48,** 413 (1932).

[2] Frédéricq, P., *Symposia Soc. Exptl. Biol.*, No. 12, 104 (1958).

[3] Frédéricq, P., *Schweiz. Z. Pathol. u. Bakteriol*, **20,** 670 (1950).

[4] Heatley, N. G., and H. W. Florey, *Brit. J. Exptl. Pathol.*, **27,** 378 (1946). Halbert, S. P., and H. J. Magnuson, *J. Immunol.*, **58,** 397 (1948). Gardner, J. F., *Brit. J. Exptl. Pathol.*, **31,** 102 (1950).

[5] Goebel, W. F., G. T. Barry, M. A. Jesaitis, and E. M. Miller, *Nature*, **176,** 700 (1955); and Goebel, W. F., and G. T. Barry, *J. Exptl. Med.*, **107,** 185 (1958).

[6] Amano, T., W. F. Goebel, and E. M. Smidth, *ibid.*, **108,** 731 (1958).

[7] Goebel, W. F., G. T. Barry, and T. Shedlovsky, *ibid.*, **103,** 577 (1956).

*THE ELUTION PROPERTIES OF TYPE 1 POLIOVIRUSES FROM AL(OH)$_3$ GEL. A POSSIBLE GENETIC ATTRIBUTE**

By Wilna A. Woods and Frederick C. Robbins

DEPARTMENT OF PEDIATRICS, WESTERN RESERVE UNIVERSITY SCHOOL OF MEDICINE, AND DEPARTMENT OF PEDIATRICS AND CONTAGIOUS DISEASES, CLEVELAND METROPOLITAN GENERAL HOSPITAL

Communicated by John H. Dingle, July 14, 1961

The adsorptive capacity of alumina gels for certain viruses has long been recognized. Various investigators have utilized this system as a method for concentrating and purifying viruses[1–5] and indeed differences in adsorption to and elution from aluminum phosphate gels have been used to distinguish between strains of influenza virus.[5] Sabin[1] found that poliovirus was adsorbed to aluminum hydroxide at an acid pH and quantitatively eluted at a pH above 7.

During the course of studies upon the infection of newborn infants with attenuated polioviruses[6] it was postulated that the high concentration of hydrochloric acid in the stomach at this age might inactivate the virus and thus interfere with the establishment of infection. The possibility was entertained that poliovirus adsorbed to alumina gel might be given by mouth. The virus would presumably remain associated with the gel in the stomach, but would be eluted in the alkaline environment of the intestine. Before pursuing this approach further, the adsorption and elution of the type 1 poliovirus vaccine strain LSc2ab was studied *in vitro* and compared to that of the prototype virulent Mahoney strain. Mahoney virus reacted with Al(OH)$_3$ gel in the manner described by Sabin.[1] However, the LSc2ab strain behaved in a very different manner in that only a very small portion of the virus that adsorbed to the gel could be eluted. It is this observation that prompted the studies reported in this communication. The phenomenon was of interest because of the possibility that it might provide an additional genetic attribute of poliovirus that would be relatively simple to determine. Such markers are of theoretical value but also have practical importance in the study of the genetic stability of the attenuated polioviruses now in wide use as vaccines. It would be particularly desirable to have some means of assessing the neurovirulence of polioviruses other than inoculation of monkeys, which is the method that is now employed.

This report presents data indicating that the way in which strains of poliovirus elute from Al(OH)$_3$ gel with alteration in pH is a characteristic that provides an additional means of identifying differences, probably physicochemical, particularly between strains of type 1 viruses, and may indeed correlate with neurovirulence.

Methods and Materials.—1. *Viruses:* The virus suspensions were pools of tissue culture fluids (TCF) from monkey kidney (MK) monolayer cultures infected with polioviruses. The following "wild type" or virulent strains were used: Mahoney (type 1), MEF1 (type 2), and Saukett (type 3). The attenuated strains LSc2ab (type 1), P712 (type 2), and Leon (type 3) were obtained from A. B. Sabin. In addition to these strains, a certain number of type 1 polioviruses isolated from human fecal specimens were studied.

2. *Preparation of Al(OH)$_3$ gel:* Alumina gel C of the Willstätter series was prepared with sterile materials according to the procedure outlined by Sabin.[1] The various preparations contained 15–18 mg Al_2O_3/ml. A single lot of gel was employed for each series of experiments in which the adsorption and elution patterns of different virus strains were compared.

3. *Titration of virus samples:* Viruses were titrated in MK monolayer tube cultures main-

tained with 1 ml of a medium containing lactalbumin hydrolysate (0.5%), ox serum ultrafiltrate (22.5%), and neutral Hanks' balanced salt solution (BSS) (77%). One hundred units of penicillin and 1 μg of streptomycin were added per ml of medium. One tenth ml of the sample to be tested was inoculated into each of 4 tubes per dilution. On the sixth day after inoculation the tubes were read for cytopathic effect (CPE). Titers are expressed as 50% tissue culture infective doses ($TCID_{50}$).

4. *Buffer solutions:* Standard M/15 phosphate buffers in the pH range 3.5–8 were used.

5. *Methods of adsorption and elution:* (*a*). A modification of the method described by Sabin[1] was used in the preliminary experiments. The stock gel was washed 10–15 times with a buffer of pH 3.5 until the pH of the suspension was below 6. Aliquots of the washed gel were dispensed into 50 ml centrifuge bottles, and the virus was added. In early experiments, tissue culture fluid containing approximately 10^8 $TCID_{50}$ of virus was added to an equal volume of gel suspension; in later experiments, a more complete adsorption was obtained by adding 0.5 ml of a virus suspension diluted with an acid buffer to contain approximately 10^4 $TCID_{50}$ per ml to a gel cake packed by centrifuging 10 ml of washed gel suspension at 2,000 rpm for 10 min. The mixture of virus, gel, and acid buffer was shaken on a Burrell wrist action shaker for 20 min at room temperature. Adsorption of the virus was allowed to proceed for 3 hr at 4°C. The gel was then sedimented by centrifugation, the supernatant fluid removed, and tested for viral content. The surface of the cake was washed with distilled water and the gel resuspended in the eluting buffer by shaking for 20 min at room temperature. The suspension was allowed to remain overnight at 4°C in order to permit elution of the virus. The gel was then removed by centrifugation and the quantity of infectious virus in the supernate again was determined. In some experiments after elution the gel was resuspended in BSS, and the resulting suspension titrated for virus. In other experiments, repeated elution of the same gel was carried out. (*b*). It was found that more reproducible results were obtained when the virus was adsorbed to a column of $Al(OH)_3$ gel, and this method was substituted for the less precise one described in the previous paragraph. The procedure was carried out entirely at room temperature. Ten ml of the gel suspension were placed in a column of 2 cm diameter with a sintered glass disk at one end. Phosphate buffer of pH 3.5 was allowed to run through the column until the pH of the effluent fluid was below 6 (usually in the range of 5.5–5.8). Excess buffer above the packed gel was then removed with suction and 9 ml of a 1:10 dilution of the virus (approximately $10^{7.5}$ $TCID_{50}$) in pH 3.5 buffer were added. The column was placed on an automatic fraction collector, and 3 ml samples were collected. Eighteen to 20 hr were required for the 9 ml of fluid containing the virus to flow through the column. The column was then washed with 15–30 ml of pH 3.5 buffer. Elution was accomplished by passing 60 ml of pH 7 buffer through the column followed by an equal quantity of buffer of pH 8. The flow rate was maintained at about 3 ml/hr except during the period of adsorption. Each 3 ml fraction was tested for pH and virus content. A Beckman model G pH meter was used for the pH determinations.

Results.—1. *Adsorption and elution of virus:* Preliminary experiments using gel suspensions were carried out with Mahoney and LSc2ab type 1 polioviruses. The results of four representative experiments are recorded in Table 1.

TABLE 1

ADSORPTION AND ELUTION OF VIRULENT AND ATTENUATED TYPE 1 POLIOVIRUSES WITH $Al(OH)_3$ GEL

Strain of virus	Virus Titer Log $TCID_{50}$/ml*			
	Before adsorption	After adsorption	Eluate	Gel after elution
Mahoney	8.2†	4.2	8.2	8.0
(virulent)	8.2	5.4	8.6	8.4
	4.2	0.2	4.7	...
	4.2	0	4.2	...
LSc2ab	8.0	3.9	4.2	7.0
(attenuated)	7.2	4.9	4.6	7.2
	4.2	0	0	...
	4.2	0	0	...

* Corrected for differences in volumes.
† Log sensitivity of determination = ± 0.3.

It is evident that both viruses were well adsorbed and to an equal degree. When concentrations of virus of approximately 10^8 $TCID_{50}$/ml were employed 0.008%–0.5% of the virus remained unadsorbed, but when the concentration was reduced to 10^4 $TCID_{50}$/ml little or no virus could be detected in the supernate after adsorption. In contrast, the two strains eluted from the gel in a very different manner. Mahoney virus eluted quantitatively. On the other hand, the LSc strain eluted poorly, and indeed it will be noted that in some experiments no virus was demonstrated in the eluate and in no instance was more than 0.25 per cent of the adsorbed virus released from the gel. It is also apparent that after elution considerable quantities of both virus strains were still associated with the gel. This latter observation is of particular importance in regard to the LSc strain since it indicates that the failure of this virus appear to in the eluate when the pH of the mixture was raised was not due to inactivation of infectious virus.

Additional experiments indicated that Mahoney virus eluted readily with a buffer of pH 7.0 but that even repeated washings with buffers of pH 7.0 or 8.0 failed to dissociate LSc virus from the gel.

Thus, it appeared that the failure of the LSc virus to elute to a significant extent from $Al(OH)_3$ gel when the pH was raised was a reproducible property that differentiated this strain from the virulent Mahoney strain.

2. *Elution patterns of standard polioviruses from columns of $Al(OH)_3$ gel:* The results obtained with aluminum hydroxide columns revealed the same difference in elution between the Mahoney and LSc type 1 strains. These data are presented in Figures 1 and 2. In Figure 1 the titer of infectious virus and pH of each 3 ml fraction is plotted. In Figure 2 the results of a comparable experiment are presented in a different manner. The amount of infectious virus recovered in each of

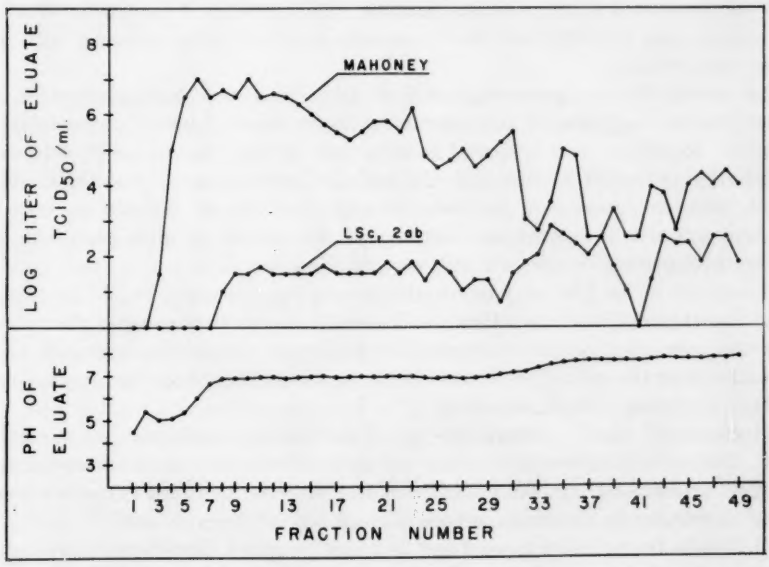

FIG. 1.—Elution pattern of Mahoney and LSc2ab viruses from an $Al(OH)_3$ column.

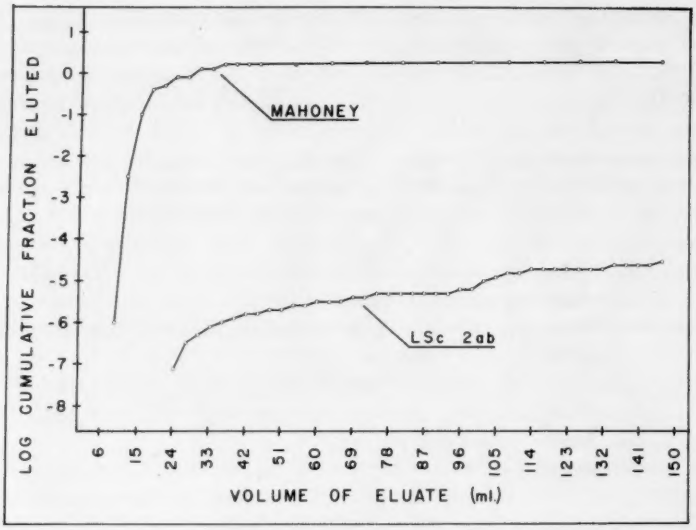

FIG. 2.—Elution of polioviruses from an $Al(OH)_3$ column (cumulative fractions).

the 3 ml samples was divided by the amount originally placed on the column. This gave the fraction of virus contained in the particular aliquot of the total eluate. These values expressed in logs were cumulated so that each point on the curve represents the proportion of the original virus contained in one aliquot of the eluate plus that contained in all preceding samples. This method of expressing the data was chosen since it permitted direct comparison of the results obtained with different virus strains.

It is evident in the figures that none of either virus was demonstrated in the effluent at the beginning of the experiment when the acid buffer was employed. However, Mahoney virus appeared in the eluate in high titer promptly following the addition of the pH 7 buffer and indeed almost simultaneously with the increase in pH, indicating passage of the buffer through the column. Within the next 21 ml there was nearly quantitative recovery of the amount of virus placed on the column with little more released with the pH 8 buffer.

The elution of the LSc virus occurred later and this amounted *in toto* to only 2.4×10^{-5} of the original virus. However, following extensive washing of the column with the more alkaline buffer, infectious virus could still be demonstrated to be associated with the gel. This confirmed the previous observation that inactivation of infectious virus was not occurring.

3. *Elution of virulent and avirulent type 2 and type 3 polioviruses:* It was naturally of interest to determine whether the same differences could be demonstrated between virulent and avirulent polioviruses of types 2 and 3. They were accordingly tested on columns by the same methods as employed for the type 1 virus.

The results for both the types 2 and 3 viruses indicated that the virulent strains were in each instance somewhat more readily eluted than the avirulent ones.

However, these differences were not great enough to permit reliable differentiation between strains by this method. Employing the method of expressing the results that were described above and illustrated in Figure 2, the total fraction eluted of the virulent type 2 strain (MEF 1) was 1.2×10^{-2}. This was almost 100-fold less than was observed for the type 1 Mahoney strain. The comparable figure for the avirulent type 2 virus (P712) was 4.7×10^{-3}. This is a measurable, but not a striking difference, although it is in the same direction as noted for the type 1 viruses with the avirulent strain eluting more poorly from the gel than the virulent one.

Results with the type 3 viruses indicated a similar difference in elution between the virulent (Saukett) and avirulent (Leon) strains, the fractions eluted being 3.7×10^{-1} and 3.1×10^{-2}, respectively. Again, although the differences were slight, they are in the same direction as noted for the other two types.

4. *Elution of wild viruses isolated from human fecal specimens:* In order to obtain additional data concerning a possible relationship between elution from $Al(OH)_3$ and virulence, a number of type 1 viruses isolated from persons with disease of varying severity or no disease were examined. The tests were performed with $Al(OH)_3$ suspensions and the virus was in each instance the tissue culture fluid from the cultures in which the original isolation was made from feces. The results are given in Table 2. It is readily apparent that although there was some

TABLE 2

ELUTION FROM $Al(OH)_3$ GEL OF TYPE 1 POLIOVIRUSES ISOLATED FROM HUMAN FECES

Source	Virus Titer Log $TCID_{50}$/ml		
	Original virus	Supernate after adsorption	Eluate
Paralytic case	3.5	0	1.2
Paralytic case	2.7	0	2.0
Nonparalytic case	4.5	0	3.1
Nonparalytic case	2.7	0	2.8
Healthy contact	2.7	0	2.5

variation all of these viruses showed an elution pattern similar to that of the Mahoney virus. Indeed, the virus that eluted most poorly was isolated from a paralytic case.

5. *Elution of viruses isolated from the feces of infants fed LSc virus:* In order to determine whether or not the elution property of poliovirus remained constant during multiplication in the human intestine, an early and a late isolate were tested from each of eight infants fed the type 1 LSc virus. The results are seen in Table 3.

In each instance the virus isolated within a few days after feeding failed to elute and thus was identical in regard to this property with the vaccine virus. No alteration was noted in the viruses isolated later in the course of infection from five of the infants. The isolates obtained at 32, 34, and 44 days, respectively, from the remaining three babies were eluted in varying degree. Thus, there was in this regard complete or partial reversion to the state characteristic of the virulent Mahoney strain. Of course, this finding could be explained by the acquisition by these children of an infection with wild type 1 viruses. However, the observations that virus could be demonstrated regularly in the feces of these infants and that there was no change in the only other property so far tested, namely, the lack of growth

TABLE 3

ELUTION FROM $Al(OH)_3$ GEL OF VIRUSES ISOLATED FROM INFANTS FED LSc VIRUS

Infant no.	Time of virus recovery*	Virus Titer Log $TCID_{50}$/ml		
		Original virus	Supernate after adsorption	Eluate
1	3	4.8	0	0
	44	3.5	0	0
2	9	5.0	0	0
	37	4.5	0	0
3	9	4.7	0	0
	26	4.5	0	0
4	2	4.5	0	0
	26	4.0	0	0
5	7	3.7	0	0
	27	2.2	0	0
6	2	4.5	0	0
	32	5.0	0	1.0
7	4	3.5	0	0
	34	5.0	0	1.5
8	2	2.7	0	0
	44	3.5	0	3.1

* Days post-feeding.

at 40°C,[7] suggest rather that alteration of the original virus has occurred during the course of multiplication in the bowel.

Discussion.—Differentiation of virus strains on the basis of their adsorption to and elution from aluminum phosphate gel[5] has been reported for influenza virus. More recently, Hodes *et al.*[8] described differences in the adsorption of type 1 polioviruses to diethylaminoethyl (DEAE) cellulose resin and suggested that there was a correlation between virulence and this physical property of the virus. The present study describes a similar differentiation of virulent and attenuated type 1 polioviruses on the basis of their elution pattern at alkaline pH from $Al(OH)_3$ gel. There is a suggestion that this physical property also may have some relationship to virulence. The elution patterns indicate that the virulent type 1 strains, which were poorly adsorbed in the study of Hodes *et al.*,[8] elute quantitatively from the alumina gel used in the present study. Differences in elution from $Al(OH)_3$ gel between virulent and avirulent types 2 and 3 viruses were much less striking than for type 1; however, so far only one set of conditions has been employed.

It would seem probable that the different behavior of viral strains with respect to elution from alumina gel or adsorption to DEAE reflect physicochemical differences in the protein component of the virus particle. The demonstration by Melnick,[9] which we have confirmed, that there are minor antigenic differences between the Mahoney and LSc2ab strains provides additional evidence that the protein of these two agents is not identical. The true significance of the differences in elution of polioviruses from $Al(OH)_3$ gel can only be determined after many more strains of virus from various sources have been examined for this property as well as for other genetic markers, in particular neurovirulence for the monkey.

Summary.—Virulent type 1 viruses eluted readily from $Al(OH)_3$ gel in the alkaline pH range; attenuated type 1 viruses eluted very poorly under the same conditions. It is postulated that this reflects differences in structure of the protein portion of the virus particle.

The standard virulent type 2 (MEF1) and type 3 (Saukett) viruses also tend to elute more readily than the corresponding attenuated P712 and Leon strains, but the differences are not so marked as with type 1 strains.

* Aided by a grant from The National Foundation.

[1] Sabin, A. B., *J. Exptl. Med.*, **56**, 307 (1931).

[2] Schaeffer, M., and W. B. Brebner, *Arch. Pathol.*, **15**, 221 (1933).

[3] Chang, S. L., P. C. G. Isaac, and N. Baine, *Am. J. Hyg.*, **57**, 253 (1953).

[4] Stevenson, R. E., S. L. Chang, N. A. Clarke, and P. W. Kabler, *Proc. Soc. Exptl. Biol. Med.*, **92**, 764 (1956).

[5] Miller, H. K., and R. W. Schlesinger, *J. Immunol.*, **75**, 155 (1955).

[6] Lepow, M. L., R. J. Warren, N. Gray, and F. C. Robbins, *Live Poliovirus Vaccines* (Washington, D. C.: Pan American Health Organization and World Health Organization, 1960), p. 302.

[7] Lwoff, A., and M. Lwoff, *C.R. Acad. Sci., Paris*, **248**, 1725 (1959).

[8] Hodes, H. L., H. D. Zepp, and E. A. Ainbender, *Virology*, **11**, 306 (1960).

[9] Melnick, J. L., and M. Benyesh-Melnick, *Live Poliovirus Vaccines* (Washington, D. C.: Pan American Health Organization and World Health Organization, 1960), p. 12.

WAVE BRANCHING PROCESSES AND INVARIANT IMBEDDING, I

BY RICHARD BELLMAN AND ROBERT KALABA

THE RAND CORPORATION, SANTA MONICA, CALIFORNIA

Communicated by S. Chandrasekhar, July 7, 1961

1. *Introduction.*—In recent years, a great deal of effort has been devoted to the use of functional equation techniques in treating particle processes of mathematical physics. This work stems on one hand from the principles of invariance of Ambarzumian and Chandrasekhar in astrophysics[1] and on the other hand from the point of regeneration techniques of Bellman and Harris[2] and Janossy. For a survey of this application of invariant imbedding to various areas of analysis and physics, see Bellman, Kalaba, and Wing,[3] where references to works of Ueno, Preisendorfer, Redheffer, and others may be found.

In reference 4, it was shown that similar techniques can be applied to the study of wave processes, using a principle of localization which generalizes completely the concept applied implicitly in the study of particle processes. In view of the duality that exists between wave and particle properties in modern physics, it is to be expected that a uniform mathematical technique will exist to treat both simultaneously.

In this introductory note, we wish to indicate how to use invariant imbedding and the principle of localization to treat wave processes in which we can have creation and destruction of waves. This is a stochastic process of branching type, completely analogous to that discussed in the particle case by Bellman and Harris; see also Harris,[5] for an up-to-date account.

We are presenting a new mathematical formulation of wave processes which overlaps with the conventional one in the case of deterministic linear processes and can serve as a definition of the physical process in the stochastic and nonlinear cases. Wave propagation in random media was treated in papers 6 and 7, using functional equation techniques.

2. *Wave Propagation and Invariant Imbedding.*—We wish to consider the intensity of reflected and transmitted waves from an inhomogeneous medium, as

pictured below, under the assumption that there is a possibility of the creation of new waves and the absorption of existing waves as a result of interactions with the medium. For the sake of simplicity, we will assume that there is a probability of $p(z)\Delta$ that a wave passing through the stratum $[z,z+\Delta]$ will be absorbed itself but will produce two waves, one of the same amplitude and phase traveling in the same direction and one of the same amplitude and phase traveling in the opposite direction, and a probability $1-p\Delta$ that the wave will continue through the stratum unchanged. In addition to this new absorption and fission process, we allow the usual reflection and transmission of waves.

Refer now to Figure 1. The medium $z \leq x \leq b$ is inhomogeneous with wave

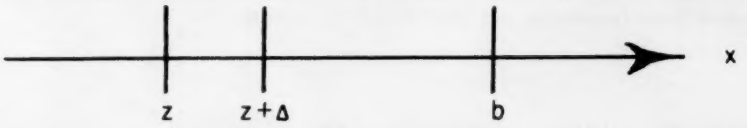

FIG. 1.—An Inhomogeneous Slab.

number $k(x)$, where, for simplicity, $k(x)$ is assumed continuous for all x. The medium to the left of $x = z$ will be taken to be homogeneous with wave number $k(z)$, while the medium to the right of $x = b$ will be taken to be homogeneous with wave number $k(b)$. As usual,[4] we take the solution (reflected wave) in the half-space $x \leq z$ to have the form

$$u(z)e^{-ik(z)(x-z)}, \tag{1}$$

where $u(z)$ is now a random variable. We wish to determine an equation for the expected value of $u(z)$, the quantity $U(z)$.

Let us enumerate the possible events in the interval $[z,z+\Delta]$ yielding terms of orders zero and one in Δ:

(*a*) An immediately reflected wave.

(*b*) Transmission through $[z,z+\Delta]$ with no interaction, reflection at $z+\Delta$, and either no interaction in $[z+\Delta,z]$ followed by transmission through the interface at $x = z$ or reflection at that interface, transmission through $[z,z+\Delta]$, reflection at $x = z+\Delta$, and transmission through $[z+\Delta,z]$ and $x = z$, or interaction in $[z+\Delta,z]$ which yields one wave passing directly through $x = z$ and one that is reflected at $x = z+\Delta$ and is ultimately transmitted through $x = z$.

(*c*) Transmission through $[z,z+\Delta]$ with an interaction yielding a wave passing directly through $x = z$ and another which is reflected at $x = z+\Delta$ and is ultimately transmitted through $x = z$.

3. *Principle of Wave Localization.*—In our paper,[4] we formulated and proved, for certain cases, the following principle of wave localization:

A plane wave traveling through an inhomogeneous medium proceeds as if there were an instantaneous transmission and reflection at each interface. These transmissions and reflections occur as if the media on each side of the interface were semi-infinite and homogeneous.

A further discussion can be found in Atkinson's paper.[8]

Our basic idea is to make use of this principle by imbedding the original problem within a class of problems by considering reflection from sections $[z,b]$ for all $z \leq b$

where b is fixed, and interconnecting the expected reflection coefficient for intervals $[z,b]$ and $[z + \Delta,b]$.

4. *Riccati Equation for Expected Reflected Wave.*—Adding up all the events listed above in section 2 we find the equation

$$U(z) = \frac{k(z) - k(z + \Delta)}{k(z) + k(z + \Delta)} + \frac{2k(z)}{k(z) + k(z + \Delta)} (1 - p(z)\Delta)e^{ik(z + \Delta)\Delta} U(z + \Delta)\Big\{(1 - p(z)\Delta)$$
$$\left[e^{ik(z)\Delta}\frac{2k(z + \Delta)}{k(z) + k(z + \Delta)} + \frac{k(z + \Delta) - k(z)}{k(z) + k(z + \Delta)} U(z)\right] + p(z)\Delta[1 + U(z)]\Big\}$$
$$+ \frac{2k(z)}{k(z) + k(z + \Delta)} p(z)\Delta\{1 + U(z)\} + o(\Delta). \quad (1)$$

Passing to the limit as $\Delta \to 0$, we obtain our desired result, the Riccati equation

$$\frac{dU}{dz} = \frac{k'}{2k} - p - 2ikU - \left(\frac{k'}{2k} + p\right)U^2, \quad (2)$$

where $k'(z) = dk/dz$.

For an initial condition we have

$$U(b) = 0. \quad (3)$$

5. *Extensions.*—In this note, our aim has been to derive the equation (4.2) for the expected reflected wave. Having done this, a number of considerations now present themselves for further consideration. Among these are questions concerning the existence of a critical length for wave branching processes, the treatment of processes involving particles of many types, the consideration of spherical and cylindrical geometries, and the calculation of moments of $u(z)$ higher than the first. Future papers will treat these in detail.

[1] Chandrasekhar, S., *Radiative Transfer* (New York: Dover, 1960).

[2] Bellman, R., and T. Harris, "On age-dependent binary branching processes," *Ann. Math.*, **55**, 280–295 (1952).

[3] Bellman, R., R. Kalaba, and G. M. Wing, "Invariant Imbedding and Mathematical Physics, I. Particle Processes," *J. of Math. Physics*, **1**, 280–308 (1960).

[4] Bellman, R., and R. Kalaba, "Functional equations, wave propagation and invariant imbedding," *J. of Math. and Mechanics*, **8**, 683–704 (1959).

[5] Harris, T., *Branching Processes* (Berlin: Springer Verlag, to appear).

[6] Bellman, R., and R. Kalaba, "Invariant imbedding and wave propagation in stochastic media," *Electromagnetic Wave Propagation* (New York: Academic Press, 1960), pp. 243–252.

[7] Bellman, R., and R. Kalaba, "Functional equations in adaptive processes and random transmission," *IRE Trans. on Circuit Theory*, **CT-6**, 271–282 (1959).

[8] Atkinson, F., "Wave propagation and the Bremmer series," *J. Math. Anal. and App.*, **1**, 255–276 (1960).

*ON THE STATE OF CREATINE IN HEART MUSCLE**

By Y. C. P. Lee† and Maurice B. Visscher

DEPARTMENT OF PHYSIOLOGY, UNIVERSITY OF MINNESOTA

Communicated July 17, 1961

It is well known[1–4] that a considerable fraction of the total creatine in heart muscle is present in such a form that upon extraction by conventional procedures, such as trichloroacetic or perchloric acid, it will react directly with the diacetyl reagent. It is conventionally called the free creatine fraction and amounts to about 7 mM per kg of rabbit heart muscle.[4] The concentration of free creatine in plasma is 0.03 mM per liter. There is therefore a steady-state difference in apparent concentration of 230 fold. Since creatine can be demonstrated to move across the muscle membrane, it would seem that there must either be a "pump" mechanism maintaining a steady-state concentration difference or the so-called free creatine must not all be actually in free solution in a compartment available for exchange with the extracellular fluids. The theoretical possibility that the membrane is virtually impermeable to creatine is discarded on the grounds that it is contrary to observation, and the possibility that there is a large source of creatine synthesis in the muscle cell is discarded also for lack of evidence for it.

In order to investigate further the state of creatine in muscle, studies have been made using isotopically labeled creatine with isolated perfused rabbit hearts. Creatine-1-C^{14} in tracer amounts has been incorporated in the perfusion fluid and the changes over time in the specific activity in the creatine phosphate and "free" creatine fractions in heart muscle measured. By such observations one can obtain information bearing upon the permeability of the cell membrane to creatine and upon the nature of the "free" creatine pool.

Methods.—Male rabbits about 3 kg body weight were anesthetized with sodium pentobarbital (50 mgm/kg) and thoracotomized under endotracheal ventilation with oxygen. After heparin (300 U.S.P. units/kg), the aorta was cannulated and perfusion of the coronaries with oxygenated saline begun as quickly as possible to avoid myocardial hypoxia. The perfusate at this stage was discarded. The heart was transferred to a temperature-controlled chamber (37°C) arranged for collection of the coronary venous outflow. After all blood was washed out, the venous outflow was returned to the reservoir system creating a closed circuit. The minimum volume used was 60 ml. The perfusion was at a pressure of 20 mm Hg maintained by finger-pump. The flow was about 25 ml per min.

The perfusion fluid was a phosphate buffered solution, NaCl 145.5, KCl 2.7, $CaCl_2$ 1.8, KH_2PO_4 0.17, Na_2HPO_4 1.48, and glucose 5.56 mM per liter. It was aerated with 100% oxygen. The initial pH was about 7.6. After a period of closed circuit perfusion, CO_2 and organic acids entered and the pH fell to 7.2–7.3.

The exchanges of creatine were studied in hearts beating spontaneously, during prolonged arrest, and also after a previously arrested heart was returned to a rhythmic contractile state. Arrest was induced by shifting to a calcium-free perfusate and in addition, introducing rapidly into the flowing perfusion fluid entering the coronary vessels 3.5 ml of a 0.20% solution of sodium citrate. The citrate rich perfusate was discarded, as was the first 50 ml of calcium-free perfusion fluid. The heart was maintained in asystole so long as the perfusion fluid was calcium-free. The beat was restored by shifting to perfusion with normal calcium level. The details of the ion effects upon arrest and recovery are complex and will be presented in another report.[5]

Creatine-1-C^{14} was added to the perfusion fluid at a concentration of 8.8 μM per 100 ml. The activity of the creatine was about 1.34 $\mu c/\mu M$. Since the entrance rate of creatine into the muscle cell is slow, it was essential to remove tracer-containing perfusate from the coronary

blood vessels and from the readily exchangeable extracellular space. Consequently, after perfusion with radioactive creatine solution, the heart was perfused with tracer-free solutions for the period of time found necessary in preliminary experiments for the venous effluent radioactivity to fall to a steady level, close to background. This required from 5 to 7 min of washout perfusion under different circumstances.

For analysis, the heart was frozen in liquid nitrogen, always after citrate arrest if the heart was not already in arrest. Previous studies[4] have demonstrated that creatine phosphate breakdown during freezing is prevented or diminished by prior calcium-lack arrest. The methods for creatine and creatine phosphate extraction and analysis have been described previously,[4] with the modification that 6% perchloric acid was used in place of trichloroacetic and neutralization with KOH allowed removal of the perchlorate. The extracts were passed through columns of Dowex-1 and Dowex-50 resins in a room at 2°C. The former retains creatine phosphate from neutral solutions but allows the creatine to pass. The creatine phosphate is eluted with ammonium formate solution, following the method of Hurlbert *et al.*[6] Dowex-50 retains creatine and allows creatine phosphate to pass with a water eluent. The radioactivity was measured with a liquid scintillation counter and specific activities calculated from the analytical concentrations and activities of creatine and creatine phosphate, respectively.

Results.—Table 1 presents the observed data from twenty-six experiments in which rabbit hearts were perfused with labeled creatine for periods from 5 to 90 min, followed by either 5 or 20 min of washout perfusion. It will be noted that the hearts tended to become edematous with longer perfusions as evidenced by a decrease in per cent dry weight, with some decrease (10%) in total creatine (per unit dry weight), and a definite decrease in the proportion of the total creatine that was present as the phosphate. These are not unexpected findings.

The more interesting observed facts relate to radioactivity present in the "free" creatine and creatine phosphate fractions, respectively. Here, contrary to what might have been predicted, the specific activity of the creatine phosphate fraction exceeds that in the "free" creatine moiety for the first 60 min of accumulation. The decline of the SA ratio after 60 min may be an artifact since the creatine phosphate concentration and fraction of total were both low and the dry weight values indicated considerable edema. The rate of rise of SA of "free"creatine from 60 to 90 min is apparently four times that in the preceding hour. The rate of rise of SA of creatine phosphate is also greater in the period 60 to 90 min than before, but the increase is very much less. It is possible that the occurrence of the edema may have resulted in some increase in trapped extracellular creatine which the standard washout perfusion of 5 min did not remove. A small difference in this quantity would create a large error, because the specific activity of the perfusate creatine was about 100 times that of the intracellular creatine, even at 90 min.

It will also be noted that when the time of washout perfusion is extended to 20 min, the observed specific activity of the creatine phosphate falls relatively little from the values obtained after 5 min of washout, while the SA of the "free" creatine declines to about 25 per cent of what it had been.

In Table 2 are shown the results of a series of experiments in which the tracer was presented to the heart muscle during periods of cardiac arrest, in comparison with the findings when the tracer was in the perfusion fluid only during a period of spontaneous beating after recovery from prolonged asystole. It may be noted that during asystole the incorporation of label in the creatine phosphate was definitely decreased, both in comparison with the incorporation in the same period of time with no prior arrest and after a period of arrest followed by recovery.

TABLE 1

CONCENTRATIONS AND SPECIFIC ACTIVITIES OF "FREE" CREATINE AND CREATINE PHOSPHATE IN PERFUSED RABBIT MYOCARDIUM

No. of rabbits	Perfusion with creatine-1-C^{14} (time in min)	Time of washout (min)	Dry wt (%)	Creatine μM/gm Dry Ventricular Muscle				Specific Activity		SA of Cr-P
				"Free" Cr	Total Cr	Bound Cr-P	Bound (%)	"Free" creatine cpm/μM (range)	Creatine from Cr-P	SA of "Free" Cr
4	5	5	14.3	30.04	66.45	36.41	54.8	173 (128–213)	276 (266–278)	1.59
2	10	5	14.9	29.85	68.47	38.63	56.1	286 (227–345)	461 (455–467)	1.61
2	15	5	14.6	30.92	65.27	34.35	52.6	391 (376–406)	696 (640–752)	1.78
5	30	7	14.5	34.50	65.80	31.30	47.5	650 (599–755)	968 (803–1,238)	1.49
3	60	7	13.7	33.21	62.29	29.08	46.7	1,141 (1,104–1,179)	1,415 (1,255–1,559)	1.24
4	90	7	11.9	33.97	60.92	26.95	44.2	3,302 (2,222–4,084)	2,440 (1,210–3,268)	0.72
3	15	20	14.8	26.41	61.60	35.19	57.1	96 (57–134)	510 (448–615)	5.31
3	30	20	13.2	24.81	55.27	30.46	55.0	183 (148–223)	772 (543–896)	4.22

TABLE 2

THE EFFECTS OF CARDIAC ARREST UPON THE INCORPORATION OF CREATINE-1-C^{14} INTO MYOCARDIAL CREATINE FRACTIONS

No. of rabbits	Perfusion with Creatine-1-C^{14} (time in min)			Time of washout (min)	Dry wt (%)	Creatine μM/gm Dry Ventricular Muscle				Specific Activity cpm/μM				SA of Cr-P
	Normal beating	Arrest	Recovery			"Free" Cr	Total Cr	Bound Cr-P	Bound (%)	"Free" creatine	S.E.	Creatine from Cr-P	S.E.	SA of "Free" Cr
2	10	..	..	5	14.9	29.85	68.47	38.63	56.1	286 (227–345)	S.E.	461 (455–467)	S.E.	1.61
7	..	10	..	7	13.4	25.75	74.14	48.40	65.3	295	±45	173	±16	0.59
4	..	..	10	5	14.3	36.49	74.96	38.47	51.3	186	±30	259	±25	1.47

Discussion.—One can schematize the possible relationships between the various forms in which creatine exists in heart muscle and its environment, and the possibilities for its movement in position or in respect to form of chemical combination as follows:

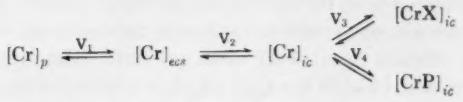

In this expression the subscript *p* indicates plasma or perfusate, *ecs* the extracellular space, and *ic* the intracellular compartment. Cr refers to creatine, CrP creatine phosphate, and CrX a hypothetical creatine complex or state which will be considered later. On *a priori* grounds, it seems likely that the capillary wall offers no great barrier to movement and that V_1 is not a rate-limiting factor in the over-all transfer process. Therefore, $(Cr)_p$ probably is equal to $(Cr)_{ecs}$. However, the cell wall proper may or may not offer impediments to creatine diffusion. The relative magnitudes of V_2, V_3, and V_4 appear to be determining as to accumulation of the tracer. The facts presented in this paper bear upon these questions. There are several possibilities as to interpretation of the observed facts and they will be presented.

In terms of the scheme presented, the analytically determined "free" creatine comprises the sum of $(Cr)_{ic}$ and $(CrX)_{ic}$. The existence of CrX as a definite chemical entity has not been demonstrated, and its occurrence is being postulated to account for the facts (1) that the specific activity of the "free" creatine fraction in heart muscle is lower than that of the creatine phosphate and (2) that upon washout for 20 min., the specific activity of the "free" fraction falls very rapidly, indicating that some moiety of that fraction is able to leave the cell freely. The creatine phosphate specific activity fell comparatively less during the 20-min washout period.

An alternative possibility to the existence of a chemical entity CrX is that the Cr pool is not a unit but consists of pools in at least two compartments within the cell with high barriers to exchange between them. This hypothesis would appear to require the existence of low permittivity "membranes" within the cell separating such pool compartments in order to account for the fact that the "free" creatine specific activity rises so slowly during accumulation and falls so rapidly during washout. Such a multicompartment system is, of course, not impossible, but since such systems are not known to exist, it seems simpler to suppose that a fraction of the "free" creatine is somehow bound in such a way that it does not exchange rapidly with the true free creatine pool. Creatine is known to complex readily with other substances.[7]

If one accepts tentatively the postulates implicit in the scheme presented, it becomes possible to suggest that $(Cr)_{ic}$ may have a value equal to $(Cr)_{ecs}$ and that there may normally be no concentration gradient whatever for creatine across the cell wall. If $V_2 \ll V_1$, and $V_4 \gg V_3$, then the facts as observed in the tracer experiments can be harmonized with the scheme.

In the experiments performed, as noted in the description of methods, a period of 5 min of washout was used routinely to remove intravascular and readily diffusible

extravascular (presumably *ecs*) label. The experimental design was therefore not adequate to a precise quantitative evaluation of the several V values. Since the SA of the perfusion fluid creatine was about 100 times that of the CrP [illegible] min, we cannot know the SA values of Cr_{ecs} and Cr_{ic} with any certainty after the washout period. A better design will be difficult to set up with an intact heart, but perhaps with thin strips of muscle one could measure the necessary variables. Nevertheless, certain facts in relation to rates are quite evident. The fact that the arrested heart shows an increase in label in the CrP which is a little less than half that found in beating hearts indicates that the reaction $CrP \rightleftharpoons Cr + P$ is proceeding during arrest, although at a slower rate. Since the oxidative metabolism of the heart is also greatly reduced by arrest, this result is not surprising. Since oxygen consumption measurements were not made in these experiments, it is not possible to say whether or not the CrP turnover was precisely proportionate to the oxidation changes. It is worth noting, however, that CrP turnover is not limited to a contraction-linked process. The increase in "free" creatine label was not less in the arrested than in the normal heart, or in one restored to beating after a 10-min period of arrest, indicating that its accumulation may be unrelated either to contractile process or to total oxidative metabolism. This deduction should be accepted with reserve, however, because the arrested heart was perfused at a lower pressure, since earlier observations showed that edema occurred quickly in perfused quiescent hearts, and the washout period was extended from the usual 5 min to 7 min, which was found necessary to bring the washout fluid to stable counts near background. Thus the conditions were altered sufficiently in the case of these seven hearts to make comparisons of absolute values of "free" creatine radioactivity dubious, but for the CrP and the SA ratios the values are undoubtedly valid, especially since extra washout time in the hearts perfused with labeled creatine during normal contraction produces exactly the opposite change in SA ratio from that found in this series.

Summary.—Studies on the rates of incorporation of creatine-1-C^{14} into the separated and analytically measured creatine phosphate and so-called "free" creatine fractions in perfused isolated rabbit hearts have shown that the specific activity of the creatine phosphate fraction rises more rapidly than does that of the "free" fraction. Upon washout the specific activity of the "free" fraction falls three times as rapidly as does that of the creatine phosphate fraction. Cardiac arrest slows but does not stop the incorporation of label in the creatine phosphate. The creatine phosphate breakdown and resynthesis is therefore not exclusively contraction-linked.

The kinetics of movement of label are incompatible with the assumption of a homogeneous "free" creatine pool. Reasons are presented for favoring the view that the fraction conventionally measured as free creatine consists of at least two chemical entities, one bound in such a way as to be freed during acid extraction. The actual concentration of free creatine in the cell need not be higher than that in the extracellular fluid to account for known facts, if one assumes the existence of a creatine complex which comprises most of the analytically determined "free" creatine.

* Aided by grant H-3212, U.S. Public Health Service.

† Established Investigator of the Minnesota Heart Association

[1] Ennor, A. H., and H. Rosenberg, *Biochem. J.*, **51**, 606 (1952).
[2] Fawaz, G., and E. S. Hawa, *Proc. Soc. Exptl. Biol. Med.*, **84**, 277 (1953).
[3] Wollenberger, A., *Am. J. Physiol.*, **150**, 733 (1947).
[4] Lee, Y. C. P., R. A. DeWall, and M. B. Visscher, *Am. J. Physiol.*, **198**, 855 (1960).
[5] Lee, Y. C. P., H. G. Richman, R. A. DeWall, and M. B. Visscher, to be published.
[6] Hurlbert, R. B., H. Schmitz, A. F. Braum, and Van R. Potter, *J. Biol. Chem.*, **209**, 23 (1954).
[7] Unpublished observations in this laboratory showing complexing with certain amino acids.

*A THEORY OF GASEOUS ANESTHETICS**

BY STANLEY L. MILLER

DEPARTMENT OF CHEMISTRY, UNIVERSITY OF CALIFORNIA AT SAN DIEGO

Communicated by Joseph E. Mayer, July 5, 1961

In the course of an investigation of gas hydrates at low temperatures and their occurrence in the solar system,[1] it was noticed that many of the gases which form hydrates, such as ethylene, nitrous oxide, chloroform, and xenon, are also gaseous anesthetics.[2] A comparison of the pressure of anesthetic necessary to maintain a person in a given stage of anesthesia and the dissociation pressure of the hydrate at 0°C shows that there is indeed a correlation. The data are shown in Table 1. The ratio of anesthetic pressure to hydrate dissociation pressure is in the range 0.1 to 0.5, except for the low value of carbon dioxide and the high values of sulfur hexafluoride and xenon. The ratios are about the same for both Structure I hydrates (Gas·6 to 10 H_2O) and the Structure II hydrates (Gas·17 H_2O).

Taking into account the uncertainties of the data, the correlation can be considered good, with some of the agreement probably being fortuitous. This correlation is as good as the correlations obtained with the Meyer-Overton lipid theory of anesthesia.[5]

The gas hydrates: The gas hydrates are clathrate compounds of a gas encaged in a distorted ice matrix (for reviews, see refs. 3 and 17). These crystalline compounds occur in two forms, and the structures have been determined[12, 17–20]. Structure I has a cubic unit cell 12.0 Å on edge containing 46 water molecules and 8 cavities. The two smaller cavities are pentagonal dodecahedra each formed by an array of 20 water molecules giving a cavity of 3.95 Å which can encage molecules with diameters of 5.1 Å or less. The six larger cavities are tetrakaidecahedra (with two opposite hexagonal faces and 12 pentagonal faces) each formed by an array of 24 water molecules, giving a cavity of 4.3 Å radius which can encage molecules with diameters of 5.8 Å or less.

Structure II hydrates have a cubic unit cell of 17.4 Å on edge containing 136 water molecules and 24 cavities. The sixteen smaller cavities are distorted pentagonal dodecahedra each formed by an array of 20 water molecules giving a cavity of 3.91 Å radius which can encage molecules with diameters of 5.0 Å or less. The eight larger cavities are hexadecahedra each formed by an array of 28 water molecules giving a cavity 4.73 Å radius which can encage molecules with diameters of 6.7 Å or less.

Gases which form hydrates but are not anesthetics: There are a number of gases,

TABLE 1

COMPARISON OF THE GAS REQUIRED FOR SURGICAL ANESTHESIA[4] AND THE DISSOCIATION PRESSURE OF THE HYDRATE AT 0°C

Gas	Pressure (atm) of anesthesia	Ref.	Dissociation pressure (atm) of hydrate at 0°C	Ref.	$P_{anesthesia}/P_{hydrate}$
		STRUCTURE I HYDRATES			
Nitrogen	29	*6*	160	*15*	0.18
Argon	20	*6*	95	*3*	0.21
Krypton	2.9	*6*	14.5	*3*	0.20
Xenon	0.85	*6,7*	1.2	*3*	0.70
Methane	4.6	*6*	26	*3*	0.18
Ethane	1.3	*5*	5.2	*3*	0.25
Ethylene	0.80	*6,9*	5.54	*3*	0.14
Acetylene	0.70	*5,9*	5.7	*3*	0.12
Cyclopropane	0.15	*6,9*	0.63	*14*	0.24
Nitrous oxide	0.90	*6,9*	10	*3*	0.09
Carbon dioxide	0.25	*10*	12.5	*3*	0.02
Methyl fluoride	0.14	*8*	2.1	*12*	0.07
Methyl chloride	0.14	*8*	0.41	*3*	0.34
CH_3CHF_2	0.45	*8*	0.82	*13*	0.55
		STRUCTURE II HYDRATES			
Chloroform	0.015	*9*	0.062	*3*	0.24
Ethyl chloride	0.04	*9*	0.27	*3*	0.15
Propane	0.9	*5*	1.74	*3*	0.5
Propene	0.4	*3,9*	4.3	*16*	0.09
Sulfur hexafluoride	3.0	*6*	1.0	*3*	3.0
Methyl iodide	0.07	*8*	0.097	*3*	0.7
Ethyl bromide	0.04	*8*	0.20	*12*	0.2
CH_2Cl_2	0.030	*8*	0.15	*3*	0.20
CF_2Cl_2	0.6	*8*	0.9	*11*	0.7
$CFCl_3$	0.15	*8*	0.54	*11*	0.28
CH_2CHCl_2	0.026	*8*	0.072	*12*	0.36

such as H_2S, SO_2, Cl_2, O_2, $CHCl_2F$, C_2H_5F, etc., which form hydrates, but are not known to have anesthetic properties. These gases exhibit acute toxic reactions at pressures lower than those probably necessary for narcosis and are therefore omitted from the table.

Gases which have no narcotic properties: Helium, hydrogen, and probably neon have no anesthetic effect, and these gases do not form hydrates.

Local anesthetics: The mechanism of action of local anesthetics which are tertiary or quaternary amines is almost certainly different from gaseous anesthetics, and therefore will not be discussed here.

The Formation of Hydrates during Anesthesia.—In order to determine if crystalline hydrates could be formed in the body during the administration of an anesthetic, it is necessary to extrapolate the dissociation pressures to 37°C, since the pressures given in the table refer to 0°C.

The dissociation pressure of a hydrate as a function of temperature is given by the integrated Clausius-Clapeyron equation

$$\log P_1/P_0 = \frac{\Delta H}{2.3R}\left(\frac{1}{T_0} - \frac{1}{T_1}\right) \qquad (1)$$

where ΔH is the enthalpy of the reaction of 1 mole of gas with n moles of liquid water to form a solid hydrate $G \cdot nH_2O$, R is the gas constant and the T's are the absolute temperatures.

For hydrates of Structure I, the ΔH's are about 16 kcal/mole[3], giving $P_{37}/P_0 = 33$. For hydrates of Structure II, the ΔH's are about 31 kcal/mole[3], giving $P_{37}/P_0 = 915$.

These figures refer to the reaction of the gas with pure water to give a hydrate, and therefore must be corrected for the effects of salts in the interstitial and intracellular fluids. Taking the salt concentration as 0.32 osmolar and omitting the effect of the dissolved anesthetic, the activity of water in interstitial fluid is lowered by 0.58 per cent. The increase in gas pressure needed to form a hydrate due to the lowering of the activity of the water is given by the equation

$$a_G = a_{H_2O}{}^{-n} \tag{2}$$

where a_G is the activity of the gas relative to the dissociation pressure of the hydrate with pure water, a_{H_2O} is the activity of water in the interstitial fluid relative to pure water, n is the ratio of water to gas in the crystalline hydrate (about 7 for Structure I hydrates and 17 for Structure II hydrates). This raises the dissociation pressure by a factor of 1.04 for Structure I hydrates, and 1.10 for Structure II hydrates.

Combining these factors, the pressure to form, for example, N_2O hydrate in interstitial fluid is 343 atm, while the observed pressure for anesthesia is 0.90 atm. This is a free energy unfavorable by $\Delta G = RT\ln[P_{hydrate}/P_{anesthesia}] = 3.6$ kcal/mole of gas or $\Delta G = 0.51$ kcal/mole of water.

For a Structure II hydrate, for example $CHCl_3$, the pressure to form a hydrate at 37°C in interstitial fluid is 63 atm, while the observed pressure for anesthesia is 0.015 atm. This gives a free energy unfavorable by 5.1 kcal/mole of gas or 0.30 kcal/mole of water.

These pressures (fugacities) of N_2O and $CHCl_3$ cannot be obtained at 37°C since these gases liquefy at much lower pressures, and in any case the hydrates of N_2O and $CHCl_3$ are not stable above 10° and 1.6°, respectively.

These hydrates could be stable at 37° if the activity of water could be increased, equation (2). This may be possible in isolated systems where small particles of ice or water can be in a metastable condition. However, since the cells are in osmotic equilibrium with the interstitial fluid, the activity of water is the same throughout the body. Therefore, it would appear to be impossible that crystalline hydrates could form during anesthesia. In addition, hydrates are formed at a definite pressure, below which the hydrate is unstable, but anesthetics exert a continuously increasing effect as the pressure is raised.

If the correlation of anesthetic potency and hydrate dissociation pressures is assumed to be more than accidental, then we must examine the interactions of gases in aqueous solution, for which the ability to form hydrates is but one expression.

Gases in Aqueous Solution.—It has been pointed out by several investigators[21] that the low solubilities, large entropies of solution, and large partial molal heat capacities of nonpolar gases in water can be interpreted to mean that the water surrounding a dissolved gas molecule is in a more highly ordered state than the water in bulk solution. This more highly ordered water is sometimes referred to as "iceberg."

Most of the theories of the structure of water assume that ice-like configurations are present in liquid water.[22] Pauling has proposed a model of liquid water which is a Structure I hydrate with the cavities occupied by water molecules instead of gas molecules.[23] Although none of these theories has been accepted as the correct description of liquid water, it seems likely that ice-like clusters, probably of several

types, do exist in liquid water. These "icebergs" would be in a dynamic state, constantly being formed and broken down.

It has also been proposed that some of the water in proteins is ice-like, and that these "icebergs" play a significant role in the properties of these polymers.[24, 25]

We will assume that these "icebergs" are present in liquid water, and that the gas molecule is also surrounded by "icebergs."

Not all the gas molecules dissolved in water are surrounded by "icebergs." A fraction of the gas molecules occupy quasi-lattice sites in the water, and this fraction depends on the gas dissolved. It is high for helium and low for xenon. An estimate of the "iceberg" present might be obtained from the partial molal entropies of solution or partial molal heat capacities, but these quantities are not accurately known or the data are not available. Therefore, we shall examine this problem from the standpoint of the binding of a gas molecule in a cavity in liquid water, in particular in a water cavity near some surface. Whether this surface is the surface of a membrane, the "surface" of a protein, mucopolysaccharide or other polymer will not alter the discussion. This treatment would also apply to the "icebergs" around gas molecules in bulk water, and this might permit the calculation of solubilities and partial molal entropies of solution for nonpolar gases.

We shall attempt to calculate the fraction of the surface covered by water which is in a more highly ordered (or icelike) state than in the liquid water. This cumbersome expression will be abbreviated "ice cover."

It has been shown that the dissociation pressure of a clathrate with a single type of cavity in terms of the fraction of cavities occupied and the binding energy in the cavity is given by the equation[26]

$$P_A = \frac{y}{1-y}\frac{kT}{2\pi a^3 g}\exp\left[w(0)/kT\right] \tag{3}$$

where P_A is the pressure of the gas, y is the fraction of cavities (or sites) occupied by the gas molecules, k is Boltzmann's constant and T is the absolute temperature. The quantity $w(0)$ is the energy of binding at the center of a preformed cavity (or site) and $2\pi a^3 g$ is the free volume of the molecule in the cavity. These latter two quantities have been calculated with some success by means of the Lennard-Jones, Devonshire theory.[3, 27] This equation is analogous to a Langmuir adsorption, in which the bound molecules are adsorbed on independent sites and there are no interactions between the adsorbed molecules.[28] Written in molar quantities this becomes,

$$P_A = \frac{y}{1-y}\frac{RT}{V_f}\exp\left(-\Delta E/RT\right) \tag{3a}$$

where V_f is the free volume per mole and ΔE is the energy of vaporization from the cavities.

We will assume that the surface under consideration has three types of water. A fraction X_w consists of "liquid water" which has no icelike structure. The second fraction X_I is icelike or "iceberg" water. These "icebergs" will be assumed to contain a cavity that can encage a gas molecule but the cavity is empty. The third fraction of the total water $X\hat{A}$ consists of "icebergs" which have gas molecules encaged in them.

The ratio of "iceberg" water to liquid water is given by

$$X_I/X_W = \exp(-\Delta G_1/RT) \tag{4}$$

where ΔG_1 is the free energy to form a mole of these cavities from liquid water. ΔG_1 is temperature dependent in a manner to make X_I greater at lower temperature. The number of empty "icebergs" does not change appreciably when dissolved gas molecules are present. When some of the empty "icebergs" become filled with gas molecules, sufficient "liquid water" is converted to "iceberg" to maintain the ratio given by equation (4).

We have from the definition of y

$$X_A/X_I = y/(1 - y) \tag{5}$$

Combining these two equations gives the ratio of surface covered with gas filled cavities to surface covered with liquid water

$$X_A/X_W = \exp(-\Delta G/RT)\, y/(1 - y) \tag{6}$$

Combining with equation (3a) for $y/(1 - y)$ gives

$$X_A/X_W = P_A \frac{V_f}{RT} \exp(\Delta E/RT) \exp(-\Delta G_1/RT) \tag{7}$$

or

$$P_A = \frac{X_A}{X_W} \frac{RT}{V_f} \exp(-\Delta E/RT) \exp(\Delta G_1/RT) \tag{7a}$$

This equation states that at a given temperature the "ice cover"/water ratio at a surface in the different stages of anesthesia is proportional to the pressure of the anesthetic. The term $(RT/V_f) \exp[-\Delta E/RT]$ is proportional to the dissociation pressure of the hydrate along the ice-hydrate-gas equilibrium extrapolated to 37°, assuming that the cavities in the "iceberg" are the same as in the hydrate. In order to have a correlation of anesthetic pressures with hydrate dissociation pressures at 0°C, the ΔG_1 term would have to compensate for the variations in ΔE. The ΔE's vary from 3 to 8 kcal for both hydrate structures. The larger ΔE's are associated with the larger molecules in most cases, but the larger molecule will only fit into a larger cavity. This larger cavity will have a greater ΔG_1 of formation than a smaller cavity, and the quantity $\Delta E - \Delta G_1$ will remain approximately constant for molecules of both hydrate structures.[29] Therefore, if we assume this model of anesthetic activity to be correct, the correlation of anesthetic potency at 37°C and the hydrate dissociation pressures at 0°C can be understood.

Anesthetics which do not form hydrates: There are many gases which have anesthetic properties but, in so far as is known, do not form hydrates. The most notable of these is diethyl ether. The list also includes hydrocarbons higher than propane, aromatic hydrocarbons, various ethers and halogenated derivatives of these compounds.

These higher molecular weight anesthetics are too large in size to enter the cavities of Structures I or II. It is as likely that these larger molecules are surrounded by "icebergs" in aqueous solution as it is for gases which form hydrates, since these larger molecules also have large entropies of solution and large partial molal heat capacities in solution. Equation (7) would apply to these gases for

which hydrates are not known. If good estimates of ΔE, ΔG_1 and V_f could be made, the correlation in Table 1 of anesthetic potency and "ice-cover" could be extended to include these larger molecules.

This argument would be strengthened if hydrates of these larger molecules could be shown to exist, and attempts are being made in this laboratory to prepare them.

Hydrogen bonding anesthetics: Alcohols, esters, ketones and aldehydes have anesthetic properties, and it seems likely that these compounds would increase the "ice cover" of membranes. In the case of acetone the hydrate is known (Structure II).[30] It is not likely that the "ice cover" formed by these compounds could be estimated by assuming that they are simply encaged in an empty "iceberg" cavity. The effects of hydrogen bonding and dipole interactions with the water would have to be taken into account. Therefore, these anesthetics will not be examined here even though they may, in the final analysis, act in the same way as non-hydrogen bonding anesthetics.

The Temperature Effect of Anesthesia.—It would be reasonable to assume that an "iceberg" without a gas molecule in it (X_I) would have the same effect as an "iceberg" containing a gas molecule (X_A), with the role of the anesthetic gas being to increase the total amount of "ice cover." This would allow an explanation of the anesthetic effect of hypothermia in the absence of an anesthetic gas. Equation (7) neglects the contribution of X_I to the anesthetic effect, but X_I which is present in any case, subtracts out and allows intercomparisons of different anesthetics as long as the temperature is held constant.

We can include the effect of X_I by taking the total "ice cover," $X_A + X_I$, as the index of anesthetic activity. This gives

$$\frac{X_A + X_I}{X_W} = \exp\left(-\Delta G_1/RT\right)\left[P_A \frac{V_f}{RT} \exp\left(\Delta E/RT\right) + 1\right] \tag{8}$$

Therefore, if we assume that equal "ice covers" give equal degrees of anesthesia, then the temperature and anesthetic pressures required to attain a given stage of anesthesia are interrelated by this equation.

We have assumed a single type of cavity, but it would be likely that several types of cavities could surround a gas molecule, and that X_I consists of several types of ice-like structures. We can allow for the different types of cavities by summing over the i types of cavities to give

$$\frac{X_A + X_I}{X_W} = \sum_i \exp\left(-\Delta G_i/RT\right)\left[P_A \frac{V_f}{RT} \exp\left(\Delta E_i/RT\right) + 1\right] \tag{9}$$

There have been to the writer's knowledge no careful studies of the change of the pressure of an anesthetic needed when the temperature of the patient is below or above 37°. Any temperature effect of anesthesia is, of course, complicated by temperature effects on nerve activity and metabolism. This point could be studied by comparing equations (8) or (9) with experimental data, using reasonable values of ΔE and ΔG. The temperature range available for the investigation with cold blooded animals might permit the evaluation of the (average) constants of equation (9).

It is of interest to consider whether the anesthesia produced by hypothermia is a carbon dioxide anesthesia, an effect on the water, or another effect. Carbon

dioxide anesthesia is attained at 0.25 atms at 37°C, and using $\Delta H = 16$ kcal in equation (1) for the extrapolation, carbon dioxide anesthesia would be attained with 0.14 atm at 30°C, which is the temperature for anesthesia by hypothermia. The partial pressure of CO_2 in arterial blood is 0.047 atm at 37°C but is lowered to 0.026 atm during hypothermia.[31] Therefore, on the basis of this extrapolation, it would appear that the normal carbon dioxide of the blood does not contribute to the anesthesia during hypothermia. This conclusion could be tested by determining the temperature required for anesthesia when the patient is in compensated metabolic alkalosis (high CO_2) and compensated metabolic acidosis (low CO_2).

Mixtures of Anesthetics.—If we assume that the sites in which an anesthetic is adsorbed are independent, then it follows that the "ice cover" will be the sum of the effects of each anesthetic. This can be expressed by the equation:

$$\sum_i P_i/P_i^0 = 1 \qquad (10)$$

where P_i^0 is the pressure of the i^{th} gas which will produce a given stage of anesthesia when used alone, and P_i is the partial pressure of this gas in the mixture. Clinical practice of using mixtures of gaseous anesthetics approximates this equation, and this relationship is in accord with the quantitative data for N_2O and CO_2 mixtures.[32] These gases both form Structure I hydrates. If the sites were not independent, the effects would still be additive, because both types of molecules can be interchanged in the same cavity.

In mixtures of anesthetics of different size, such as chloroform and cyclopropane, the cyclopropane can enter the cavity occupied by the chloroform, but not the reverse. Therefore, if the sites were not independent, in that the iceberg around the chloroform extended a sufficient distance to form an empty cavity of smaller size, then the cyclopropane would stabilize the chloroform "iceberg" in a non-additive manner. This effect is shown by the stabilization of Structure II hydrates by small molecules which occupy the smaller holes of the Structure II lattice, forming double hydrates (for example, $CHCl_3 \cdot 2H_2S \cdot 17H_2O$ instead of $CHCl_3 \cdot 17H_2O$ when no H_2S is present). The question whether the sites are independent or not can be easily tested experimentally.

The Lipid Theory of Narcosis.—The Meyer-Overton theory of narcosis states that anesthetics are lipid soluble gases, the index of anesthetic potency being the oil/water partition coefficient times the solubility in water. Ferguson[33] and Brink and Posternak[34] have used the activity of the anesthetic gas relative to the liquid to correlate anesthetic activity. This choice of standard state, which is arbitrary, implies that equal degrees of anesthesia are produced when equal mole fractions (or volume fractions) of anesthetic are present in the lipid parts of a membrane or other structure which are lipid in character. This treatment has been extended by Mullins[5] to take into account the more advanced ideas of solution theory.

This correlation of the chemical activity of the anesthetic and its potency can be considered as rather good. There can also be no question that anesthetics enter the lipid membranes. The problem is where do the anesthetics exert their effect. Correlations of anesthetic activity do not answer this question, especially if several different properties of the anesthetic give about equally good correlations.

The Mechanism of Action of Anesthetics.—There are many hypotheses of the

mechanism of narcosis that could be proposed in the light of this theory. It is possible that the "ice cover" lowers the conductance, "stiffens up" the lipid membrane, "plugs up" the pores of the membrane, etc. There are also several hypotheses which do not involve mechanical obstructions and which are more accessible to experimental test.

Narcotic agents raise the threshold for conduction along the nerve,[35] and the threshold would be increased by an increase in the capacity of the membrane and associated aqueous double layer. It is possible that an "ice cover" could increase this capacity. At the interface between mercury and aqueous salts, there is an anomalous increase in the differential capacity between the mercury and the outer Helmholtz plane.[36] The anomalous capacity is present when the mercury has a positive surface charge. An explanation offered for this effect is that the water near the mercury is "ice-like." It is interesting to note that this anomalous capacity is markedly increased in the presence of n-heptyl alcohol,[37] which is also a narcotic.

This hypothesis could be tested by measuring the changes in capacitance in the presence of different gaseous anesthetics at the nodes of Ranvier or at unmyelinated nerves. Although the mercury-aqueous salt interface is not a model for a nerve, this system permits the study of the effect of anesthetics on the "ice cover" and the resulting anomalous capacity without the complications due to lipid solubility and changes in permeability and voltage.

It is possible that the anesthetic exerts its effect on the mechanism of permeability change during conduction. In Nachmansohn's theory,[38] this effect would be on acetylcholine esterase, the receptor protein or the storage protein. The effect of anesthetics on the binding constants or enzyme activity could be measured *in vitro*.

From general considerations, it is apparent that the major effect of gaseous anesthetics is on transmission at synapses (including neurons and the neuromuscular junction).

It has been demonstrated *in vitro* that the sympathetic ganglion is more sensitive to a given level of anesthetic than a node of Ranvier, although the effect is similar.[39] A capacitance change in the membrane is likely to exhibit a greater overall influence at a synapse than at a nerve, because the presynaptic membrane and postsynaptic membrane form in a sense a condenser in themselves. The relative influence of the capacitance change would depend on the details of the interlocking of the two membranes. The "ice cover" produced by anesthetics could also affect the binding, hydrolysis and diffusion of neurohumoral transmitters.

Summary.—There is a good correlation between the pressure of a gaseous anesthetic required for surgical anesthesia and the dissociation pressure of the corresponding gas hydrate at 0°C. However, it is shown that a gas hydrate will not form in the body with the pressures of anesthetic used. Although the gas hydrates are not formed, the anesthetic will increase the amount of "icebergs" in the water, some of which are present in the absence of the gas. This idea is examined in terms of the "ice cover" at a membrane or the surface of a protein. The amount of this "ice cover" will be proportional to the dissociation pressure of the hydrate, and this may account for the correlation of anesthetic pressures and hydrate dissociation pressures. The increase in "ice cover" on lowering the temperature and its relationship to hypothermia is also examined. Several effects that the "ice cover" might have on nerve conduction and transmission are discussed, and some experi-

ments to test this hypothesis are suggested.

Note added in proof.—Since this article was submitted, a paper by L. Pauling has appeared (*Science*, **134,** 15 (1961)) in which a similar theory is presented. Pauling proposes that microcrystals of hydrate are formed during anesthesia, these crystals being stabilized by side chains of proteins. In spite of any possible stabilization of hydrate crystals by protein side chains, it appears doubtful that crystals could be formed. The gas-filled "icebergs" could be considered equivalent to Pauling's microcrystals, except that the "icebergs" are much smaller and are not crystals in the usual sense.

* This research was supported by a Research Grant (G-13968) from the National Science Foundation.

[1] Miller, S. L., these PROCEEDINGS, (to appear).

[2] The term gaseous anesthetic will also be used here for anesthetics which are liquids at room temperature and frequently referred to as volatile anesthetics.

[3] Van der Waals, J. H., and J. C. Platteeuw, *Advances in Chemical Physics* II, 1 (1959).

[4] The anesthetic pressures from the literature references have been adjusted to the pressure necessary to maintain a person (or animal) in the third plane of the third stage of anesthesia. The pressure of anesthetic necessary to maintain this stage of anesthesia is the figure of interest, since the pressure necessary to induce anesthesia is a problem in rates of transport. Many of the anesthetic pressures given are uncertain, especially for the halogenated hydrocarbons. These values refer mostly to animal experiments which are not strictly comparable to anesthetic action on humans. In many cases there are toxic reactions superimposed on the anesthetic activity which are difficult to allow for.

[5] Mullins, L. J., *Chem. Revs.*, **54,** 289 (1954).

[6] Carpenter, F. G., *Am. J. Physiol.*, **178,** 505 (1954). The values given have been normalized by a factor of 1.60.

[7] Cullen, S. C., and E. G. Gross, *Science*, **113,** 580 (1951); Pittenger, C. B., *et al.*, *Anesthesiology*, **14,** 10 (1953).

[8] Von Oettinger, W. F., *The Halogenated Hydrocarbons, Toxicity and Potential Dangers*, Public Health Service Publication 414 (Washington, D. C.: U. S. Government Printing Office, 1955).

[9] Adriani, J., *The Pharmacology of Anesthetic Drugs* (Springfield, Illinois: Charles C Thomas, 1952).

[10] McAleavy, J. C., *et al.*, *Anesthesiology*, **22,** 260 (1961).

[11] Chinworth, H. E., and D. L. Katz, *Refrig. Eng.*, **54,** 359 (1947).

[12] Stackelberg, M. von, and H. R. Müller, *Z. Elektrochem.*, **58,** 25 (1954).

[13] Stackelberg, M. von, and W. Jahns, *Z. Elektrochem.*, **58,** 162 (1954).

[14] Miller, S. L., unpublished experiments.

[15] Van Cleeff, A., and G. Diepen, *Rec. trav. chim.*, **79,** 582 (1960).

[16] Reamer, H. H., F. T. Selleck, and B. H. Sage, *J. Petrol. Technol.*, **4,** 197 (1952).

[17] Stackelberg, M. von, *Naturwissenschaften*, **36,** 327, 359 (1949).

[18] Pauling, L., and R. E. Marsh, these PROCEEDINGS, **38,** 112 (1952).

[19] Claussen, W. F., *J. Chem. Phys.*, **19,** 259, 662, 1425 (1951).

[20] Stackelberg, M. von, and H. R. Müller, *J. Chem. Phys.*, **19,** 1319 (1951).

[21] Eley, D. D., *Trans. Faraday Soc.*, **40,** 184 (1944); Frank, H. S., and M. W. Evans, *J. Chem. Phys.*, **13,** 507 (1945); Claussen, W. F., and M. F. Polglase, *J. Am. Chem. Soc.*, **74,** 4817 (1952).

[22] For examples, see Bernal, J. D., and R. H. Fowler, *J. Chem. Phys.*, **1,** 515 (1933); Hall, L., *Phys. Rev.*, **73,** 775 (1948); Pople, J. A., *Proc. Roy. Soc.* (*London*), **202A,** 163 (1951); Litovitz, T. A., and E. H. Carnevale, *J. Appl. Phys.*, **26,** 816 (1955); Smith, A. H., and A. W. Lawson, *J. Chem. Phys.*, **22,** 351 (1954); Frank, H. S., and W. Y. Wen, *Discussions Faraday Soc.*, **24,** 133 (1957); Frank, H. S., *Proc. Roy. Soc.* (*London*), **A247,** 481 (1958).

[23] Pauling, L., in *The Nature of the Chemical Bond* (Ithaca, New York: Cornell University Press, 3rd ed., 1960), p. 472; *Hydrogen Bonding*, ed. G. Hadzi (London: Pergamon Press, 1959), p. 1; Frank, H. S., and Quist, A. S., *J. Chem. Phys.*, **34,** 604 (1961).

[24] Klotz, I. M., *Science*, **128,** 815 (1958); Klotz, I. M., and S. W. Luborsky, *J. Am. Chem. Soc.*, **81,** 5119 (1959).

[25] Szent-Györgyi, A., *Bioenergetics* (New York: Academic Press, Inc., 1957).
[26] van der Waals, J. H., *Trans. Faraday Soc.*, **52,** 184 (1956).
[27] Barrer, R. M. and W. I. Stuart, *Proc. Roy. Soc.* (*London*), **A243,** 172 (1957).
[28] Fowler, R., and E. A. Guggenheim, *Statistical Thermodynamics* (London; Cambridge University Press, 1939), p. 426.
[29] The large cavity needed for SF_6 and the (probably) small ΔE may account for its high value of $P_{\text{anesthesia}}/P_{\text{hydrate}}$.
[30] Quist, A. S., and H. S. Frank, *J. Phys. Chem.*, **65,** 560 (1961).
[31] Severinghaus, J. W., *Ann. N. Y. Acad. Sci.*, **80,** 384 (1959).
[32] McAleavy, J. C., *et al.*, *Anesthesiology*, **22,** 260 (1961).
[33] Ferguson, J., *Proc. Roy. Soc.* (*London*), **B127,** 387 (1939).
[34] Brink, F., and J. M. Posternak, *J. Cellular Comp. Physiol.*, **32,** 211 (1948).
[35] Tasaki, I., in *Handbook of Physiology*, ed. John Field (Washington, D. C.: American Physiological Society, 1959), vol. 1, p. 114.
[36] Grahame, D. C., *J. Chem. Phys.*, **23,** 1725 (1955); *J. Am. Chem. Soc.*, **79,** 2093 (1957).
[37] Grahame, D. C., *Chem. Revs.*, **41,** 496 (1947).
[38] Nachmansohn, D., *Chemical and Molecular Basis of Nerve Activity* (New York: Academic Press, 1959).
[39] Larrabee, M. G., J. G. Ramas, and E. Bulbring, *J. Cellular Comp. Physiol.*, **40,** 461 (1952).

INFORMATION TO CONTRIBUTORS

THE PROCEEDINGS is the official organ of the NATIONAL ACADEMY OF SCIENCES and of the NATIONAL RESEARCH COUNCIL for the publication of brief accounts of important current researches of members of the ACADEMY and of the COUNCIL and of other American investigators. The PROCEEDINGS will aim especially to secure prompt publication of original announcements of discoveries and wide circulation of the results of American research among investigators in other countries and in all branches of science.

ARTICLES should be brief. The viewpoint should be comprehensive in giving the relation of the paper to previous publications of the author or of others and in exhibiting, where practicable, the significance of the work for other branches of science. Elaborate technical details of the work and long tables of data should be avoided, but authors should be precise in making clear the new results and should give some record of the methods and data upon which they are based.

MANUSCRIPTS should be prepared with a current number of the PROCEEDINGS as a model in matters of form, and should be typewritten in duplicate with double spacing, the author retaining one copy. Illustrations should be confined to text figures of simple character, though more elaborate illustration may be allowed in special instances to authors willing to pay for their preparation and insertion. Particular attention should be given to arranging tabular matter in a simple and concise manner.

MANUSCRIPTS will be accepted only from members of the Academy who will assume responsibility for the propriety and scientific standards of the paper and for any printing costs in excess of those allowed them by the Academy. Manuscripts should be addressed to THE PROCEEDINGS OF THE NATIONAL ACADEMY OF SCIENCES, 2101 Constitution Ave., Washington 25, D. C.

GALLEY PROOF will be sent, with the understanding that charges for author's corrections shall be billed to him. Authors should therefore make final revisions on the typewritten manuscripts. Original artwork or figures will be returned if requested when the manuscript is submitted. Because of time limitations, page proofs will not be sent.

REPRINTS should be ordered when proof is returned, on the reprint order form which will be enclosed with the proof. They will be furnished at cost, approximately as follows:

SCHEDULE OF REPRINT RATES (POSTAGE NOT INCLUDED)

Quantity	*up to 4 pp.*	*up to 8 pp.*	*up to 12 pp.*	*Standard Covers*
50	$ 7.85	$15.10	$22.30	$6.90
100	8.95	17.30	25.60	8.40
150	10.10	19.50	28.95	9.95
add'l 100's	2.20	4.40	6.60	3.05

CONTENTS

	Page
BIOCHEMISTRY.—THE KINETICS OF FORMATION OF NATIVE RIBONUCLEASE DURING OXIDATION OF THE REDUCED POLYPEPTIDE CHAIN . . . . . *By C. B. Anfinsen, E. Haber, M. Sela, and F. H. White, Jr.*	1309
BIOCHEMISTRY.—PHOTOSYNTHETIC PHOSPHORYLATION AND MOLECULAR OXYGEN . . . . . *By Daniel I. Arnon, M. Losada, F. R. Whatley, H. Y. Tsujimoto, D. O. Hall, and A. A. Horton*	1314
BIOCHEMISTRY.—NONCYCLIC PHOTOPHOSPHORYLATION IN PHOTOSYNTHETIC BACTERIA . . . . . *By M. Nozaki, K. Tagawa, and Daniel I. Arnon*	1334
BIOCHEMISTRY.—AN INTERPRETATION OF THE KINETIC BEHAVIOR OF MODEL SUBSTRATES OF α-CHYMOTRYPSIN . . . . . *By George Hein and Carl Niemann*	1341
BIOCHEMISTRY.—AN ELECTRON SPIN RESONANCE ANALYSIS OF THE MECHANISM OF SUCCINIC DEHYDROGENASE ACTIVITY . *By Thomas C. Hollocher, Jr., and Barry Commoner*	1355
BIOCHEMISTRY.—FREE RADICALS IN SURVIVING TISSUES . . . . . *By Barry Commoner and Jessie L. Ternberg*	1374
BIOCHEMISTRY.—VARIATION IN BASE COMPOSITION OF RIBONUCLEIC ACID IN *Escherichia coli* . . . . . *By Melvin Santer, David C. Teller, and Lida Shilna*	1384
BIOCHEMISTRY.—IDENTIFICATION OF 5′ LINKED ADENOSINE AS END GROUP OF TMV-RNA . . . . . *By T. Sugiyama and H. Fraenkel-Conrat*	1393
BIOCHEMISTRY.—REACTION OF CARCINOGENS WITH ACRIDINE . . . . . *By A. Szent-Györgyi and Jane McLaughlin*	1397
BIOCHEMISTRY.—METALS AND CHARGE TRANSFER . . . . *By Albert Szent-Györgyi*	1398
BIOCHEMISTRY.—THE ENZYMATIC SYNTHESIS OF RNA: NEAREST-NEIGHBOR BASE FREQUENCIES . . . . . *By Samuel B. Weiss and Tokumasa Nakamoto*	1400
BIOCHEMISTRY.—THE ENZYMATIC SYNTHESIS OF RNA: COMPLEMENTARY INTERACTION WITH DNA . . *By E. Peter Geiduschek, Tokumasa Nakamoto, and Samuel B. Weiss*	1405
BIOCHEMISTRY.—STUDIES ON THE KINETICS OF PROTEIN SYNTHESIS IN YEAST . . . . . *By R. J. Young, H. K. Kihara, and H. O. Halvorson*	1415
BIOCHEMISTRY.—BIOCHEMICAL CONTROL OF STOMATAL OPENING IN LEAVES . . . . . *By Israel Zelitch*	1423
CHEMISTRY.—THE PROTON IRRADIATION OF METHANE, AMMONIA, AND WATER AT 77°K . . . . . *By Rainer Berger*	1434
GENETICS.—THE STAGE OF THE GENOME-PLASMON INTERACTION IN THE RESTORATION OF FERTILITY TO CYTOPLASMICALLY POLLEN-STERILE MAIZE . *By Janson G. Buchert*	1436
GENETICS.—ENZYME COMPLEMENTATION IN MIXED EXTRACTS OF MUTANTS FROM THE *Salmonella* HISTIDINE B LOCUS . . . . . *By John C. Loper*	1440
GENETICS.—DENSITY DIFFERENCES BETWEEN GENETIC MARKERS IN PNEUMOCOCCAL TRANSFORMING PRINCIPLE . . *By Ronald Rolfe and Harriett Ephrussi-Taylor*	1450
GENETICS.—SECOND-GENERATION HYBRIDS OF THE SPECIES OF *Taricha* . . . . . *By Victor C. Twitty*	1461
GENETICS.—ORGANIZATION OF THE SALIVARY-GLAND CHROMOSOME AS REVEALED BY THE PATTERN OF INCORPORATION OF H^3-THYMIDINE . . . . . *By Philip S. Woods, H. Gay, and A. Sengün*	1486
MATHEMATICS.—ON THE SUPERSOLVABILITY OF BICYCLIC GROUPS . . *By Jesse Douglas*	1493
MATHEMATICS.—A SIMPLIFIED PROOF OF VON NEUMANN'S COORDINATIZATION THEOREM . . . . . *By Israel Halperin*	1495
MICROBIOLOGY.—COLICINE V. . . . . *By John J. Hutton and Walther F. Goebel*	1498
MICROBIOLOGY.—THE ELUTION PROPERTIES OF TYPE 1 POLIOVIRUSES FROM $Al(OH)_3$ GEL. A POSSIBLE GENETIC ATTRIBUTE . . *By Wilna A. Woods and Frederick C. Robbins*	1501
PHYSICS.—WAVE BRANCHING PROCESSES AND INVARIANT IMBEDDING, I . . . . . *By Richard Bellman and Robert Kalaba*	1507
PHYSIOLOGY.—ON THE STATE OF CREATINE IN HEART MUSCLE . . . . . *By Y. C. P. Lee and Maurice B. Visscher*	1510
PHYSIOLOGY.—A THEORY OF GASEOUS ANESTHETICS . . . . *By Stanley L. Miller*	1515